

# A new species group of *Strumigenys* (Hymenoptera, Formicidae) from Ecuador, with a description of its mandible morphology

Douglas B. Booher<sup>1,2,\*</sup>, Philipp O. Hoenle<sup>3,\*</sup>

**1** Yale Center for Biodiversity and Global Change, 165 Prospect Street, New Haven, CT 06520-8106, USA  
**2** Georgia Museum of Natural History, 101 Cedar Street, Athens, GA 30602, USA **3** Ecological Networks, Department of Biology, Technical University of Darmstadt, Darmstadt, Germany

Corresponding authors: Douglas B. Booher ([dbooher@antmuseum.com](mailto:dbooher@antmuseum.com));

Philipp O. Hoenle ([philipp.hoenle92@gmail.com](mailto:philipp.hoenle92@gmail.com))

---

Academic editor: Brian L. Fisher | Received 14 December 2020 | Accepted 5 March 2021 | Published 5 May 2021

---

<http://zoobank.org/96B950D5-4973-4137-81EF-8030E91272C4>

---

**Citation:** Booher DB, Hoenle PO (2021) A new species group of *Strumigenys* (Hymenoptera, Formicidae) from Ecuador, with a description of its mandible morphology. ZooKeys 1036: 1–19. <https://doi.org/10.3897/zookeys.1036.62034>

---

## Abstract

*Strumigenys* is one of the most diverse ant genera in the world and arguably the most morphologically diverse, exhibiting an exceptional range of mandible shape and function. A new species, *Strumigenys ayersthey* sp. nov., discovered in the Chocó region of Ecuador is described. With two morphological characters, this species is shown to be a morphologically unique outlier among *Strumigenys* globally, having predominately smooth and shining cuticle surface sculpturing and long trap-jaw mandibles. Using  $\mu$ CT scans, we produced 3D images of the worker ant and static images to examine and compare mandible articular morphologies with most morphologically similar members of the *mandibularis* species group. Cuticular, pilosity, and articular mandible morphological differences supports placing the new species in its own new species group.

## Keywords

3D scan,  $\mu$ CT, LaMSA (latch-mediated spring-actuation), Myrmicinae, Northwest Ecuador, power amplified, *Strumigenys ayersthey*, taxonomy, tropical forest

---

\* Authors contributed equally.

## Introduction

Ecuador has one of the highest animal and plant species richness of any country, both in terms of species per area and total species richness (Sierra et al. 2002). This unusually high diversity is due to the three very distinct bioregions within Ecuador: the Amazon basin in eastern Ecuador, the Chocó-Darién bioregion in the northwest, and the Tumbesian drylands in the southern portion of the country (Sierra et al. 2002). Of these, the areas west of the Andes have been the least studied, and particularly the Chocó-Darién is a hotspot for new, previously unknown ant species (Donoso and Ramón 2009; Donoso et al. 2009; Salazar and Donoso 2013; Salazar et al. 2015; Donoso 2017; Hoenle et al. 2020). The *Strumigenys* fauna of Ecuador currently includes 51 species (Salazar et al. 2015), several of which are endemic (e.g., *Strumigenys madrigalae* Lattke and Aguirre 2015). Here, we report the finding of another likely endemic *Strumigenys* species from the Ecuadorian Chocó, contributing to a better understanding of this hyperdiverse region.

*Strumigenys* is one of the most diverse ant genera known with currently 852 extant and four fossil species, and is present on all continents except Antarctica (Guénard et al. 2017; Bolton 2020). Over the past two decades this genus received much taxonomic attention, but given the number of recent species descriptions, it is certain that many species are still waiting to be discovered (e.g., Booher et al. 2019; Sarnat et al. 2019; Dong and Kim 2020). *Strumigenys* are comparatively small ants (most < 4 mm) and are primarily litter dwelling although there are a few arboreal species (Bolton 2000). Most species assessed for diet are specialist predators of entomobryomorph Collembola (springtails), which may have led them to evolve a range of peculiar mandible forms to facilitate predation of fast-moving prey (Wesson and Wesson 1939; Wilson 1953; Masuko 1984; Dejean 1985; Brown and Wilson 1995; Masuko 2009; Lattke et al. 2018; Gray et al. 2019; Booher et al. 2021). Most spectacular, many *Strumigenys* possess trap-jaws, fast-snapping mandibles that function via a power amplified latch-mediated spring-actuation (LaMSA) (Booher et al. 2021; Ilton et al. 2018; Longo et al. 2019) akin to a biological mousetrap (Gronenberg 1996; Larabee and Suarez 2014). Performance and evolution of the trigger and latch system has been studied in detail, however there has been little attention given to additional undefined mandibular morphology that may contribute to the stability of trap-jaw movement in *Strumigenys* and other trap-jaw ants (Gronenberg 1996; Larabee et al. 2018; Booher et al. 2021). Within *Strumigenys*, the LaMSA mechanism has evolved independently multiple times, with each evolution convergent in morphology, function, and performance (Booher et al. 2021). However, the morphological variation in articular surfaces and articular processes involved in mandible movement across *Strumigenys* with or without LaMSA is morphologically variable and not well understood (Booher, unpublished data, Silva and Feitosa 2019). Here, we construct and define the single species *ayersthey* species group, describe the mandible articular morphology in detail within the description of the previously unknown *S. ayersthey* sp. nov., and compare it to that of morphologically similar members of the *S. mandibularis* species group to support species group separation.

## Materials and methods

### Sampling and geographic origins

The specimen of *Strumigenys ayersthey* sp. nov. was collected during a field trip to the Reserva Río Canandé in Ecuador (Esmeraldas Province) on 2 May 2018 (Fig. 1.). The reserve belongs to the Chocó-Darién bioregion, and is characterized by evergreen tropical forest with a wet season from January to March, and a dry season from September to December. The reserve contains low- to mid-elevation forest spanning a range of approximately 200 to 600 m. The specimen was collected in old-growth forest, along the ridge of small plateau at 507 m elevation. The specimen was collected alive by hand, and later preserved in a vial containing 96% ethanol. The Ministerio de Ambiente de Ecuador issued the permits for collection (MAE-DNB-CM-2017-0068) and exportation (41-2018-EXP-CM-FAU-DNB/MA).

### Photographs

We took stacking images with a Canon EOS 7D with a MPE 65mm lens (Canon, Tokyo, Japan). We used Helicon Focus Version 7 (Helicon Soft Ltd., Kharkiv, Ukraine) to focus stack multiple images, and added a scale and brightness adjustments with Adobe Photoshop CS6 13.0 (Adobe Inc., San Kaso, CA, USA). All images presented are available online and can be viewed on AntWeb (Antweb 2020), where it can be identified by a specimen-level code affixed to the pin.

### Synchrotron X-Ray micro-computed-tomography (SR $\mu$ CT) scan

The SR $\mu$ CT scan of the sample was recorded at P05 at PETRA III, Deutsches Elektronen-Synchrotron DESY in Hamburg, Germany. We used absorption contrast tomography with an energy of 11 keV, a sample-detector distance of 20 mm, and a magnification of 9.97 resulting in an effective pixel size of 0.642  $\mu$ m.

The dataset has been cropped, positioned, and visualized in VGStudio MAX 3.0 (build 109953; Volume Graphics GmbH, Heidelberg, Germany). Amira 5.6 (FEI Visualization Sciences Group, Mérignac Cedex, France) was used to digitally remove the cardboard the specimen was glued onto and to make a surface model of the scan data. Fiji (Schindelin et al. 2012) was then used to convert the resulting surface model to U3D.

### Morphological data

The measurements, indices, and morphological terminology used in species-group definitions and species descriptions in this study are based on Bolton (2000), and the mandible articular terminology is based on two studies (Table 1) (Silva and Feitosa 2019; Richter et al. 2019). We compared analogous terms for these studies, and

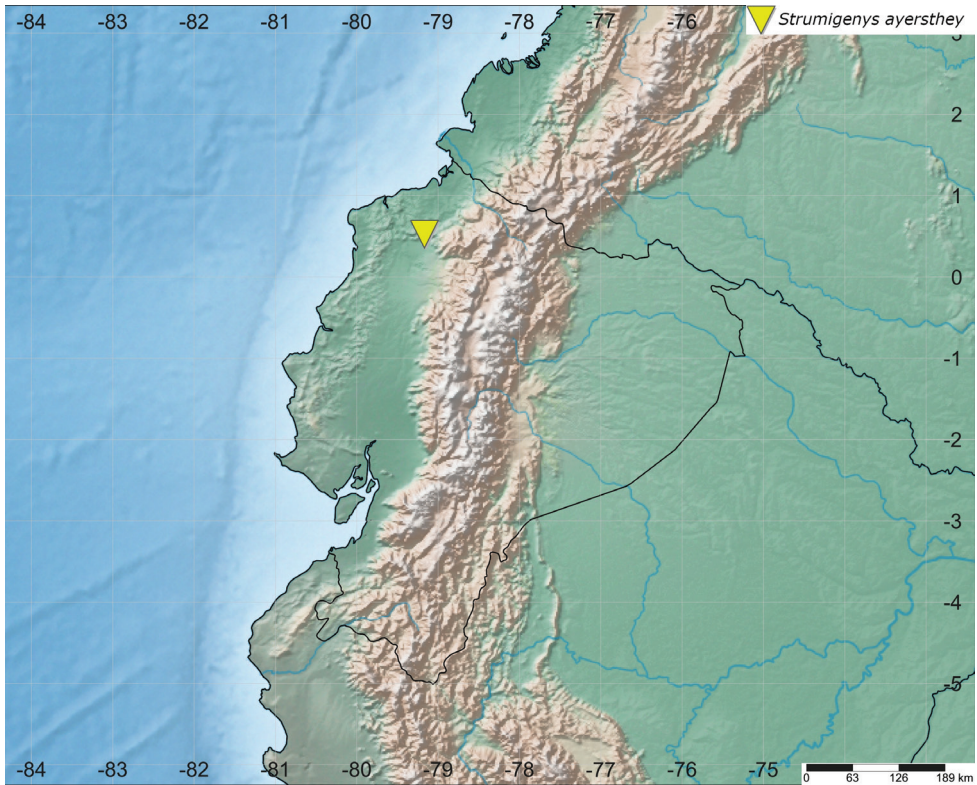


**Figure 1.** Location of the holotype collection of *S. ayersthey* sp. nov. in Ecuador (Reserva Río Canandé, Esmeraldas Province). Distribution map generated with SimpleMappr (Shorthouse 2010).

added our own terminology for features that were not included in these studies in best agreement with terminology already in use. Measurements were taken using the measurement application of the LAS-X Leica software using a Leica IC90 E digital camera and Leica M165 C microscope with either a 1.0× or 1.6× PLANAPO objective. Measurements and indices are presented as a single value mean of three independent measures; measurements are expressed in millimeters to three decimal places. Global morphological mandible index data were assimilated by DBB (Booher et al. 2021). Specimens were identified without head surface sculpture visually from species imaged and hosted on AntWeb (Antweb 2020). The data was plotted with JMP version 15.0.0 statistical software. Softening specimens and visual confirmation of trap-jaw mechanisms through visual manipulations of specimen were done as described in Booher et al. (2020). For this study, we examined mandible morphology in the following *mandibularis*-group species: *S. planeti* CASENT0873025, *S. biolleyi* CASENT0747760, *S. cordovens* CASENT0609666, and *S. smithi* from Ecuador in author DB's collection.

**Table 1.** Comparison of morphological features of *Strumigenys ayersthey* sp. nov. with those described in *Strumigenys* spp. (Silva and Feitosa 2019), and the Myrmicine ant *Wasmannia affinis* (Richter et al. 2019). *Strumigenys ayersthey* sp. nov. has several features previously not reported, but may be shared with many other *Strumigenys*. Presence refers to the reporting of each morphological feature: S – *Strumigenys* including *S. ayersthey*, SA – only reported in this publication in *S. ayersthey*, W – reported in *Wasmannia affinis*.

This study	Abbreviation		Presence	Definition	Figure
	Silva and Feitosa 2019	Richter et al. 2019			
aba	NA	apab	SA&W	apodeme attachment location of the abductor muscle	Fig. 6
ada	NA	apad	SA&W	apodeme attachment location of the adductor muscle	Fig. 6
clp	clp	cl	S&W	clypeus	Fig. 5
dfc	NA	dma (of head)	SA&W	dorsal mandibular articular surface of clypeus	Fig. 5
dmap	dmap	dma (of mandible)	S&W	dorsal articular process of mandible	Figs 5, 6
lbp	lplb	lbrp	S&W	labral articular process	Figs 5, 6
lbh	NA	NA	SA	labral hood of basal mandibular process insertion	Fig. 5
lbm	labrum	lbr	S&W	labrum	Fig. 5
lmap	lmap	abs (abductor swelling)	S&W	lateral articular process of mandible	Figs 5, 6
md	mandible	mandible	S&W	mandible	Fig. 5
vmap	vmap	vma (of mandible)	S&W	ventral articular process of mandible	Figs 5, 6
vpc	NA	NA	SA	ventral articular process of clypeus	Fig. 5
lmah	NA	absa (of head)	S&W	articular area of the abductor swelling	NA
vmah	NA	vma (of head)	S&W	ventral mandibular articulation	NA
bpm	bpm	NA	S	basal process of mandible	Figs 5, 6

## Measurement definitions

- CI** Cephalic index.  $HW/HL \times 100$ ;
- EL** Eye length. Maximum length of eye as measured in oblique view of the head to show full surface of eye;
- FL** Femur length. Maximum length of hind femur;
- HL** Head length. Maximum length of head in full-face view, excluding mandibles, measured from anterior most point of clypeal margin to midpoint of a line across the posterior margin;
- HW** Head width. Maximum width of head in full-face view, measured in the same plane as HL;
- MI** Mandible index.  $ML/HL \times 100$ ;
- ML** Mandible length. The straight-line length of mandible at full closure, measured in the same plane as HL, from mandibular apex to anterior clypeal margin;
- PW** Pronotum width. Maximum width of pronotum in dorsal view;
- SI** Scape index.  $SL/HW \times 100$ ;
- SL** Scape length. Length of antennal scape excluding the basal condylar bulb;
- TL** Total body length;
- WL** Weber's Length.

## Results

### Key to *Strumigenys ayersthey* sp. nov.

- 1 Head in full face view absent of sculpture, smooth and shining; mandible relatively long MI 65; pilosity consisting of nearly uniform sub-erect to erect filiform setae.....***Strumigenys ayersthey* sp. nov. (Ecuador)**
- Head in full face view usually with at least some sculpture, if smooth and shining; mandible is relatively short MI < 40; pilosity variable but not usually consisting of nearly uniform sub-erect to erect filiform setae.....**Couplet 1 in Bolton (2000; Key to Nearctic and Neotropical *Strumigenys*)**

### *Strumigenys ayersthey* group

The *ayersthey* group contains one member and exhibits most morphological resemblance to the *mandibularis* group (Bolton 2000), from which it is most easily separated by differences in sculpture and pilosity. *Strumigenys ayersthey* sp. nov. has little to no sculpture anywhere on its body and has only fine simple to flagellate setae, whereas *mandibularis* species group members are predominately sculptured and not shining with mostly decumbent to appressed apically expanded or flattened setae. Also separating these two groups are morphological differences in dorsal articular processes of mandibles, in *S. ayersthey* sp. nov. these processes project from the dorsal surface at the base of each mandible without distinct lamellate lateral edges. In *mandibularis* species-group members, these processes arise from laterally expanded lamella at the base of mandibles that are continuous with the dorsal surface of each mandible. *Strumigenys ayersthey* sp. nov. can be distinguished from all other *Strumigenys* species by shining sculpture, MI 65, and ML 41, other *Strumigenys* predominately lacking sculpture and shining have MI < 40 and ML < 0.25 (Fig. 2). The following diagnosis is adapted and expanded from the *mandibularis* species-group diagnosis (Bolton 2000).

### *Strumigenys ayersthey* species group: diagnosis of worker.

- Bulla of femoral gland not easily visible but appears as a faint streak along the medial dorsal surface.
- Scape not dorsally flattened.
- Apical fork of mandible with one well-developed intercalary tooth. Mandible with two conspicuous acute preapical teeth; both approximately the same length. Preapical dentition not crowded near apex. MI 65.
  - Anterior clypeal margin usually shallowly convex.
  - Leading edge of scape usually with all setae standing and directed toward apex of the scape. Scape slender, the subbasal curve extremely shallow; relatively long, SI 110.
  - Preocular carina in profile short, terminating before level of eye.

## Global distributions of relative mandible size

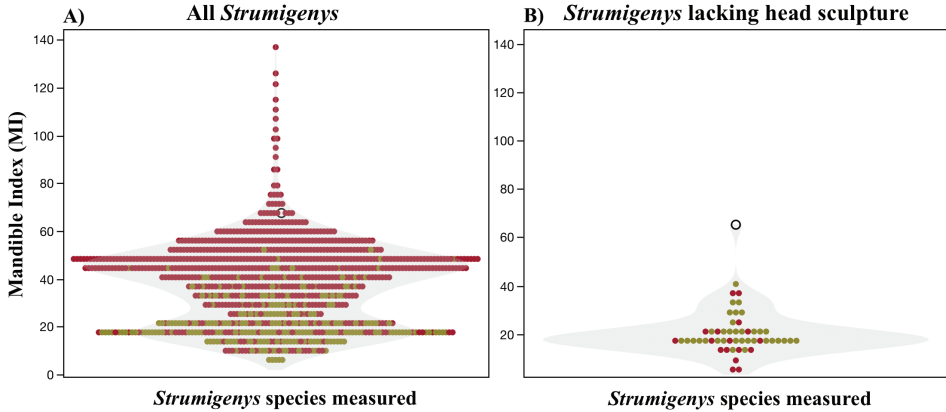


**Figure 2.** Comparisons of MI among *Strumigenys* spp. **A** accounts of 961 species and morphospecies globally representing all species groups **B** MI of 52 *Strumigenys* identified as not smooth and shining cuticular surface of the head in full frontal view. Light yellow points are species without trap-jaws, dark red points are those with trap-jaws. *Strumigenys ayersthey* sp. nov. is marked with an open black circle and possesses trap-jaw mandible morphology.

- Upper margin of the antennal scrobe not sharply defined behind level of eye.
- Ventrolateral margin of head continuous and not obviously concave in front of eye.
  - Postbuccal impression absent.
  - Propodeum with minute teeth with a lower propodeal tooth-like lobe at base of declivity that is slightly less developed than the upper propodeal tooth, the two linked by a lamella.
    - Ventral surface of petiole with spongiform tissue.
    - Pilosity. Pronotal humeral setae flagellate and indistinguishable from neighboring background pilosity of similarly shaped simple standing to flagellate setae. Standing setae on head and mesosoma not differentiated from ground pilosity, abundant and simple to flagellate.
      - Sculpture. Head and mesosoma predominantly or entirely free of sculpture and shining, usually with a smooth area on mesopleuron.
      - Basal process of mandible arises dorsally with a locking angle estimated between 180 and 200°.
      - Dorsal articular process of mandibles bluntly pointed arising evenly from the dorsal surface without a distinct lateral lamella.
      - Basal mandibular process arising in dorsal most plane of mandibles.
      - Processes of clypeus present as a pair of small tooth like laminar ridges each positioned between the basal mandibular and dorsal articular processes of mandibles in closed position.

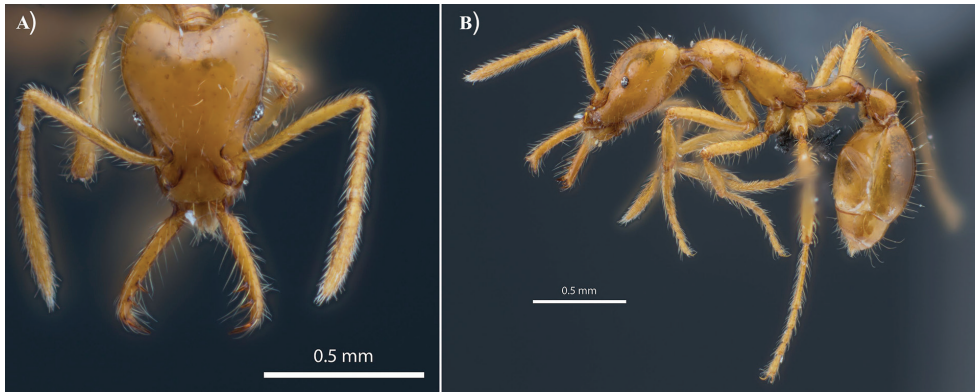


**Figure 3.** Images of **A** head in full-face view and **B** profile of Holotype specimen of *Strumigenys ayersthey* sp. nov. (CASENT0875770) [MEPN].

***Strumigenys ayersthey* sp. nov.**

<http://zoobank.org/235F1F9D-A33F-4C75-959F-C52B9BC5FD41>

**Type material examined. Holotype worker:** Ecuador: Esmeraldas Province, Reserva Río Canandé, 2 May 2018, Elevation 507m, 0.5263, -79.1682, Part of diversity study Hoenle & Blüthgen plot F1N31, hand-sampling on forest floor in primary forest, specimen broke in several parts, leg. P. Hoenle. Specimen identifier code (casent0875770), deposited at [MEPN] (Museo de Colecciones Biológicas Gustavo Orcés, Escuela Politécnica Nacional, Quito, Ecuador).

**Holotype worker measurements** (n = 1): HL = (0.609); HW = (0.480); ML = (left = 0.383, right = 0.411), the left mandible is slightly shorter than the right mandible; PW = (0.303); SL = (0.530); FL = (0.568); EL = (0.07); WL = (0.683); CI = (78.82); MI = (65.19); SI = (110.42).

**Description. Mandibles** with five teeth; two preapical teeth, apicodorsal and apicoventral teeth, and an intercalary tooth. The two preapical teeth are well developed and spiniform with nearly equal lengths and are longer than the width of the mandible where they arise (first preapical tooth = 0.056, second preapical tooth = 0.050). These teeth are located in the apical third of mandible and separated by a distance approximately equal their length (0.051). Apicodorsal (0.78) and apicoventral (0.73) teeth spiniform and of nearly equal length and with a well-developed intercalary tooth (0.38) arising just above the apicoventral tooth. Basal portion of mandible with four processes, three articular processes (dorsal, lateral, and ventral articular processes) and a latching process (basal mandibular process; Fig. 5). The dorsal articular process extends posteriorly from the basal dorsal surface without a distinct lateral ridge and terminating as a small bulbous point. The ventral articular process extends from the latero-posterior basal portion of the mandible as a dorsal to ventral cuticular ridge from and is continuously connected to the lateral articular process. The lateral articular process is dilated, with the medial portion extending laterally away from a line drawn verti-

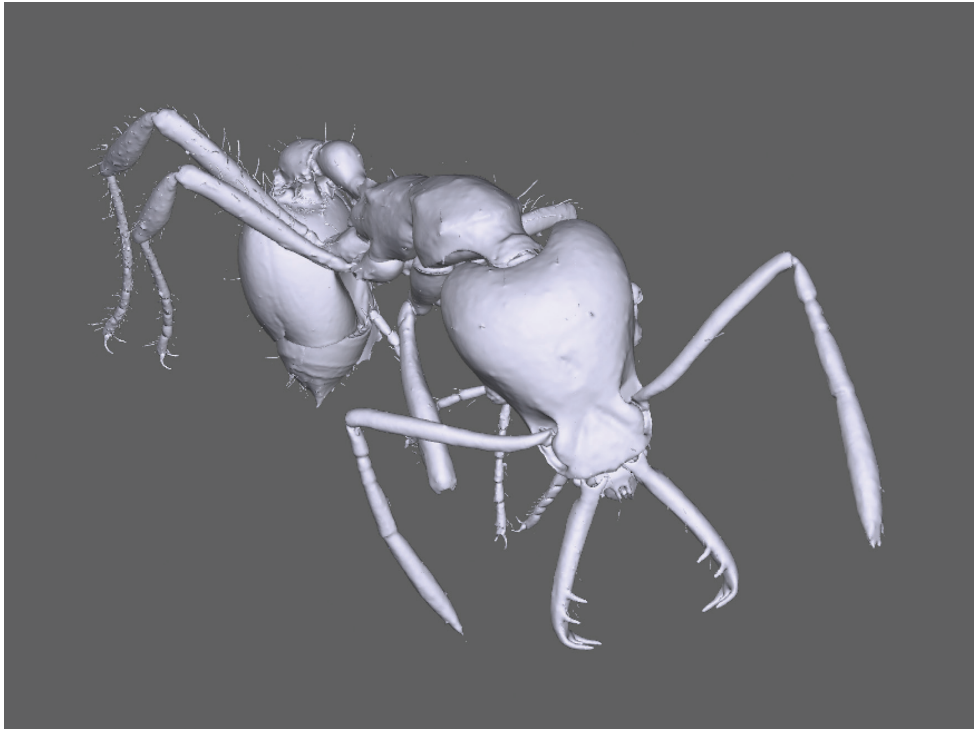


**Figure 4.** 3D scan of *Strumigenys ayersthey* sp. nov. assembled by  $\mu$ CT.

cally from the posterior-most positions of the dorsal and ventral processes. In full face view, the lateral articular process appears as a lateral bulge below the dorsal ridge of the dorsal articular process and shadows the ventral process (Fig. 6). The dorsal area between the basal process and dorsal articular process is indented and when mandibles are closed the process of the clypeus extends into this cavity (Fig. 5).

**Clypeus** ca.  $1.5 \times$  as wide as long. Eye apparent (0.070) with 15 or 16 pigmented ommatidia. Scape sub-cylindrical with shallowly curved subbasal bend. Ventrolateral margin of head in front of eye not sharply defined, strongly indented or concave. Post-buccal impression absent. Preocular carina and upper margin of the antennal scrobe in profile short, terminating anterior of eye.

**Mesosoma** shallowly and gradually impressed between pronotum and propodeum. Declivity of propodeum with two bluntly rounded triangular teeth that are just longer than the lamella connecting them (upper tooth = 0.062, lower tooth = 0.50, lamella at shallowest point between = 0.046).

In profile view, bulla of propodeal spiracle located at dorsal-most position of propodeum with propodeal spiracle opening facing postero-dorsally and forming lateral bulges that disrupt the outline in dorsal view. Spiracle opening much narrower than EL (.022). Petiolar node longer (0.127) than wide (0.113). Postpetiolar disc longer (0.185) than wide (0.153.). First gastral tergite with no basigastral costulae past the limbus.

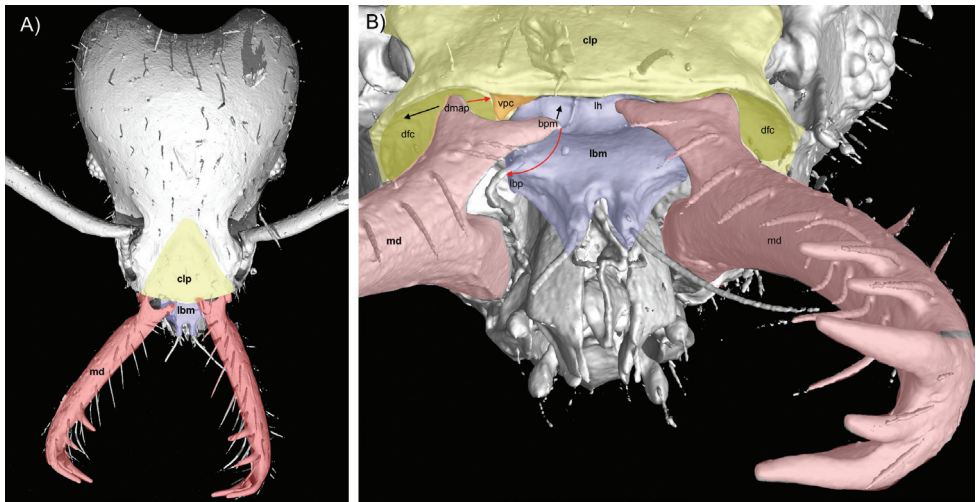


**Figure 5.** Colorized  $\mu$ CT surface renders of the head of *S. ayersthey* sp. nov. **A** head in full face view and **B** view from apex of mandibles looking towards base of mandibles. Black arrows represent closing motions and red arrows represent opening motions of mandibles. Abbreviations: **bpm** – basal process of mandible, **clp** – clypeus (yellow), **dfc** – dorsal articular surface of oral cavity (green), **dmap** – dorsal articular process of mandible, **lbp** – labral articular process, **lh** – labral hood, **lbm** – labrum (lavender), **md** – mandible (red), **vmap** – ventral articular process of mandible, **vpc** – ventral articular process of clypeus in orange. As the mandibles open towards latched position, the labrum (lbm) hinges upwards such that the basal mandibular process (bpm) latches into the complementary pocket of the labrum (lbp) and the dorsal articular process of the mandible (dmap) articulates freely within the dorsal articular surface of the oral cavity (dfc) around the ventral process of the clypeus (vpc). The labral hood (lh) and the ventral processes of the clypeus (vpc) forms a pair of pockets housing the basal mandibular process (bpm) of each mandible.

**Sculpture.** Head and rest of body smooth and shining and without obvious sculpture other than piliferous punctations where setae arise. Basigastral sculpture limited to costulae within the limbus and do not extend onto the surface of the first gastral tergite.

**Pilosity.** The background pilosity of all surfaces (mandibles, head, mesosoma, petiole, postpetiole, abdomen, and legs) are covered in evenly spaced simple to subflagellate erect to suberect setae that vary in length and are apically pointed. Head without differentiated apicoscrobial setae and leading edge of scape also without differentiated setae, pilosity of scape on all surfaces consists of short erect simple setae tending to point towards apex, none are recurved as to point to the base, and scape pilosity is similar to those elsewhere on head. Differentiated longer subflagellate to flagellate setae are limited to a pair straddling the midline on the anterior margin of clypeus that extend over mandibles when closed, a lateral pair on pronotal shoulders, a pair arising from ventral portion of propodeal spiracle, one to two pairs on the dorsum of petiole, and postpetiole. The majority of pilosity on gaster consist of slightly longer subflagellate setae than those on mesosoma.

**Spongiform appendages.** Length of lateral lobe of petiole weakly developed and visible only as a thin carinae along posterior third of node; expanded as a thin cuticular

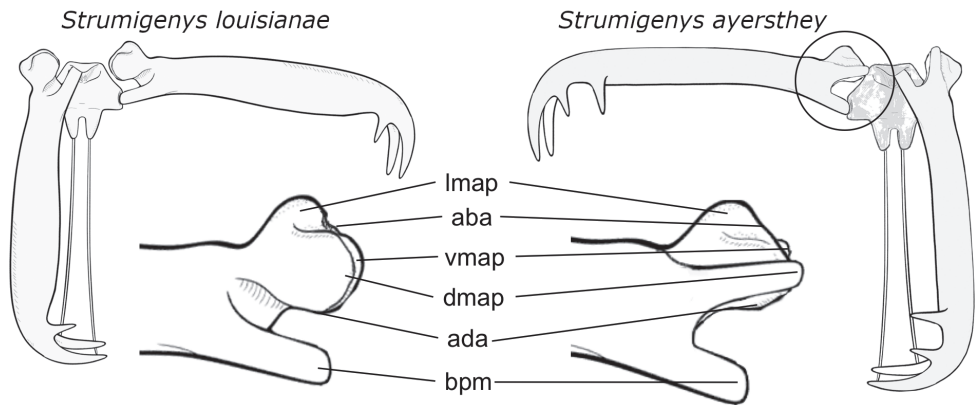


**Figure 6.** Comparison of the mandibles between *S. louisianae* (left) and *S. ayersthey* sp. nov. (right). Abbreviations: **aba** – apodeme attachment location of the abductor muscle, **ada** – apodeme attachment location of the adductor muscle, **bpm** – basal process of mandible, **dmap** – dorsal articular process of mandible, **lmap** – lateral articular process of mandible, **vmap** – ventral articular process of mandible. Illustrations adapted from Booher et al. (2021).

flange just behind the node in dorsal view. Subpetiolar flange developed as a thin cuticular narrow flange deepest posteriorly (0.046). Lateral lobes of postpetiole distinct and separated from the anterior flange of the post petiolar disc and do not connect posteriorly leaving a medial posterior gap along the posterior portion of disc (most easily seen in dorsal view). In profile, ventral lobe of postpetiole also weakly-developed (0.053 in depth) and much narrower than the exposed height of postpetiolar node (0.149).

**Color.** Yellow uniform light reddish brown.

**Queen and male.** Unknown.

**Etymology.** Many cultures have recognized a spectrum of genders between and beyond the binary of male and female. However, by following a rule exemplified in the International Code of Nomenclature (ICZN 1999) for how to name species after individuals, one might conclude only binary gender assignments possible when assigning new species names derived from Latin. Dubois (2007) provides clarification to this rule stating that there is no need to amend or Latinize personal names – and therefore no need to assign gender. In contrast to the traditional naming practices that identify individuals as one of two distinct genders, we have chosen a non-Latinized portmanteau honoring the artist Jeremy Ayers and representing people that do not identify with conventional binary gender assignments, *Strumigenys ayersthey*. The ‘they’ recognizes non-binary gender identifiers in order to reflect recent evolution in English pronoun use - ‘they, them, their’ and address a more inclusive and expansive understanding of non-neutral gender identification. *Strumigenys ayersthey* sp. nov. is thus inclusively named in honor of Jeremy Ayers for the multitude of humans among the spectrum of gender who have been unrepresented under traditional naming practices. Jeremy was a multifaceted and beloved Athens-based (GA, USA) artist and activist whose humanity and achievements defied the limits of categorized classification. Jer-

emy brought an intellectual and playful, Pan-like curiosity to every aspect of his life. He was a writer, philosopher, painter, musician, activist, photographer, gardener, and exploder of boundaries who transformed the culture that surrounded him. His deep appreciation of the variety and minute details of the natural world astounded all who knew him. In the spirit of Jeremy, we also propose that the -they suffix can be used for singular honorific names of non-binary identifiers in compliance with the ICZN.

## Discussion

As morphological convergence is rampant among *Strumigenys* morphotypes (short or long mandible species) it is difficult to determine by morphology alone how species are related (Ward et al. 2014). However, within biogeographic regions, species groups of morphologically similar *Strumigenys* species are often phylogenetically most closely related (Booher 2021). As such, morphological species groups are relevant and useful for identification as well as evolutionary research (Booher et al. 2021). In the construction of *Strumigenys* morphological species groups, differences in the position, presence, and shape of pilosity are of major importance. For example, the direction and shape of hairs along the clypeal margin and along the leading edge of the scape separates several Nearctic species groups, e.g., *pulchella*, *ornata*, and *talpa* groups (Bolton 2000). Similarly, slight differences in sculpturing help to identify similar species, but major differences in sculpture (i.e., having sculpture present across most cuticular surfaces compared to no sculpture) do not occur among species within any *Strumigenys* species group. We further justify the formation of a new single species group with differences in basal mandibular morphology from most morphologically similar *mandibularis*-group members.

The general mandibular morphology of LaMSA *Strumigenys* has been well described with the base of the mandible having three articular processes; the dorsal and ventral articulatory processes are responsible for holding mandibles in place during movement and a third lateral process is attached via apodemes to opening muscles (Fig. 6) (Silva and Feitosa 2019), alternatively termed the abductor swelling of the mandible or 'atala' (Richter et al. 2019; Richter et al. 2020). Although articular morphology of mandibles has been described in LaMSA *Strumigenys* and more generally in the more typical ant genera *Wasmannia* (Richter et al. 2019), *Formica*, and *Brachyponera* (Richter et al. 2020), there has not yet been a comparison in morphological features between them and there are a few important differences associated with the derived morphology of trap-jaws in *Strumigenys* (Table 1). Most morphological features in *S. ayersthey* have homologous features shared with other ants, however there are a few features that are not shared or have not been previously reported and are worth discussing. A most apparent difference is the dorsal articulation of the mandible and head. In what is described in *Wasmannia* and other ants, mandibles are tightly connected to the head capsule with primary and secondary joints, with

the “secondary joint (dmah-dmap) formed by a ventrolateral longitudinal smooth elongation of the clypeus... which articulates with a smooth dorsolateral area on the mandibular base” (Richter 2019). In *S. ayersthey* sp. nov., this secondary joint is not connected to the head and the dmap moves freely within the dfc. We hypothesize that in contrast to typical ants, the clypeal articular process present in *S. ayersthey* helps to stabilize dorsal mandible articular movement. A second morphological feature important to note, is the derived labral hood (lh) present in *S. ayersthey*. This dorsal expansion of the basal area of the labrum is highly sclerotized, hypothesized to reduce damage from self-piercing and over-rotation, and is common to trap-jaw *Strumigenys* (Booher et al. 2021). We provide a table of mandible terminology (Table 1), however a more extensive comparative study across ants is needed to truly understand homology of mandible morphology.

Less prominent morphological features differ between trap-jaw *Strumigenys* and, for instance, mandible dentition has been used as focal distinguishing character between species groups. *Strumigenys ayersthey*, although most similar to members of the *mandibularis*-group, the dorsal articular process of the mandible differs in shape with *mandibularis*-group species. In members of *mandibularis* species group the dorsal articular process arises from a laterally extending dorsal surface forming a shelf like lamellate ridge at the basal portion of the mandible. In dorsal view, this lamellate process overhangs the lateral articular process obscuring most of it from view. In *S. ayersthey* sp. nov., the lateral corner of the dorsal articular surface is gradually rounded and does not form a lamellate margin. Additionally, in the only species with a detached mandible that could be visually inspected by us (*S. planeti*) the posteriormost articular surface of the dorsal process contained three small bulbous points connected by indented lamellae, wherein *S. ayersthey* sp. nov. there is a single bulbous articular point. Therefore, *S. ayersthey* sp. nov. is an exceptional morphological outlier and a rare addition to the hyperdiverse genus *Strumigenys*. It does not fit cleanly into any of Bolton’s species groups, nor can existing species-group definitions envelope this species with minor changes – hence, we placed it as the only member of a new species group. We find morphological articular structure of mandibles are important taxonomic characters and should be investigated in future taxonomic works in this genus.

Our species description includes a  $\mu$ CT 3D render of the holotype worker, and its surface model is freely available for download (Suppl. material 1). This offers any reader virtual morphological details of the new species and the ability to view morphological features at all angles. 3D imaging techniques, and in particular micro-computed X-ray tomography ( $\mu$ CT), are being frequently used in taxonomy and functional morphology, particular in ants (Faulwetter et al. 2013; Akkari et al. 2015; Garcia et al. 2017; Sarnat et al. 2017; Staab et al. 2018). For *Strumigenys*, they already lead to detailed morphological analysis, and  $\mu$ CT scans of Fijian *Strumigenys* have even been suggested as a tool for teaching with augmented reality (Sarnat et al. 2019). In our case, the  $\mu$ CT scan facilitated additional descriptions of mandibular morphology and function of *S. ayersthey* sp. nov.

The discovery of *Strumigenys ayersthey* sp. nov. advanced our understanding of the global morphology of this genus: Its unique combination of almost no surface sculpturing and long trap-jaw mandibles make it stand out among nearly a thousand other *Strumigenys* species. Because of *S. ayersthey* sp. nov. unusual morphology, information about its general biology could prove to be valuable. However, subsequent attempts in obtaining more specimens at the previous location with Winkler traps in 2019 have failed, and a large ecological ant study in the Canandé reserve did not reveal any more specimens. *Strumigenys ayersthey* sp. nov. can therefore be considered as rare. The discovery of such an unusual rare ant highlights the importance of scientific exploration and conservation of the Chocó region in Ecuador, which is at the same time one of the most biodiverse and threatened areas on our planet (Dinerstein et al. 1995; Olson and Dinerstein 1998; Myers et al. 2000).

## Acknowledgements

We thank the Fundación Jocotoco and the associated Tesoro Escondido for logistic support and their permission to do research on their forest properties. First, we like to thank Adriana Argoti and Adrian Brückner for help during field collection. We are grateful for the local support from the park staff in the Canandé and Tesoro Escondido reserve, that made the field collection easier and made two great field stays possible: Bryan Amayo, Alcides Zombrano, Roberto de la Cruz, Jorge Zambrano, Amado de la Cruz, Yadria Giler, Patricio Encarnación and Vanessa Moreira.

We thank musician and artist Michael Stipe for contributing to the etymology in honor of a hero to many and dear friend to those that knew him, Jeremy Ayers. We further thank the support from the LGBTQIA+ and gender dynamic community, for which we hope this species furthers pride. Additional thanks to Adrienne Truscott for input and suggestions.

Further, we like to thank Sebastian Schmelzle for providing and editing the  $\mu$ CT scans. We thank Roberto Keller for comments on the functional aspects of the trap-jaw, and James Trager for his Latin expertise. We thank Christoph von Beeren for the use of his photostacking equipment. David Donoso, Martin Schäfer and Nico Blüthgen provided supervision and logistic support for the studies in Ecuador, and without them this discovery would not have been possible.

The SR $\mu$ CT data of the single *Strumigenys ayersthey* sp. nov. specimen was acquired within the project NOVA (Network for Online Visualization and synergistic Analysis of tomographic data) funded by the German Federal Ministry of Education and Research (05K16VKB) within the call for proposals “Erforschung kondensierter Materie an Großgeräten” 2016/2019. We thank the proposers of the NOVA project Michael Heethoff (Technische Universität Darmstadt), Vincent Heuveline (Heidelberg University), and Jürgen Becker (Karlsruhe Institute of Technology). We thank the associated partners of the NOVA project Felix Beckmann from the HelmholtzZentrum Geesthacht, and Andreas Kopmann and Wolfgang Mexner from

the Karlsruhe Institute of Technology. We acknowledge DESY (Hamburg, Germany), a member of the Helmholtz Association HGF, for the provision of experimental facilities. Parts of this research were carried out at PETRA III and we would like to thank Jörg Hammel and Fabian Wilde for assistance in using the experimental station at P05 and reconstruction of the data.

Finally, we are grateful for the suggestions from two anonymous reviewers and Brian L. Fisher, which substantially improved the manuscript.

We acknowledge support by the Open Access Publishing Fund of Technische Universität Darmstadt. PH was supported by a scholarship from the German National Academic Foundation.

## References

- Akkari N, Enghoff H, Metscher BD (2015) A new dimension in documenting new species: high-detail imaging for Myriapod taxonomy and first 3D cybertype of a new millipede species (Diplopoda, Julida, Julidae). *PLoS ONE* 10(8): e9135243. <https://doi.org/10.1371/journal.pone.0135243>
- AntWeb (2020) AntWeb. Version 8.45.1. California Academy of Science. <https://www.antweb.org> <https://doi.org/10.1596/0-8213-3295-3> eb.org [Accessed on 21 November 2020]
- Booher DB, Gibson JC, Liu C, Longino JT, Fisher BL, Janda M, Narula N, Toulkeridou E, Mikheyev AS, Suarez AV, Economo EP (2021) Functional innovation promotes diversification of form in the evolution of an ultrafast trap-jaw mechanism in ants. *PLOS Biology* 19(3): e3001031. <https://doi.org/10.1371/journal.pbio.3001031>
- Booher DB, Prebus MM, Lubertazzi D (2019) A taxonomic revision of the *Strumigenys nitens* and *simulans* groups (Hymenoptera: Formicidae), two Caribbean radiations of leaf litter ants. *Zootaxa* 4656: 335–358. <https://doi.org/10.11646/zootaxa.4656.2.7>
- Bolton B (2000) The ant tribe Dacetini. *Memoirs of the American Entomological Institute* 65: 1–1028.
- Bolton B (2020) An online catalog of the ants of the world. <http://antcat.org> [Accessed on 16 July 2020]
- Brown WL, Wilson EO (1959) The evolution of the dacetine ants. *The Quarterly Review Biology* 34: 278–294. <https://doi.org/10.1086/402828>
- Dinerstein EA, Olsen DM, Graham DJ, Webster AL, Primm SA, Bookbinder MP, Ledec G (1995) Conservation Assessment of the Terrestrial Ecoregions of Latin America and the Caribbean. The World Bank, Washington, 129 pp. <https://doi.org/10.1596/0-8213-3295-3>
- Dong MS, Kim SK (2020) A taxonomic study on the genus *Strumigenys* Smith, 1860 (Hymenoptera: Formicidae) from Korea with a description of new species. *Asian Myrmecology* 12(e012001): 1–21.
- Donoso DA, Salazar F, Maza F, Cárdenas RE, Dangles O (2009) Diversity and distribution of type specimens deposited in the Invertebrate section of the Museum of Zoology QCAZ, Quito, Ecuador. *Annales de la Société Entomologique de France* 45(4): 437–454. <https://doi.org/10.1080/00379271.2009.10697628>

- Donoso DA, Ramón G (2009) Composition of a high diversity leaf litter ant community (Hymenoptera: Formicidae) from an Ecuadorian pre-montane rainforest. *Annales de la Société Entomologique de France* 45(4): 487–499. <https://doi.org/10.1080/00379271.2009.10697631>
- Donoso DA (2017) Tropical ant communities are in long-term equilibrium. *Ecological Indicators* 83: 515–523. <https://doi.org/10.1016/j.ecolind.2017.03.022>
- Dubois A (2007) Genitives of species and subspecies nomina derived from personal names should not be emended. *Zootaxa* 1550(1): 49–68. <https://doi.org/10.11646/zootaxa.1550.1.2>
- Faulwetter S, Vasileiadou A, Kouratoras M, Dailianis T, Arvanitidis C (2013) Micro-computed tomography: Introducing new dimensions to taxonomy. *ZooKeys* 264: 1–45. <https://doi.org/10.3897/zookeys.263.4261>
- Garcia FH, Fischer G, Liu C, Audisio TL, Alpert GD, Fisher BL, Economo EP (2017) X-Ray microtomography for ant taxonomy: An exploration and case study with two new *Tera-taner* (Hymenoptera, Formicidae, Myrmicinae) species from Madagascar. *PLoS ONE* 12: e0172641. <https://doi.org/10.1371/journal.pone.0172641>
- Guénard B, Weiser M, Gomez K, Narula N, Economo EP (2017) The Global Ant Biodiversity Informatics (GABI) database: a synthesis of ant species geographic distributions. *Myrmecological News* 24: 83–89.
- Gray KW, Cover SP, Johnson RA, Rabeling C (2018) The dacetine ant *Strumigenys arizonica*, an apparent obligate commensal of the fungus-growing ant *Trachymyrmex arizonensis* in southwestern North America. *Insectes Sociaux* 65: 401–410. <https://doi.org/10.1007/s00040-018-0625-8>
- Gronenberg W, Tautz J, Hölldobler B (1993) Fast trap jaws and giant neurons in the ant *Odontomachus*. *Science* 262: 561–563. <https://doi.org/10.1126/science.262.5133.561>
- Gronenberg W (1996) The trap-jaw mechanism in the dacetine ants *Daceton armigerum* and *Strumigenys* sp. *Journal of Experimental Biology* 199: 2021–2033.
- Hoenle PO, Lattke JE, Donoso DA, von Beeren C, Heethoff, M, Schmelzle S, Argoti A, Camacho L, Ströbel B, Blüthgen N (2020) *Odontomachus davidsoni* sp. nov. (Hymenoptera: Formicidae), a new conspicuous trap-jaw ant from Ecuador. *ZooKeys* 948: 75–105. <https://doi.org/10.3897/zookeys.948.48701>
- ICZN [International Commission on Zoological Nomenclature] (1999) International code of zoological nomenclature. Fourth Edition. The International Trust for Zoological Nomenclature, London.
- Ilton M, Bhamla MS, Ma X, Cox SM, Fitchett LL, Kim Y, Koh J, Krishnamurthy D, Kuo C-Y, Temel FZ, Crosby AJ, Prakash M, Sutton GP, Wood RJ, Azizi E, Bergbreiter S, Patek SN (2018) The principles of cascading power limits in small, fast biological and engineered systems. *Science* 360(6387): eaao1082. <https://doi.org/10.1126/science.aao1082>
- International Code of Nomenclature (2020) International Code of Nomenclature (5<sup>th</sup> edn.), Article 31.1. <https://www.iczn.org/the-code/the-international-code-of-zoological-nomenclature/the-code-online/> [Accessed on 20 November 2020]
- Larabee FJ, Smith AA, Suarez AV (2018) Snap-jaw morphology is specialized for high-speed power amplification in the Dracula ant, *Mystridium camillae*. *Royal Society Open Science* (12): e181447. <https://doi.org/10.1098/rsos.181447>

- Larabee FJ, Suarez A (2014) The evolution and functional morphology of trap-jaw ants (Hymenoptera: Formicidae). *Myrmecological News* 20: 25–36.
- Lattke JE, Da Silva TSR, Delsinne T (2018) Taxonomy and natural history of *Strumigenys thaxteri* Wheeler and *Strumigenys reticeps* (Kempf) (Hymenoptera: Formicidae). *Zootaxa* 4438: 137–147. <https://doi.org/10.11646/zootaxa.4438.1.6>
- Lattke JE, Aguirre N (2015) Two new *Strumigenys* F. Smith (Hymenoptera: Formicidae: Myrmicinae) from montane forests of Ecuador. *Sociobiology* 62(2): 175–180. <https://doi.org/10.13102/sociobiology.v62i2.175-180>
- Longo SJ, Cox SM, Azizi E, Ilton M, Olberding JP, St Pierre R, Patek SN (2019) Beyond power amplification: latch-mediated spring actuation is an emerging framework for the study of diverse elastic systems. *Journal of Experimental Biology* 222: jeb197889. <https://doi.org/10.1242/jeb.197889>
- Masuko K (1984) Studies on the Predatory Biology of Oriental Dacetine Ants (Hymenoptera, Formicidae). 1. Some Japanese Species of *Strumigenys*, *Pentastruma*, and *Epitritus*, and a Malaysian *Labidogenys*, with Special Reference to Hunting Tactics in Short-Mandibulate Forms. *Insectes Sociaux* 31: 429–451. <https://doi.org/10.1007/BF02223658>
- Masuko K (2009) Studies on the predatory biology of Oriental dacetine ants (Hymenoptera: Formicidae) II. Novel prey specialization in *Pyramica benten*. *Journal of Natural History* 43: 825–841. <https://doi.org/10.1080/00222930802610543>
- Myers N, Mittermeier RA, Mittermeier CG, da Fonseca GAB, Kent J (2000) Biodiversity hotspots for conservation priorities. *Nature* 403(6772): 853–858. <https://doi.org/10.1038/35002501>
- Olson DM, Dinerstein E (1998) The Global 200: a representation approach to conserving the Earth's most biologically valuable ecoregions. *Conservation Biology* 12(3): 502–515. <https://doi.org/10.1046/j.1523-1739.1998.012003502.x>
- Richter A, Garcia FH, Keller RA, Billen J, Economo E, Beutel RG (2020) Comparative analysis of worker head anatomy of *Formica* and *Brachyponera* (Hymenoptera: Formicidae). *Arthropod Systematics & Phylogeny* 78(1): 133–170.
- Richter A, Keller RA, Rosumek FB, Economo EP, Garcia FH, Beutel RG (2019) The cephalic anatomy of workers of the ant species *Wasmannia affinis* (Formicidae, Hymenoptera, Insecta) and its evolutionary implications. *Arthropod Structure & Development* (49): 26–49. <https://doi.org/10.1016/j.asd.2019.02.002>
- Salazar F, Donoso DA (2013) New ant (Hymenoptera: Formicidae) records for Ecuador deposited at the Carl Rettenmeyer ant collection in the QCAZ Museum. *Boletín Técnico* 11, Serie Zoológica 8–9: 151–177.
- Salazar F, Reyes-Bueno F, Sanmartin D, Donoso DA (2015) Mapping continental Ecuadorian ant species. *Sociobiology* 62(2): 132–162. <https://doi.org/10.13102/sociobiology.v62i2.132-162>
- Sarnat EM, Hita Garcia F, Dudley K, Liu C, Fischer G, Economo EP (2019) Ready species one: exploring the use of augmented reality to enhance systematic biology with a revision of Fijian *Strumigenys* (Hymenoptera: Formicidae). *Insect Systematics and Diversity* 3(6): 6: 1–43. <https://doi.org/10.1093/isd/ixz005>
- Sarnat EM, Friedman NR, Fischer G, Lecroq-Bennet B, Economo EP (2017) Rise of the spiny ants: diversification, ecology and function of extreme traits in the hyperdiverse genus *Pheidole*

- (Hymenoptera: Formicidae). *Biological of the Linnaean Society* 122: 514–538. <https://doi.org/10.1093/biolinnean/blx081>
- Schindelin J, Arganda-Carreras I, Frise E, Kaynig V, Longair M, Pietzsch T, Preibisch S, Rueden C, Saalfeld S, Schmid B, Tinevez J-Y, White DJ, Hartenstein V, Eliceiri K, Tomancak P, Cardona A (2012) Fiji: an open-source platform for biological-image analysis. *Nature Methods* 9(7): 676–682. <https://doi.org/10.1038/nmeth.2019>
- Shorthouse DP (2010) SimpleMappr, an online tool to produce publication-quality point maps. <https://www.simplemappr.net> [Accessed July 03, 2020]
- Sierra R, Campos F, Chamberlin J (2002) Diversity conservation priorities: ecosystem risk and representativeness in continental Ecuador. *Landscape and Urban Planning* 59: 95–110. [https://doi.org/10.1016/S0169-2046\(02\)00006-3](https://doi.org/10.1016/S0169-2046(02)00006-3)
- Silva TSR, Feitosa RM (2019) Using controlled vocabularies in anatomical vocabulary: a case study with *Strumigenys*. *Arthropod Structure & Development* 52: e100877. <https://doi.org/10.1016/j.asd.2019.100877>
- Staab M, Garcia FH, Liu C, Xu ZH, Economo EP (2018) Systematics of the ant genus *Proceratium* Roger (Hymenoptera, Formicidae, Proceratiinae) in China – with descriptions of three new species based on micro-CT enhanced next-generation-morphology. *ZooKeys* 770: 137–192. <https://doi.org/10.3897/zookeys.770.24908>
- Ward PS, Brady SG, Fisher BL, Schultz TR (2014) The evolution of myrmicine ants: phylogeny and biogeography of a hyperdiverse ant clade (Hymenoptera: Formicidae). *Systematic Entomology* 40: 61–81. <https://doi.org/10.1111/syen.12090>
- Wesson LG, Wesson RG (1939) Notes on *Strumigenys* from southern Ohio, with descriptions of six new species. *Psyche* 46: 91–112. <https://doi.org/10.1155/1939/94785>
- Wilson EO (1953) The ecology of some North American dacetine ants. *Annals of the Entomological Society of America* 46: 479–495. <https://doi.org/10.1093/aesa/46.4.479>

## Supplementary material I

### *Strumigenys ayersthey* 3D pdf

Authors: Douglas D. Booher, Philipp O. Hoenle

Data type: 3D PDF file

Explanation note: 3D surface render of *Strumigenys ayersthey*. This is the same file as Figure 4.

Copyright notice: This dataset is made available under the Open Database License (<http://opendatacommons.org/licenses/odbl/1.0/>). The Open Database License (ODbL) is a license agreement intended to allow users to freely share, modify, and use this Dataset while maintaining this same freedom for others, provided that the original source and author(s) are credited.

Link: <https://doi.org/10.3897/zookeys.1036.62034.suppl1>

## Supplementary material 2

### *Strumigenys ayersthey* apodeme attachments

Authors: Douglas B. Booher, Philipp O. Hoenle

Data type: PNG image

Explanation note: Highlight of *Strumigenys ayersthey* apodome attachments from one slice from the  $\mu$ CT scan.

Copyright notice: This dataset is made available under the Open Database License (<http://opendatacommons.org/licenses/odbl/1.0/>). The Open Database License (ODbL) is a license agreement intended to allow users to freely share, modify, and use this Dataset while maintaining this same freedom for others, provided that the original source and author(s) are credited.

Link: <https://doi.org/10.3897/zookeys.1036.62034.suppl2>



# Two new species of *Archaeopodagrion* (Odonata, Philogeniidae) from the western foothills of the Tropical Andes, with biological observations and distributional records

Vanessa Amaya-Vallejo<sup>1,2</sup>, Cornelio Bota-Sierra<sup>3,4</sup>,  
Rodolfo Novelo-Gutiérrez<sup>3</sup>, Melissa Sánchez-Herrera<sup>1,2</sup>

**1** Laboratorio de Zoología y Ecología Acuática, Universidad de los Andes, Bogotá DC, Colombia **2** Grupo de investigación en Genética Evolutiva, Filogeografía y Ecología de Biodiversidad Neotropical, Universidad del Rosario, Bogotá DC, Colombia **3** Red de Biodiversidad y Sistemática, Instituto de Ecología AC, Xalapa, Veracruz, México **4** Grupo de Entomología, Universidad de Antioquia, Medellín, Antioquia, Colombia

Corresponding authors: Vanessa Amaya-Vallejo ([v.amaya10@uniandes.edu.co](mailto:v.amaya10@uniandes.edu.co));  
Melissa Sanchez-Herrera ([melsanc@gmail.com](mailto:melsanc@gmail.com))

---

Academic editor: N. von Ellenrieder | Received 10 February 2021 | Accepted 16 March 2021 | Published 5 May 2021

<http://zoobank.org/4AEAB9EA-D40F-4A08-8029-63A6ACDAE262>

---

**Citation:** Amaya-Vallejo V, Bota-Sierra C, Novelo-Gutiérrez R, Sánchez-Herrera M (2021) Two new species of *Archaeopodagrion* (Odonata, Philogeniidae) from the western foothills of the Tropical Andes, with biological observations and distributional records. ZooKeys 1036: 21–38. <https://doi.org/10.3897/zookeys.1036.64230>

---

## Abstract

Two new species of the damselfly genus *Archaeopodagrion*, *A. recurvatum* **sp. nov.** and *A. mayi* **sp. nov.**, are described from the confluence of the Tropical Andes and the Tumbes-Chocó-Magdalena biodiversity hotspots. Adults differ from the other known species in the shape of female posterior lobe of pronotum and male structures of cerci and paraprocts; the larva differs from other *Archaeopodagrion* species in the caudal lamellae structure and in the mandibular formula. The two new species are diagnosed, a morphological key to all known males and females in the genus is provided, and geographical distributions are updated. Finally, observations on habitat preferences for each newly described species are provided.

## Keywords

Biodiversity hotspots, Colombia, damselfly, Ecuador, female, larva, male

## Introduction

*Archaeopodagrion* is a genus of Neotropical damselflies endemic to the rainforests of the Tropical Andes and the Tumbes-Chocó-Magdalena biodiversity hotspots. This genus has been poorly known; for a long time only the type species *A. bicorne* Kennedy, 1939 and the elusive *A. bilobatum* Kennedy, 1946 were reported from Ecuador, but in the last decade two more species were described: *A. armatum* Tennessen & Johnson, 2010 from southern Ecuador, and *A. fernandoi* Bota-Sierra, 2017 from Colombia, extending the distributional range of the genus almost 700 km north along the Andes.

Here, two new species of *Archaeopodagrion* from localities in Colombia and Ecuador are presented, extending the distribution of the genus further north within the western Andean foothills. Morphological descriptions accompanied with photographs of the diagnostic traits for both species are provided. Additionally, two updated keys for the adults of the known species of *Archaeopodagrion*, one for males (6 spp.) and another one for females (4 spp.) are presented. For *A. recurvatum* sp. nov. the morphological description of the penultimate instar larva is also provided. Besides the morphological descriptions, biological notes, a new distribution map, and some taxonomic remarks are offered, thus adding to the known diversity of this rare genus.

## Materials and methods

Male and female adults and a female larva were collected for *A. recurvatum* but only male adults were collected for *A. mayi*. The F-1 (penultimate instar) larva was preserved in 80% ethanol, the adults were steeped in 96% ethanol for twelve hours and then dried. Specimens are deposited in the ANDES Entomology Museum, Universidad de Los Andes, and the CEUA Entomology Museum, Universidad de Antioquia.

Photographs of morphological structures were taken with a Nikon DS-U3 camera mounted on a Nikon SMZ25 stereomicroscope, and processed with the program NIS elements AR version 4.5. Descriptions were made by examining specimens under a Zeiss Stemi SV6 stereomicroscope, and measurements (in mm) taken with an ocular micrometer and a ruler. Wing nomenclature follows Riek and Kukalová-Peck (1984). Mandible nomenclature follows Watson (1956); labium nomenclature follows Corbet (1953). Wing measurements follow Bechly (1996) and head measurements follow Tennessen (2017). Abbreviations are as follows:

- AL** Abdomen length: maximum length of the abdomen, measured from the first (S1) to the 10<sup>th</sup> abdominal segment (S10) and including the caudal appendages (cerci and paraprocts), in dorsal view;
- FWL** Forewing (FW) length: maximum length of the forewing, measured from the first cross-vein (ax0) to the furthest point of the wing tip;
- HWL** Hindwing (HW) length: maximum length of the hindwing, measured from the first cross-vein to the furthest point of the wing tip;

<b>WHW</b>	Hindwing width: maximum width of the hindwing, measured from the nodus to the furthest point of the wing's posterior edge;
<b>HFL</b>	Hind femur length: maximum length of the hind femur in lateral view;
<b>HWd</b>	Head width: maximum width of the head, measured across compound eyes in dorsal view;
<b>PtL</b>	Pterostigma (Pt) length;
<b>Px</b>	Postnodal crossveins;
<b>CL</b>	Cercus length: maximum width of the cercus, measured from the insertion in S10 to the furthest point of the cercus tip in dorsal view;
<b>S1–10</b>	Abdominal segments;
<b>TL</b>	Total length: maximum length of the specimen, measured from the furthest edge of the labrum to the 10 <sup>th</sup> abdominal segment (S10) including the caudal appendages (cerci and paraprocts), in dorsal view;
<b>PpL</b>	Paraproct length: maximum length of the paraprocts, measured from the insertion in S10 to the furthest point of the paraproct tip in dorsal view;
<b>EpL</b>	Epiproct length: maximum length of the epiproct, measured from the insertion in S10 to the furthest point of the epiproct tip in dorsal view.

## Depositories

<b>ANDES-E</b>	Entomology collection, Natural History Museum, Universidad de Los Andes, Bogotá, Cundinamarca, Colombia;
<b>CEUA</b>	Entomology collection, Universidad de Antioquia, Medellín, Antioquia, Colombia.

## Results

### *Archaeopodagrion recurvatum* sp. nov.

<http://zoobank.org/1E28E29E-1352-494F-B77B-6A7DF0E24E44>

Figures 1–6

**Type material. Holotype:** 1 adult male, Colombia, Valle del Cauca Department, Dagua Municipality, Farallones Natural National Park, Alto Anchicayá, La Riqueza stream, 3.6094167°N, 76.8845°W, 670 m, taken with aerial net while perched in riparian vegetation, 4 February 2020, VAV and MSH leg. (ANDES-E). **Paratypes:** 1 male, 1 female as teneral, same data as holotype; 1 F-1 female larva, same data as holotype, D-net, sand/pebbles bottom in shallow La Riqueza stream bank, but collected 9 July 2016, VAV leg. (ANDES-E). 1 teneral male, 1 adult female, Colombia, Risaralda Department, Santa Cecilia, Alto Amurrapá Reserve, Ranas de Cristal stream, 5.32033°N, 76.17357°W, 620 m, taken with aerial net while perched in riparian vegetation along stream, 31 January 2017, CBJ and JSH leg. (CEUA).

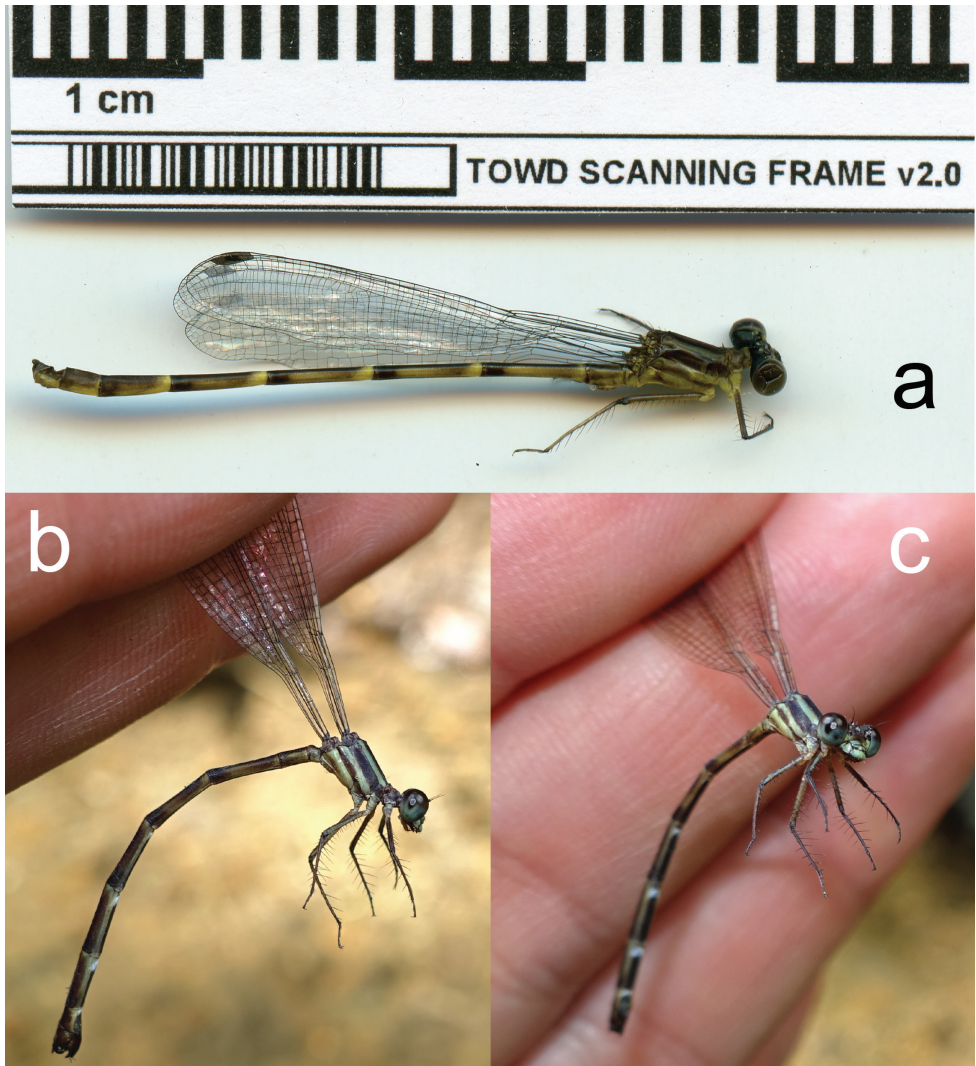


**Figure 1.** Full body lateral scans and photographs of *Archaeopodagrion recurvatum* **A** male holotype **B** and **C** female paratype. Scale bar: 1 cm.

**Diagnosis.** *Archaeopodagrion recurvatum* lacks the tubercle bearing a hair pencil on the midlength of each paraproct and also lacks a well-developed internal tooth on the cercus, a character present only in *A. bilobatum* and *A. bicorne*. Among the females, *A. recurvatum* differs from the other three females described (females of *A. bilobatum* and *A. mayi* are unknown) by the unique shape of the posterior lobe of the pronotum (Fig. 3B, C). The larvae of *A. recurvatum* lacks the fleshy tubercles or spiniform setae present in the caudal lamellae of *A. fernandoi*; also *A. recurvatum* has a slenderer body than *A. fernandoi* and a different mandibular formula, since the molar crest in the left mandible of *A. recurvatum* possesses twice as many teeth as in *A. fernandoi*. The adults of *A. recurvatum* are also the smallest of the genus (male total length 35.0–38.0 mm,

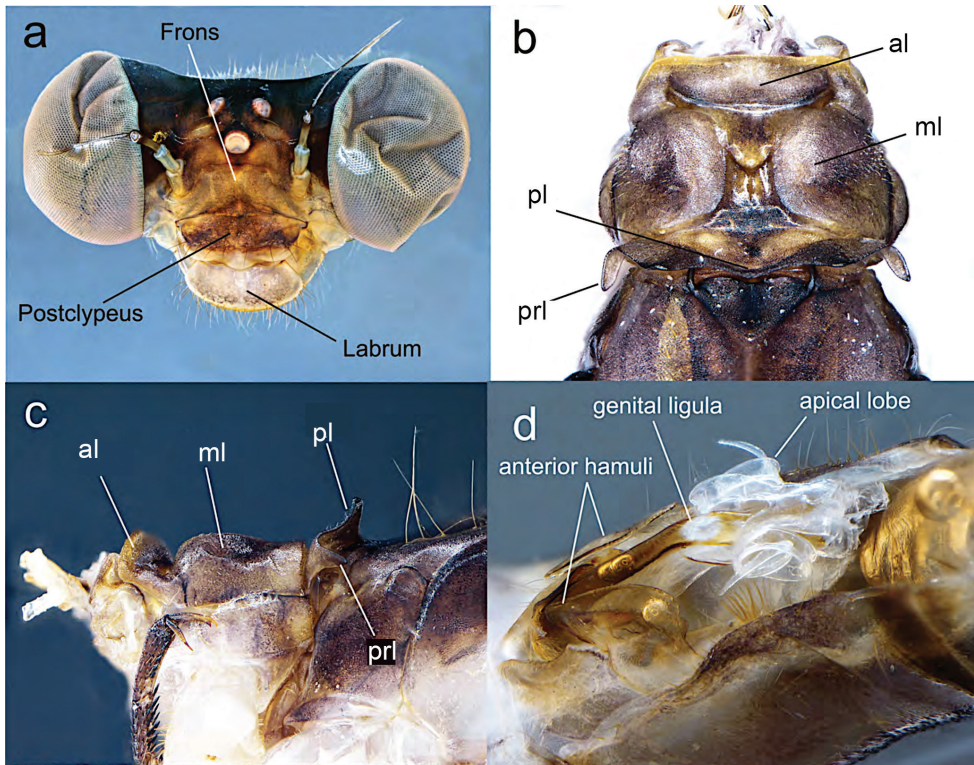


**Figure 2.** Diagnostic characters of male holotype of *Archaeopodagrion recurvatum* **A** head, frontal view **B** pronotum, dorsal view **C** pronotum, lateral view **D** genital ligula. Abbreviations: anterior lobe (al), middle lobe (ml), posterior lobe (pl), pronotal lobe (prl).

female 34.0 mm), with the average length in the genus ranging from 37.5 mm for males and 36.5 mm for females in the smaller known specimens of *A. armatum*, to 45.0 mm for males and 42.0 mm for females in *A. fernandoi* (Kennedy 1946; Tennessen and Johnson 2010; Bota-Sierra 2017).

**Description. Male holotype.** Small-sized damselfly, thorax brown with pale yellow stripes, abdomen brown with pale yellow spots, cerci in dorsal view conspicuously recurved, paraproct tips upturned, with tips contacting distal margin of cerci (Fig. 1A–C). **Measurements:** holotype: TL 35; AL 28.1; FWL 21.2; HWL 20.9; WHW 2.3; FW PtL 1.1; HW PtL 1.2; HWd 4.6; HFL 4. Risaralda paratype: TL 38; AL 30; FWL 24; HWL 23.1; WHW 2.3; FW PtL 1.2; HW PtL 1.5; HWd 5.1; HFL 4. **Head:** eyes in life dark gray, with black borders; labium grayish brown, dark brown medially, with long pale setae; labrum and anteclypeus yellow, postclypeus brown, frons grayish brown; vertex, occiput and rear of head black, anterior and postero-dorsal surface of vertex and occiput with sculptured surface that refracts light producing green to red metallic colors; some scattered, dark brown setae on dorsum of head; occiput straight, dark brown with long, brown setae along entire width; antennae dark brown except base, basal half of first antennomere pale yellow (Fig. 2A). **Thorax:** prothorax light

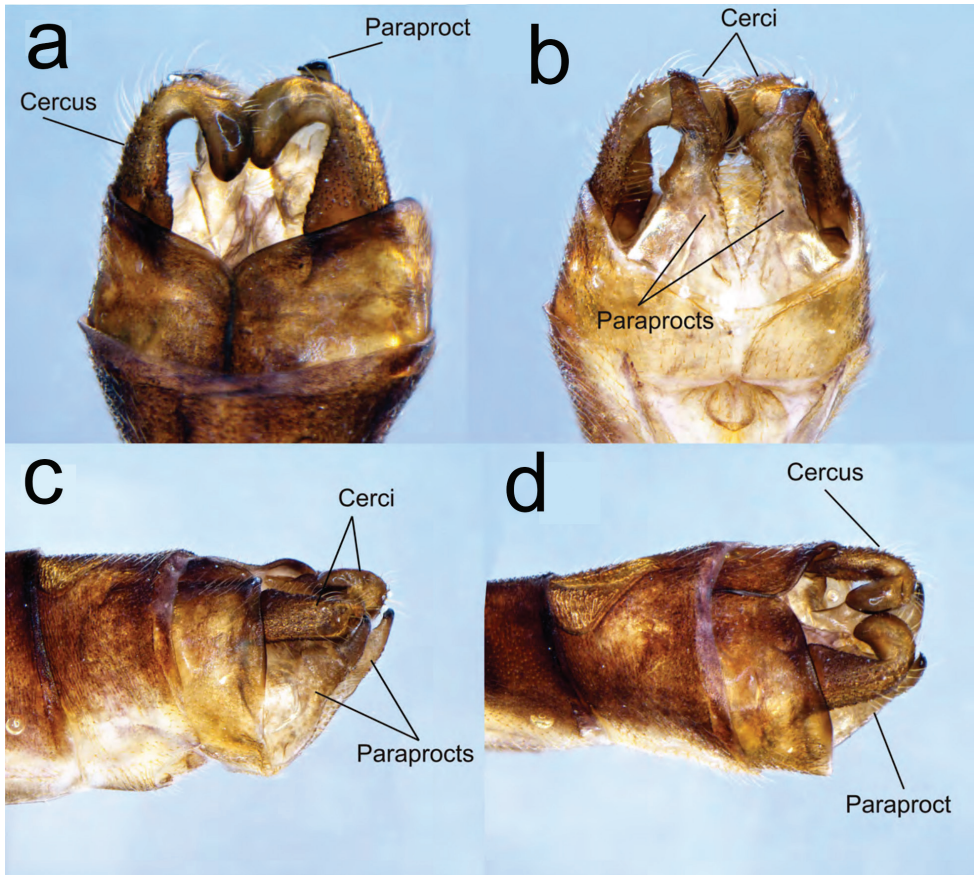


**Figure 3.** Caudal appendages of teneral male paratype of *Archaeopodagrion recurvatum* **A** dorsal view **B** ventral view **C** lateral view **D** dorsolateral view. Caudal appendages might show postmortem distortions.

brown. Anterior lobe strongly convex in lateral view, middle and posterior lobes with a deep medial depression, pronotal lobe prolonged laterally into trapezoid processes with a conspicuous spine directed toward mesinfraepisternum (Fig. 2B, C). Middorsal carina of pterothorax brown, mesepisternum brown with a yellowish wide stripe reaching humeral suture. Mesinfraepisternum and mesepimeron brown, metepisternum yellowish along the anterior half, becoming light brown near wing base; metinfraepisternum brown near metepisternum, the posterior half yellowish. Metepimeron yellow, with a slight brown stripe below metathoracic suture. Venter of thorax and coxae yellowish, femora, tibia and claws tan brown. Leg spines 2–4 times longer than spaces between bases of adjacent spines, these spaces increasing distally. Wings hyaline; Px 16–17 in FW, 15–16 in HW; Pt surmounting two to two and a half cells, dark brown with very narrow pale edges next to enclosing veins (Fig. 1A). **Abdomen:** S1–2 completely light brown; S3–7 light brown dorsally with narrow basal pale-yellow mark connecting to yellow lateral mark and then forming a yellow triangular mark reaching ventral side in S7–8. S9–10 dark brown dorsally, slightly yellow ventrally, S10 with a conspicuous

central cleft (Fig. 2A). Genital ligula with two lateroapical recurved flagella as in other species described for the genus (Fig. 2D). Cerci light brown, strongly recurved medio anteriorly with tips touching, giving a heart-shaped appearance, armed with some small denticles along inner margins; paraprocts in lateral view slightly longer than cerci but with divergent acuminate apex strongly recurved dorsally and armed with a small, blunt tooth at the tip (Fig. 3A–D).

**Female paratype. Measurements:** TL 34; AL 26.8; FWL 22; HWL 21.1; WHW 7.1; FW PtL 1.1; HW PtL 1.2; HWd 5.1; HFL 4. **Head:** black except: labium pale yellow; labrum mandible base, genae and anteclypeus yellowish blue; postclypeus greyish brown with two yellow spots; antefrons greyish brown, postfrons brown, both with sculptured surface which extends to foramen except for lustrous space between antennae base and eyes, two yellowish blue elongated spots between antenna base and each lateral ocellus; antennae dark brown, base and basal half of first antennomere pale yellow; postocular lobe slightly protruding posteriorly beyond level of hind margin of compound eye, paraorbital carina distinct (Fig. 4A). **Thorax:** brown with antehumeral and metepisternal yellowish blue stripe, metepimeron pale yellow with a slight brown stripe below metathoracic suture (Fig. 1B, C). Posterior lobe of pronotum convex laterally with a small, angled projection (Fig. 4B, C). Metathoracic legs missing, coxae yellowish blue, femora dark brown externally and yellowish blue internally, tibiae and tarsi brown, armature brown. Eight spurs on the external side of right mesofemur and seven on left mesofemur, each as long as space between them or shorter, gradually increasing in size toward the apex. Eight spurs on the anterior side of right mesotibia and seven on left mesotibia, longer than the spaces between them and gradually decreasing in size toward apex. Tarsal claws with a supplementary tooth. Wings smoky. Pt dark brown surmounting two to two and a half cells, Px 18 in FW and 16 in HW. **Abdomen:** dark brown except light brown sides of S1–2, apical incomplete rings from S3 to S7 connected to ventrolateral stripes, and S8 ventrolateral stripe. Genital valves brown, internal edges of gv1 and gv2 serrulated, gv3 and gv4 with a large triangular process over the base of long and slender black styli (Fig. 4D).

**Larva.** Penultimate instar F-1, medium size for Zygoptera. Body mostly glabrous, light brown to yellowish; antennae long, light brown. Head large, flattened, abdomen convex dorsally, flattened ventrally. Caudal lamellae saccoid, violaceous, with a long, pale terminal filament. **Measurements:** TL 13; AL 6; HWd 2; HFL 3; Ep 3.9; Pp 3.5. **Head:** yellowish brown, almost as wide as long, subhexagonal. Labrum brown, mostly covered by minute spinules, with a large, glabrous, oval, median area and anterior margin widely emarginate medially, with a row of long, white setae as described for *A. fernandoi* (Novelo-Gutiérrez et al. 2020). Clypeus light yellow, with few setae. Frons large, yellowish brown, flat, very finely rugose. Vertex flat, dark brown, with three large white ocelli. Antennae long, 7-segmented, glabrous, all segments yellowish brown, scape barrel-shaped, thicker, pedicel cylindrical, antennomere 3 longest, antennomere 7 shortest, size proportions: 0.30, 0.37, 1.0, 0.55, 0.39, 0.20, 0.10; compound eyes large, not bulging, ventrolateral margin covered with a row of short setae, occiput large, cephalic lobes quadrangular; external margins covered with longitudinal rows of minute spines; occipital margin widely concave (Fig. 5A). Mandibles

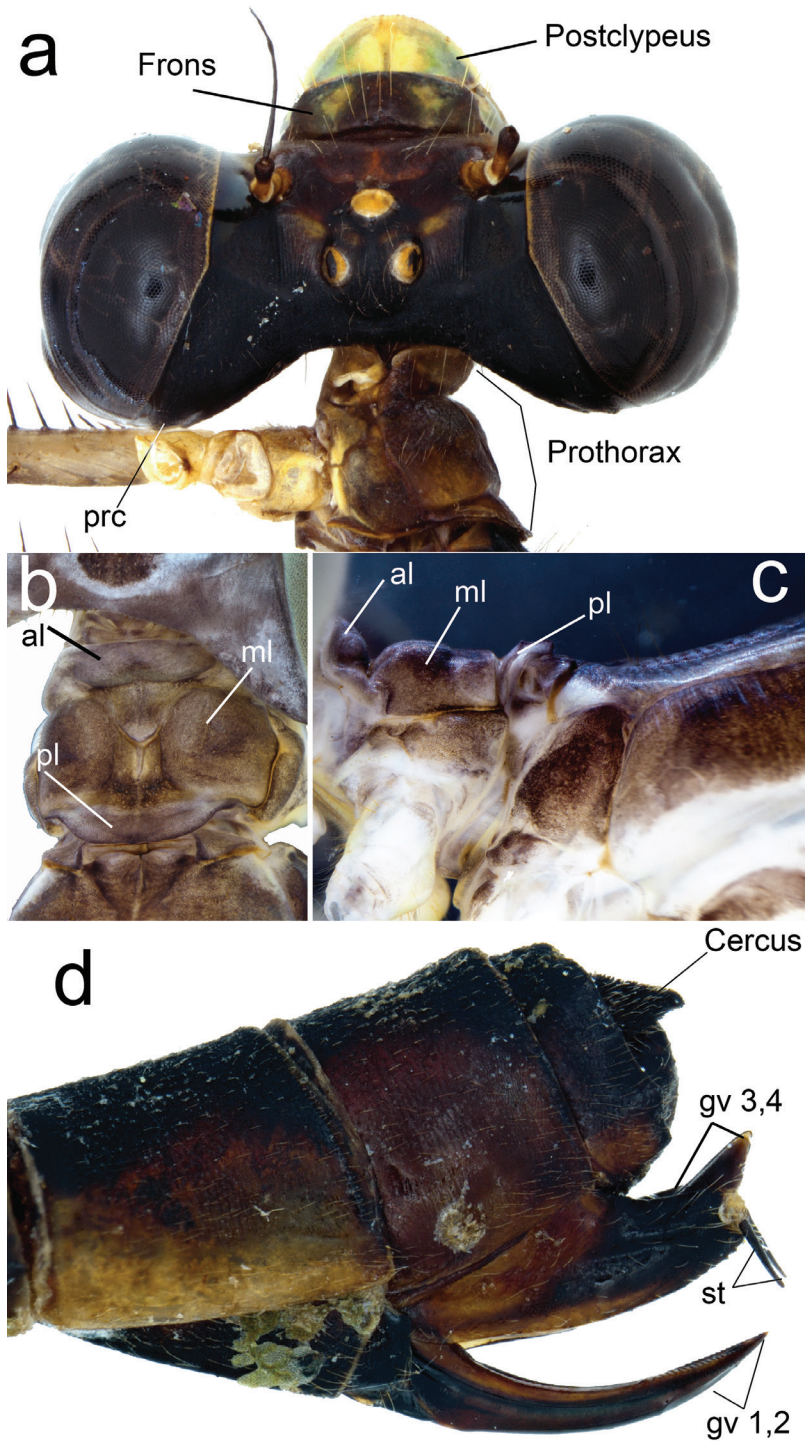


**Figure 4.** Diagnostic characters of female paratype of *Archaeopodagrion recurvatum* **A** head, dorsal view **B** pronotum, dorsal view **C** pronotum, lateral view **D** ovipositor, lateral view. Abbreviations: anterior lobe (al), genital valvae (gv), middle lobe (ml), posterior lobe (pl), paraorbital carina (prc), styli (st).

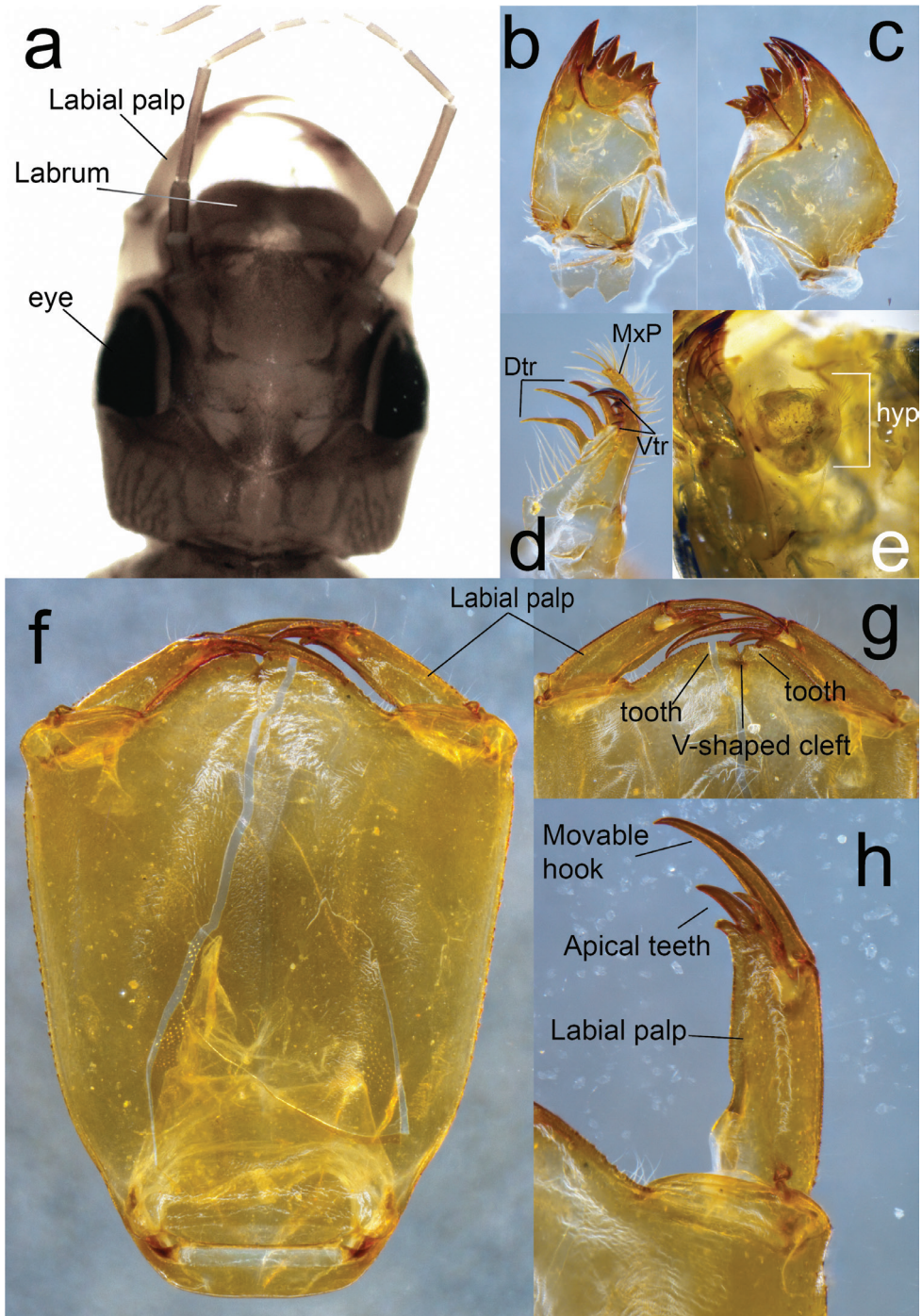


**Figure 5.** Diagnostic characters of F-1 larva of *Archaeopodagrion recurvatum* **A** head, dorsal view **B** right mandible, lateral view **C** left mandible, lateral view **D** galeolacinia, lateral view **E** hypopharynx, dorsal view **F** ligula, ventral view **G** close up of the medial cleft of the ligula, ventral view **H** detail of the labial palp, ventral view. Abbreviations: dorsal teeth (Dtr), hypopharynx (hyp), maxillary palp (MxP), ventral teeth (Vtr).

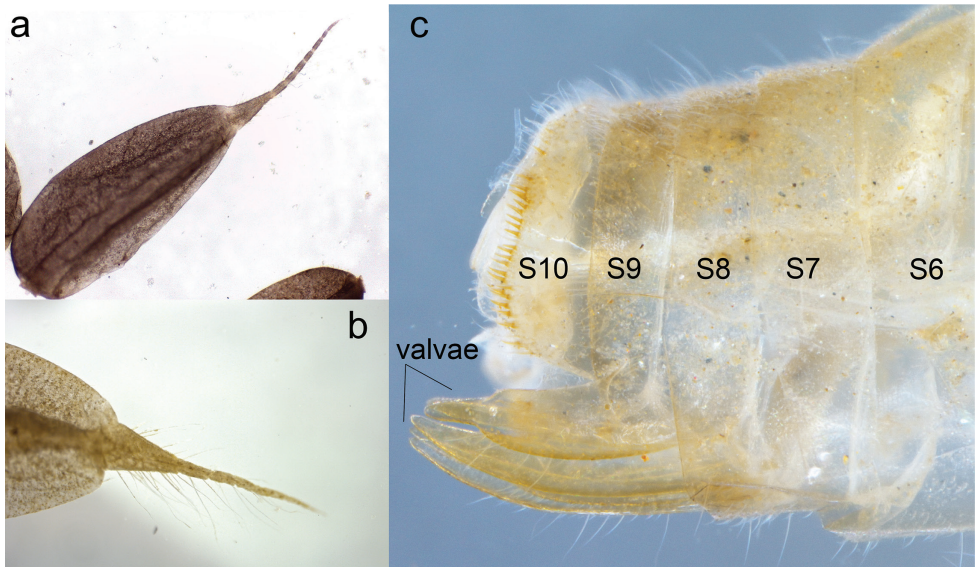


**Figure 6.** Diagnostic characters of F-1 larva of *Archaeopodagrion recurvatum* **A** epiproct, dorsal view **B** paraproct, dorsal view **C** last segments of the abdomen, lateral view.

(Fig. 5B, C) with a movable molar crest, strongly carinate along ventro-lateral margin, baso-lateral margins covered with stout, short spines; formula: R 1+2345 y a ( $m^1$ ) b, L1+2345 0 a ( $m^4$ ) bd,  $a > b$  in both mandibles. Galeolacinia (Fig. 4D) with seven teeth, three dorsal teeth of similar length and robustness, all of them slightly incurved, four ventral teeth with similar sizes and robustness, apical tooth the largest, the basal tooth preceded by a row of approximately six short stiff setae; maxillary palp setose, slightly incurved, ending in a spine shorter than apical tooth of Galeolacinia. Hypopharynx (Fig. 5E) trapezoid, slightly sclerotized, pale yellow, with the distal rounded corners bearing a conspicuous row of long, anteriorly directed white setae; anterior margin slightly rounded, posterior margin slightly concave, shorter. Labium: prementum-postmentum articulation nearly reaching posterior margin of procoxae. Prementum yellow, subrectangular,  $0.43 \times$  longer than its widest part, glabrous, shiny, lateral margins finely serrulate, subparallel, gradually converging basally; ligula convex, prominent, distal margin finely serrulated with a short V-shaped median cleft, a minute spine on each side of cleft in dorsal view; labial palp yellow, large, parallel-sided, lateral margin with some short spines on basal third, mesial margin smooth, apical lobe short, ending in three short hooks of different sizes, median hook largest, internal hook shortest; movable hook brown, slightly incurved, sharply-pointed, almost as long as labial palp (Fig. 5F). **Thorax:** narrower than head, covered with minute setae. Pronotal disc light brown, anterior margin slightly concave, lateral margins strongly produced medially, forming a pronounced, almost acute-angled convexity; posterior margin convex; propleuron spiny, ventral margin widely V-shaped. Pterothorax pale brown with wide, irregular dark-brown spots, ventral margin of mesopleuron ser-

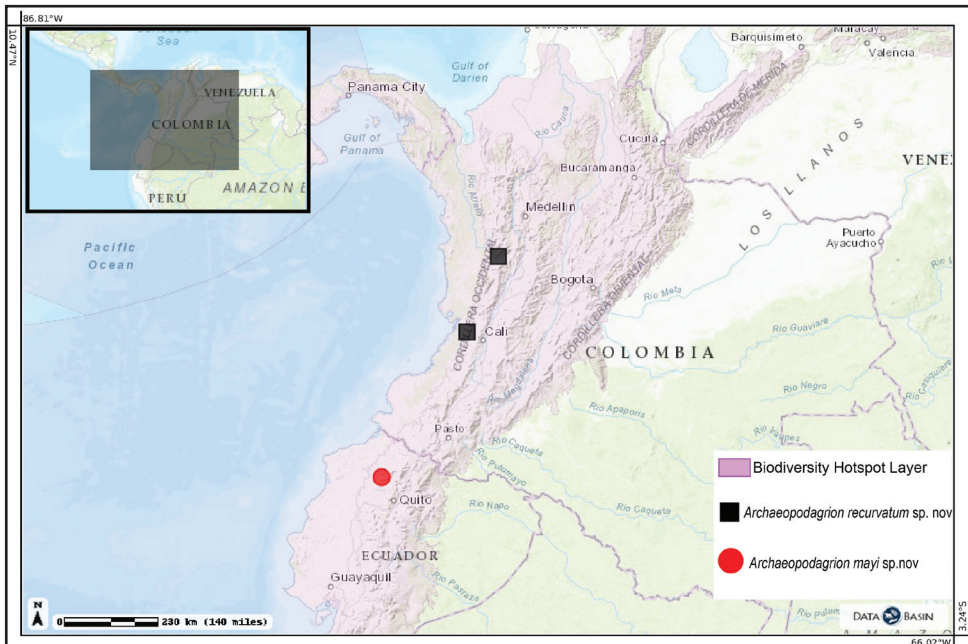


**Figure 7.** Distribution map for the new species of *Archaeopodagrion*. Black dots represent type localities.

rate. Legs long, yellowish brown, fore legs darker. Femora granulose, tibiae setose. Tarsi pale, with a ventral, longitudinal double row of spiniform setae; tarsal claws simple, all with pulvilliform empodium. Anterior and posterior wing sheaths slightly divergent, reaching the basal half and posterior margin of S4, respectively. **Abdomen:** convex dorsally, flat ventrally, slightly narrowing posteriorly. Tergum including posterior margins of S1–10 light brown, covered with minute white setae. Sternum bare, creamy pale. S3–5 distorted, the female gonapophyses surpassing well beyond posterior margin of S10, lateral valvae creamy-pale, ventrally setose, central valvae yellow, smooth, longer, all roundly pointed (Fig. 6C), as in *A. fernandoi* (Novelo-Gutiérrez et al. 2020). Cerci not visible. Caudal lamellae pale violet, saccoid, with abundant, long white setae on dorsum, with a long pale, setose, gradually tapering terminal filament. Epiproct (Fig. 6A) lacking fleshy tubercles or spiniform setae along midline; terminal filament divided into 7 segments, almost 1/3 shorter than the saccoid portion length of epiproct. Paraproct (Fig. 6B) without fleshy tubercles or spiniform setae; terminal filament shorter than saccoid portion length of epiproct, divided into seven segments covered with long, white setae. S8–9 bearing genital valvae (Fig. 6C).

**Distribution.** Known only from the holotype and paratype localities on the western slope foothills of the West Andean Cordillera at the Colombian departments of Risaralda and Valle del Cauca (Fig. 7).

**Etymology.** Named *recurvatum* (from the Latin *recurvatum*: curved inwards, with tips that are directed back to the point of origin) due to the peculiar structure of the male's cerci.

***Archaeopodagrion mayi* sp. nov.**

<http://zoobank.org/65471F12-C179-47E5-8114-9514E5458214>

Figures 8–10

**Type material.** *Holotype*: 1 adult male, and 1 adult male *paratype*, both Ecuador, Imbabura Province, Reserva Natural Los Cedros, near Cascada Vieja Trail, 0.308986°N, 78.779328°W, 500 m, taken with aerial net while perched in lianas hanging from a small stream canyon wall, 4 December 2013, MSH leg. (ANDES-E).

**Diagnosis.** The males of *Archaeopodagrion mayi* are medium-sized, with total length ranging from 40.0 to 43.0 mm. They present a tubercle bearing a hair pencil on the midlength of each paraproct, a character shared with the males of *A. armatum* and *A. fernandoi*, and lack a well-developed internal tooth on cercus, a character shared only with *A. recurvatum*.

**Description.** **Male holotype.** Medium-sized damselfly, thorax brown with greenish yellow stripes, abdomen dark brown dorsally and light brown ventrally, with greenish yellow pale spots (Fig. 8). Abdominal appendages with characteristic morphology, comprising cylindrical cerci with tips directed posteroventrally, longer than paraprocts, and paraprocts with tips acute and directed dorsally (Fig. 10A–D). **Measurements:** holotype: TL 40; AL 34.1; FWL 26.5; HWL 25; WHW 2.5; FW PtL 1.2; HW PtL 1.5; HWd 4.1; HFL 4; CL 2. Paratype: TL 43; AL 36; FWL 26.5; HWL 25; WHW 2.3; FW PtL 1; HW PtL 1.3; HWd 4.1; HFL 4; CL 1.8. **Head:** eyes brown; head black except: labium, labrum mandible base, genae, and anteclypeus pale greenish yellow; labium and labrum with long, pale setae; postclypeus greyish yellow, antefrons and postfrons dark brown, both with sculptured surface except lustrous space between antennae base and eyes and extending to occipital foramen; antennae dark-brown except pale yellow base, postocular lobe slightly protruding posteriorly beyond level of hind margin of compound eye, paraorbital carina distinct (Fig. 9A). **Thorax:** prothorax bright yellow with brown spots, pterothorax brown with antehumeral and metepisternal yellow

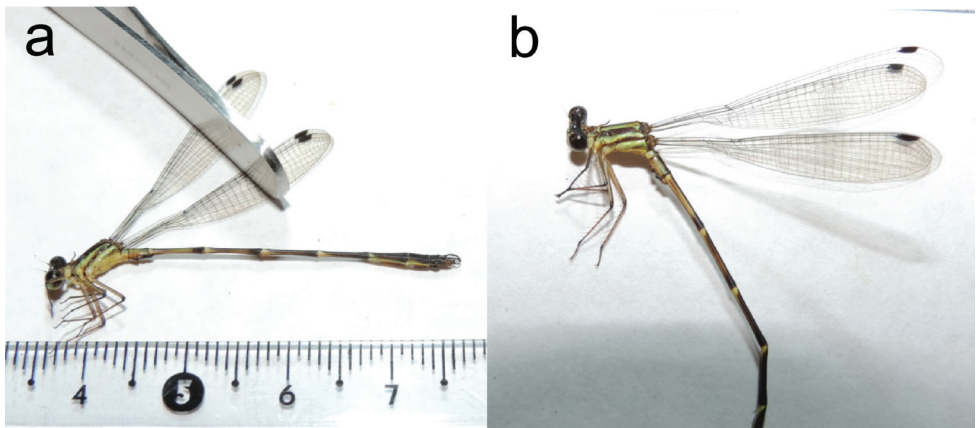


**Figure 8.** Full body lateral photographs of *Archaeopodagrion mayi* **A** male holotype **B** male holotype head and thorax closeup. Scale bar: 1 cm.

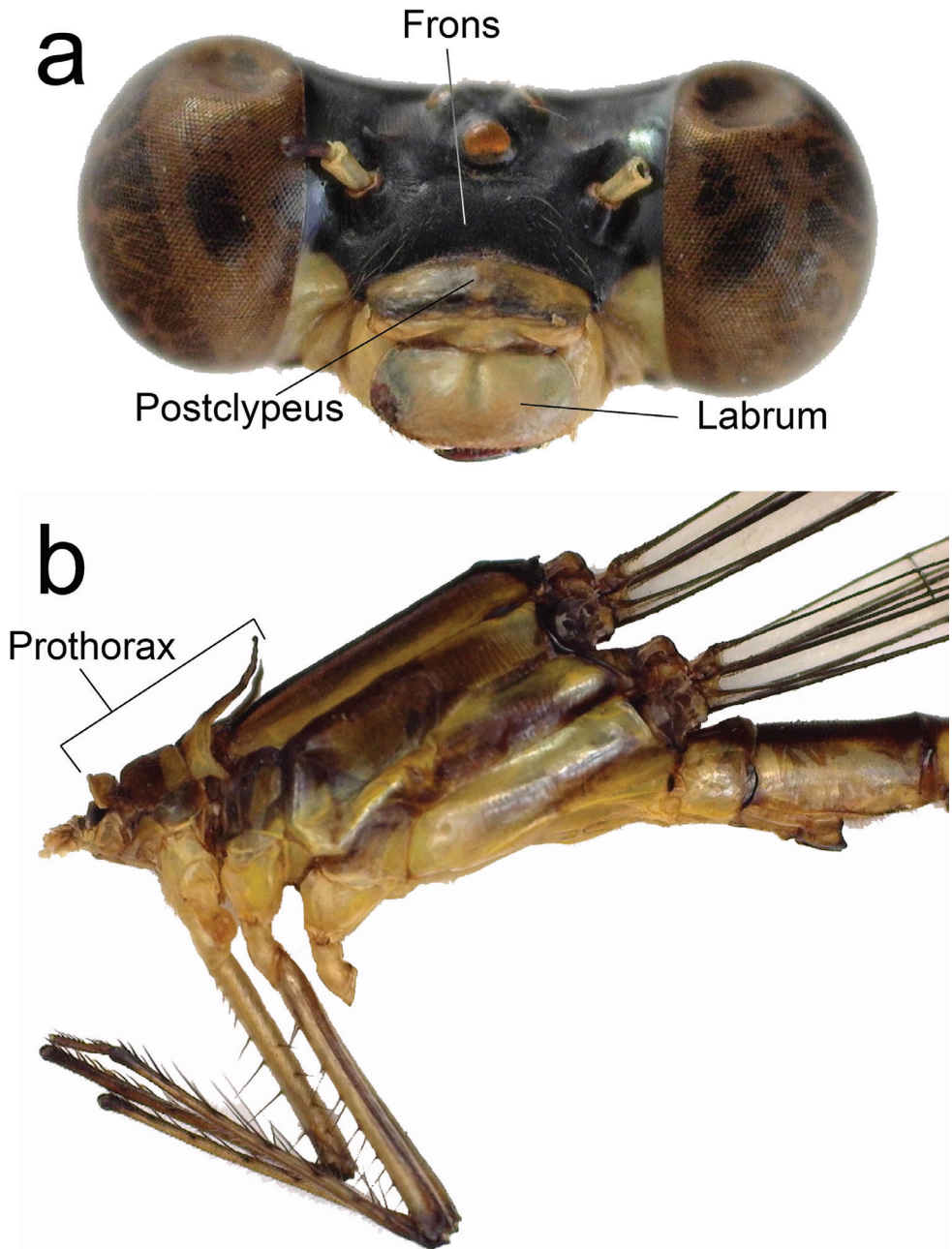


**Figure 9.** Diagnostic characters of male holotype of *Archaeopodagrion mayi* **A** head, frontal view **B** thorax, lateral view.

stripe, metepimeron brown with a yellow stripe below metathoracic suture (Figs 8B, 9B). Anterior lobe of the prothorax subquadrate, middle lobes arcuate medially (Fig. 10A), the posterior lobe of pronotum convex, prolonged laterally into two pairs of processes: one on superior margin and the other on inferior margin; superior pro-

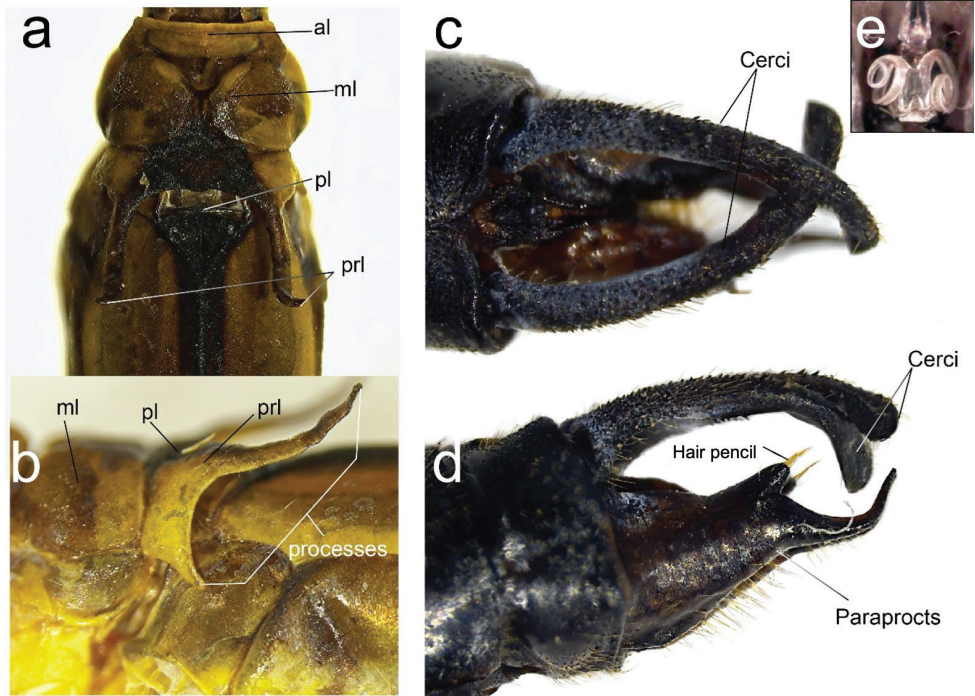


**Figure 10.** Diagnostic characters of male holotype of *Archaeopodagrion mayi* **A** pronotum, dorsal view **B** pronotum, lateral view **C** caudal appendages, dorsal view **D** caudal appendages, lateral view **E** genital ligula, ventral view. Caudal appendages might show postmortem distortions. Abbreviations: anterior lobe (al), middle lobe (ml), posterior lobe (pl), pronotal lobe (prl).

cesses long, curved dorsoposteriorly, their tips blunt and extending over a third of the pterothorax; inferior processes shorter, less than half the length of superior processes, and extending posteroventrally (Fig. 10B). Venter of thorax and coxae yellow, femora dark brown externally and pale brown internally, tibiae, tarsi and armature brown. Leg spines 2–3 times longer than spaces between bases of adjacent spines, interval between spurs subequal along all legs. Tarsal claws with supplementary tooth. Wings hyaline. Pt dark brown surmounting two to two and a half cells, ratio between distal and proximal length approximately 1:1. Px 18 in FW and 16 in HW. **Abdomen:** dark brown, S1 and S2 with yellow lateral stripes, S3–7 dark brown dorsally with narrow basal yellow ring connecting laterally to yellow stripe along ventral side in S7 and S8. S9 and S10 dark brown (Fig. 8). Cercus cylindrical, covered with denticles and scattered short setae, in lateral view longer than paraproct (Fig. 10C, D); paraprocts in lateral view with a strong ventral tubercle located at midlength, the tubercle bearing a conspicuous hair pencil apically, tips of paraprocts recurved, acute, hook shaped (Fig. 10D). Genital ligula with two lateroapical recurved flagella as in the other species described for the genus.

**Distribution.** Known only from the holotype and paratype locality in the western foothills of the Ecuadorian Andes in Imbabura Province (Fig. 7).

**Etymology.** Named *mayi*, an adjective in the genitive case, after Dr. Michael L. May for his great contributions on the study of odonates, whose work ranges from basic taxonomy and systematics to complex ecological and physiological questions related to migratory patterns and to the body temperature regulation of dragonflies. Dr. May has established the foundation for many research topics in Odonatology and has supported the development of several odonatologists and their research.

### Biological observations

The specimens of *A. recurvatum* were collected at two different locations with similar characteristics along the Colombian Western Andean foothills, where the climate is tropical, with temperatures ranging from 22 °C to 27 °C, high precipitation (> 3000 mm per year [Pravettoni 2019]) and tropical rainforest as the predominant vegetation. They were found on small to medium-sized fast flowing streams, with sand and gravel substrates surrounded by a mix of boulders and exposed bedrocks, interspersed with waterfalls, pools and rapids, within primary and undisturbed forests. The waters were clear, clean, and highly oxygenated. *Archaeopodagrion recurvatum* coexisted there with damselflies of other families such as Heteragrionidae, Polythoridae, and Platystictidae. Those streams are highly dependent on precipitation: during the wet season, the stream water level can increase 0.50 to 1.0 m, decreasing in the same proportion during the dry season. When the waters recede, apparently there are more available spaces for adults to emerge, using semi-submerged large stones and sticks as attachment substrate. Amaya-Vallejo (2009) identified odonate assemblages associated with different habitats within the Anchicayá zone, thus classifying most of the species inhabiting the previously described streams as stenoecious, or able to live only in a restricted range of habitats.

*Archaeopodagrion mayi* was collected at Los Cedros Natural Reserve in Ecuador. This reserve is located in the southernmost area of the Cordillera de la Plata, lying on the western side of the Andes mountains. The temperature generally fluctuates between 16–25 °C and the humidity can be as high as 100% due to the high level of precipitation (> 3000 mm per year [Pravettoni 2019]). The dominant type of vegetation is tropical rainforest. The specimens were found in a swampy trail left by a stream located inside a small canyon; the walls were covered with long roots and lianas. Both males were perching at the end of these roots, with their wings open as in individuals of *Heteragrion* and somewhat resembling females of this genus. The collection trip occurred right after the dry season and the climatic conditions were similar to the ones in the Colombian locations. The stream water level may have been reduced and *A. mayi* may have the same emergence habits as *A. recurvatum*. Polythoridae and Heteragrionidae were collected at the same place and considering the characteristics of the habitat and the classification made by Amaya-Vallejo (2009), *A. mayi* may also be a stenoecious species thus sharing similar habitat requirements with *A. recurvatum*. Despite the habitat requirements for both species, due to lack of surveys we suggest these to be data deficient category for the IUCN red species list.

## Taxonomic remarks

The phylogenetic position of *Archaeopodagrion* was expected to be close to the Malagasy genus *Tatocnemis* based on morphological characteristics (Rácenis 1959). Dijkstra et al. (2014) proposed the family Philogeniidae for *Archaeopodagrion* and *Philogenia* genera based on molecular evidence only, but morphologically, the only character shared by them is the coiled flagella on genital ligula, with no further evidence of other reliable diagnostic characters (Bota-Sierra 2017). With the description of the larva of *Archaeopodagrion* (Novelo-Gutiérrez et al. 2020), some important taxonomic information supported Philogeniidae as a monophyletic group including the shape of the antennae and the caudal lamellae, the structure of the galeolacinia of the maxilla, the maxillary palp and the distointernal margins of tibiae and the prementum. Autapomorphic characters separating larvae of *Archaeopodagrion* from those of *Philogenia* become less apparent with the description of *A. recurvatum* because the caudal lamellae with basal, spiny, fleshy tubercles present in *A. fernandoi* are lacking in *A. recurvatum*. We propose that the mandibular formula is the most reliable character for separating larvae of *Archaeopodagrion* and *Philogenia*, following Novelo-Gutiérrez et al. (2020): the molar lobe in the right mandible of *Archaeopodagrion* does not present m denticles but it does in *Philogenia*, the molar lobe in the left mandible of *Archaeopodagrion* has only two m denticles but the number varies in *Philogenia*, and the tooth d in the left mandible of *Archaeopodagrion* is small, bluntly-pointed and close to tooth b whereas in *Philogenia* the shape is different and its position is quite variable.

## Updated key for the adults of *Archaeopodagrion* (modified from Bota-Sierra 2017)

### Key to males

- |   |  |                             |
|---|--|-----------------------------|
| 1 | Paraprocts with a tubercle bearing a hair pencil (Fig. 10D) .....  | 2                           |
| – | Paraprocts lacking a tubercle bearing a hair pencil.....   | 4                           |
| 2 | Paraproct apex with two pointed processes.....   | <b><i>A. armatum</i></b>    |
| – | Paraproct apex ending in a single process (Fig. 10C) .....   | 3                           |
| 3 | Tips of paraprocts slightly recurved, shorter in length compared to cercus in lateral view.....                        | <b><i>A. fernandoi</i></b>  |
| – | Tips of paraprocts strongly recurved, paraproct subequal in length compared to cercus in lateral view (Fig. 10D) ..... | <b><i>A. mayi</i></b>       |
| 4 | Cerci with a sharp tooth internally.....   | 5                           |
| – | Cercus lacking an internal sharp tooth (Fig. 3A–D).....  | <b><i>A. recurvatum</i></b> |
| 5 | Cercus with an internal sharp tooth at midlength; cercus slightly curved in lateral view.....                          | <b><i>A. bicorne</i></b>    |
| – | Cercus with an internal sharp tooth at basal 1/4; cercus strongly curved in lateral view.....                          | <b><i>A. bilobatum</i></b>  |

## Key to females

Note: the females of *A. bilobatum* and *A. mayi* are unknown.

- 1       Posterior lobe of pronotum convex or with projections at posterolateral corners.....**2**
- Posterior lobe of pronotum laterally with a large, arched, hollowed out recurved quadrate process ..... *A. armatum*
- 2       Posterior lobe of pronotum convex with lateral small angled projections (Fig. 4B, C).....*A. recurvatum*
- Posterior lobe of pronotum with posterolateral projections blunt or rounded....**3**
- 3       Posterolateral projections on posterior lobe of pronotum acute.... *A. fernandoi*
- Posterolateral projections on posterior lobe of pronotum wide and rounded..... *A. bicorne*

## Acknowledgements

Authors sincerely thank the Colombian National Authority for Environmental Licenses (ANLA) and Colombian National Natural Parks (PNN) for the fieldwork and specimen collection permits (005-2016, 010-2019). Extended thanks to the Pacific Energy Company (EPSA-CELSIA) for granting the access to their lodging facilities in Campamento Yatacué (Anchicayá zone). Also, thanks to Juliana Sandoval-Hernández (JSH) for her help during field work at Santa Cecilia, Fausto and Jose Decaux for help and lodging in la Reserva Los Cedros, and Juan Pablo Monguí and Emilio Realpe for fieldwork assistance in Anchicayá. Additional thanks to Dr. José Antonio Gómez-Anaya for the image's edition, Dr. Christopher Beatty for the proofreading of the manuscript as an English native speaker, and Dr. Ken Tennesen and Dr. Rosser Garrison for their insightful comments and careful review of the manuscript.

VAV and MSH acknowledge the financial assistance rendered by the Colombian Ministry of Science (COLCIENCIAS–Crecimiento Verde Grant no. 80740-147-2019, code 122280863907) for fieldwork expeditions to PNN Farallones de Cali. VAV thanks Universidad de Los Andes for funding fieldwork expeditions through the Proyecto Semilla Grant (INV-2018-48-1355). MSH thanks the National Geographic Society for funding collection expeditions in Ecuador through the Waitt Explorer Grant W265–13. CBS acknowledges the Rufford Foundation Grant 19846-1 for field work at Santa Cecilia.

## References

- Amaya-Vallejo V (2009) Ensamblajes de odonatos como indicadores del estado ecológico de dos hábitats diferentes en la Central Hidroeléctrica del río Anchicayá, PNN Farallones de Cali. MSc Thesis. Universidad de Los Andes, Bogotá.

- Bechly G (1996) Morphologische Untersuchungen am Flügelgeäder der rezenten Libellen und deren Stammgruppenvertreter (Insecta; Pterygota; Odonata) unter besonderer Berücksichtigung der phylogentischen Systematik und des Grundplanes der Odonata. *Petalura* 2: 1–402.
- Bota-Sierra CA (2017) Two new species of the family Philogeniidae (Odonata: Zygoptera) from the Western Colombian Andes. *International Journal of Odonatology* 20: 137–150. <https://doi.org/10.1080/13887890.2017.1344733>
- Corbet P (1953) A terminology for the labium of larval Odonata. *Entomologist* 86: 191–196.
- Dijkstra KDB, Kalkman VJ, Dow RA, Stokvis FR, Van Tol J (2014) Redefining the damselfly families: A comprehensive molecular phylogeny of Zygoptera (Odonata). *Systematic Entomology* 39: 68–96. <https://doi.org/10.1111/syen.12035>
- Kennedy CH (1946) *Archaeopodagrion bilobatum*, n. sp., from Central Ecuador (Odonata: Megapodagrioninae). *Annals of the Entomological Society of America* 39: 171–176. <https://doi.org/10.1093/aesa/39.2.171>
- Novelo-Gutiérrez R, Bota-Sierra CA, Amaya-Vallejo V (2020) Description of the larva of the genus *Archaeopodagrion* Kennedy, 1939 (Zygoptera: Philogeniidae). *Zootaxa* 4816: 325–332. <https://doi.org/10.11646/zootaxa.4816.3.3>
- Pravettoni R (2019) Precipitation in the Andes. <https://www.grida.no/resources/12820>
- Rácenis J (1959) Lista de los odonatos del Perú. *Acta Biológica Venezuelica* 2: 467–522.
- Riek EF, Kukalová-Peck J (1984) A new interpretation of dragonfly wing venation based upon Early Upper Carboniferous fossils from Argentina (Insecta: Odonatoidea) and basic character states in pterygote wings. *Canadian Journal of Zoology* 62: 1150–1166. <https://doi.org/10.1139/z84-166>
- Tennessen KJ (2017) A method for determining stadium number of late-stage dragonfly nymphs (Odonata: Anisoptera). *Entomological News* 126: 299–306. <https://doi.org/10.3157/021.126.0407>
- Tennessen KJ, Johnson JT (2010) *Archaeopodagrion armatum* sp. nov. from Ecuador (Odonata: Megapodagrionidae). *International Journal of Odonatology* 13: 89–95. <https://doi.org/10.1080/13887890.2010.9748362>
- Watson MC (1956) The utilization of mandibular armature in taxonomic studies of anisopterous nymphs. *Transactions of the American Entomological Society* 81: 155–202.

# New species of the genus *Pseudolathra* Casey, 1905 (Coleoptera, Staphylinidae, Paederinae) from the Northwestern District of China

Xiaoyan Li<sup>1</sup>, Yanpeng Cai<sup>3</sup>, Hongzhang Zhou<sup>2</sup>

**1** Hebei Key Laboratory of Animal Diversity, College of Life Science, Langfang Normal University, Langfang 065000, China **2** Key Laboratory of Zoological Systematics and Evolution, Institute of Zoology, Chinese Academy of Sciences, 1 Beichen West Rd., Chaoyang District, Beijing 100101, China **3** Morphological Laboratory, Guizhou University of Traditional Chinese Medicine, Guiyang, 550025, Guizhou, China

Corresponding author: Hongzhang Zhou ([zhouhz@ioz.ac.cn](mailto:zhouhz@ioz.ac.cn))

---

Academic editor: Jan Klimaszewski | Received 3 November 2020 | Accepted 8 April 2021 | Published 5 May 2021

---

<http://zoobank.org/979D8628-AA45-435B-963B-67AD6057134B>

---

**Citation:** Li X, Cai Y, Zhou H (2021) New species of the genus *Pseudolathra* Casey, 1905 (Coleoptera, Staphylinidae, Paederinae) from the Northwestern District of China. ZooKeys 1036: 39–45. <https://doi.org/10.3897/zookeys.1036.60139>

---

## Abstract

Two new species of the genus *Pseudolathra* Casey, 1905 from mainland China are reported in this paper, namely *Pseudolathra gansuensis* Li & Zhou, **sp. nov.** and *P. assingi* Li & Zhou, **sp. nov.** This genus is reported for the first time from Gansu Province, Northwest China. Both species are described in detail and supplemented with color plates of normal light photos of the habitus, sternites VII–IX and details of aedeagal structures in different views.

## Keywords

Lathrobiini, new species, rove beetles, taxonomy

## Introduction

The genus *Pseudolathra* Casey, 1905 (Staphylinidae, Paederinae) is a rove beetle genus in the subtribe Lathrobiina with well-developed hind wings, commonly found during light trapping or in debris (Assing 2012). The genus occurs in all zoogeographic

regions, though most of the species have been recorded from the East Palaearctic and Oriental regions and many species have restricted distributions (Rougement 2015; Assing 2018, 2019; Li et al. 2019). So far, there are about 100 species recorded worldwide in the genus. More and more species of the subtribe Lathrobiina will be moved into *Pseudolathra* from related genera within the subtribe, so the exact number of species in the genus is still pending (Li et al 2013; Kocian and Hlaváč 2018).

Based on the most recent knowledge, the genus *Pseudolathra* was composed of 9 Chinese species by 2019 (Herman 2003; Assing 2012, 2013a, b, 2014; Li et al. 2013; Peng et al. 2014; Li et al. 2019), all characterized by the punctures on the forebody, while the middle area of the pronotum is impunctate; the punctures of the elytra are distinctly aligned in rows. Based on material collected recently, two new species from mainland China are described and illustrated here, namely *Pseudolathra gansuensis* Li & Zhou, sp. nov. and *P. assingi* Li & Zhou, sp. nov., both from Gansu province, China, which can be placed in the *P. unicolor* species group in the subgenus *Allolathra* based on the diagnostic characters of that group (Assing 2012). Thus, there are currently 11 species of *Pseudolathra* known from China. The type specimens are deposited in the Institute of Zoology, Chinese Academy of Sciences, Beijing (IZCAS).

## Material and methods

The dried specimens were softened in hot water at 60 °C for about 8 hours for dissection of the terminalia. The male genitalia were soaked in a 10% KOH solution (30 °C) for about 20–40 minutes (depending on the degree of sclerotization). The surrounding soft tissues were immediately removed and the remaining dissected parts are preserved in glycerin in plastic microvials with stoppers, pinned together with the source specimen for subsequent observation and photography. For each species, 3–5 specimens were dissected.

Observations, dissections and measurements were done under a Zeiss SteREO Discovery V20 stereomicroscope. Photos of the habitus, sternites and genitalia were taken with a Zeiss AxioCam MRc 5 camera attached to a Zeiss Axio Zoom V16 Stereo Zoom Microscope. Photos were processed and stacked with the Zen 2012 (Blue version) and Helicon Focus imaging softwares. All specimens listed in the present study were deposited in the Institute of Zoology, Chinese Academy of Sciences, Beijing (IZCAS).

The following abbreviations are used in the descriptions:

- AEL** Aedeagus length (length of the aedeagus from apex of dorsal plate to base of aedeagal capsule);
- BL** Body length (measured from anterior margin of labrum to end of abdomen);
- EL** Elytra length (measured from humeral angle to posterior margin);
- EW** Elytra width (width of elytra across the widest part);
- EYL** Eye length (length of eye in dorsal view);
- FL** Forebody length (measured from anterior margin of labrum to posterior margin of elytra);

- HL** Head length (measured from anterior margin of clypeal to posterior constriction);  
**HW** Head width (greatest width of head, including eyes);  
**PL** Pronotum length (measured from anterior margin to posterior margin);  
**POL** Postocular length (measured from posterior margin of eye to posterior constriction of head);  
**PW** Pronotum width (greatest width of pronotum).

## Taxonomy

### *Pseudolathra gansuensis* Li & Zhou, sp. nov.

<http://zoobank.org/2ACAA0B6-4CD7-47E4-AF05-334C7E3D8FF5>

Fig. 1

**Type specimens. Holotype:** ♂, CHINA: Gansu Province, Lanzhou City, Shifogou National Forest Park, Shifogou (石佛沟), 17.V. 2015, coll. Meng Wang (IZCAS). **Paratypes:** 4 ♂♂, 6 ♀♀, same data as holotype (IZCAS).

**Description.** BL: 4.4–4.6 mm; FL: 2.4–2.5 mm. HL: 0.67 mm; HW: 0.62 mm; PL: 0.73 mm; PW: 0.64mm; EL: 0.93 mm; EW: 0.81 mm; EYL: 0.21mm; POL: 0.25mm.

**Body** (Fig. 1A) elongate, brownish yellow; legs and antennae pale brown.

**Head** (Fig. 1A) nearly square, slightly longer than wide and about 1.08 times as long as wide; punctures on vertex of head sparse and coarse, dense around eyes, intervals between punctures larger than diameter of a puncture; eyes big and slightly protruding, postocular portion approximately 0.73–0.76 times as long as eye length.

**Pronotum** (Fig. 1A) oblong, slightly elongated, 1.14–1.16 times as long as wide, longer and broader than head. Anterior angles visible and posterior angles rounded, both sides straight. Longitudinal midline portion impunctate, both sides with dense and large punctures much denser and coarser than those of head and arranged in two compact rows generally; interstices with fine microsculpture.

**Elytra** parallel-sided, longer than wide, longer than pronotum; punctures on surface arranged in 7 series in dorsal view; interstices without microsculpture. Hind wings fully developed.

**Abdomen** approximately as broad as elytra, wider than head or pronotum; punctures very fine and dense; interstices with microsculpture; posterior margin of tergite VII with palisade fringe.

**Male. Sternite VII** (Fig. 1B) with a slight protrusion in middle, both sides of which slightly notched and surface with short hair slope to middle. Sternite VIII (Fig. 1C) with posterior excision narrow and deep, not quite reaching middle of sternite.

**Aedeagus** (Fig. 1D–F), AEL= 0.91–0.93 mm long, length/width = 3.29. Dorsal plate fused with median lobe. Ventral process strongly sclerotized and curved ventrally (Fig. 1D–E). Middle lobe with apex round in dorsal or ventral view and internal sac with several strongly sclerotized and acute structures.

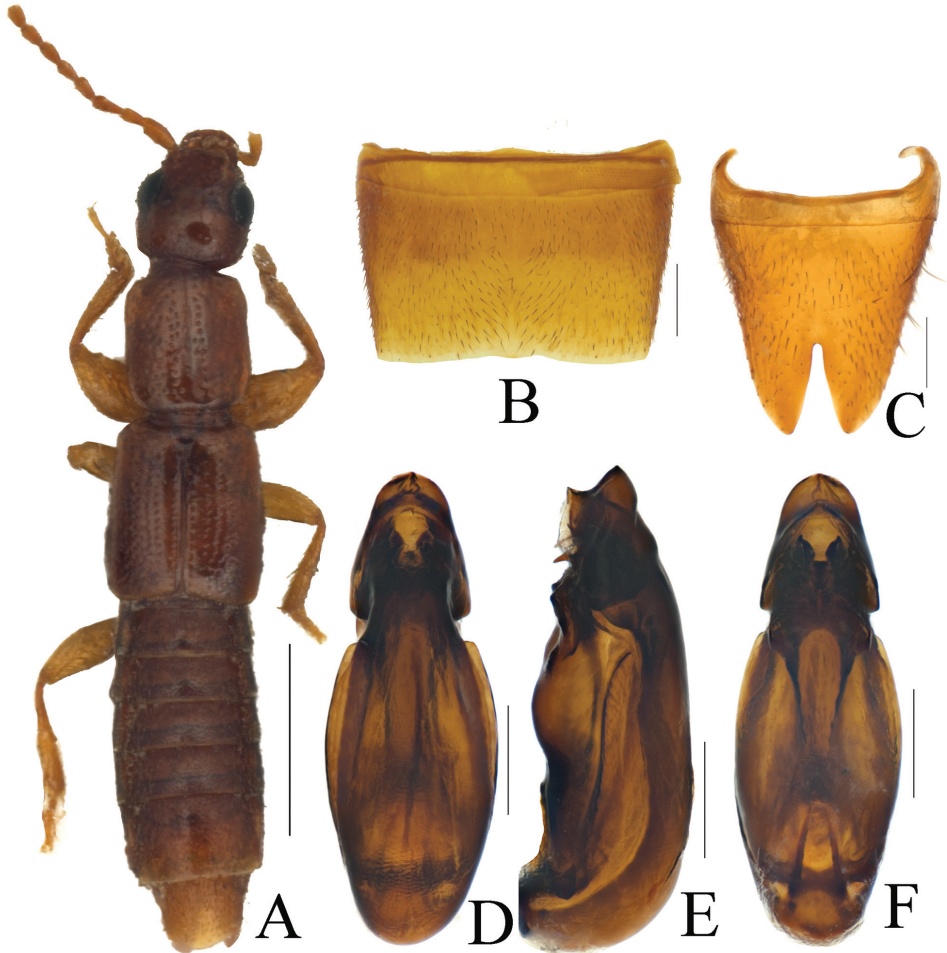


**Figure 1.** *Pseudolathra gansuensis* Li & Zhou, sp. nov., morphology **A** habitus **B** male sternite VII **C** male sternite VIII **D** aedeagus, dorsal view **E** aedeagus, lateral view **F** aedeagus, ventral view. Scale bars: 1.0 mm (**A**); 0.2 mm (**B–G**).

**Distribution and remarks.** The species is known only from Gansu Province and the specimens were collected by light traps.

**Comparative notes.** The new species is similar to *P. assingi* sp. nov. in habitus, but it can be distinguished from the latter by the deep notch in male sternites VII–VIII (Figs 1B, C, 2B, C), and the characteristics of the median lobe and interior armatures of the aedeagus are distinctly different (Fig. 1E–G).

The new species has a very similar aedeagus to *P. pulchella* (Kraatz, 1859), whereas the ventral protrusions of the median lobe are thinner than in the latter species. On the other hand, the middle notch of sternite VIII is distinctly deeper and narrower than in *P. pulchella* (Fig. 1B–C; Assing 2012: 315: figs 33–34; 321: 38–39).

**Etymology.** The specific epithet is derived from the type locality, Gansu Province in Northwest China.

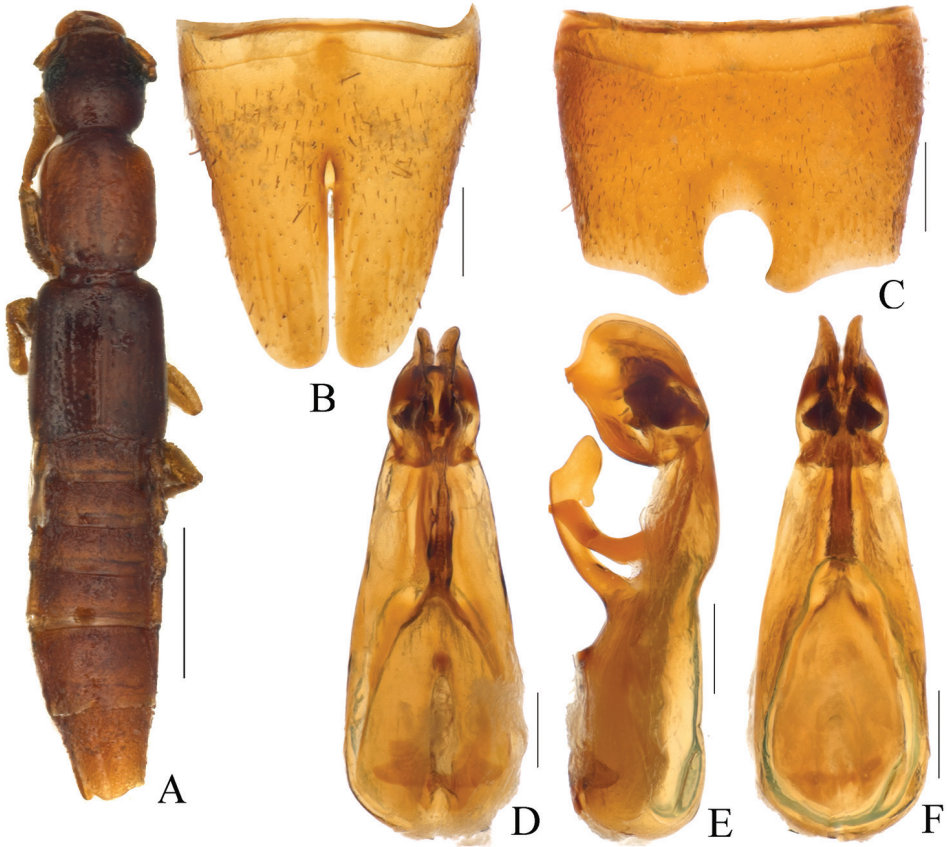


**Figure 2.** *Pseudolathra assingi* Li & Zhou, sp. nov., morphology **A** forebody **B** male sternite VII **C** male sternite VIII **D** aedeagus, ventral view **E** aedeagus, lateral view **F** aedeagus, dorsal view. Scale bars: 1.0 mm (**A**); 0.2 mm (**B–G**).

*Pseudolathra assingi* Li & Zhou, sp. nov.

<http://zoobank.org/7074F6B1-BB93-4C58-A4D4-07DBE8C1829E>

Fig. 2

**Type specimens.** *Holotype*: ♂, CHINA: Gansu Province, Lanzhou City, Shifogou National Forest Park, Shifogou (石佛沟), 17.V. 2015, coll. Meng Wang (IZCAS). *Paratypes*: 1 ♂, 5 ♀♀, same data as holotype (IZCAS).

**Description.** BL: 5.4–5.7 mm; FL: 2.8–3.1 mm. HL: 0.72 mm; HW: 0.72 mm; PL: 0.93 mm; PW: 0.78 mm; EL: 1.12 mm; EW: 0.93 mm; EYL: 0.29 mm; POL: 0.29 mm.

**Body** (Fig. 1A) elongate, brownish yellow; legs and antennae straw yellow.

**Head** (Fig. 1A) round, slightly wider than long and about 1.08 times as long as wide; punctures on vertex of head and around the eyes dense and coarse, with intervals between punctures as large as the diameter of a puncture; eyes big and flat, postocular approximately as long as eye.

**Pronotum** (Fig. 1A) oblong, slightly elongated, 1.09–1.11 times as long as wide, 1.28–1.30 times as long and 1.07–1.09 times as broad as head; both anterior angles and posterior angles rounded, sides straight. Longitudinal midline portion impunctate; punctures on each side dense and larger than those of head and generally arranged in rows; interstices glossy with fine microsculpture.

**Elytra** parallel-sided, longer than wide, slightly longer than pronotum; punctures on surface arranged in 5 series in dorsal view; interstices glossy with fine microsculpture. Hind wings fully developed.

**Abdomen** approximately as broad as elytra, wider than head or pronotum; punctures of posterior tergites very fine and dense, whereas basal area with punctures larger than the former; interstices with fine microsculpture; posterior margin of tergite VII with palisade fringe.

**Male. Sternite VII** (Fig. 1B) with a round notch in middle, prominent on both sides. Sternite VIII (Fig. 1C) with posterior excision narrow and deep and about 2/3 length of this sternite, basal part with a half-fusiform depression.

**Aedeagus** (Fig. 2D–F). AEL= 1.17 mm, length/width = 2.8. Dorsal plate fused with median lobe. Ventral process with a strongly sclerotized structure, curved ventrally and with apex irregularly formed (Fig. 2D–E). Middle lobe narrow in middle and bilobed posteriorly. Internal sac with several strongly sclerotized structures inside.

**Distribution and remarks.** The species is known only from Gansu Province and the specimens were collected by light traps.

**Comparative notes.** In addition to being similar to the previous species as described above, *P. assingi* sp. nov. also closely resembles *P. glabra* Peng, Li & Zhao, 2014, with differences as follows: 1) the former species has black head and elytra, whereas the latter one has brown head and elytra; 2) the notch of sternite VII, the ventral process, the hooks and the internal sac of the aedeagus differ significantly between the two species (Fig. 2E–G; Peng et al. 2014: 598, fig. 1B, D–E).

**Etymology.** The specific epithet is from the given name of entomologist Dr. Volker Assing, in recognition of his great scientific contributions to the Chinese fauna of the genus *Pseudolathra*.

## Acknowledgements

We are grateful to Dr. Volker Assing (Hannover, Germany) for sending valuable e-prints of publications on this group and Yanli Yue (岳艳丽, Sichuan Agriculture University) for sending the valuable specimens described in this study, and to the subject editor Dr. Jan Klimaszewski and reviewers Dr. Peng Zhong (彭中, Shanghai Normal University) and Dr. Daniel Whitmore (Stuttgart) for their sincere comments on the manuscript. This study was financially supported by the Natural Science Foundation of Hebei Province (C2019408016), Research Funds for the Universities in Hebei Province (ZD2020123, JYT202001), 333 talent projects of Hebei Province (A202002007) and the National Natural Science Foundation of China (NSFC31760629).

## References

- Assing V (2012) The *Pseudolathra* species of the East Palaearctic and the Oriental regions (Coleoptera: Staphylinidae: Paederinae). *Beiträge zur Entomologie* 62: 299–330. <https://doi.org/10.21248/contrib.entomol.62.2.299-330>
- Assing V (2013a) A revision of *Pseudolathra* of the East Palaearctic and Oriental regions. II. Six new species and additional records, with notes on some New World species (Coleoptera: Staphylinidae: Paederinae). *Linzer Biologische Beiträge* 45: 205–227.
- Assing V (2013b) A revision of Palaearctic and Oriental *Pseudolathra* III. Seven new species and additional records (Coleoptera: Staphylinidae: Paederinae). *Entomologische Blätter und Coleoptera* 109: 271–284.
- Assing V (2014) A revision of Palaearctic and Oriental *Pseudolathra*. IV. New species, new combinations and additional records (Coleoptera: Staphylinidae: Paederinae). *Linzer Biologische Beiträge* 46(2): 1151–1166.
- Assing V (2018) A revision of Palaearctic and Oriental *Pseudolathra*. V. Two new species from Cambodia and Thailand, and additional records (Coleoptera: Staphylinidae: Paederinae). *Linzer Biologische Beiträge* 50(2): 1005–1014.
- Assing V (2019) Monograph of the Staphylinidae of Crete (Greece). Part I. Diversity and endemism (Insecta: Coleoptera). *Linzer Biologische Beiträge* 69(2): 197–238. <https://doi.org/10.21248/contrib.entomol.69.2.197-239>
- Casey TL (1905) A revision of the American Paederini. *Transactions of the Academy of Science of Saint Louis* xv: 17–248. <https://doi.org/10.5962/bhl.title.9845>
- Herman LH (2003) Nomenclatural Changes in the Paederinae (Coleoptera: Staphylinidae). *American Museum Novitates* 3416(1): 1–28. [https://doi.org/10.1206/0003-0082\(2003\)416%3C0001:NCITPC%3E2.0.CO;2](https://doi.org/10.1206/0003-0082(2003)416%3C0001:NCITPC%3E2.0.CO;2)
- Kraatz G (1859) Die Staphylinen-Fauna von Ostindien, insbesondere der Insel Ceylan. *Archiv für Naturgeschichte* 25(1): 1–196. <https://doi.org/10.5962/bhl.title.66002>
- Kocian M, Hlaváč P (2018) Review of the genus *Pseudolathra* Casey, 1905 (Coleoptera: Staphylinidae: Paederinae) of Réunion Island *Zootaxa* 4531(3): 437–443. <https://doi.org/10.11646/zootaxa.4531.3.8>
- Li XY, Solodovnikov A, Zhou HZ (2013) The genus *Pseudolathra* in China: new species and new records (Coleoptera, Staphylinidae, Paederinae). *ZooKeys* 356: 1–9. <https://doi.org/10.3897/zookeys.356.5979>
- Li LZ, Hu JY, Peng Z, Tang L, Yin ZW, Zhao M J (2019) Staphylinidae. In: Yang XK (Ed.) *Catalogue of Chinese Coleoptera* (Vol. 3). Science Press, Beijing, 343–406.
- Peng Z, Li LZ, Zhao MJ (2014) A new species and additional records of *Pseudolathra* Casey (Coleoptera: Staphylinidae: Paederinae) from southern China. *Zootaxa* 3878(6): 597–600. <https://doi.org/10.11646/zootaxa.3878.6.7>
- Rougemont G de (2015) A new Oriental and Papuan *Pseudolathra* (Coleoptera, Staphylinidae, Paederinae). *Linzer Biologische Beiträge* 47(2): 1785–1799.



# Two new cryptic species of *Microhyla* Tschudi, 1838 (Amphibia, Anura, Microhylidae) related to the *M. heymonsi* group from central Vietnam

Chung Van Hoang<sup>1,2,9</sup>, Tao Thien Nguyen<sup>3</sup>, Hoa Thi Ninh<sup>3</sup>, Anh Mai Luong<sup>4</sup>,  
Cuong The Pham<sup>4,5</sup>, Truong Quang Nguyen<sup>4,5</sup>, Nikolai L. Orlov<sup>6</sup>, Youhua Chen<sup>1</sup>,  
Bin Wang<sup>1</sup>, Thomas Ziegler<sup>7,8</sup>, Jianping Jiang<sup>1,2</sup>

**1** CAS Key Laboratory of Mountain Ecological Restoration and Bioresource Utilization and Ecological Restoration and Biodiversity Conservation Key Laboratory of Sichuan Province, Chengdu Institute of Biology, Chinese Academy of Sciences, Chengdu 610041, China **2** University of Chinese Academy of Sciences, Beijing 810000, China **3** Vietnam National Museum of Nature, Vietnam Academy of Science and Technology, 18 Hoang Quoc Viet Road, Hanoi, Vietnam **4** Institute of Ecology and Biological Resources, Vietnam Academy of Science and Technology, 18 Hoang Quoc Viet Road, Hanoi, Vietnam **5** Graduate University of Science and Technology, Vietnam Academy of Science and Technology, 18 Hoang Quoc Viet Road, Cau Giay, Hanoi, Vietnam **6** Zoological Institute, Russian Academy of Sciences, Universitetskaya nab 1, St. Petersburg 199034, Russia **7** AG Zoologischer Garten Köln, Riehler Strasse 173, D-50735 Cologne, Germany **8** Institute of Zoology, University of Cologne, Zùlpicher Strasse 47b, D-50674 Cologne, Germany **9** Forest Resources and Environment Center, 300 Ngoc Hoi Road, Thanh Tri, Hanoi, Vietnam

Corresponding authors: Jianping Jiang ([jiangjp@cib.ac.cn](mailto:jiangjp@cib.ac.cn)); Tao Thien Nguyen ([nguyenthientao@gmail.com](mailto:nguyenthientao@gmail.com))

Academic editor: J. Penner | Received 27 July 2020 | Accepted 26 February 2021 | Published 5 May 2021

<http://zoobank.org/45F76C89-6B58-44B7-980F-0BFE455A2CEE>

**Citation:** Hoang CV, Nguyen TT, Ninh HT, Luong AM, Pham CT, Nguyen TQ, Orlov NL, Chen YH, Wang B, Ziegler T, Jiang JP (2021) Two new cryptic species of *Microhyla* Tschudi, 1838 (Amphibia, Anura, Microhylidae) related to the *M. heymonsi* group from central Vietnam. ZooKeys 1036: 47–74. <https://doi.org/10.3897/zookeys.1036.56919>

## Abstract

The *Microhyla heymonsi* species complex from central Vietnam was examined, and based upon morphological and molecular evidence, two new species are described. The discovery of *Microhyla daklakensis* **sp. nov.** and *Microhyla ninhthuanensis* **sp. nov.** brings the total number of known species in the genus to 46 and the species number of *Microhyla* in Vietnam to 13. The Truong Son Range harbors the highest diversity of the genus *Microhyla* with 11 recorded species so far. However, this apparent micro-endemic diversity is at risk because of habitat loss by deforestation, which highlights the necessity of further research leading to improved conservation measures.

## Keywords

*Microhyla*, new species, central Vietnam, morphology, molecular phylogeny

## Introduction

The genus *Microhyla* Tschudi, 1838 currently contains 44 species, which are distributed from India and Sri Lanka eastwards to the Ryukyu Archipelago of Japan and southwards to Indonesia (Hoang et al. 2020; Gorin et al. 2021; Frost 2021). Recently, Gorin et al. (2021) described a new genus *Nanohyla* from the *Microhyla* – *Glyphoglossus* assemblage (currently called the *Microhyla* – *Nanohyla* – *Glyphoglossus* assemblage). Recent studies have discovered highly divergent mitochondrial DNA lineages indicating a high degree of undiagnosed diversity in the genus (Hasan et al. 2012, 2014, 2015; Howlader et al. 2015; Matsui et al. 2005, 2011, 2013; Seshadri et al. 2016; Wijayathilaka et al. 2016; Yuan et al. 2016; Zhang et al. 2018; Nguyen et al. 2019; Li et al. 2019; Poyarkov et al. 2019; Hoang et al. 2020). Remarkably, 23 new species have been described during the last decade (Frost 2021).

In Vietnam, nine species of *Microhyla* have been recorded to date (Frost 2021), with the greatest species diversity occurring in the central and southern parts of the Truong Son Range, also known as the Central Highlands or the Tay Nguyen Plateau (Fig. 1). This mountain range harbors the highest diversity of amphibians in the Indochina region with a high degree of local endemism, and it is considered as a hotspot for new species discoveries (Bain and Hurley 2011; Geissler et al. 2015; Nguyen et al. 2019). This mountain range also appears to be one of the centers of radiation for the genus *Microhyla* (Poyarkov et al. 2014; Gorin et al. 2020). The following species have been described since 2010: *M. aurantiventris* Nguyen, Poyarkov, Nguyen, Nguyen, Tran, Gorin, Murphy & Nguyen, 2019; *M. darevskii* Poyarkov, Vassilieva, Orlov, Galoyan, Tran, Le, Kretova & Geissler, 2014; *M. mukhlesuri* Hasan, Islam, Kuramoto, Kurabayashi & Sumida, 2014; *M. neglecta* Poyarkov, Nguyen, Trofimets & Gorin, 2020; *M. pineticola* Poyarkov, Vassilieva, Orlov, Galoyan, Tran, Le, Kretova & Geissler, 2014 (Bain and Nguyen 2004; Hoang et al. 2013; Inger et al. 1999; Poyarkov et al. 2014; Nguyen et al. 2019; Poyarkov et al. 2020).

Heymon's narrow-mouthed frog, *Microhyla heymonsi* Vogt, 1911, was originally described from Taiwan based on eight male specimens (ZMB 54906–54913). Apart from Taiwan, this species has a wide distribution (Jang-Liaw and Chou 2015), and is reported from across East and Southeast Asia, from mainland China through Sumatra (Amphibia Web 2020; Frost 2021). Recently, Garg et al. (2019) demonstrated that *M. heymonsi* represents a complex of species, and that the current number of recognized *Microhyla* species may be underestimated. Garg et al. (2019) revealed six and Gorin et al. (2020) revealed seven or eight genetic lineages within *M. 'heymonsi'*.

During our recent field surveys in Kon Tum, Dak Lak, Lam Dong, and Ninh Thuan provinces in central Vietnam between 2016 and 2019, a number of microhylid frog specimens were collected that morphologically resembled *M. 'heymonsi'*. However, morphological and molecular analyses showed that these populations represent independent evolutionary lineages. The population from Lam Dong Province was recently

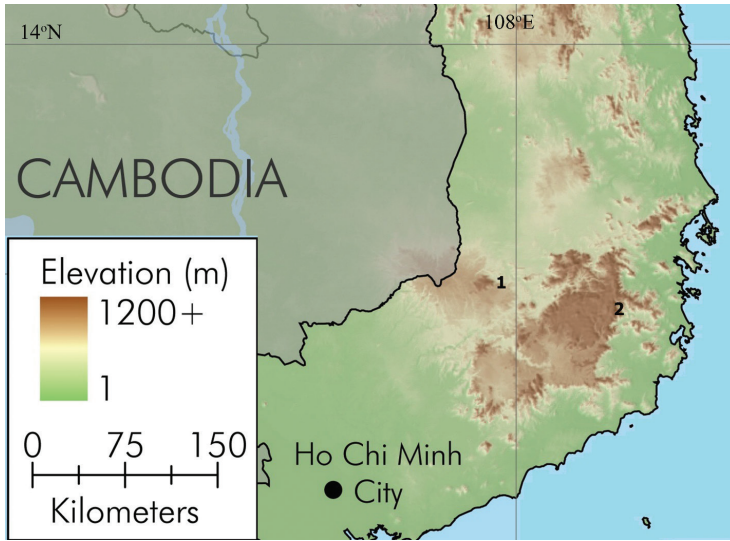


**Figure 1.** Map showing the type localities of *Microhyla ninhthuanensis* sp. nov. in Ninh Thuan Province (2) and *Microhyla daklakensis* sp. nov. in Dak Lak Province (1) in Tay Nguyen Plateau (Central Highlands) of Vietnam (EJ Sterling and K Koy kindly provided the map).

described as *M. neglecta* (Poyarkov et al. 2020). Two further populations remained that could not be assigned to any known species of *Microhyla*. Herein, we describe these two populations of *Microhyla* from central Vietnam as two new species.

## Materials and methods

### Sampling

Field surveys were conducted in Kon Tum, Dak Lak, Lam Dong, and Ninh Thuan provinces, Vietnam (Fig. 1) in June 2016, April and May 2018 and April 2019 by C.V. Hoang, A.M. Luong, Y.T. Nguyen, H.T. Ninh, N. L. Orlov, L. Iogansen (hereafter C.V. Hoang et al.). Geographic coordinates and elevations were obtained using a Garmin GPSMAP 78S (WGS 84 data). After photographing specimens in life, they were euthanized in a closed vessel with a piece of cotton wool containing ethyl acetate (Simmons 2002). Specimens were fixed in 70% ethanol for five hours, and then later transferred to 70% ethanol for permanent storage. Tissue samples were preserved separately in 70% ethanol prior to specimen fixation. Specimens referred to in this paper are deposited in the collections of the Vietnam National Museum of Nature (VNMN), Hanoi, Vietnam; Institute of Ecology and Biological Resources (IEBR), Hanoi, Vietnam; Chengdu Institute of Biology (CIB), Chengdu, Sichuan, China; and the Zoological Institute of the Russian Academy of Sciences (ZISP), St. Petersburg, Russia. Sex was determined by the direct observation of calling males in life or by gonadal dissection. Further information on the specimens is provided in Suppl. material 1: Table S1.

## Molecular analyses

Extraction of genomic DNA from 41 tissue samples (Suppl. material 1: Table S2) was carried out using the TIANamp Genomic DNA kit (Tiangen Biotech, Beijing, China), following the manufacturers' instructions. We amplified a 1979 base pair (bp) fragment that encodes part of the 12S rRNA gene, the complete tRNA Val gene, and part of the 16S rRNA gene that was used recently for *Microhylla* (Nguyen et al. 2019). The polymerase chain reaction (PCR) was performed using an Eppendorf PCR machine in 25 µl reactions containing 12 µl of Mastermix, 6 µl of water, 1 µl of each primer at a concentration of 10 pmol/µl, and 5 µl of DNA. We have amplified in multiple fragments: Fragment first, primers: 12SAL (5'-AAACTGGGATTAGATACCC-CACTAT-3'; forward), 16S2000H (5'-GTGATTAYGCTACCTTTGCACGGT-3'; reverse) (Zhang et al. 2008) used in the PCR and sequencing; and fragment second, primers: LR-N-13398 (5'-CGCCTGTTTACCAAAAACAT -3'; forward), LR-J 12887 (5'-CCGGTCTGAACTCAGATCACGT -3'; reverse) (Simon 1994) used in the PCR and sequencing. PCR conditions: 94 °C for 5 minutes of initial denaturation; with 35 cycles of denaturation at 94 °C for 30 s, annealing at 56 °C for 30 s, and extension at 72 °C for 45 s; and the final extension at 72 °C for 7 minutes. PCR products were sent to Tsingke Biological Technology company for sequencing (<http://www.tsingke.net>). The obtained sequences were deposited in GenBank under the accession numbers MT808928–MT808963 and MT819964–MT819968 (Suppl. material 1: Table S2).

In addition to the 41 sequences of the collected samples in this work, we used 76 available sequences of 12S rRNA–16S rRNA from GenBank (Garg et al. 2019) for phylogenetic analyses. Sequences of *Kaloula pulchra* Gray, 1831 were included in the analysis as outgroup (Van Bocxlaer et al. 2006). Locality information and accession numbers for all sequences included in the analysis can be found in Suppl. material 1: Table S2.

Phylogenetic trees were constructed by using Maximum Likelihood (ML) and Bayesian Inference (BI) analyses. Chromas Pro software (Technelysium Pty Ltd., Tewantin, Australia) was used to edit the sequences, and then aligned using the ClustalW (Thompson et al. 1997) option in MEGA 7.0 (Kumar et al. 2016) with default parameters and subsequently optimized manually in BioEdit 7.0.5.2 (Hall 1999). We then checked the initial alignments by eye and made slight adjustments. Prior to Bayesian tests, phylogenetic analyses were performed in MrBayes 3.2 (Ronquist et al. 2012). We chose the optimum substitution models for entire sequences using Kakusan 4 (Tanabe 2011) based on the Akaike information criterion (AIC). The best model selected for ML was the general time reversible model (GTR: Tavaré 1986) with a gamma shape parameter (G: 0.202 in ML and 0.226 in BI). The BI summarized two independent runs of four Markov Chains for 10 000 000 generations. A tree was sampled every 100 generations and a consensus topology was calculated for 70 000 trees after discarding the first 30 001 trees (burn-in = 3 000 000) (Nguyen et al. 2017). We checked parameter estimations and convergence using Tracer version 1.5 (Rambaut and Drummond 2009). The strength of nodal support in the ML tree was analyzed using non-paramet-

ric bootstrapping (MLBS) with 1000 replicates. We regarded tree nodes in the ML tree with bootstrap values of 75% or greater as sufficiently resolved (Hillis and Bull 1993; Huelsenbeck and Hillis 1993), and nodes with a BPP of 95% or greater as significant in the BI analysis (Leaché and Reeder 2002).

## Morphological analysis

All measurements were taken from 63 preserved specimens (Suppl. material 1: Table S4) with a digital caliper to the nearest 0.01 mm under a dissecting microscope. The following morphological characteristics were taken following Matsui (2011); Matsui et al. (2013), and Poyarkov et al. (2014), with some modifications:

<b>SVL</b>	snout-vent length (measured from the tip of snout to cloaca);
<b>HL</b>	head length (measured from tip of snout to hind border of jaw angle, but not measured parallel with the median line as done by Matsui 2011);
<b>SL</b>	snout length (measured from the anterior corner of eye to the tip of snout);
<b>EL</b>	eye length (measured as the distance between the anterior and posterior corners of the eye);
<b>N-EL</b>	nostril-eye length (measured as the distance between the anterior corner of the eye and the nostril);
<b>HW</b>	head width (measured as the maximum width of the head on the level of mouth angles in ventral view);
<b>IND</b>	internarial distance (measured as the distance between central points of nostrils);
<b>IOD</b>	interorbital distance (measured as the shortest distance between the medial edges of eyeballs in dorsal view);
<b>UEW</b>	upper eyelid width (measured as the widest distance from the medial edge of eyeball to the lateral edge of the upper eyelid);
<b>FLL</b>	forelimb length (measured as length of straightened forelimb to tip of third finger);
<b>LAL</b>	lower arm and hand length (measured as distance from elbow to tip of third finger);
<b>HAL</b>	hand length (measured from proximal end of outer palmar [metacarpal] tubercle to tip of third finger);
<b>IPTL</b>	inner palmar tubercle length (measured as maximal distance from proximal to distal ends of inner palmar tubercle);
<b>OPTL</b>	outer palmar tubercle length (measured as maximal diameter of outer palmar tubercle);
<b>HLL</b>	hindlimb length (measured as length of straightened hindlimb from groin to tip of fourth toe);
<b>TL</b>	tibia length (taken as the distance between the knee and tibiotarsal articulation);
<b>FL</b>	foot length (measured from distal end of tibia to tip of toe IV);

<b>IMTL</b>	inner metatarsal tubercle length (taken as maximal length of inner metatarsal tubercle);
<b>1TOEL</b>	first toe length (from distal end of inner metatarsal tubercle to tip of first toe);
<b>OMTL</b>	outer metatarsal tubercle length;
<b>1FW</b>	first finger width (measured at the distal phalanx);
<b>1–3FLO</b>	finger lengths, outer side ( <b>O</b> ) of the first-third;
<b>2–4FLI</b>	finger lengths, inner side ( <b>I</b> ) of the second-fourth;
<b>2–4FDW</b>	finger disk diameters;
<b>1–5TDW</b>	toe disk diameters.

Terminology for describing eye coloration in life followed Glaw and Vences (1997) and webbing formula followed Savage (1975).

## Morphological comparisons

A total of 45 species (Suppl. material 1: Table S5) was compared based on examined specimens (Suppl. material 1: Table S4) and from data in the literature: Boulenger (1897, 1900, 1920); Smith (1923); Parker (1928, 1934); Andersson (1942); Bourret (1942); Parker and Osman (1948); Pillai (1977); Inger and Frogner (1979); Inger (1989); Dutta and Ray (2000); Bain and Nguyen (2004); Das et al. (2007); Das and Haas (2010); Fei et al. (2012); Matsui (2011); Matsui et al. (2013); Hasan et al. (2014); Poyarkov et al. (2014); Howlader et al. (2015); Seshadri et al. (2016); Wijayathilaka et al. (2016); Khatiwada et al. (2017); Zhang et al. (2018); Nguyen et al. (2019); Garg et al. (2019); Poyarkov et al. (2019); Li et al. (2019); and Hoang et al. (2020).

## Principal component analysis (PCA)

Measurements were used to compare the morphometric difference between the four males and six females of the population from Dak Lak Province and the nine males and two females of the population from Ninh Thuan Province vs. the eight males and two females of *M. 'heymonsi'* from Kon Tum Province. All statistical analyses were performed using PAST 2.17b software (Hammer et al. 2001).

## Results

### Sequence variations

The final alignment of 12S rRNA–16S rRNA contained 1979 numbers of characters. Of these, 1222 sites were conserved and 731 sites exhibited variation, with 587 characters being parsimony-informative. The transition-transversion bias (R) was estimated as 1.279. Nucleotide frequencies were A = 31.64%, T = 23.96%, C = 23.09%, and G = 21.31% (data for ingroup only).

## Interspecific uncorrected p-distances

The genetic divergence of the population from Ninh Thuan Province and its congeners ranged from 3.6% (*M. heymonsi* sensu stricto from Taiwan) to 13.2–13.4% (*M. laterite*). The genetic divergence of the population from Dak Lak Province and its congeners ranged from 2.4–2.9% (the *M. 'heymonsi'* population from Kon Tum Province) to 12.4–13.4% (*M. nanapollexa*). These values were higher than the genetic distances between other recognized species of *Microhyla* (i.e., 2.4% between *M. fanjingshanensis* and *M. beilunensis*, *M. borneensis* and *M. malang*; 2.4% between *M. okinavensis* and *M. beilunensis*; 2.2% between *M. okinavensis* and *M. mixtura*) (Suppl. material 1: Table S3). Our results support those of Garg et al. (2019) and Gorin et al. (2020), clearly indicating that the *M. 'heymonsi'* clade represents a complex of several species, either representing previously available names or so far unrecognized diversity.

## Phylogenetic relationships

The BI and ML analyses produced topologies with  $-\ln L = 15327.579$  and  $12672.916$ , respectively. BI and ML analyses obtained similar topologies (Fig. 2) that differed only at several poorly supported basal nodes. Our matrilineal genealogy was consistent with previous studies based on mt DNA (e.g., Matsui et al. 2005, 2011; Hasan et al. 2012; Matsui et al. 2013; Howlader et al. 2015; Wijayathilaka et al. 2016; Seshadri et al. 2016; Yuan et al. 2016; Khatiwada et al. 2017; Nguyen et al. 2019; Garg et al. 2019; and Hoang et al. 2020). As shown in previous molecular analyses (Matsui et al. 2011; Peloso et al. 2016), Asian *Microhyla* species were divided into two geographical subgroups: the Southeast Asian subgroup was recently named as *Nanohyla* by Gorin et al. (2021), with eight known species: *N. annamensis*, *N. annectens*, *N. hongiaoensis*, *N. marmorata*, *N. nanapollexa*, *N. perparva*, *N. petrigena*, and *N. pulchella*; and Pan-Asian, including all other South, Southeast, and East Asian members (Fig. 2). Among the known taxa, molecular data are presented for the first time for four poorly known species: *N. annamensis*, *N. hongiaoensis*, *N. pulchella*, and *M. pineticola*. Molecular results further revealed *M. heymonsi* to represent a complex consisting of multiple species.

## Morphological analysis

The two new forms could be assigned to the genus *Microhyla* based both on the molecular phylogenetic data and the following morphological characters: size relatively small; maxillary and vomerine teeth absent; vomer divided into two parts, disappearing at the posterior edge of the choana; tongue round posteriorly; skin smooth or with tubercles; tympanum hidden; palate with one or two rows of horizontal skin ridges; fingers without webbing; toes slightly webbed or free of webbing; metacarpal tubercles two or three; and the absence of skin ridge or skin projection between the subarticular tubercles of toes III and IV.

The two new forms differ from other known species of *Microhyla* by having a medium body size, stocky habit, round snout, smooth skin on dorsum, disks on distal end

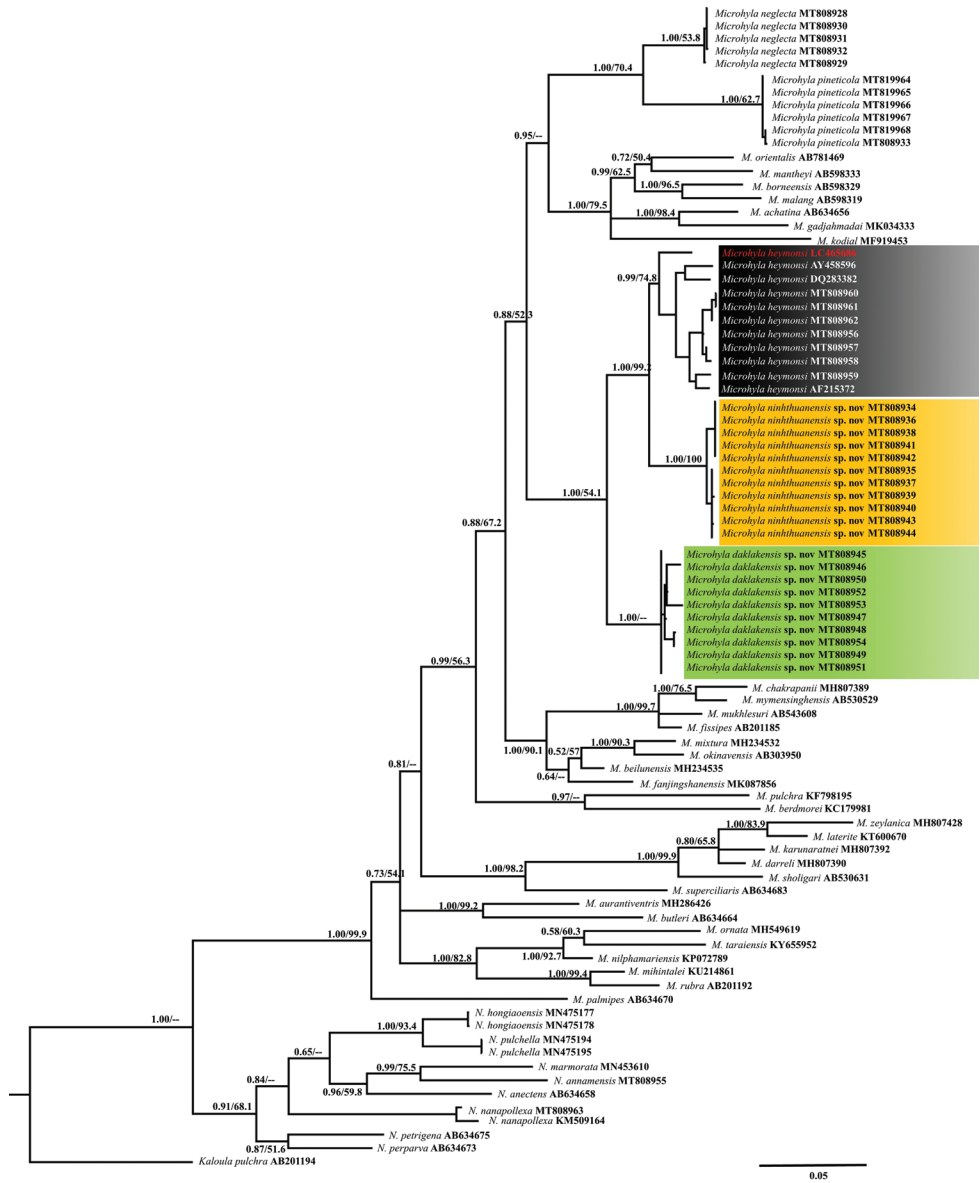


**Figure 2.** Bayesian Inference of the matrilineal genealogy of *Microhyla* derived from the analysis of 1979 bp of 12S rRNA–16S rRNA mtDNA sequences. Numbers above and below branches are Bayesian posterior probabilities and ML bootstrap values. The scale bar represents 0.05 nucleotide substitutions per site.

of toes present, dorsal median longitudinal grooves on finger disks present, superciliary tubercles absent, light dorsomedial vertebral line present (morphological characters and distribution data for each species are summarized in Suppl. material 1: Table S5).

The two new forms of *Microhyla* from Dak Lak and Ninh Thuan provinces can also be separated from *M. 'heymonsi'* based on morphometric data. We extracted three principal

component axes in the PCA result with eigenvalues greater than 0.01, the first two component axes accounted for 93.49% (in males) and 81.80% (in females) of the variation (Suppl. material 1: Table S6). The first two principal component axes could separate the new forms from *M. 'heymonsi'* by 23 characters (Fig. 7), mainly based on limb and head measurements, namely: SVL, HL, HW, SL, EL, N-EL, IND, IOD, UEW, FLL, LAL, HAL, IPTL, OPTL, 1FL, 3FDW, HLL, TL, FL, 1TOEL, IMTL, OMTL, and 3TDD (Suppl. material 1: Table S6). In males, species with a larger and positive score on PC1 reflected shorter SVL, HL, HW, SL, EL, N-EL, IND, IOD, UEW, FLL, LAL, HAL, IPTL, OPTL, 1FL, HLL, TL, and FL; while a negative score signified smaller 3FDW, 1TOEL, IMTL, OMTL, and 3TDD. The PC2 with positive scores were associated with species with larger morphological traits with all 23 characters, whereas no negative scores were associated with species (Suppl. material 1: Table S6). In females, species with a larger and positive score on PC1 reflected shorter SVL, HL, HW, SL, EL, N-EL, IOD, UEW, FLL, LAL, HAL, IPTL, OPTL, 1FL, HLL, TL, and FL; while a negative score signified smaller IND, 3FDW, 1TOEL, IMTL, OMTL, and 3TDD. The PC2 with positive scores were associated with species with larger SVL, HL, HW, SL, EL, N-EL, IOD, UEW, FLL, LAL, HAL, IPTL, OPTL, 1FL, HLL, TL, FL, 1TOEL, IMTL, OMTL, and 3TDD while a negative score signified smaller IND and 3FDW (Suppl. material 1: Table S6).

### Taxonomic conclusions

Based upon the phylogenetic analyses of 12S rRNA–16S rRNA sequences, the two populations clearly differ from all other species of *Microhyla* for which comparable genetic data are available, and the observed differences in mtDNA sequences were congruent with other morphological data. Accordingly, we describe the two new species as follows.

#### *Microhyla ninhthuanensis* sp. nov.

<http://zoobank.org/C458EC2A-C0AE-4BF6-B886-772A85A81911>

Figures 3M, 4G, H, 5J, K, L; Table 1; Suppl. material 1: Tables S4–S5

**Holotype.** VNMN 2021.01 (HAO 73), adult male, collected in Phuoc Binh National Park, Bac Ai District, Ninh Thuan Province, Vietnam (11°59'3.71"N, 108°44'51.63"E, ca. 305 m a.s.l., Fig. 1); leg. C.V. Hoang et al., 28 April 2018.

**Paratypes.** (n = 10) All collected by C.V. Hoang et al. at the same location as the holotype: IEBR.A 4841–4843 (HAO74, HAO76, HAO77), VNMN 2021.02–2021.05 (HAO78, HAO79, HAO80, HAO184), CIB (HAO185) eight adult males and ZISP 14253–14254 (HAO75, HAO186) two adult females, collected on Phuoc Binh National Park, Bac Ai District, Ninh Thuan Province, Vietnam (11°59'3.71"N, 108°44'51.63"E, ca. 305 m a.s.l., Fig. 1), 28 April 2018.

**Diagnosis.** *Microhyla ninhthuanensis* sp. nov. is distinguished from its congeners by a combination of the following morphological characters: 1) body stocky, size medium (SVL 17.3–18.8 mm, n = 9 males; 21.6–23.6 mm, n = 2 females). 2) dorsum smooth; 3) head triangular, snout round in profile; 4) finger I shorter than one-half



**Figure 3.** Dorsolateral and ventral views of the specimens in life: comparative specimen of *Microhyla neglecta* (VNMN 07344, male) (**A, B**); (VNMN 07673, female) (**C, D**); comparative specimen of *M. pineticola* (VNMN 07441, female) (**E, F**) and (VNMN 07455, male) (**G, H**). Photographs by CV Hoang and NL Orlov.



**Figure 3.** Continued. Dorsolateral and ventral views of the specimens in life: comparative specimen of *M. 'heymonsi'* (KPMĐ2018.42, male) (**I, J**); the holotype of *Microhyla daklakensis* sp. nov. (VNMN 06877, male) (**K, L**); the paratype of *Microhyla ninhthuanensis* sp. nov. (ZISP 14254 (HAO186), female) (**M**). Photographs by CV Hoang and NL Orlov.

the length of finger II; 5) tips of all outer fingers dilated, forming disks, with a median longitudinal groove visible dorsally; 6) tips of all toes distinctly dilated into disks, with a weak median longitudinal groove visible dorsally, producing the appearance of two scutes; 7) inner metacarpal tubercle oval and prominent, paired outer metacarpal tubercle divided by a waist into two equal-sized parts: outer part quite round, inner part quite crescent; 8) tibiotarsal articulation of straightened limb not reaching snout; 9) webbing basal: I2 – 2½II2 – 3III3 – 4IV4⅓ – 3V; 10) inner metatarsal tubercles oval, prominent and outer metatarsal tubercles round; 11) upper eyelid without supraciliary spines; 12) narrow faint brown stripe extending from rear corner of eye to axilla; 13) light thin vertebral stripe present, canthus rostralis with dark lines; 14) small

**Table 1.** Selected diagnostic characters for the comparisons between the species of the *Microhyla heymonsi* group.

	<i>M. 'heymonsi'</i>	<i>Microhyla daklakensis</i> sp. nov.	<i>Microhyla ninhthuanensis</i> sp. nov.
SVL M	16.5–22.0	17.7–20.1	17.3–18.8
SVL F	18.0–26.5	22.9–26.8	21.6–23.6
Habit	Stocky	Stocky	Stocky
Snout profile	rounded, obtusely pointed	rounded	rounded
Dorsal skin	smooth	smooth	smooth
F1 vs. F2	F1 ≤ ½ F2	F1 > ½ F2	F1 ≤ ½ F2
Disks on distal end of fingers	present	present	present
Dorsal median longitudinal line grooves on finger disks	usually present	present	present
Disks on distal end of toes	present	present	present
Dorsal peripheral grooves on toe disks	usually present	present	present
Presence or absence of superciliary tubercles	absent	absent	absent
Presence or absence of light dorsomedial (vertebral) line	present	present	present
Tibiotarsal articulation	shorter than snout	shorter than snout	shorter than snout
Foot webbing	I2 – 2½II2 – 3III3 – 4IV4½ – 3V	I2 – 2½II2 – 3III3 – 4IV4½ – 3V	I2 – 2½II2 – 3III3 – 4IV4½ – 3V
Distribution	S China, NE India, SE Asia to Sumatra	Dak Lak	Ninh Thuan

dark round spot at mid-dorsum, divided by a light vertebral stripe; 15) dorsum pinkish brown with dark brown marking in X-shape between eyes and arm, along vertebral and dorsolateral region stripes form wavy dust strip towards the groin, a small dark marking ‘( )’-shaped in the center of the dorsum and mid-dorsal line; 16) an even black lateral stripe from above arm, almost reaching groin; 17) chin dark grey; throat white with scattered dark grey dusting; chest and belly creamy white.

**Description of holotype.** Habitus stocky, size medium, SVL 18.20 mm; head wider than long (HL/HW 0.83); snout long, abruptly round in dorsal view, projecting beyond margin of lower jaw, longer than diameter of eye (SL/EL 1.24); eyes small, slightly protuberant, pupil round (Fig. 4G); dorsal surface of head flat, loreal region acute; indistinct canthus rostralis; nostril oval, lateral, closer to tip of snout (N-EL 1.33) than to eye (EL 1.95); interorbital distance wide, greater than internarial distance (IOD/IND 1.28); and internarial distance wide, greater than upper eyelid width (IND/UEW 1.18); tympanum hidden, supratympanic fold weak, from posterior corner of eye to arm insertion; vomerine teeth absent, tongue without papillae, oval and free at the rear half of its length; slit-like openings to a small vocal sac.

Forelimbs short, about three times shorter than hindlimbs (FLL/HLL 0.31); hand two times shorter than forelimb length (HAL/FLL 0.43); fingers slender, free of webbing, round in cross-section, skin fringes of fingers weak; first finger shorter than one-half the length of the second finger (1FLO/2FLO 0.44), second finger slightly shorter than fourth (2FLI/4FLI 0.98), latter much longer than first, and much shorter than third (2FLI/3FLI 0.74); relative finger lengths: I < II < IV < III (Fig. 5K). All disks bearing narrow peripheral grooves, dorsal finger tips with median longitudinal grooves producing the appearance of two scutes; relative finger disk widths: I < IV < II < III; nuptial pad absent; subarticular

tubercles on fingers distinct, round, finger subarticular tubercle formula: 1:1:2:2 (given for fingers I:II:III:IV, respectively); inner metacarpal tubercle (IPTL 0.48) oval, prominent; a paired outer metacarpal tubercle divided by a waistline into two equal-sized parts: outer part quite round, inner part quite crescent (OPTL 0.47) (Fig. 5K).

Hindlimbs slender and slightly short (HLL 31.62), tibia length longer than half of snout-vent length (TL/SVL 0.58); tibiotarsal articulation at straightened limb not reaching snout; foot longer than tibia (FL/TL 1.32); relative toe lengths: I<II<V<III<IV; tarsus smooth, inner tarsal fold absent; tips of all toes distinctly dilated into disks, slightly wider than those of fingers (3TDW 0.53, 3FDW/3TDW 0.93), dorsally all toes with median longitudinal grooves at disks; relative toe disk widths: I<V<II<III=IV; webbing between toes basal and poorly developed, webbing formula: I2 – 2½II2 – 3III3 – 4IV4½ – 3V; subarticular tubercles prominent, all present, circular, formula 1, 1, 2, 3, 2; inner metatarsal tubercle elongated, oval, large and prominent, length (IMTL 0.78); outer metatarsal tubercle round, elevated and very well distinct, smaller (OMTL 0.38) than length of inner metatarsal tubercle (Fig. 5L).

Dorsal surface of head and body smooth, flank shagreened, dorsal surface smooth, including fingers and toes, fore and hind limbs; ventral surfaces smooth.

**Coloration of holotype in life.** Dorsal surface of head and trunk pinkish brown with a dark brown marking in X-shape between eyes to arm, dorsolateral stripes form wavy dust strip towards the groin; a small dark marking in '( )'-shape in the center of the dorsum and a mid-dorsal line extending from the tip of snout to vent. Flanks and lateral surface of head dark, a dark lateral stripe running from snout tip to nostril, fading towards upper jaw. Chin dark grey; throat white with scattered dark grey dusting; chest and belly creamy white. Limbs dorsally with narrow indistinct dark brown cross-bars; fingers and toes dorsally brown with dark brown cross-bars; forelimbs ventrally creamy white, hindlimbs ventrally with creamy white thigh becoming dark grey toward shank, foot. Iris bicolored, golden in upper one-third, dark copper in its lower two-thirds; pupil oval, horizontal, black.

**Coloration of holotype in preservative.** After preservation in ethanol, dorsal coloration changed from light brown to greyish pink (Fig. 4G), ventral surface of chest, belly, and limbs changed from creamy white to whitish beige (Fig. 4H); dorsal pattern: dark spots on dorsum and stripes on dorsal surfaces of limbs unchanged, dark brown pattern changed to dark grey; iris completely black, pupil round, white.

**Variation.** Specimens vary in body size, dorsal markings, and black scapular spots. Adult males smaller than adult females, adult males with small vocal sac (Suppl. material 1: Table S4).

**Comparisons.** *Microhyla ninththuanensis* sp. nov. is morphologically most similar to *M. heymonsi* sensu stricto (Fig. 2), but differs by having: 1) a snout round in profile (vs. snout obtusely pointed in *M. heymonsi* sensu stricto), 2) pinkish brown dorsal surface with a dark brown marking in X-shape between eyes to insertion of the arms (vs. dorsal surface red to grayish red with a dark brown marking in X-shape and a vague V-shape dark brown marking in *M. heymonsi* sensu stricto (Vogt, 1913)). Detailed comparisons between *M. ninththuanensis* sp. nov. and other members of the *M. heymonsi* group are shown in Table 1 and Suppl. material 1: Table S5.

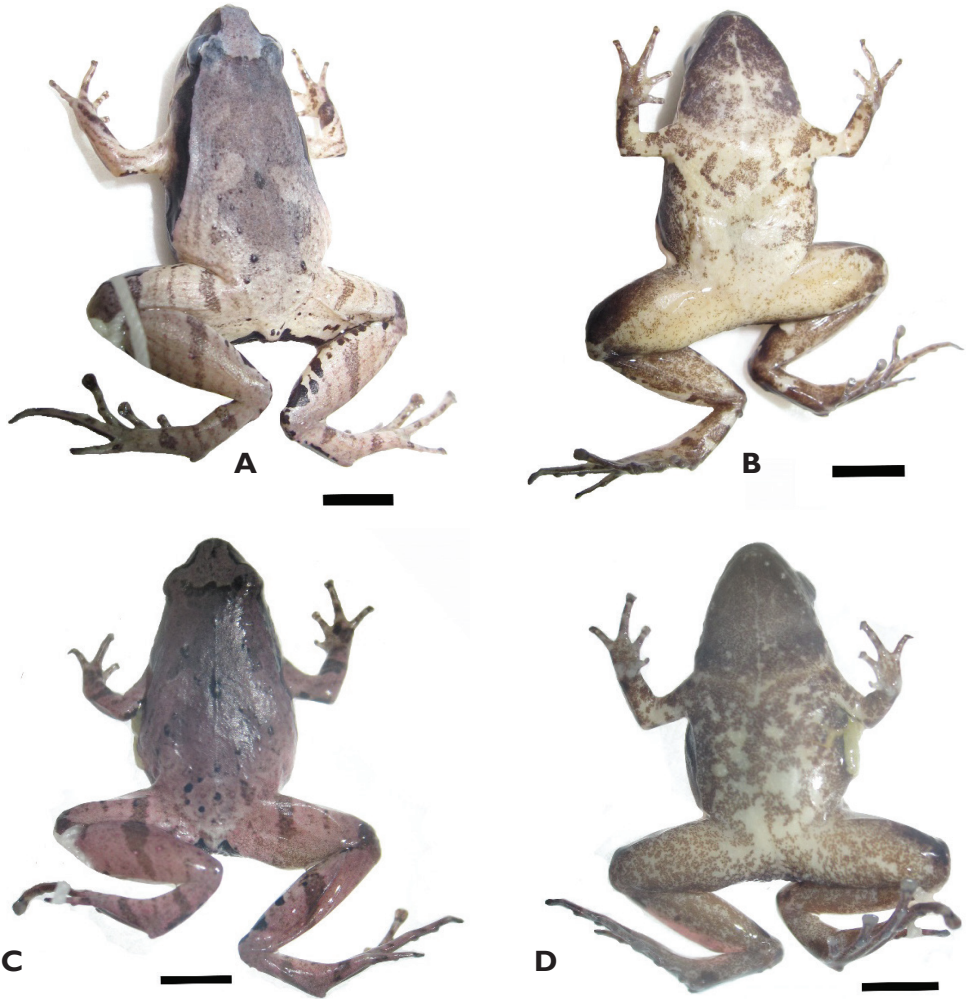


**Figure 4.** Dorsolateral and ventral views of the specimens in preservative: comparative specimen of *Microhyala neglecta* (VNMN 07344, male) (**A, B**), comparative specimen of *M. pineticola* (VNMN 07719, male) (**C, D**). Photographs by CV Hoang. Scale bars 4 mm.

**Etymology.** Specific epithet is in reference to the type locality, Ninh Thuan Province. We recommend “Ninh Thuan narrow-mouth frog” as the common English name and “Nhái bầu ninh thuận” as the Vietnamese name.

**Natural history.** All specimens were collected at night from 19:00 to 23:00 h on the ground near the banks of a small stream in the forest and on the sides of a recently constructed road next to the devastated forests (Fig. 6B). Larval stages and eggs of the new species are unknown.

**Distribution.** *Microhyala ninhthuanensis* sp. nov. is currently only known from the type locality in Phuoc Binh National Park, Ninh Thuan Province, Vietnam (Fig. 1). The species was recorded at an elevation of ca. 300 m a.s.l.

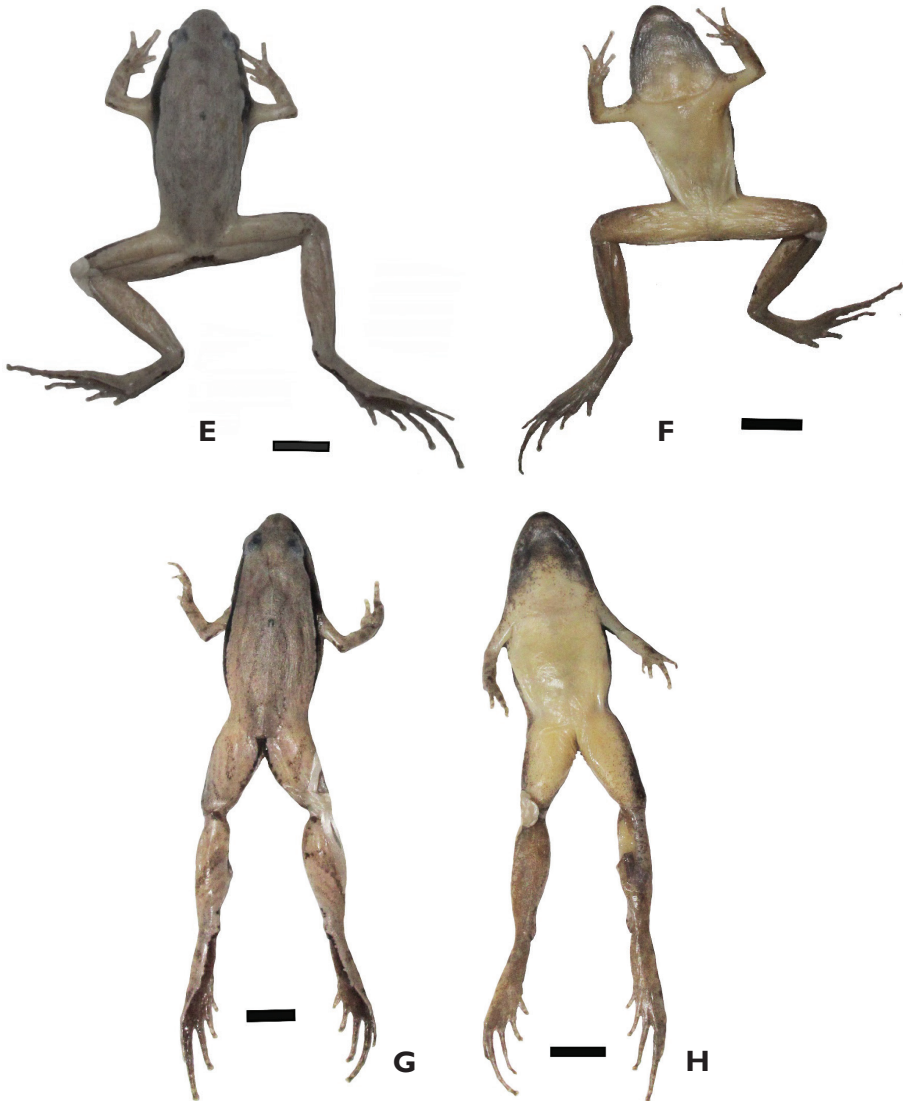


**Figure 4.** Continued. Dorsolateral and ventral views of the specimens in preservative: the holotype of *Microhyla daklakensis* sp. nov. (VNMN 06877, male) (**E, F**); and the holotype of *Microhyla ninhthuanensis* sp. nov. (VNMN 2021.01, male) (**G, H**). Photographs by CV Hoang. Scale bars 4 mm.

**Conservation status.** Currently, the evergreen forest in Phuoc Binh National Park is connected with other forests in Tay Nguyen Plateau. Based on its habitat and altitudinal range, the new species is likely to be endemic to Tay Nguyen Plateau. However, the extent of its actual distribution range requires further study. Given the available information, we suggest *Microhyla ninhthuanensis* sp. nov. be considered as Data Deficient following IUCN's Red List categories (IUCN Standards and Petitions Subcommittee 2001).

***Microhyla daklakensis* sp. nov.**

<http://zoobank.org/F1830785-835D-45AD-8416-ABD9BBE5F27D>

Figures 3K, L, 4E, F, 5G, H, I; Table 1; Suppl. material 1: Tables S4–S5

**Holotype.** VNMN 06877, adult male, collected in Nam Ka Nature Reserve, Krong No District, Dak Lak Province, Vietnam (12°20'25.39"N, 108°1'23.67"E, ca. 519 m a.s.l., Fig. 1); 27 May 2018, leg C.V. Hoang et al.

**Paratypes.** (n = 9) All collected by C.V. Hoang et al. at the same location as the holotype: IEBR.A 4845-4746 (VNMN 06817, VNMN 06884), CIB (VNMN 06902) three adult males and VNMN 06818, CIB (VNMN 06858), ZISP 14249, 14250, 14251, 14252 (VNMN 06867, VNMN 06868, VNMN 06869, VNMN 06887), six adult females, collected on Nam Ka NR, Krong No District, Dak Lak Province, Vietnam (12°20'25.39"N, 108°1'23.67"E, ca. 519 m a.s.l., Fig. 1), 27 May 2018.

**Diagnosis.** (1) *Microhyla daklakensis* sp. nov. is distinguished from its congeners by a combination of the following morphological characters: 1) body stocky, size medium (SVL 17.7–20.1 mm n = 4 males; 21.1–23.8 mm, n = 6 females), 2) dorsum smooth; 3) snout round in profile; 4) finger I longer than one-half the length of the finger II; 5) tips of all outer fingers dilated, forming disks, with a median longitudinal groove visible dorsally; 6) tips of all toes distinctly dilated into disks, with a weak median longitudinal groove visible dorsally, producing the appearance of two scutes; 7) inner metacarpal tubercle oval and prominent, paired outer metacarpal tubercle divided by a waistline into two equal-sized parts: outer part quite round, inner part crescent-shaped; 8) tibiotarsal articulation of straightened limb not reaching snout; 9) webbing basal: I2 – 2½II2 – 3III3 – 4IV4½ – 3V; 10) inner metatarsal tubercles oval, prominent and outer metatarsal tubercles round; 11) upper eyelid without supraciliary spines; 12) narrow faint brown stripe extending from rear corner of eye to axilla; 13) thin, pale vertebral stripe present, canthus rostralis with dark lines; 14) small dark round spot at mid-dorsum, divided by a light vertebral stripe; 15) dorsal surface yellowish brown, a dark brown marking in V-shape between eyes to insertion of arms; 16) vertebral and dorsolateral stripes form wavy dust strip towards the groin; 17) a small dark marking in '( )'-shape on the center of the dorsum and mid-dorsal line; 18) an evenly colored black lateral stripe from above the insertion of the arms, almost reaching groin; 19) chin dark grey; throat white with scattered dark grey dusting; chest and belly creamy white.

**Description of holotype.** Habitus stocky, size medium SVL 19.07 mm; head wider than long (HL/HW 0.82); snout long, abruptly round in dorsal view, projecting beyond margin of lower jaw, longer than diameter of eye (SL/EL 1.34); eyes comparatively small, slightly protuberant, pupil round (Fig. 5G); dorsal surface of head flat, canthus rostralis round; loreal region steep, weakly concave; nostril round, lateral, above canthus rostralis, closer to tip of snout (N-EL 1.20) than to eye (EL 1.79), interorbital distance wide (IOD 1.90) much greater than the internarial distance (IND 1.62) and the upper eyelid width (UEW 1.15); pineal spot absent, tympanum hidden, supratympanic fold weak, running from posterior corner of eye to arm insertion;

vomerine teeth absent, tongue without papillae, roundly spatulate and free at the rear half of its length; slit-like openings to a median vocal sac (Fig. 6G).

Forelimbs comparatively short, about three times shorter than hindlimbs (FLL/HLL 0.33); hand two times shorter than forelimb length (HAL/FLL 0.44); fingers slender, free of webbing, round in cross-section, no skin fringes on fingers present, dorsoventrally flattened, skin fringes of fingers weak; first finger well-developed, longer than one-half the length of the second finger (1FLO/2FLO 0.57), second finger slightly shorter than fourth (2FLI/4FLI 0.89), latter much longer than first, and much shorter than third (2FLI/3FLI 0.60), relative finger lengths: I < II < IV < III (Fig. 5H); all disks bearing narrow peripheral grooves, dorsal finger tips with median longitudinal grooves producing the appearance of two scutes, grooves present in all fingers; relative finger disk widths: I < IV < II < III; nuptial pad absent; subarticular tubercles on fingers distinct, round, finger subarticular tubercle formula: 1:1:2:2 (given for fingers I:II:III:IV, respectively); inner metacarpal tubercle oval (IPTL 0.55), elongated and prominent; subarticular tubercles and outer metacarpal tubercle (OPTL 0.61) split unclearly with a weak groove (Fig. 5H).

Hindlimbs slender and slightly short (HLL 30.99), tibia length longer than half of snout-vent length (TL/SVL 0.53); tibiotarsal articulation at straightened limb not reaching snout; foot longer than tibia (FL/TL 1.36); relative toe lengths: I < II < V < III < IV; tarsus smooth, inner tarsal fold absent; tips of all toes distinctly dilated into disks, slightly wider than those of fingers (3TDW 0.63, 3FDW/3TDW 0.83), dorsally all toes with median longitudinal grooves at disks; relative toe disk widths: I < V < II < III < IV; webbing between toes basal and poorly developed (Fig. 5I), webbing formula: I2 – 2½II2 – 3III3 – 4IV4½ – 3V; subarticular tubercles on toes small, prominent, round, formula 1, 1, 2, 3, 2; inner metatarsal tubercle elongated, oval, large and prominent, length (IMTL 0.52) shorter than half of first toe (1TOEL 2.57); outer metatarsal tubercle round, elevated and very distinct, slightly shorter (OMTL 0.52) than length of inner metatarsal tubercle (Fig. 5I).

Skin: Dorsal surface of head and body smooth, flanks smoothly shagreened, dorsal surface of fore and hind limbs, including fingers and toes, smooth; ventral surfaces smooth (Fig. 3K, L).

**Coloration of holotype in life.** Dorsal surface of head and trunk yellowish brown to light brown with a dark brown marking in a V-shape between eyes to insertion of arms. Vertebral and dorsolateral stripes forming a wavy dust stripe towards the groin. A small dark brown marking in ‘( )’-shape in the center of the dorsum and mid-dorsal line. Flanks and lateral surface of head dark, a darker lateral stripe running from snout tip to nostril, fading towards the upper jaw and the belly, fading into belly as dusting. Chin dark grey; throat white with scattered dark grey dusting; chest and belly creamy white. Limbs dorsally with narrow indistinct dark brown cross-bars; fingers and toes dorsally brown with dark brown cross-bars; forelimbs ventrally creamy white, hindlimbs ventrally with creamy white thigh changing to dark grey toward shank and foot. Iris bicolored, golden in upper one-third, dark copper in lower two-thirds; pupil oval, horizontal, black (Figs 3K, 4L).

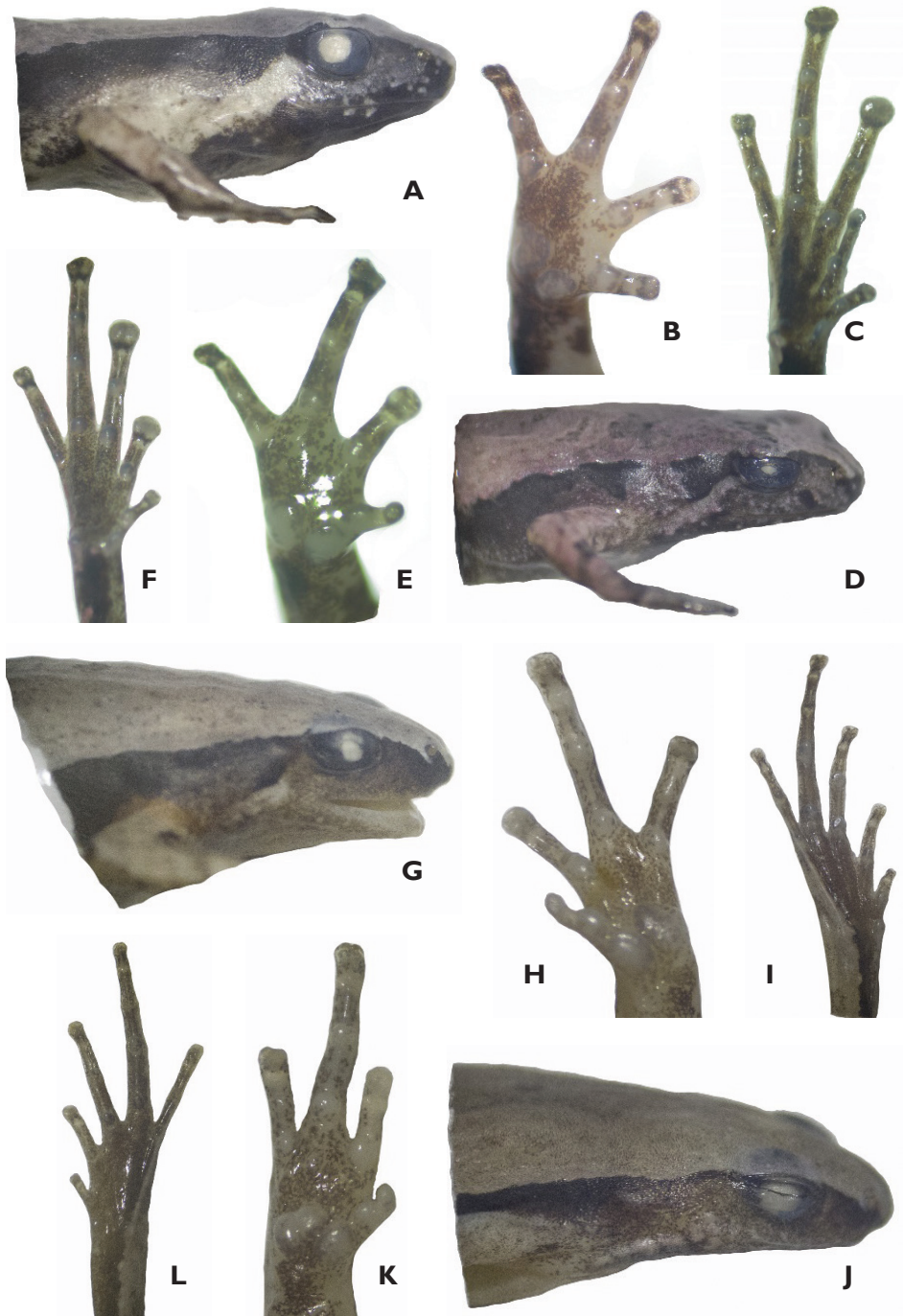


**Figure 5.** Lateral view of the head, right hand and right foot of *Microhyla neglecta* (VNMN 07344, male) (A, B, C); comparative specimen of *Microhyla pineticola* (VNMN 07719, male) (D, E, F); *Microhyla daklakensis* sp. nov. (VNMN 06877, male) (G, H, I); and *Microhyla ninhthuanensis* sp. nov. (HAO73, male) (J, K, L). Photographs by CV Hoang.



**Figure 6.** Habitat of *Microhyla daklakensis* sp. nov. in Nam Ka NR, Dak Lak Province (**A**); and of *Microhyla ninhthuanensis* sp. nov. in Phuoc Binh NP, Ninh Thuan Province (**B**), Vietnam. Photos by C. V. Hoang.

**Coloration of holotype in preservative.** After preservation in ethanol, the dorsal coloration changed from brown to whitish grey (Fig. 4E), and the ventral surface of chest, belly, and limbs changed from creamy white to whitish beige (Fig. 4F). The dorsal pattern, dark spots on the dorsum and stripes on the dorsal surfaces of the limbs are unchanged, dark brown pattern on the dorsum changed to dark grey; iris completely black, pupil round, white.

**Variation.** (Suppl. material 1: Table S4, Fig. 3). Paratypes vary in body size, dorsal color pattern, and shape of black scapular spots. Adult males are smaller than adult females and have a distinct vocal sac (Suppl. material 1: Table S4).

**Comparisons.** *Microhyla daklakensis* sp. nov. is morphologically similar to *M. ninthuanensis* from Ninh Thuan Province and *M. heymonsi* sensu stricto (Fig. 2), but differs by having: 1) a snout round in profile (vs. snout obtusely pointed in *M. heymonsi* sensu stricto), 2) finger I longer than one-half the length of the finger II (vs. finger I shorter than one-half the length of the finger II in the new form from Ninh Thuan and *M. heymonsi* sensu stricto), 3) dorsal surface yellowish brown with a dark brown marking in V-shape between the eyes and the insertion of the arms (vs. pinkish brown dorsal surface with a dark brown marking in X-shape between eyes and insertion of the arms in the new form from Ninh Thuan, and dorsal surface red to grayish red with a dark brown X-shaped marking and a vague V-shaped dark brown marking in *M. heymonsi* sensu stricto (Vogt, 1913). Detailed comparisons between *Microhyla daklakensis* sp. nov. and other members of the *M. heymonsi* group are shown in Table 1 and Suppl. material 1: Table S5.

**Etymology.** Specific epithet is in reference to the type locality, Dak Lak Province. We recommend “Dak Lak narrow-mouth frog” as the common English name and “Nhái bầu dak lak” as the Vietnamese name.

**Natural history.** All specimens were collected at night from 19:00 to 23:00 h on the ground near the banks of small temporary ponds formed after heavy rain, along the edges of the forest and on the sides of a recently constructed road next to the devastated forests (Fig. 6A). The new species was found in sympatry with four congeners including *M. berdmorei*, *M. butleri*, *M. mukhlesuri*, and *M. pulchra*, all of which were reproducing simultaneously with the new species in the same breeding site. Other anurans such as *Fejervarya limnocharis*, *Occidozyga* cf. *lima*, and *Occidozyga martensii* also occurred in sympatry. Larval stages and eggs of the new species are unknown.

**Distribution.** *Microhyla daklakensis* sp. nov. is currently known only from the type locality in Nam Ka Nature Reserve, Krong No District, Dak Lak Province, Vietnam (Fig. 1). The species was recorded at an elevation of ca. 500 m a.s.l.

**Conservation status.** Currently, the evergreen forest in Nam Ka Nature Reserve, Dak Lak Province, is connected with other forests in the Tay Nguyen Plateau. The extent of its actual distribution range requires further study. Given the available information, we suggest *Microhyla daklakensis* sp. nov. be considered as Data Deficient following IUCN’s Red List categories (IUCN Standards and Petitions Subcommittee 2017).

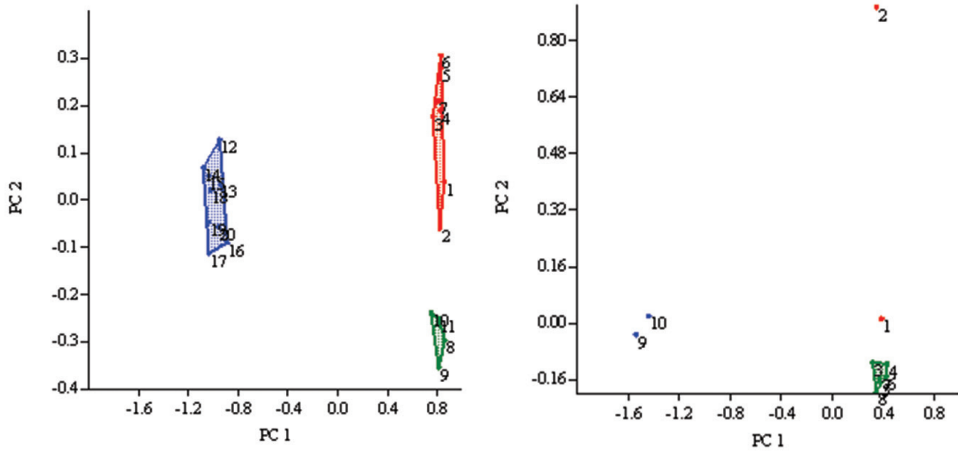


**Figure 7.** Plots of the first principal component (PC1) versus the second (PC2) for the males and the females of *Microhyla ninhthuanensis* sp. nov. (blue), *Microhyla daklakensis* sp. nov. (green), and *Microhyla 'heymonsi'* (red).

## Discussion

Our matrilineal genealogy is consistent with those of Matsui et al. (2011), Peloso et al. (2016), Nguyen et al. (2019), Garg et al. (2019), and Gorin et al. (2020, 2021). The BI and ML genealogy showed that the monophyly of Microhylinae was not supported and the relationships among microhylid subfamilies remained unresolved (Nguyen et al. 2019) (Fig. 2). In our phylogenetic analyses using a 12S rRNA–16S rRNA gene fragment, *M. ninhthuanensis* was recovered as sister to *M. heymonsi* sensu stricto with high nodal support values (1.00/99.2) and in turn, this clade was sister to *M. daklakensis* with nodal support values (1.00/54.1). Furthermore, the results of morphometric analyses (PCA) indicated *M. ninhthuanensis* to be distinct from *M. daklakensis* and *M. 'heymonsi'*.

The discovery of *M. ninhthuanensis* and *M. daklakensis* brings the total number of known species in the genus *Microhyla* to 46 and the species number in Vietnam to 12. The Truong Son Range harbors the highest diversity of the genus *Microhyla* with ten recorded species so far. It shows that there is still an underestimation of species diversity in the *Microhyla* genus (especially *M. heymonsi* group). We strongly recommend focused research to elucidate the taxonomic issues of the *M. heymonsi* group.

In terms of conservation concern, habitat loss is one of the greatest threats to amphibians in Southeast Asia, and the amphibians of the region appear to be particularly vulnerable to habitat alterations (Rowley et al. 2010a, 2010b, 2016). The need for further biological exploration in this region in concert with improved conservation measures is urgent due to intensified logging and road construction, along with increasing agricultural pressure and other human activities (De Koninck 1999; Kuznetsov and Kuznetsova 2011; Laurance 2007; Meijer 1973; Meyfroidt and Lambin 2008).

## Acknowledgements

We would like to thank the directorates of the Bi Doup-Nui Ba National Park, Phuoc Binh National Park, Nam Ka Nature Reserve and Forest Protection Department of Kon Tum Province for supporting our work and issuing relevant permits. Many thanks to L. Iogansen, A. Ostroshabov (St. Petersburg), and T. Y. Nguyen (Hanoi) for their assistance. Thanks to E. J. Sterling (New York) and K. Koy (Berkeley) for providing the map. Research of TTN is funded by the Vietnam National Foundation for Science and Technology Development (NAFOSTED, Grant Number 106.05-2019.334). This research is supported by the Strategic Priority Research Program of the Chinese Academy of Sciences (XDA23080101), NSFC (31471964), The World Academy of Sciences (TWAS), CAS- TWAS president fellowship program, RFBR 19-54-54003 Vietnam, the State program AAAA-A19-119082990107-3 and Ideal Wild.

## References

- Andersson LG (1942) A small collection of frogs from Annam collected in the years 1938–39 by Bertil Bjorkegren. *Arkiv for Zoologi* 34A(6): 1–11.
- Bain RH, Hurley MM (2011) A biogeographic synthesis of the amphibians and reptiles of Indochina. *Bulletin of the American Museum of Natural History*: 1–138. <https://doi.org/10.1206/360.1>
- Bain RH, Nguyen QT (2004) Three new species of narrow-mouth frogs (Genus: *Microhyla*) from Indochina, with comments on *Microhyla annamensis* and *Microhyla palmipes*. *Copeia* (3): 507–524. <https://doi.org/10.1643/CH-04-020R2>
- Boulenger GA (1897) Descriptions of new Malay frogs. In: Hornell J (Ed.) *The Annals and magazine of natural history; zoology, botany, and geology being a continuation of the Annals combined with Loudon and Charlesworth's Magazine of Natural History*. Taylor and Francis, Ltd., London, 106–108. <https://doi.org/10.1080/00222939708680508>
- Boulenger GA (1900) Descriptions of new batrachians and reptiles from the Larut Hills, Perak. In: Hornell J (Ed.) *The Annals and magazine of natural history; zoology, botany, and geology being a continuation of the Annals combined with Loudon and Charlesworth's Magazine of Natural History*. Taylor and Francis, Ltd., London, 186–193. <https://doi.org/10.1080/00222930008678356>
- Boulenger GA (1920) IX. Descriptions of three new frogs in the collection of the British Museum. *Journal of Natural History* 6: 106–108. <https://doi.org/10.1080/00222932008632416>
- Bourret R (1942) *Les Batraciens de l'Indochine*. Institut Océanographique de l'Indochine, Ha Noi, x + 547 pp. + 4 pls. Chen, L.S. (1929) Description of a new species of *Microhyla* from Kwangtung, South China. *China Journal of Science and Arts* 10: 338–339.
- Das I, Haas A (2010) New species of *Microhyla* from Sarawak: Old World's smallest frogs crawl out of miniature pitcher plants on Borneo (Amphibia: Anura: Microhylidae). *Zootaxa* 2571: 37–52. <https://doi.org/10.11646/zootaxa.2571.1.2>

- Das I, Yaakob NS, Sukumaran J (2007) A new species of *Microhyla* (Anura: Microhylidae) from the Malay Peninsula. *Hamadryad* 31(2): 304–314.
- De Koninck R (1999) Deforestation in Viet Nam. International Research Centre, Ottawa, 100 pp.
- Dutta SK, Ray P (2000) *Microhyla sholigari*, a new species of microhylid frog (Anura: Microhylidae) from Karnataka, India. *Hamadryad* 25: 38–44.
- Fei L, Ye C, Jiang JP (2012) Colored Atlas of Chinese Amphibians and Their Distributions. Sichuan Publishing Group, Sichuan Publishing House of Science and Technology, Sichuan, 619 pp.
- Frost DR (2021) Amphibian Species of the World: An Online Reference. Version 6.0. Electronic Database accessible. American Museum of Natural History, New York. <http://research.amnh.org/herpetology/amphibia/index.html> [accessed 2 February 2021]
- Garg S, Suyesh R, Das A, Jiang JP, Wijayathilaka N, Amarasinghe AAT, Alhadi F, Vineeth KK, Aravind NA, Senevirathne G, Meegaskumbura M, Biju SD (2018 “2019”) Systematic revision of *Microhyla* (Microhylidae) frogs of South Asia: a molecular, morphological, and acoustic assessment. *Vertebrate Zoology*. *Senckenberg* 69: 1–71.
- Geissler P, Hartmann T, Ihlow F, Rödder D, Poyarkov NA, Nguyen QT, Ziegler T, Böhme W (2015) The Lower Mekong: an insurmountable barrier to amphibians in southern Indochina? *Biological Journal of the Linnean Society* 114(4): 905–914. <https://doi.org/10.1111/bij.12444>
- Glaw F, Vences M (1997) Anuran eye colouration: definitions, variation, taxonomic implications and possible functions. In: Bohme W, Bischoff W, Ziegler T (Eds) *Herpetologia Bonnensis*, Bonn, 125–138.
- Gorin VA, Solovyeva EN, Hasan M, Okamiya H, Karunarathna DMSS, Pawangkhanant P, de Silva A, Juthong W, Milto KD, Nguyen TL, Suwannapoom C, Haas A, Bickford DP, Das I, Poyarkov NA (2020) A little frog leaps a long way: compounded colonizations of the Indian Subcontinent discovered in the tiny Oriental frog genus *Microhyla* (Amphibia: Microhylidae). *PeerJ* 8: e9411. <https://doi.org/10.7717/peerj.9411>
- Gorin VA, Scherz MD, Korost DV, Poyarkov NA (2021) Consequences of parallel miniaturisation in Microhyliinae (Anura, Microhylidae), with the description of a new genus of diminutive South East Asian frogs. *Zoosystematics and Evolution* 97: 21–54. <https://doi.org/10.3897/zse.97.57968>
- Hall TA (1999) BioEdit: a user-friendly biological sequence alignment editor and analysis program for Windows 95/98/NT. In: *Nucleic acids symposium series*. Information Retrieval Ltd., London, 95–98.
- Hammer O, Harper DAT, Ryan PD (2001) PAST: Paleontological Statistics software package for education and data analysis. *Palaeontologia Electronica* 4(1): 1–9.
- Hasan M, Islam MM, Khan MMR, Alam MS, Kurabayashi A, Igawa T, Kuramoto M, Sumida M (2012) Cryptic anuran biodiversity in Bangladesh revealed by mitochondrial 16S rRNA gene sequences. *Zoological Science* 29(3): 162–172. <https://doi.org/10.2108/zsj.29.162>
- Hasan M, Islam MM, Kuramoto M, Kurabayashi A, Sumida M (2014) Description of two new species of *Microhyla* (Anura: Microhylidae) from Bangladesh. *Zootaxa* 3755(5): 401–408. <https://doi.org/10.11646/zootaxa.3755.5.1>

- Hasan M, Razzaque MA, Sarker AK, Kuramoto M, Sumida M (2015) Genetic variation, advertisement call, and morphometry of *Microhyla nilphamariensis* from Bangladesh. *Philippine Journal of Systematic Biology* 9: 63–80.
- Hillis DM, Bull JJ (1993) An empirical test of bootstrapping as a method for assessing confidence in phylogenetic analysis. *Systematic Biology* 42: 182–192. <https://doi.org/10.1093/sysbio/42.2.182>
- Hoang VC, Nguyen QT, Pham TC, Nguyen TT (2013) Herpetofaunal diversity of Kon Ka Kinh National Park, Gia Lai Province. In: Proceedings of the 5<sup>th</sup> National Scientific Conference on Ecology and Biological Resources. Hanoi Agricultural Publisher, Hanoi, 401–409.
- Hoang VC, Luong MA, Nguyen QT, Orlov N, Chen Y, Wang B, Jiang JP (2020) A new species of *Microhyla* (Amphibia: Anura: Microhylidae) from Langbian Plateau, Central Vietnam. *Asian Herpetological Research* 11(3): 161–182.
- Howlader MSA, Nair A, Gopalan SV, Merilä J (2015) A New Species of *Microhyla* (Anura: Microhylidae) from Nilphamari, Bangladesh. *PLOS One* 10(3): e0119825. <https://doi.org/10.1371/journal.pone.0119825>
- Huelsenbeck JP, Hillis DM (1993) Success of phylogenetic methods in the four-taxon case. *Systematic Biology* 42(3): 247–264. <https://doi.org/10.1093/sysbio/42.3.247>
- Inger RF (1989) Four new species of frogs from Borneo. *Malayan Nature Journal* 42: 229–243.
- Inger RF, Frogner KJ (1979) New species of narrow-mouth frogs (genus *Microhyla*) from Borneo. *The Sarawak Museum Journal* 27: 311–322.
- Inger RF, Darevsky IS, Orlov NL (1999) Frogs of Vietnam: a report on new collections. *Feldiana Zoology* 92: 1–46.
- IUCN Standards and Petitions Subcommittee (2017) Guidelines for Using the IUCN Red List Categories and Criteria. Version 13. Prepared by the Standards and Petitions Subcommittee. <http://www.iucnredlist.org/documents/RedListGuidelines.pdf> [accessed January 2021]
- Khatiwada JR, Shu GC, Wang SH, Thapa A, Wang B, Jiang JP (2017) A new species of the genus *Microhyla* (Anura: Microhylidae) from Eastern Nepal. *Zootaxa* 4254(2): 221–239. <https://doi.org/10.11646/zootaxa.4254.2.4>
- Kumar S, Stecher G, Tamura K (2016) MEGA7: Molecular Evolutionary Genetics Analysis version 7.0 for bigger datasets. *Molecular Biology and Evolution* 33(7): 1870–1874. <https://doi.org/10.1093/molbev/msw054>
- Kuznetsov A, Kuznetsova S (2011) Botany of Bidoup-Nui Ba National Park. In: D. Nguyen and Kuznetsov, A. (Eds.), Biodiversity and Ecological Characteristics of Bidoup Nui Ba National Park. Vietnam Academy of Science and Technology Publishing House for Science and Technology, Hanoi, 37–105.
- Laurance WF (2007) Forest destruction in tropical Asia. *Current Science* 93(11): 1544–1550.
- Leaché AD, Reeder TW (2002) Molecular systematics of the eastern fence lizard (*Sceloporus undulatus*): a comparison of parsimony, likelihood, and Bayesian approaches. *Systematic Biology* 51: 44–68. <https://doi.org/10.1080/106351502753475871>
- Li S, Zhang M, Xu N, Lu J, Jiang JP, Liu J, Wei G, Wang B (2019) A new species of the genus *Microhyla* (Amphibia: Anura: Microhylidae) from Guizhou Province, China. *Zootaxa* 4624: 551–575. <https://doi.org/10.11646/zootaxa.4624.4.7>

- Matsui M, Ito H, Shimada T, Ota H, Saidapur SK, Khonsue W, Tanaka-Ueno T, Wu GF (2005) Taxonomic relationships within the Pan-Oriental narrow-mouth toad *Microhyla ornata* as revealed by mtDNA analysis (Amphibia, Anura, Microhylidae). *Zoological Science* 22(4): 489–495. <https://doi.org/10.2108/zsj.22.489>
- Matsui M (2011) Taxonomic revision of one of the Old World's smallest frogs, with description of a new Bornean *Microhyla* (Amphibia, Microhylidae). *Zootaxa* 2814(1): 33–49. <https://doi.org/10.11646/zootaxa.2814.1.3>
- Matsui M, Hamidy A, Belabut DM, Ahmad N, Panha S, Sudin A, Khonsue W, Oh HS, Yong HS, Jiang JP (2011) Systematic relationships of Oriental tiny frogs of the family Microhylidae (Amphibia, Anura) as revealed by mtDNA genealogy. *Molecular Phylogenetics and Evolution* 61(1): 167–176. <https://doi.org/10.1016/j.ympev.2011.05.015>
- Matsui M, Hamidy A, Eto K (2013) Description of a new species of *Microhyla* from Bali, Indonesia (Amphibia, Anura). *Zootaxa* 3670(4): 579–590. <https://doi.org/10.11646/zootaxa.3670.4.9>
- Meijer W (1973) Devastation and regeneration of lowland dipterocarp forests in Southeast Asia. *BioScience* 23(9): 528–533. <https://doi.org/10.2307/1296481>
- Meyfroidt P, Lambin EF (2008) Forest transition in Vietnam and its environmental impacts. *Global Change Biology* 14(6): 1319–1336. <https://doi.org/10.1111/j.1365-2486.2008.01575.x>
- Nguyen TL, Poyarkov NA, Nguyen TT, Nguyen TA, Tran VH, Gorin VA, Murphy RW, Nguyen NS (2019) A new species of the genus *Microhyla* Tschudi, 1838 (Amphibia: Anura: Microhylidae) from Tay Nguyen Plateau, Central Vietnam. *Zootaxa* 4543: 549–580. <https://doi.org/10.11646/zootaxa.4543.4.4>
- Nguyen TT, Pham TC, Nguyen TQT, Ninh TH, Ziegler T (2017) A new species of *Rhacophorus* (Amphibia: Anura: Rhacophoridae) from Vietnam. *Asian Herpetological Research* 8: 221–234.
- Parker HW (1928) The brevicipitid frogs of the genus *Microhyla*. *Journal of Natural History* 2(11): 473–499. <https://doi.org/10.1080/00222932808672911>
- Parker HW (1934) Monograph of the frogs of the family Microhylidae. Trustees of the British Museum, London, 212 pp.
- Parker HW, Osman HWC (1948) Frogs of the genus *Microhyla* from Ceylon. *Journal of Natural History* 1(10): 759–764. <https://doi.org/10.1080/00222934808653944>
- Peloso PL, Frost DR, Richards SJ, Rodrigues MT, Donnellan S, Matsui M, Raxworthy CJ, Biju S, Lemmon EM, Lemmon AR (2016) The impact of anchored phylogenomics and taxon sampling on phylogenetic inference in narrow-mouthed frogs (Anura, Microhylidae). *Cladistics* 32 (2): 113–140. <https://doi.org/10.1111/cla.12118>
- Pillai R (1977) On two frogs of the family Microhylidae from Andamans including a new species. *Proceedings of the Indian Academy of Sciences, Section-B*: 135–138.
- Posada D, Crandall KA (1998) Modeltest: testing the model of DNA substitution. *Bioinformatics* 14(9): 817–818. <https://doi.org/10.1093/bioinformatics/14.9.817>
- Poyarkov NA, Vassilieva AB, Orlov N, Galoyan EA, Tran D, Le TTD, Kretova VD, Geissler P (2014) Taxonomy and distribution of narrow-mouth frogs of the genus *Microhyla* Tschudi,

- 1838 (Anura: Microhylidae) from Vietnam with descriptions of five new species. *Russian Journal of Herpetology* 21(2): 89–148.
- Poyarkov NA, Gorin AV, Zaw T, Kretova DV, Gogoleva SS, Pawangkhanant P, Che J (2019) On the road to Mandalay: contribution to the *Microhyla* Tschudi, 1838 (Amphibia: Anura: Microhylidae) fauna of Myanmar with description of two new species. *Zoological Research* 40(4): 244–276. <https://doi.org/10.24272/j.issn.2095-8137.2019.044>
- Poyarkov NA, Nguyen VT, Trofimets VA, Gorin AV (2020) A new cryptic species of the genus *Microhyla* (Amphibia: Microhylidae) from Langbian Plateau, Vietnam. *Taprobanica. The Journal of Asian Biodiversity* 9: 136–163. <https://doi.org/10.47605/taprov9i2.228>
- Rambaut A, Drummond A (2009) TRACER, version 1.5. <http://beast.community/tracer>
- Ronquist F, Teslenko M, van der Mark P, Ayres DL, Darling A, Höhna S, Larget B, Liu L, Suchard MA, Huelsenbeck JP (2012) MrBayes 3.2: efficient Bayesian phylogenetic inference and model choice across a large model space. *Systematic Biology* 61: 539–542. <https://doi.org/10.1093/sysbio/sys029>
- Rowley JJ, Brown R, Bain R, Kusriani M, Inger RE, Stuart BL, Wogan G, Thy N, Chan-ard T, Cao TT (2010a) Impending conservation crisis for southeast Asian amphibians. *Biology Letters* 6(3): 336–338. <https://doi.org/10.1098/rsbl.2009.0793>
- Rowley JJ, Hoang DH, Le TTD, Dau QV, Cao TT (2010b) A new species of *Leptolalax* (Anura: Megophryidae) from Vietnam and further information on *Leptolalax tuberosus*. *Zootaxa* 2660: 33–45.
- Rowley JJ, Tran TAD, Le TTD, Dau QV, Peloso PLV, Nguyen QT, Hoang DH, Nguyen TT, Ziegler T (2016) Five new, microendemic Asian leaf-litter frogs (*Leptolalax*) from the southern Annamite mountains, Vietnam. *Zootaxa* 4085(1): 063–102. <https://doi.org/10.11646/zootaxa.4085.1.3>
- Savage JM (1975) Systematics and distribution of the Mexican and Central American stream frogs related to *Eleutherodactylus rugulosus*. *Copeia* 1975: 254–306. <https://doi.org/10.2307/1442883>
- Seshadri KS, Singal R, Priti H, Ravikanth G, Vidisha MK, Saurabh S, Pratik M, Gururaja KV (2016) *Microhyla laterite* sp. nov., a new species of *Microhyla* Tschudi, 1838 (Amphibia: Anura: Microhylidae) from a laterite rock formation in South West India. *PLOS One* 11(3): e0149727. <https://doi.org/10.1371/journal.pone.0149727>
- Simmons JE (2002) *Herpetological collecting and collections management*. Revised edition. Society for the Study of Amphibians and Reptiles. *Herpetological Circular* 31: 1–153.
- Simon C, Frati F, Beckenbach A, Crespi B, Liu H, Flook P (1994) Evolution, Weighting, and Phylogenetic Utility of Mitochondrial Gene Sequences and a Compilation of Conserved Polymerase Chain Reaction Primers. *Annals of the Entomological Society of America* 87(6): 651–701. <https://doi.org/10.1093/aesa/87.6.651>
- Smith M (1923) Notes on reptiles and batrachians from Siam and Indo-China (No. 2). *Journal of the Natural History Society of Siam* 6(1): 47–53.
- Tanabe AS (2011) Kakusan 4 and Aminosan: two programs for comparing nonpartitioned, proportional and separate models for combined molecular phylogenetic analyses of multi-locus sequence data. *Molecular Ecology Resources* 11: 914–921. <https://doi.org/10.1111/j.1755-0998.2011.03021.x>

- Tavaré S (1986) Some probabilistic and statistical problems in the analysis of DNA sequences. Lectures on Mathematics in the Life Sciences 17: 57–86.
- Thompson JD, Gibson TJ, Plewniak F, Jeanmougin F, Higgins DG (1997) The CLUSTAL\_X windows interface: flexible strategies for multiple sequence alignment aided by quality analysis tools. *Nucleic acids research* 25(24): 4876–4882. <https://doi.org/10.1093/nar/25.24.4876>
- Tschudi JJ (1838) Classification der Batrachier mit Berücksichtigung der fossilen Thiere dieser Abtheilung der Reptilien. Petitpierre, Neuchâtel, 99 pp. <https://doi.org/10.5962/bhl.title.4883>
- Van Bocxlaer I, Roelants K, Biju SD, Nagaraju J, Bossuyt F (2006) Late Cretaceous vicariance in Gondwanan amphibians. *PLOS One* 1: e74. <https://doi.org/10.1371/journal.pone.0000074>
- Vineeth KK, Radhakrishna U, Godwin R, Anwasha S, Rajashekhar KP, Aravind N (2018) A new species of *Microhyla* Tschudi, 1838 (Anura: Microhylidae) from West Coast of India: an integrative taxonomic approach. *Zootaxa* 4420: 151–179. <https://doi.org/10.11646/zootaxa.4420.2.1>
- Vogt T (1913) Über die Reptilien- und Amphibienfanna der Insel Hainan. *Sitzungsberichte der Gesellschaft Naturforschender Freunde zu Berlin, Berlin*, 219–221.
- Wijayathilaka N, Garg S, Senevirathne G, Karunarathna N (2016) A new species of *Microhyla* (Anura: Microhylidae) from Sri Lanka: an integrative taxonomic approach. *Zootaxa* 4066(3): 331–342. <https://doi.org/10.11646/zootaxa.4066.3.9>
- Yuan ZY, Suwannapoom C, Yan F, Poyarkov NA, Nguyen SN, Chen HM, Chomdej S, Murphy RW, Che J (2016) Red River barrier and Pleistocene climatic fluctuations shaped the genetic structure of *Microhyla fissipes* complex (Anura: Microhylidae) in southern China and Indochina. *Current Zoology* 62(6): 531–543. <https://doi.org/10.1093/cz/zow042>
- Zhang MH, Fei L, Ye CY, Wang YF, Wang B, Jiang JP (2018) A new species of genus *Microhyla* (Amphibia: Anura: Microhylidae) from Zhejiang Province, China. *Asian Herpetological Research* 9: 135–148.
- Zhang P, Papenfuss TJ, Wake MH, Qu L, Wake DB (2008) Phylogeny and biogeography of the family Salamandridae (Amphibia: Caudata) inferred from complete mitochondrial genomes. *Molecular Phylogenetics and Evolution* 49(6): 586–597. <https://doi.org/10.1016/j.ympev.2008.08.020>

## Supplementary material I

### Tables S1–S6

Authors: Chung Van Hoang, Tao Thien Nguyen, Hoa Thi Ninh, Anh Mai Luong, Cuong The Pham, Truong Quang Nguyen, Nikolai L. Orlov, Youhua Chen, Bin Wang, Thomas Ziegler, Jianping Jiang

Data type: species data

Explanation note: **Table S1.** Specimens of *Microhyla* and *Nanohyla* used in the morphological and molecular analyses. **Table S2.** Specimens and sequences of *Microhyla* and outgroup Microhylidae representatives used in molecular analyses. **Table S3.** Uncorrected (“p”) distance matrix showing percentage pair-wise genetic divergence 12S rRNA16S rRNA between members of the *Microhyla* species group. **Table S4.** Measurements (in mm) and proportions of the type series of *M. neglecta*, *M. pineticola*, *Microhyla ninhthuanensis* sp. nov., *Microhyla daklakensis* sp. nov., and *M. 'heymonsi'*. **Table S5.** Selected diagnostic characters for the species in the genus *Microhyla* (modified from Poyakov et al. 2014; Nguyen et al. 2019). All measurements are given in millimeters (mm). **Table S6.** Variable loadings for principal components with Eigenvalue greater than 0.01, from morphometric characters corrected by SVL. All measurements are given in millimeters (mm).

Copyright notice: This dataset is made available under the Open Database License (<http://opendatacommons.org/licenses/odbl/1.0/>). The Open Database License (ODbL) is a license agreement intended to allow users to freely share, modify, and use this Dataset while maintaining this same freedom for others, provided that the original source and author(s) are credited.

Link: <https://doi.org/10.3897/zookeys.1036.56919.suppl1>

# Revision and phylogeny of the genus *Loxoneptera* Hampson, 1896 (Lepidoptera, Crambidae, Pyraustinae), based on morphology and molecular data

Lanbin Xiang<sup>1\*</sup>, Kai Chen<sup>1,3\*</sup>, Dandan Zhang<sup>1,2</sup>

**1** School of Life Sciences, Sun Yat-sen University, Guangzhou, Guangdong 510275, China **2** School of Ecology, Sun Yat-sen University, Guangzhou, Guangdong 510275, China **3** School of Life Sciences, Jiaying University, Meizhou, 514015, China

Corresponding author: Dandan Zhang ([zhangdd6@mail.sysu.edu.cn](mailto:zhangdd6@mail.sysu.edu.cn))

Academic editor: Colin Plant | Received 1 February 2021 | Accepted 22 March 2021 | Published 5 May 2021

<http://zoobank.org/B6A437B0-E1B5-4E67-B526-53084C5185FE>

**Citation:** Xiang L, Chen K, Zhang D (2021) Revision and phylogeny of the genus *Loxoneptera* Hampson, 1896 (Lepidoptera, Crambidae, Pyraustinae), based on morphology and molecular data. ZooKeys 1036: 75–98. <https://doi.org/10.3897/zookeys.1036.63814>

## Abstract

The genus *Loxoneptera* Hampson, 1896 is revised based on external appearance and genitalia. It is comprised of eleven species, of which three are described as new species from China: *L. crassiuncata* Chen & Zhang, **sp. nov.**, *L. triangularis* Chen & Zhang, **sp. nov.**, and *L. rectacerosa* Chen & Zhang, **sp. nov.**; six species are proposed as new combinations: *L. carnealis* (Swinhoe, 1895), **comb. nov.**, *L. medialis* (Caradja, 1925), **comb. nov.**, *L. pentasaris* (Meyrick, 1932), **comb. nov.**, *L. bipunctalis* (Hampson, 1912), **comb. nov.**, *L. brevipalpis* (Snellen, 1890), **comb. nov.**, and *L. dichroma* (Moore, 1888), **comb. nov.** A new replacement name, *L. hampsoni* Chen & Zhang, **nom. nov.**, is proposed for *L. carnealis* Hampson, 1896, the type species of the genus, because it is a secondary homonym of *L. carnealis* (Swinhoe, 1895), **comb. nov.** External characters and genitalia morphology of all species are figured. Nucleotide sequences of COI, 16S rRNA, 28S rRNA, and EF-1 $\alpha$  were used for the molecular analysis and phylogeny of *Loxoneptera* species.

## Keywords

*Calamochrous*, China, molecular phylogeny, new combinations, new species

\* These authors contributed to the work equally and should be regarded as co-first authors.

## Introduction

The genus *Loxoneptera* was established as a monotypic genus by Hampson (1896), based on *L. carnealis* Hampson, 1896 from Sikkim and Assam. Subsequently, Swinhoe (1906) described a new species, *L. albicostalis*, from Padang, Sumatra, mainly based on appearance of the wings. The genus was not investigated again until Chen et al. (2018) who, for the first time, recorded these two species in China (see also Nuss et al. 2003–2021). They noted that *Loxoneptera* was paraphyletic, with respect to two species of *Calamochrous* Lederer, 1863, i.e., *C. carnealis* (Swinhoe, 1895) and *C. medialis* Caradja, 1925, appeared as terminal lineages within *Loxoneptera* clade based on a molecular phylogenetic analysis. But *C. carnealis* and *C. medialis* were not transferred to *Loxoneptera* in their study.

Within the additional Chinese specimens collected, three undescribed species of *Loxoneptera* were recognised. Moreover, a few species of *Calamochrous* and *Anania* Hübner, 1823 were found to be congeneric with species of *Loxoneptera*. The aim of this study is to diagnose *Loxoneptera* based on external and genital characters, to clarify the species included in the genus, and to provide a preliminary phylogenetic hypothesis based on selected genetic markers.

## Materials and methods

The material studied, including the types of the newly described species, are all deposited at the Museum of Biology, Sun Yat-sen University, China (**SYSBM**) except those stored in the following institutions: Insect Collection of the College of Life Sciences, Nankai University, China (**NKU**), Forest Canopy Ecology Lab, Yunnan, China (**FCEL**), “Grigore Antipa” National Museum of Natural History, Romania (**MGAB**), and Natural History Museum, London, United Kingdom (**NHMUK**). Slides of genitalic dissections were prepared according to Robinson (1976) and Li and Zheng (1996), with some modifications. Genitalia terminology follow Klots (1970), Munroe (1976), Maes (1995), and Kristensen (2003). Images of the adults were taken using a Canon EOS 60D camera provided with a Canon 100 mm macro lens; the genitalia images were taken using Zeiss Axio Scope.A1 in combination with a Zeiss AxioCam camera and the Axio Vision SE64 program on a Windows PC; source images were then aligned and stacked on Helicon Focus to obtain a fully sharpened composite image. All images were edited using Adobe Photoshop SC5.

Ten species in four genera were included in the molecular phylogenetic analyses (Table 1). *Euclasta stoetzneri* (Caradja, 1927) was chosen as the outgroup because it has been inferred as sister-group of Pyraustini and Portnetomorphini in Pyraustinae (Mally et al. 2019). One species of *Sclerocona* Meyrick, 1890 and three species of *Eumorphobotys* Munroe & Mutuura, 1969 were also included as related genera to *Loxoneptera* according to Chen et al. (2018). Total DNA was extracted from two legs, and

**Table 1.** Species sampled for the molecular phylogenetic analysis.

Genus	Species	Voucher	Locality	GenBank accession number				References
				COI	16S	EF-1 $\alpha$	28S	
<i>Eumorphobotys</i>	<i>eumorphalis</i>	SYSULEP0046	Fujian	MG739574	MG739586	MG739598	MG739609	Chen et al. 2018
		SYSULEP0047	Fujian	MG739575	MG739587	MG739599	MG739610	Chen et al. 2018
	<i>concauvuncus</i>	SYSULEP0042	Yunnan	MG739571	MG739583	MG739595	MG739606	Chen et al. 2018
		SYSULEP0175	Guangxi	MG739581	MG739593	MG739604	MG739616	Chen et al. 2018
	<i>horakae</i>	SYSULEP0043	Sichuan	MG739572	MG739584	MG739596	MG739607	Chen et al. 2018
SYSULEP0172		Sichuan	MG739580	MG739592	N/A	MG739615	Chen et al. 2018	
<i>Loxoneptera</i>	<i>hampsoni</i>	SYSULEP0166	Hainan	MG739579	MG739591	MG739603	MG739614	Chen et al. 2018
		SYSULEP0174	Hainan	MW736545	MW736550	MW736555	MW728364	Present study
	<i>albicastalis</i>	SYSULEP0162	Yunnan	MG739578	MG739590	MG739602	MG739613	Chen et al. 2018
		<i>medialis</i>	SYSULEP0096	Hainan	MG739576	MG739588	MG739600	MG739611
	SYSULEP0171		Guangdong	MW736546	MW736551	MW736556	MW728365	Present study
	SYSULEP0173	Guangdong	MW736547	MW736552	N/A	N/A	Present study	
	<i>rectacerosa</i>	SYSULEP0170	Yunnan	MW736548	MW736553	N/A	N/A	Present study
	<i>carnealis</i>	SYSULEP0044	Guizhou	MG739573	MG739585	MG739597	MG739608	Chen et al. 2018
		SYSULEP0186	Yunnan	MW736549	MW736554	MW736557	MW728366	Present study
	<i>Sclerocona</i>	<i>acutella</i>	SYSULEP0152	Macau	MG739577	MG739589	MG739601	MG739612
<i>Euclasta</i>	<i>stoetzneri</i>	SYSULEP0334	Shannxi	MT738696	MT734412	MT724335	MT734404	Zhang et al. 2020

sometimes from the abdomen of the dry specimens using the TIANGEN DNA extraction kit following the manufacturer's instructions. The nucleotide sequences of two mitochondrial genes, cytochrome c oxidase subunit I (COI) and 16S ribosomal RNA (16S rRNA), and two nuclear genes, 28S ribosomal RNA (28S rRNA) and Elongation factor-1 alpha (EF-1 $\alpha$ ) were selected for study. Primers used in this study and all PCRs performed are the same as in Zhang et al. (2020). PCR products were confirmed with 1.5% agarose gel electrophoresis in TAE buffer, then were purified and direct-sequenced at Majorbio Bio-pharm Technology Co., Ltd (Guangzhou), utilising the same primers used for PCR amplification.

The sequences were aligned using Clustal W (Thompson et al. 1994) in MEGA 6 (Tamura et al. 2013) with default settings. The aligned matrix was corrected by eye. Gaps were treated as missing data. Phylogenetic analyses were inferred using Bayesian inference (BI) method in MrBayes 3.2.6 (Ronquist et al. 2012) and maximum likelihood (ML) in RAxML 8.2.10 (Stamatakis 2014). BI analysis was run with independent parameters for the COI, the 16S rRNA and 28S rRNA gene partitions under the GTR + G model, the EF-1 $\alpha$  gene partition under the GTR + G + I model, as suggested by jModelTest 0.1.1 (Posada 2008). Two independent runs, each with four Markov Chain Monte Carlo (MCMC) simulations, were performed for 20 million generations sampled every 1000<sup>th</sup> generation. The first 25% trees were discarded as burn-in, and posterior probabilities (PP) were determined from remaining trees. ML analysis was executed under the GTR + G model for all gene partitions and with 1000 iterations for the bootstrap test. The pairwise Kimura 2-Parameter (K2P) distances between species were calculated from the COI gene using MEGA 6 (Tamura et al. 2013).

## Results

### Phylogenetic relationships

The concatenated dataset of four genes consisted of 2511 nucleotide positions (658 for COI, 463 for 16S rRNA, 619 for 28S rRNA, and 771 for EF-1 $\alpha$ ). Both BI and ML analyses of the concatenated dataset inferred congruent topologies with only subtle differences in posterior probability and bootstrap values probability (Fig. 1). The monophyly of *Loxoneptera* is strongly supported in BI but weakly supported in ML (PP = 0.93, BS = 65). *Eumorphobotys* is in a sister group position to *Loxoneptera* with robust support (PP = 1.00, BS = 100).

The results of the current phylogenetic analyses support that the undescribed species (here named as *L. rectacerosa* sp. nov.) should be placed in *Loxoneptera*, and that *L. carnealis* (Swinhoe, 1895) comb. nov. and *L. medialis* (Caradja, 1925) comb. nov. should be transferred from *Calamochrous* Lederer, 1863 to *Loxoneptera*. Within the genus, *L. medialis* + *L. rectacerosa* form a sister group with robust support (PP = 1.00, BS = 99), while *L. carnealis* is the sister group to *L. medialis* + *L. rectacerosa* (PP = 1.00, BS = 100). *Loxoneptera albicostalis* is associated with the clade *L. carnealis* + (*L. medialis* + *L. rectacerosa*), although with relatively low support (PP = 0.78, BS = 52). *Loxoneptera hampsoni* is the first-diverging species with strong support in the BI analysis (PP = 0.93), but with relatively low support in the ML analysis (BS = 65).

Pairwise distances of the barcoding region (COI) are given in Table 2. The genetic distances between *Loxoneptera* and other genera range from 7.7% (*Eumorphobotys*) to 12.4% (*Sclerocona*). Interspecific genetic distances within *Loxoneptera* range from 4.2% (*L. medialis* to *L. rectacerosa*) to 11.2% (*L. hampsoni* to *L. carnealis*), while intraspecific genetic distances in *Loxoneptera* range from 0 % (*L. medialis*) to 0.3% (*L. carnealis*).

### Taxonomic account

#### *Loxoneptera* Hampson, 1896

*Loxoneptera* Hampson, 1896: 405. Type species: *Loxoneptera carnealis* Hampson, 1896, by original designation.

**Diagnosis.** In external appearance, the species of *Loxoneptera* are similar to species of *Eumorphobotys* Munroe & Mutuura, 1969 in the long and porrect labial palpus, the usually concolorous wings with no obvious pattern and the straight termen of forewing, but can be best distinguished by the triangular uncus, the rod-shaped dorsal projection of transtilla bearing long and thick hair at the apex, and the hook-shaped ventral sella in the male genitalia. In the female genitalia, the ductus bursae of *Loxoneptera* is shorter and stouter than that of *Eumorphobotys*. These two genera are also different in the shape of the signum, if present a nearly rhomboid signum with connected carina, or reduced into a keel-like carina in *Loxoneptera*, and a nar-

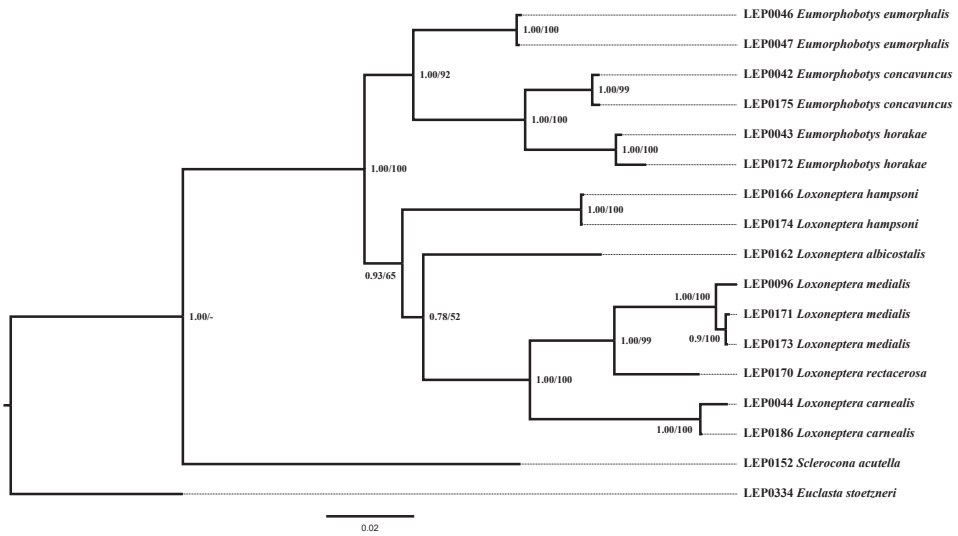


**Figure 1.** Phylogenetic hypothesis inferred from Bayesian inference. Numbers on branches indicate Bayesian posterior probabilities and ML bootstrap values, respectively.

rowly rhomboid signum with carina interrupted in *Eumorphobotys*. Eighth sternite in males of *Loxoneptera* is slightly sclerotised, with two slender and sclerotised anterolateral processes.

**Description. Head.** Frons oblique, slightly protruding. Vertex with moderately raised scales projecting between antennae. Labial palpus  $\sim 2\text{--}2.5 \times$  eye diameter; second segment obliquely upward, third segment long and porrect. Maxillary palpus small. **Thorax.** Legs unmodified usually, outer spur  $1/3$  to  $1/2$  the length of inner spur, sometimes outer spur minute. **Wings.** Forewing elongated triangular, termen obliquely straight to slightly curved; discal cell  $\sim 1/2$  length of wing,  $R_1$  from  $\sim 3/4$  of anterior margin of cell,  $R_3$  and  $R_4$  stalked to more than half of  $R_4$ ,  $R_5$  free from anterior angle of cell, parallel to stalked  $R_3+R_4$  at base, then diverging, discocellular veins concavely curved,  $M_1$  close to  $R_5$  at base, free from discocellular veins and close to anterior angle of cell,  $M_2$ ,  $M_3$  and  $CuA_1$  from posterior angle of cell,  $CuA_2$  from  $4/5$  of the posterior margin of cell, 1A faintly sinuate to tornus; 2A forming complete loop and distally recurved before joining 1A; usually only with orbicular and reniform stigmata, sometimes no pattern. Hindwing fan-shaped, termen rounded; discal cell less than half length of wing,  $Sc+R_1$  and  $Rs$  anastomosed to half of  $Rs$ , discocellulars concave,  $M_2$ ,  $M_3$  and  $CuA_1$  from posterior angle of discal cell,  $CuA_2$  from  $4/5$  of the posterior margin of cell; without obviously spot. **Abdomen.** Eighth sternite in male with two slender and sclerotised anterolateral processes, pointed or slightly stout (Fig. 14).

**Male genitalia.** Uncus triangular, glabrous or with few hair-like setae. Tegumen trapezoid. Saccus nearly triangular. Transtilla with developed ventral process, extending a rod-shaped projection dorsad, usually long, curved, and slender, and terminal part with many long hairs. Valva tongue-shaped; dorsal sella membranous, ventral sella



usually with a hook-shaped, strongly sclerotised process, dorso-distal sella presented as a sclerite and usually extended as a long, hook-shaped, sclerotised process; editum absent or not obvious; sacculus broad. Juxta with basal part rivet-shaped, remainder usually with two long and slender bifid arms. Phallus tubular, vesica with spine-shaped cornuti and sometimes deciduous cornuti.

**Female genitalia.** Ovipositor lobes flat, densely setose. Anterior apophyses longer than posterior apophyses. Antrum sclerotised, cup-shaped or bowl-shaped; colliculum well developed and sclerotised; ductus seminalis entering near anterior end of colliculum; ductus bursae short and stout, almost as long as length of corpus bursae; corpus bursae oval, appendix bursae oval or absent, signum nearly rhomboid, with a carina not interrupted in middle, sometimes signum reduced into a carina, sometimes absent.

**Distribution.** China, India, Indonesia, Malaysia.

### Key to species of *Loxoneptera*

- 1 Forewing reddish brown; hindwing black-brown in male, with a triangular patch presented near the posterior angle of cell ..... **2**
- Forewing colour paler, not reddish brown; hindwing pale yellow, triangular patch absent..... **3**
- 2 Costal band of forewing white, fringe white and with basal 1/4 black-brown (Fig. 4), a small triangular indentation presented on the 1/3 of posterior margin in male; ventral sella with a long hook-shaped process; vesica without cornutus (Fig. 16) ..... ***L. albicostalis***
- Costal band of forewing brown, fringe pale yellow and with basal half black-brown (Fig. 5), posterior margin of male smooth; ventral sella with a relatively short and stick-like process; vesica with a horn-shaped, strongly sclerotised cornutus apically (Fig. 17) ..... ***L. crassiuncata***
- 3 Forewing with pale yellow stripes between veins, posterior margin with a small triangular indentation and a group of black-brown scales in male (Fig. 2); juxta medially concave inwardly (Fig. 15)..... ***L. hampsoni***
- Forewing without pale yellow stripe between veins, posterior margin arc-shaped, without indentation and a group of black-brown scales in male; juxta normal..... **4**
- 4 Distal part of phallus with a long and pointed spine, longer than the length of phallus (Fig. 18) ..... ***L. carnealis***
- Distal part of phallus without spine, or spine shorter than the length of phallus..... **5**
- 5 Distal part of juxta with a strongly sclerotised and narrowly triangular process (Fig. 19) ..... ***L. triangularis***
- Distal part of juxta without process..... **6**
- 6 Distal end of phallus densely decorated with short spines (Fig. 22) ..... ***L. pentasaris***
- Distal end of phallus not decorated with short spines ..... **7**

- 7 Dorsal margin of valva forming a break angle subapically (Fig. 20) ..... *L. rectacerosa*  
 – Dorsal margin of valva without break angle ..... **8**  
 8 Dorsal margin of valva convex, dorso-distal sella extended outwards and not beyond the end of valva (Fig. 21) ..... *L. medialis*  
 – Dorsal margin of valva somewhat concave, dorso-distal sella extended ventrad and beyond the ventral margin of valva ..... **9**  
 9 Forewing with a stripe along posterior margin of cell (Fig. 13); ventral-distal wall of phallus weakly sclerotised and obliquely extended into a process (Fig. 25) ..... *L. dichroma*  
 – Forewing absent stripe on posterior margin of cell; wall of phallus not sclerotised ..... **10**  
 10 Distal part of phallus with a heavily sclerotised, spiny and thumb-shaped cornutus (Fig. 24) ..... *L. brevipalpis*  
 – Distal part of phallus with a weakly sclerotised, slice-shaped cornutus (Fig. 23) ..... *L. bipunctalis*

***Loxoneptera hampsoni* Chen & Zhang, nom. nov.**

Figs 2, 3, 15, 26

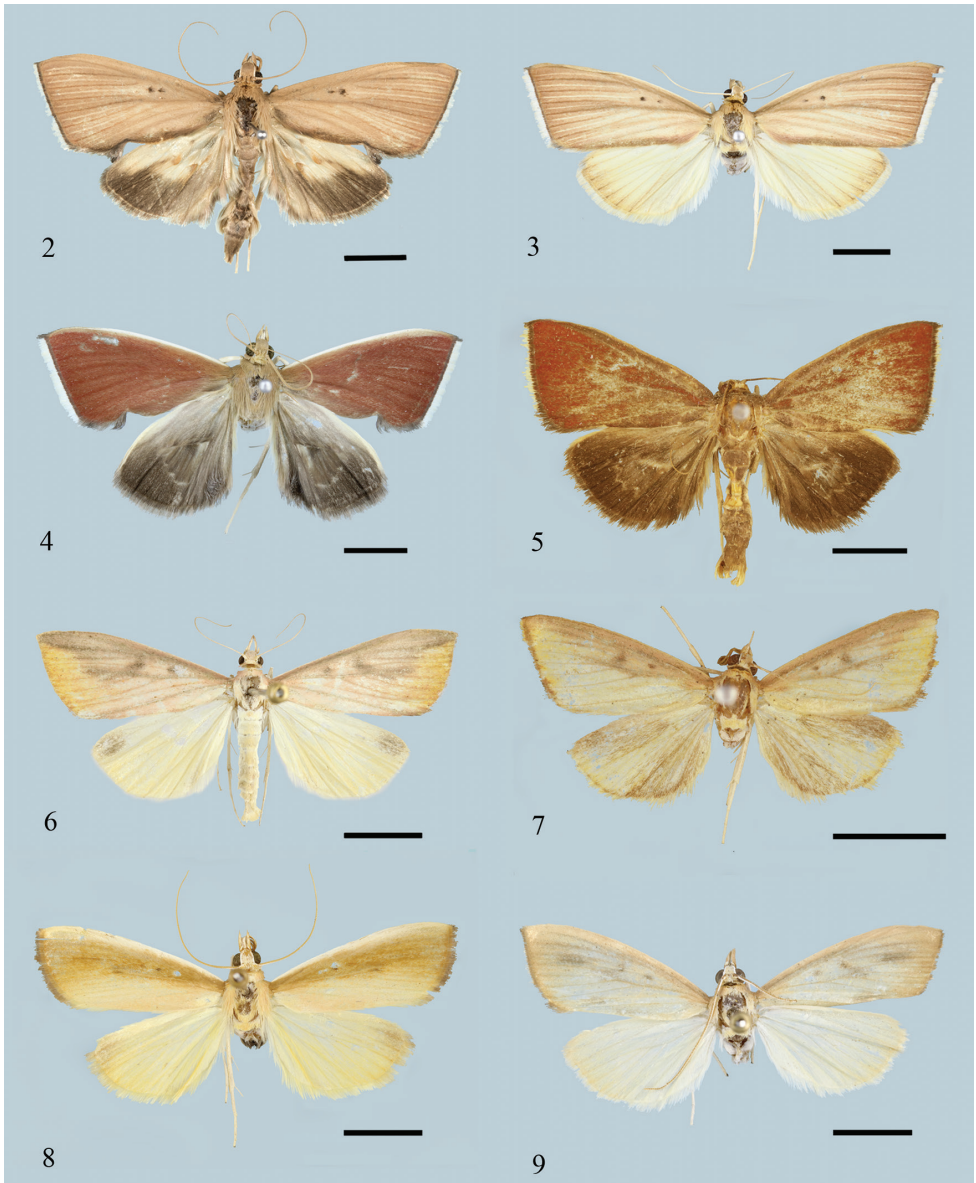
*Loxoneptera carnealis* Hampson, 1896: 406, fig. 219 (a junior secondary homonym of *Notaspis carnealis* Swinhoe, 1895). TL: India (Sikkim). TD: NHMUK.

**Material examined. Type material.** Type ♂, Sikkim, O. Müller [Coll.], Pyralidae Brit. Mus. Slide No. 9752 (NHMUK).

**Other material examined. CHINA. Hainan:** 1♂, Mt. Limushan, 5.V.2011, leg. Zhang Dandan & Yang Lijun; 1♂1♀, Mt. Limushan, 6.V.2011, leg. Zhang Dandan & Yang Lifeng, genitalia slide no. SYSU0117 (♂), no. SYSU0130 (♀); 1♂1♀, Mt. Limushan, 19.17°N, 109.73°E, alt. 662 m, 20.V.2013, leg. Li Jinwei, genitalia slide no. SYSU0929 (♂), no. SYSU0991 (♀), molecular voucher no. LEP0166 (♂), no. LEP0174 (♀). **Yunnan:** 2♂, Mengla, Xishuangbanna, 4, 6.X.2004, leg. R. L. Kitching, genitalia slide no. FCEL0003 (FCEL). **Tibet:** 1♂, 80K, Medog County, 29.66°N, 95.49°E, alt. 2059 m, 8.VIII.2017, leg. Qi Mujie & Yang Xiaofei (NKU); 1♀, Beibeng Village, Medog County, 29.24°N, 95.17°E, alt. 987 m, 12.VIII.2017, leg. Qi Mujie & Yang Xiaofei (NKU); 1♀, Beibeng Village, Medog County, 29.25°N, 95.18°E, alt. 810 m, 15.VIII.2017, leg. Qi Mujie & Yang Xiaofei (NKU).

**Diagnosis.** *Loxoneptera hampsoni* is easily distinguished from other *Loxoneptera* species as follows: forewing with distinct, black-brown and point-like orbicular and reniform stigmata, bearing pale yellow stripes between veins, and veins with ochre-brown scales forming streaks; dorsal sella with a long and slender rod-shaped extension in the male genitalia.

**Redescription. Head.** Frons brown, with white lateral bands. Vertex brown, mixed with some white erected scales. Labial palpus dark brown, with white scales on ventral



**Figures 2–9.** Adults of *Loxoneptera* spp. **2** *L. hampsoni* nom. nov., male (Tibet) **3** *L. hampsoni* nom. nov., female (Hainan) **4** *L. albicostalis*, male (Yunnan) **5** *L. crassiuncata* sp. nov., paratype, male (Yunnan) **6** *L. carnealis*, male (Yunnan) **7** *L. triangularis* sp. nov., holotype, male (Yunnan) **8** *L. rectacerosa* sp. nov., holotype, male (Yunnan) **9** *L. medialis*, male (Guangdong). Scale bars: 5.0 mm.

side. Maxillary palpus brown. Antennae brown. **Thorax.** Dorsal side, patagia and tegula yellowish brown, ventral side grey white. Foreleg yellowish brown, dorsal tarsus grey white; ventral femur and tibia of midleg and hindleg grey white, others pale yellow. **Wings.** Wingspan 29.0–36.0 mm. Forewing termen straight, a small triangular indentation presented on 1/3 of posterior margin in male, and with a group of black-brown

scales; yellowish brown, mixed with ochre-brown scales, pale yellow stripes presented between veins, and veins covered with ochre-brown scales forming streaks; orbicular stigma appearing as a black point, reniform stigma black, small and round; fringe white, basal 1/5 black-brown. Hindwing in male black-brown on terminal area, remaining areas pale yellow, a triangular patch present near posterior angle of cell, slightly concave and densely covered with pale brown scales; in female pale yellow, mixed with ochre-brown scales on termen; fringe brown in male, pale yellow in female. **Abdomen.** Dorsal side of abdomen black-brown, ventral side grey white; 5<sup>th</sup> abdominal segment with a group of pale yellow scales on each side in male; sternite VIII in male slightly sclerotised with two pointed anterolateral processes.

**Male genitalia** (Fig. 15). Uncus somewhat wide and short, distally narrowly rounded, without setae. Saccus narrow. Dorsal projection of transtilla relatively thick and slightly curved, ~ 1/2 length of costa, distally bearing hair almost as long as projection. Valva with dorsal margin slightly concave, ventral margin nearly paralleled with dorsal margin, apex truncate; costa wide; dorsal sella membranous, rod-shaped, rather slender, and fragile; ventral sella sclerotised, with a somewhat straight, hook-shaped process; dorso-distal sella with a pointed process extended beyond ventral margin of valva; sacculus broad. Juxta heart-shaped, middle part concave inwardly, with wide arms. Phallus with vesica bearing two groups of spine-shaped cornuti, one longer and curved, another short and straight.

**Female genitalia** (Fig. 26). Anterior apophyses 1.5 × as long as posterior apophyses. Lamella postvaginalis with weakly sclerotised transversely wrinkles, with dense and tiny spines; lamella antevaginalis with two curved and sclerotised notches. Antrum weakly sclerotised, cup-shaped, width 3 × as long as length; colliculum well developed and heavily sclerotised, expanded in middle part, length of colliculum ~ 1/3 of ductus bursae; ductus bursae slightly longer than length of corpus bursae; corpus bursae oval, appendix bursae arising from lateral side, small; signum broadly rhomboid, maximal length less than half width of corpus bursae, carina well-developed, laterally bearing with dense tiny spines, other two arms short and stout.

**Distribution.** China (Hainan, Yunnan, Tibet), India.

**Etymology.** The species is renamed after the last name of George Hampson, who proposed the genus *Loxoneptera* in 1896.

**Remarks.** According to the characters of the male and female genitalia, *Calamochrous carnealis* (Swinhoe, 1895) is transferred to *Loxoneptera* in this paper, which creates a secondary homonym of *Loxoneptera carnealis* Hampson, 1896, the type species of *Loxoneptera*. The specific name of *Loxoneptera carnealis* Hampson, 1896 is not valid, therefore we give it a new replacement name, i.e., *Loxoneptera hampsoni* nom. nov.

### ***Loxoneptera albicostalis* Swinhoe, 1906**

Figs 4, 14, 16

*Loxoneptera albicostalis* Swinhoe, 1906: 415.

**Material examined. Type material.** Type ♂, Padang, W. Sumatra, Pyralidae Brit. Mus. Slide No. 9753 (NHMUK).

**Other material examined. CHINA. Yunnan:** 1♂, Jingpo Village, Nabang, Yingjiang Country, 24.71°N, 97.39°E, alt. 231 m, 2.VIII.2013, leg. Teng Kaijian et al., genitalia slide no. ZDD12108 (NKU).

**Diagnosis.** In appearance, *Loxoneptera albicostalis* is extremely similar to *L. crassiuncata* and *Eumorphobotys horakae* Chen & Zhang, 2018 in the wing shape, the clean reddish brown forewing and the dark brown hindwing, but can be distinguished by the whiter costa of both wings, a group of dark brown scales on the posterior margin of forewing, and a group of scales on each side of the 5<sup>th</sup> abdominal segment in male. The underside of forewing in *L. albicostalis* is smoky brown, while that of *E. horakae* is pale yellow from anterior margin of cell to posterior margin. The male genitalia resemble that of *L. crassiuncata* but can be differentiated by the shorter and stouter uncus, the relatively longer and slender dorsal projection of transtilla, nearly triangular dorsal sella, the long and hook-shaped process of the ventral sella, as well as the absence of the spine-shaped cornutus in phallus.

**Redescription. Head.** Frons brown. Vertex brown, mixed with some yellow erected scales. Labial palpus dark brown, with white scales on ventral side. Maxillary palpus brown. Antennae yellowish brown. **Thorax.** Dorsal side, patagia and tegula brown, ventral side grey white. Legs pale yellow to grey white; hindleg basal outer spur 1/5 of basal inner spur. **Wings.** Wingspan 32.0–36.0 mm. Forewing wide, reddish brown, without pattern; costal area white, mixed with pale brown scales at apex; termen straight; a small triangular indentation presented on the 1/3 of posterior margin in male, and with a group of black-brown scales; fringe white, with basal 1/4 black-brown. Hindwing black-brown, costa area pale yellow; a triangular patch presented near the posterior angle of cell, densely covered with pale brown scales; fringe black-brown. Underside smoky dark brown on forewing, and pale brown on posterior margin area. **Abdomen.** Dorsal side black-brown, ventral side grey white; abdominal segment V with a group of dark scales on each side in male; sternite VIII in male slightly sclerotised with two pointed anterolateral processes.

**Male genitalia** (Fig. 16). Uncus wide and short, distally broadly rounded, with few hair-like setae. Saccus rounded. Dorsal projection of transtilla relatively thick and slightly curved, ~ 1/3 length of costa, distally bearing hairs longer than projection. Valvae with dorsal margin slightly straight, ventral margin sinuated, apex narrowly rounded; costa narrow; dorsal sella membranous with several setae, nearly triangular; ventral sella with a long, hook-shaped, and sclerotised process; dorso-distal sella bearing a short sclerotised process distally; sacculus broad, extended dorsad a triangular protrusion in middle. Juxta shield-shaped, middle part weakly sclerotised. Phallus slowly narrow to end, vesica mostly granulated.

**Female genitalia.** Unknown.

**Distribution.** China (Yunnan), Indonesia (Sumatra), Malaysia.

**Remarks.** The forewing colour of the type material of *Loxoneptera albicostalis* is pale yellow tinged with some reddish brown scales and differs from the specimen collected in China. No obvious difference could be found in the male genitalia between the type specimen and the Chinese specimen.

***Loxoneptera crassiuncata* Chen & Zhang, sp. nov.**

<http://zoobank.org/E03FEF8B-F4B4-4DCD-9192-5971917D4729>

Figs 5, 17

**Material examined. Type material.** Holotype, ♂, CHINA: Yunnan: Mengla, Xishuangbanna, 4.IX.2004, leg. R. L. Kitching, genitalia slide no. FCEL0010 (FCEL). Paratypes: CHINA: Yunnan: 1♂, Mengla, Xishuangbanna, 28.IX.2004, leg. R. L. Kitching; 1♂, Mengla, Xishuangbanna, 29.IX.2004, leg. R. L. Kitching, genitalia slide no. FCEL0012 (FCEL).

**Diagnosis.** *Loxoneptera crassiuncata* is similar to *L. albicostalis* in reddish brown forewing colour but male specimens can be distinguished by the unbroken posterior margin of forewing (without a small triangular indentation), without a group of black-brown scales, and abdominal segment V without a group of dark scales. In the male genitalia, it can be differentiated by the longer and slender uncus, the shorter and stouter dorsal projection of transtilla, the slender and rod-shaped dorsal sella, the relatively shorter and slightly curved process of the ventral sella, as well as the presence of a horn-shaped cornutus in phallus.

**Description. Head.** Frons brown. Vertex brown. Labial palpus brown, with white scales on ventral side. Maxillary palpus brown, broadened distally with scales. Antennae dark brown. **Thorax.** Dorsal side, patagia and tegula brown, ventral side grey white. Legs yellowish white or pale yellow, dorsal of midlegs and hindlegs yellowish brown; hindleg with basal outer spur 1/4 of inner spur. **Wings.** Wingspan 29.0–31.0 mm. Forewing wide, termen nearly straight; reddish brown, brown at basal half of posterior portion, costal band brown, without pattern; fringe pale yellow, basal half and the posterior angle black-brown. Underside greyish brown. Hindwing black-brown, pale yellow on anterior margin; a triangular patch presented near the posterior angle of cell, the margin of triangular patch with pale yellow scales and the outer margin dentate; fringe black-brown. Underside greyish brown. **Abdomen.** Dorsal side of abdomen brown, ventral side pale yellow; sternite VIII in male slightly sclerotised with two pointed anterolateral processes.

**Male genitalia** (Fig. 17). Uncus slightly narrow, distally narrowly rounded, with several setae. Saccus narrow. Dorsal projection of transtilla rather thick and straight, ~ 1/4 length of costa, distally bearing setae ~ 2 × length of projection. Valva with dorsal margin slightly concave, ventral margin nearly parallel with dorsal margin, and apex slightly truncate; costa narrow; dorsal sella membranous, long and slender, rod-shaped and fragile; ventral sella with a stick-like and strongly sclerotised process; dorso-distal sella with a short stick-like process, pointed apically; sacculus broad, extended dorsad with a triangular protrusion in the middle. Juxta with basal part narrow, two arms rather broad. Phallus stout, vesica with a horn-shaped and strongly sclerotised cornutus apically.

**Female genitalia.** Unknown.

**Distribution.** China (Yunnan).

**Etymology.** The specific name is derived from the Latin *crassi-* (thick) and *uncatus* (horn-shaped), referring to the shape of cornuti in the phallus.

***Loxoneptera carnealis* (Swinhoe, 1895), comb. nov.**

Figs 6, 18, 27

*Notaspis carnealis* Swinhoe, 1895: 302.*Calamochrous carnealis* (Swinhoe): Hampson, 1896: 420.

**Material examined. Type material.** Type ♂, Khasi Hills., 95-224, Cherra Punji (NHMUK). Syntype: 1♂, Cherra Punji, Swinhoe Coll., Brit. Mus. 1926-239 (NHMUK).

**Other material examined. CHINA. Guangdong:** 6♂, Shimentai Reserve, Yingde, 27.V.2012, leg. Yang Lijun & Jia Qianju. **Guizhou:** 1♂, Maolan Reserve, 25.13°N, 107.87°E, alt. 797 m, 12.VII.2013, leg. Chen Xiaohua, genitalia slide no. SYSU0165, molecular voucher no. LEP0044; 1♀, Banzhai Village, Maolan Reserve, 25.23°N, 108.03°E, alt. 530 m, 11.VIII.2018, leg. Zheng Meiling et al. (NKU). **Yunnan:** 6♂, Baihualing Reserve, Baoshan, alt. 1520 m, 12–13.VIII.2007, leg. Zhang Dandan, genitalia slide no. LJW12064, no. LJW12098; 2♂1♀, Tropical Botanical Garden, Xishuangbanna, 21.92°N, 101.27°E, alt. 606 m, 22.XI.2017, leg. Chen Kai & Liu Qingming, genitalia slide no. SYSU0986 (♂), no. SYSU0985 (♀), molecular voucher no. LEP0186; 1♂, Tropical Botanical Garden, Xishuangbanna, alt. 550 m, 13.III.2014, leg. Zhang Zhenguang, molecular voucher no. LEP0169 (NKU); 2♂, Mengla, 1000 m, 11–12.VII.2012, leg. Kitching & Ashton, genitalia slide no. FCEL0005 (FCEL).

**Diagnosis.** This species is similar to *Loxoneptera triangularis* in appearance, but can be distinguished by the following characters: forewing mixed with reddish brown scales, a distinct dark brown stripe appearing near posterior angle of cell; apex of hindwing with a dark brown patch; dorso-distal sella with a hook-shaped process; distal end of phallus with a spine-shaped process, longer than phallus length.

**Redescription. Head.** Frons pale reddish brown, with white lateral bands. Vertex pale brown, mixed with some reddish brown erect scales. Labial palpus reddish brown, with white scales on ventral side. Maxillary palpus reddish brown, broadened distally with scales. Antennae yellowish brown. **Thorax.** Dorsal patagia and tegula ochre-brown, ventral side grey-white. Legs pale yellow to grey-white; hindleg basal outer spur 2/5 of basal inner spur. **Wings.** Wingspan 22.0–29.0 mm. Forewing yellowish brown, densely mixed with reddish brown scales; dark brown from costal margin to posterior margin of cell; costal margin white; orbicular stigma appearing as a black-brown point, reniform stigma black, appearing as a thick streak on discocellulars; a distinct dark brown stripe appearing near posterior angle of cell; fringe black-brown. Hindwing pale yellow, apex with a dark brown patch; fringe pale yellow. Underside of forewing pale yellow, black-brown from costal margin to posterior margin of cell. **Abdomen.** Dorsal side of abdomen black-brown, ventral side grey white; sternite VIII in male slightly sclerotised with two pointed anterolateral processes.

**Male genitalia** (Fig. 18). Uncus long, triangular, distally narrowly rounded, with few hair-like setae. Saccus rounded. Dorsal projection of transtilla relatively slender and slightly curved, ~ 3/4 length of costa, distally bearing hair ~ 1/2 length of projection,

basal 1/3 broad. Valva with dorsal margin slightly convex, ventral margin sinuated, apex narrowly rounded; costa narrow; dorsal sella membranous with several setae, nearly rectangular; ventral sella with short, finger-shaped, and weakly sclerotised process; dorso-distal sella bearing a hook-shaped, strongly sclerotised process, basal broad with two small spines; sacculus broad. Juxta with basal part narrow, two arms long and slender, pointed apically. Phallus short, distal part with a long and pointed spine, slightly curved, as long as the length of phallus.

**Female genitalia** (Fig. 27). Anterior apophyses  $1.5 \times$  as long as posterior apophyses. Antrum weakly sclerotised, cup-shaped; colliculum well developed, length of colliculum  $\sim 2/7$  of ductus bursae; basal ductus seminalis expanded and sclerotised; ductus bursae short and stout, as long as length of corpus bursae; corpus bursae oval, without appendix bursae and signum.

**Distribution.** China (Guangdong, Guizhou, Yunnan), India.

***Loxoneptera triangularis* Chen & Zhang, sp. nov.**

<http://zoobank.org/A58926C8-3A03-4017-89BB-F613163F7686>

Figs 7, 19

**Material examined. Type material.** Holotype, ♂, **CHINA: Yunnan:** Mengla, Xishuangbanna, 7.X.2004, leg. R. L. Kitching, genitalia slide no. FCEL0004 (FCEL). Paratype: **CHINA: Yunnan:** 1♂, Mengla, Xishuangbanna, 4.X.2004, leg. R. L. Kitching.

**Diagnosis.** Externally, *Loxoneptera triangularis* resembles *L. carnealis* in the wing shape, but can be distinguished by the smaller wings, and costal and posterior areas of hindwing dark brown. In the male genitalia, it can be differentiated by the process on the dorso-distal sella with a strongly sclerotised stick, distal part of juxta with a strongly sclerotised and narrowly triangular process, and distal phallus with a relatively short and hook-shaped spine.

**Description. Head.** Frons pale yellow, with white lateral bands, basal white bands mixed with reddish brown scales. Vertex pale yellow. Labial palpus reddish brown, ventral side with white scales. Maxillary palpus reddish brown, broadened distally with scales. Antennae yellowish brown. **Thorax.** Dorsal side, patagia and tegula yellowish brown, mixed with reddish brown scales, ventral side grey white. Legs pale yellow. **Wings.** Wingspan 23.0–25.0 mm. Forewing pale yellow, termen dark brown, as well as from costal margin to posterior margin of cell, apex mixed with reddish brown scales; orbicular stigma weak, appearing as a dark brown point, reniform stigma black-brown and weak; fringe dark brown. Underside of forewing black from costal margin to posterior margin of cell. Hindwing pale yellow between  $CuA_2$  and  $M_2$ , remainders dark brown, without pattern, fringe yellow brown. **Abdomen.** Dorsal side of abdomen pale brown, ventral side grey white; sternite VIII in male slightly sclerotised with two stout anterolateral processes.

**Male genitalia** (Fig. 19). Uncus long and slender, distally narrowly rounded, with few hair-like setae. Saccus rounded. Dorsal projection of transtilla relatively slender and slightly curved, approximately as long as length of costa, distally bearing hair  $\sim$

1/4 length of projection, basal 1/3 broad. Valva with dorsal margin slightly convex, ventral margin sinuated, apex narrowly rounded; costa slightly curved; dorsal sella membranous, with several setae, ventral sella with a small, hook-shaped and sclerotised process, narrow and pointed apically; dorso-distal sella with a long, stick-like, strongly sclerotised process, broad at terminal part, then pointed at apex; sacculus broad. Juxta shield-shaped, strongly sclerotised, distal part broad, with a strongly sclerotised and narrowly triangular process. Phallus long, distal end with a long and hook-shaped spine, narrow and pointed apically.

**Female genitalia.** Unknown.

**Distribution.** China (Yunnan).

**Etymology.** The specific name derived from the Latin *triangularis*, referring to the triangular process in the end of juxta.

***Loxoneptera rectacerosa* Chen & Zhang, sp. nov.**

<http://zoobank.org/FF3B831C-02BE-407A-ABC2-F49CAEEBE759>

Figs 8, 20

**Material examined. Type material.** Holotype, ♂, CHINA: Yunnan: Yexianggu, Xishuangbanna, 22.17°N, 100.87°E, alt. 762 m, 18.VII.2014, leg. Teng Kaijian et al., genitalia slide no. ZDD12059, molecular voucher no. LEP0170 (NKU).

**Diagnosis.** *Loxoneptera rectacerosa* resembles *L. medialis* in wing pattern, but the forewing of *L. rectacerosa* is brown from the costal margin to posterior margin of the cell, and white on costal margin, whereas it is pale yellow in *L. medialis*. In the male genitalia, dorsal margin of valva of *L. rectacerosa* makes a turn in the end, forming a distinct obtuse subapical angle; the process of the dorso-distal sella is smaller and shorter than that of *L. medialis*; distal end of phallus has a small and triangular sclerite, vesica is just with a group of spines.

**Description. Head.** Frons pale yellow, with white lateral bands. Vertex pale yellow. Labial palpus brown, with white scales on ventral side. Maxillary palpus brown, broadened distally with scales. Antennae yellowish brown. **Thorax.** Dorsal side, patagia and tegula yellowish brown, ventral side grey white. Legs white to yellowish white. **Wings.** Wingspan 29.0 mm. Forewing brown, mixed with reddish brown scales, costal margin white, posterior area pale yellow; orbicular stigma weak, appearing as a dark brown point, reniform stigma absent; fringe black-brown. Hindwing pale yellow, without any spot, apex mixed with a few pale brown scales. Underside of forewing black on cell. **Abdomen.** Dorsal side of abdomen pale brown, ventral side grey white; sternite VIII in male slightly sclerotised with two stout anterolateral processes.

**Male genitalia** (Fig. 20). Uncus long and slender, distally narrowly rounded, with few hair-like setae. Saccus rounded. Dorsal projection of transtilla relatively slender and slightly curved, ~ as long as length of costa, distally bearing hair ~ 1/4 length of projection, basal 1/3 broad. Valva with dorsal margin slightly convex, ventral margin sinuated, apex slightly pointed; costa straight, and making a turn on 1/5 of the end,

forming a break angle on dorsal margin of valva subapically; dorsal sella membranous, with several setae; ventral sella with a hook-shaped and strongly sclerotised process, narrow and pointed apically; dorso-distal sella with a short and weakly sclerotised process; sacculus broad. Juxta with basal part narrow, two arms long and slender, pointed apically. Phallus long and slightly curved, distal end with a semi-circular sclerite, vesica with a group of short, straight, spine-shaped cornuti.

**Female genitalia.** Unknown.

**Distribution.** China (Yunnan).

**Etymology.** The specific name derived from the Latin *rect-* (straight) and *arcerosus* (spine-shaped), referring to the shape of cornuti in phallus.

***Loxoneptera medialis* (Caradja, 1925), comb. nov.**

Figs 9, 21, 28

*Calamochrous medialis* Caradja, 1925: 363.

**Material examined. Type material.** Holotype, ♂, Canton, Type, Car.[adja], Gen. Praep.[Prep.] EGM 3 (MGAB).

**Other material examined. CHINA. Guangdong:** 1♂, Dongmei Village, Potou District, Zhanjiang, 10.IV.2016, leg. Li Zhiqiang & Li Jun, genitalia slide no. SYSU0987, molecular voucher no. LEP0171; 1♀, Liuzhang Village, Beihe Country, Leizhou, 9.IV.2016, leg. Li Zhiqiang & Li Jun, genitalia slide no. SYSU0990, molecular voucher no. LEP0173. **Hainan:** 1♂, Jianling Reserve, 18.87°N, 110.27°E, alt. 143 m, 8.IX.2013, leg. Chen Xiaohua, genitalia slide no. SYSU0180, molecular voucher no. LEP0096.

**Diagnosis.** The wing shape of *Loxoneptera medialis* is similar to *L. rectacerosa* but can be distinguished by the light yellow forewing and costal margin. In the male genitalia, it can be distinguished by longer spinous process on dorso-distal sella, distal end of phallus with a small and pointed spine, and vesica with two groups of short, spine-shaped cornuti.

**Redescription. Head.** Frons pale yellow, with white lateral bands. Vertex pale yellow. Labial palpus pale yellow, with white scales on ventral side. Maxillary palpus pale yellow, mixed with white scales, broadened distally with scales. Antennae yellowish brown. **Thorax.** Dorsal side, patagia and tegula yellowish brown, ventral side grey white. Legs yellowish white. **Wings.** Wingspan 25.0–30.0 mm. Forewing pale yellow, costal and terminal areas reddish brown; orbicular stigma weak, dark brown, reniform stigma weak, black-brown, appearing as a thick line on discocellulars; a weak, dark-brown stripe appearing between  $M_2$  and  $CuA_1$ ; fringe black-brown. Hindwing pale yellow, termen mixed with brown scales, without pattern. Underside of forewing pale yellow, without any spot. **Abdomen.** Dorsal side of abdomen black-brown, ventral side grey white; sternite VIII in male slightly sclerotised with bifurcate anterolateral processes.

**Male genitalia** (Fig. 21). Uncus long and slender, distally narrowly rounded, with few hair-like setae. Saccus rounded. Dorsal projection of transtilla relatively slender

and slightly curved, approximately as long as length of costa, distally bearing hair  $\sim 1/3$  length of projection, basal  $1/3$  broad. Valva with dorsal margin slightly convex, ventral margin sinuated, apex slightly pointed; costa slightly curved; dorsal sella appearing as a broad, slightly curved and stick-like sclerite, with several setae; ventral sella sclerotised, with a long, straight and stick-like process, narrow and pointed apically, apex slightly curved; dorso-distal sella with a pointed, hook-like, and strongly sclerotised process, as long as the process on ventral sella. Sacculus broad. Juxta with basal part narrow, two arms long and slender, pointed apically. Phallus short, basal  $1/2$  broad, distal end with a small pointed spine, and vesica with two groups of short, spine-shaped cornuti.

**Female genitalia** (Fig. 28). Anterior apophyses  $1.5 \times$  as long as posterior apophyses; lamella postvaginalis trapezoidal and strongly sclerotised, with distinct transversely wrinkles, covered with dense and tiny spines; lamella antevaginalis strongly sclerotised, appearing as a small, triangular sclerite, covered with many dense and tiny spines. Antrum strongly sclerotised, cup-shaped; colliculum well developed and strongly sclerotised; ductus bursae short and stout,  $\sim 1/2$  length of corpus bursae; corpus bursae oval, signum weak, reduced into a long carina, laterally bearing with some tiny spines, without appendix bursae.

**Distribution.** China (Guangdong, Hainan).

***Loxoneptera pentasaris* (Meyrick, 1932), comb. nov.**

Figs 10, 22

*Calamochrous pentasaris* Meyrick, 1932: 317.

**Material examined. Type material.** Holotype, ♂, [India] Datarpur, Hoshiarpur. Officer-in-charge, 21.12.1927, Pyralidae Brit. Mus. Slide No. 9747 (NHMUK).

**Diagnosis.** Wingspan 28.0 mm. *Loxoneptera pentasaris* is best distinguished from other *Loxoneptera* species by greyish ochreous forewing with a white costal band, and without pattern. In the male genitalia, this species is similar to *L. medialis* in the shape of dorsal projection of transtilla, ventral sella and valva, but can be distinguished by the triangular dorsal sella, process of dorso-distal sella extending ventrad, distal margin of phallus densely decorated with short spines.

**Distribution.** India.

***Loxoneptera bipunctalis* (Hampson, 1912), comb. nov.**

Figs 11, 23

*Calamochrous bipunctalis* Hampson, 1912: 1269.

**Material examined. Type material.** Type ♂, S. India, Palani Hills [Palnis], Campbell 1907.365, Pyralidae Brit. Mus. Slide No. 9750 (NHMUK).



**Figures 10–13.** Adults of *Loxoneptera* spp. **10** *L. pentasaris*, holotype, male (India) **11** *L. bipunctalis*, type, male (India) **12** *L. brevipalpis*, holotype, male (India) **13** *L. dichroma*, type, male (India). Scale bars: 5.0 mm.

**Diagnosis.** Wingspan 34.0 mm. In appearance, *Loxoneptera bipunctalis* is best distinguished from other *Loxoneptera* species by pale ochreous yellow forewing, two blackish orbicular stigmata, and interrupted postmedial line of forewing. In the male genitalia, this species is similar to *L. brevipalpis* and *L. dichroma* but can be distinguished by the longer process of dorso-distal sella and the weakly sclerotised, slice-shaped cornutus of phallus.

**Distribution.** India.

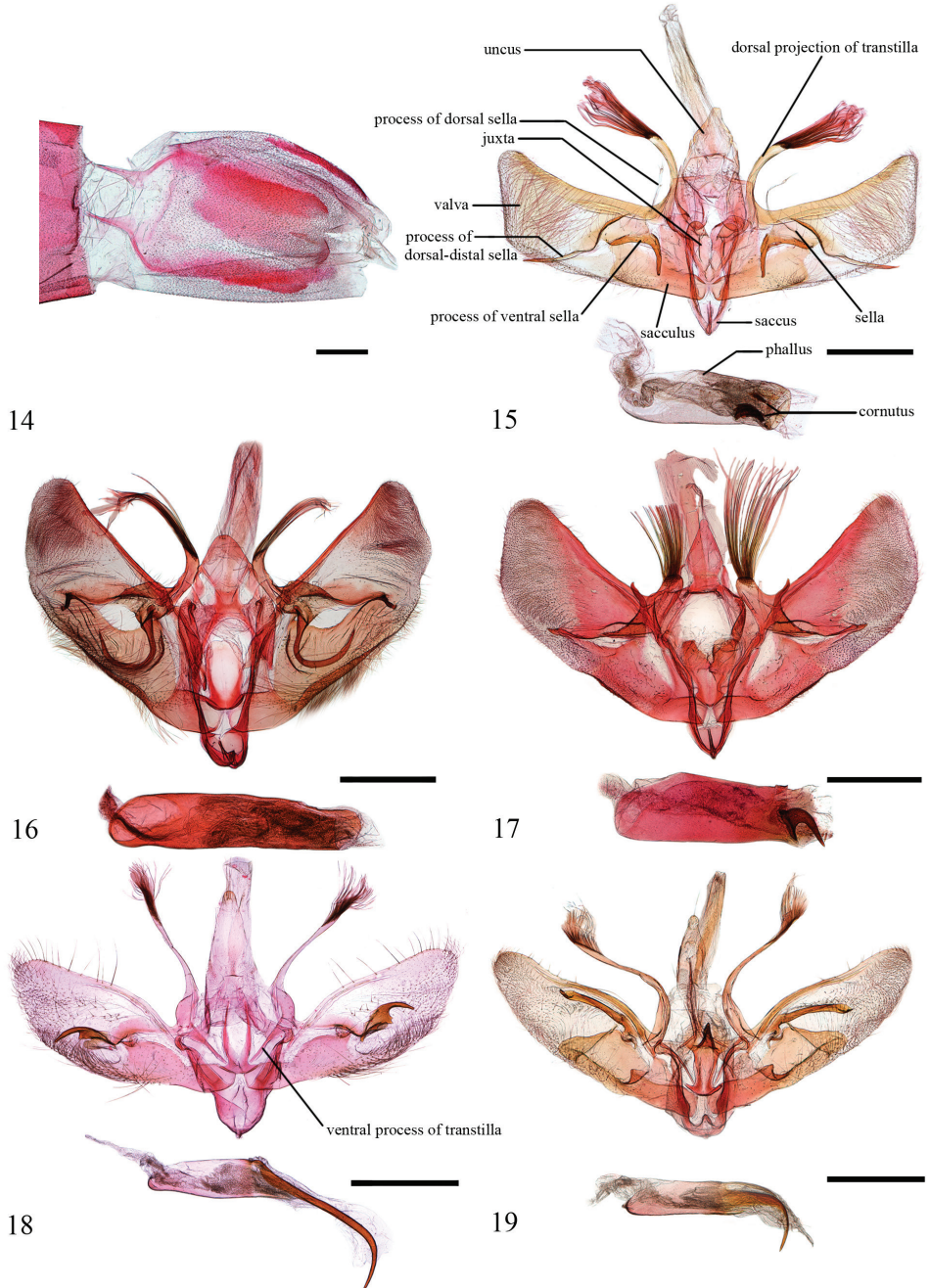
***Loxoneptera brevipalpis* (Snellen, 1890), comb. nov.**

Figs 12, 24

*Calamochrous brevipalpis* Snellen, 1890: 599.

**Material examined. Type material.** Holotype, ♂, Sikkim, O. Möller, Pyralidae Brit. Mus. Slide No. 9748 (NHMUK).

**Diagnosis.** Wingspan 33.0 mm. This species is distinguished by dull luteous forewing suffused with ochreous scales and bearing indistinct orbicular and reniform stigmata, lustrous hindwing suffused with grey scales along the costa. In the male genitalia, this species is similar to *L. dichroma* in the shape of the dorsal projection of the transtilla, ventral sella and valva, as well as by the process of dorso-distal sella extended



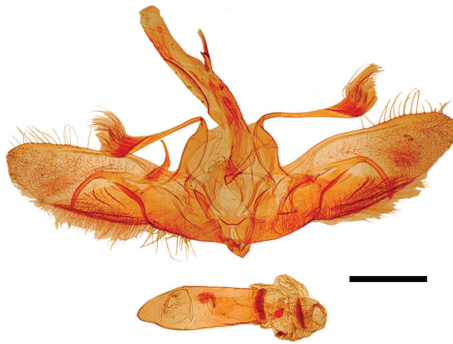
**Figures 14–19.** **14** The sternite VIII in male of *L. albicostalis* **15–19** Male genitalia of *Loxoneptera* spp. **15** *L. hampsoni* nom. nov., Hainan (genitalia slide no. SYSU0929) **16** *L. albicostalis*, Yunnan (genitalia slide no. ZDD12108) **17** *L. crassiuncata* sp. nov., Yunnan (genitalia slide no. FCEL0010) **18** *L. carnealis*, Guizhou (genitalia slide no. SYSU0165) **19** *L. triangularis* sp. nov., Yunnan (genitalia slide no. FCEL0004). Scale bars: 1.0 mm.



20



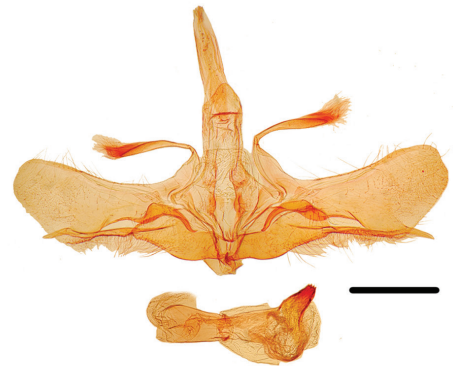
21



22



23

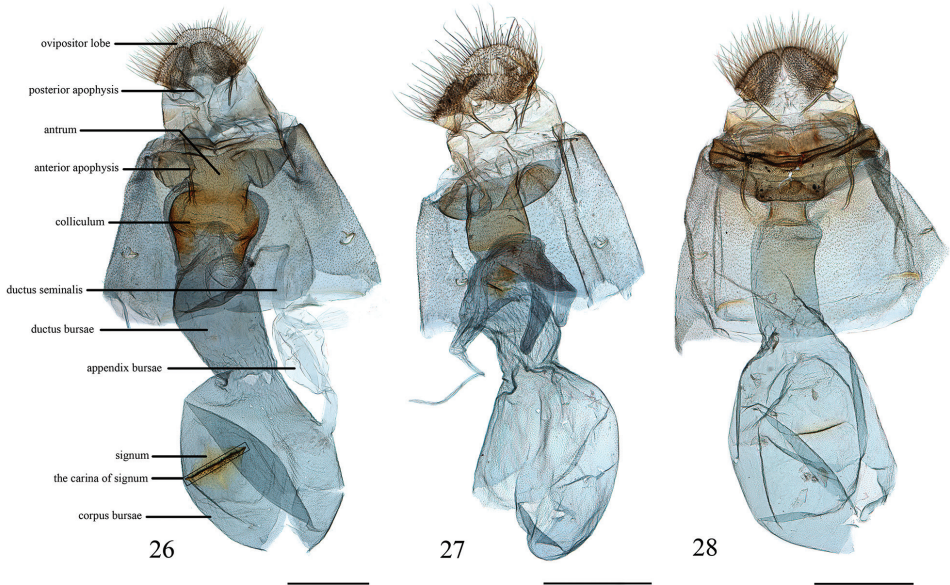


24



25

**Figures 20–25.** Male genitalia of *Loxoneptera* spp. **20** *L. rectacerosa* sp. nov., Yunnan (genitalia slide no. ZDD12059) **21** *L. medialis*, Guangdong (genitalia slide no. SYSU0987) **22** *L. pentasaris*, India (Pyralidae Brit. Mus. Slide No. 9747) **23** *L. bipunctalis*, India (Pyralidae Brit. Mus. Slide No. 9750) **24** *L. brevivalpis*, India (Pyralidae Brit. Mus. Slide No. 9748) **25** *L. dichroma*, India (Pyralidae Brit. Mus. Slide No. 9749). Scale bars: 1.0 mm.



**Figures 26–28.** Female genitalia of *Loxoneptera* spp. **26** *L. hampsoni* nom. nov., Hainan (genitalia slide no. SYSU0991) **27** *L. carnalis*, Yunnan (genitalia slide no. SYSU0985) **28** *L. medialis*, Guangdong (genitalia slide no. SYSU0990). Scale bars: 1.0 mm.

ventrad and beyond the ventral margin of valva. *Loxoneptera brevipalpis* can be distinguished by the thick and heavily sclerotised process of dorso-distal sella, and the heavily sclerotised, spiny, thumb-shaped cornutus.

**Distribution.** India (Sikkim).

***Loxoneptera dichroma* (Moore, 1888), comb. nov.**

Figs 13, 25

*Ebulea dichroma* Moore, 1888: 223.

*Calamochrous dichroma* (Moore): Snellen, 1890: 599.

*Anania dichroma* (Moore): Nuss et al. 2003–2021, Global Information System on Pyraloidea.

**Material examined.** *Type material.* Type ♂, Darjeeling [Darjiling], Pyralidae Brit. Mus. Slide No. 9749 (NHMUK).

**Diagnosis.** Wingspan 34.0 mm. This species can be distinguished by having a brown stripe along posterior margin of the discal cell in forewing, and ventral-distal wall of phallus is weakly sclerotised and obliquely extended into a process.

**Distribution.** India.

## Discussion

The monophyly of *Loxoneptera* is strongly supported by the results of the molecular analysis. The dorsal projection of the transtilla in the male genitalia is a putative synapomorphy for the genus. It is shared by eleven species of *Loxoneptera* and can be used to separate them from most other pyraustine genera. In addition, two provisional infrageneric groups of the species of *Loxoneptera* are recognised by proportional lengths of the dorsal projection of the transtilla with its distal hair. The tree topology (Fig. 1) supports this morphological trait: *L. rectacerosa* is more closely related to *L. medialis* and *L. carnealis* (all bearing a relatively short hair, < 1/2 length of the dorsal projection of the transtilla) than to *L. albicostalis* and *L. hampsoni* (both bearing a relatively long hair, as long as or longer than the dorsal projection of the transtilla). Based on the proportional length of the dorsal projection of the transtilla with its distal hair, we additionally place *L. triangularis* and *L. crassiuncata*, as well as *L. pentasaris*, *L. bipunctalis*, *L. brevivalpis*, and *L. dichroma* (not included in the molecular analysis because no fresh specimen could be accessed) in their respective subgroups: *L. triangularis*, *L. bipunctalis*, *L. brevivalpis*, *L. dichroma*, and *L. pentasaris* resemble *L. rectacerosa*, *L. medialis*, and *L. carnealis* by the relatively short hair on the dorsal projection of the transtilla, while *L. crassiuncata* resembles *L. albicostalis* and *L. hampsoni* by the relatively long hair. The relationships among all these species need further study on more nucleotide sequences and freshly collected specimens.

After examining three specimens of *Calamochrous chilonalis* (the type species of *Calamochrous*) deposited in NHMUK, we confirm that it is quite different from those *Loxoneptera* species formerly placed in *Calamochrous*. Among these specimens, one is the paratype of which the abdomen was lost; the other two, collected in Minca, Colombia, were dissected and identified by Dr Koen V. N. Maes (Pyralidae Brit. Mus. Slide No. 762 male, 19967 female). Morphologically, *C. chilonalis* differs from *Loxoneptera* species by the relatively narrow forewing with arch termen, the conical, densely setose uncus, the narrowly triangular transtilla, the scale-like editum, as well as the long and slender ductus bursae. Maes (pers. comm.) also mentioned that *Calamochrous* species are restricted to the Nearctic region, while *Loxoneptera* species are distributed in the Oriental region.

## Acknowledgements

Grateful thanks to Prof. Houhun Li (Nankai University, China) and Prof. Akihiro Nakamura (Forest Canopy Ecology Lab, Yunnan, China) for the loan of some specimens, to Dr. David Lees and Dr. Geoff Martin (both Natural History Museum, United Kingdom) and Dr. Mihai Stănescu (“Grigore Antipa” National Museum of Natural History, Romania) for helping to access specimens deposited at their institutions. We are also grateful to Dr. Robert B. Angus (Natural History Museum, London, United Kingdom) for critical reviews of the manuscript and for linguistic assistance. This project was supported by the National Natural Science Foundation of China (Grant No. 31672330), Program of the Ministry of Science and Technology of the People of Republic of China (2015FY210300).

## References

- Chen K, Zhang DD, Stănescu M (2018) Revision of the genus *Eumorphobotys* with descriptions of two new species (Lepidoptera, Crambidae, Pyraustinae). *Zootaxa* 4472(3): 489–504. <https://doi.org/10.11646/zootaxa.4472.3.4>
- Hampson GF (1896) *Moths. The Fauna of British India, including Ceylon and Burma*. Taylor and Francis, London, 594 pp.
- Hampson GF (1912) The moths of India. Supplementary paper to the volumes in “The fauna of British India.” Series IV. Part V. *The Journal of the Bombay Natural History Society* 21: 1222–1272.
- Klots AB (1970) Lepidoptera. In: Tuxen SL (Ed.) *Taxonomist’s glossary of genitalia in insects* (2<sup>nd</sup> revised and enlarged edition). Munksgaard, Copenhagen, 115–130.
- Kristensen NP (2003) Skeleton and muscles: adults. In: Kristensen NP (Ed.) *Lepidoptera, Moths and Butterflies – Volume 2: Evolution, Systematics, and Biogeography Handbook of Zoology IV* (35). Walter de Gruyter, Berlin & New York, 39–131. <https://doi.org/10.1515/9783110893724.39>
- Li HH, Zheng ZM (1996) Methods and techniques of specimens of Microlepidoptera. *Journal of Shaanxi Normal University (Natural Science Edition)* 24: 63–70.
- Maes KVN (1995) A comparative morphological study of the adult Crambidae (Lepidoptera, Pyraloidea). *Bulletin et Annales de la Société Royale Belge d’Entomologie* 131: 383–434.
- Mally R, Hayden JE, Neinhuis C, Jordal BH, Nuss M (2019) The phylogenetic systematics of Spilomelinae and Pyraustinae (Lepidoptera: Pyraloidea: Crambidae) inferred from DNA and morphology. *Arthropod Systematics & Phylogeny* 77(1): 141–204.
- Meyrick E (1932) *Exotic Microlepidoptera*. Vol. IV. Pt. 10. Taylor and Francis, London, 289–320.
- Moore F (1888) Descriptions of Indian Lepidoptera Heterocera from the collection of the late Mr. W. S. Atkinson. In: Hewitson WC, Moore F (Eds) *Descriptions of new Indian Lepidopterous Insects from the Collection of the Late Mr. W.S. Atkinson* 3. Asiatic Society of Bengal/ Taylor & Francis, Calcutta / London, 199–299.
- Munroe EG (1976) Pyraloidea Pyralidae comprising the subfamily Pyraustinae tribe Pyraustini (part). In: Dominick RB, Dominick T, Ferguson DC, Franclemont JG, Hodges RW, Munroe EG (Eds) *The Moths of America North of Mexico*. Classey EW Ltd and The Wedge Entomological Research Foundation, London, 78 pp.
- Nuss M, Landry B, Mally R, Vegliante F, Tränkner A, Bauer F, Hayden J, Segerer A, Schouten R, Li H, Trofimova T, Solis MA, De Prins J, Speidel W (2003–2021) *Global Information System on Pyraloidea*. <http://www.pyraloidea.org>
- Posada D (2008) jModelTest: Phylogenetic model averaging. *Molecular Biology and Evolution* 25: 1253–1256. <https://doi.org/10.1093/molbev/msn083>
- Robinson GS (1976) The preparation of slides of Lepidoptera genitalia with special reference to the Microlepidoptera. *Entomologist’s Gazette* 27: 127–132.
- Ronquist F, Teslenko M, van der Mark P, Ayres DL, Darling A, Höhna S, Larget B, Liu L, Suchard MA, Huelsenbeck JP (2012) MrBayes 3.2: Efficient Bayesian Phylogenetic Inference and Model Choice Across a Large Model Space. *Systematic biology* 61: 539–542. <https://doi.org/10.1093/sysbio/sys029>

- Snellen PCT (1890) A catalogue of the Pyralidina of Sikkim collected by Henry J. Elwes and the late Otto Möller, with notes by H. J. Elwes. *Transactions of the Entomological Society of London* 38: 557–647. <https://doi.org/10.1111/j.1365-2311.1890.tb03031.x>
- Stamatakis A (2014) RAxML version 8: a tool for phylogenetic analysis and post-analysis of large phylogenies. *Bioinformatics* 30: 1312–1313. <https://doi.org/10.1093/bioinformatics/btu033>
- Swinhoe C (1906) New and little-known species of Eastern and Australian Heterocera. *Annals and Magazine of Natural History, including Zoology, Botany and Geology* 18: 403–416. <https://doi.org/10.1080/00222930608562637>
- Tamura K, Stecher G, Peterson D, Filipski A, Kumar S (2013) MEGA6: Molecular Evolutionary Genetics Analysis Version 6.0. *Molecular Biology and Evolution* 30: 2725–2729. <https://doi.org/10.1093/molbev/mst197>
- Thompson JD, Higgins DG, Gibson TJ (1994) CLUSTAL W: improving the sensitivity of progressive multiple sequence alignment through sequence weighting, position-specific gap penalties and weight matrix choice. *Nucleic Acids Research* 22: 4673–4680. <https://doi.org/10.1093/nar/22.22.4673>
- Zhang DD, Chen K, Xiang LB (2020) Revision of the genus *Epiparbattia* Caradja, 1925 (Lepidoptera, Crambidae, Pyraustinae), based on morphology and molecular data. *ZooKeys* 960: 143–155. <https://doi.org/10.3897/zookeys.960.54986>

# First fossil record of the mayfly family Vietnamellidae (Insecta, Ephemeroptera) from Burmese Amber confirms its Oriental origin and gives new insights into its evolution

Roman J. Godunko<sup>1,2,3</sup>, Alexander V. Martynov<sup>4</sup>, Arnold H. Staniczek<sup>5</sup>

**1** Biology Centre of the Czech Academy of Sciences, Institute of Entomology, Branišovská 31, 37005 České Budějovice, Czech Republic **2** Department of Invertebrate Zoology and Hydrobiology, University of Łódź, Banacha 12/16, 90237 Łódź, Poland **3** State Museum of Natural History, National Academy of Sciences of Ukraine, Teatralna 18, 79008, Lviv, Ukraine **4** National Museum of Natural History, National Academy of Sciences of Ukraine, Bohdan Khmelnytsky 15, 01030, Kyiv, Ukraine **5** Department of Entomology, State Museum of Natural History Stuttgart, Rosenstein 1, 70191, Stuttgart, Germany

Corresponding author: Arnold H. Staniczek ([arnold.staniczek@smns-bw.de](mailto:arnold.staniczek@smns-bw.de))

Academic editor: L. Pereira-da-Conceicao | Received 25 March 2021 | Accepted 19 April 2021 | Published 10 May 2021

<http://zoobank.org/F4A99588-18BD-4B91-8DB4-3368AF1D7984>

**Citation:** Godunko RJ, Martynov AV, Staniczek AH (2021) First fossil record of the mayfly family Vietnamellidae (Insecta, Ephemeroptera) from Burmese Amber confirms its Oriental origin and gives new insights into its evolution. ZooKeys 1036: 99–120. <https://doi.org/10.3897/zookeys.1036.66435>

## Abstract

The small, monophyletic mayfly family Vietnamellidae Allen, 1984 has so far only been known from a few extant species of the genus *Vietnamella* Tshernova, 1972, which are all distributed in the Oriental Realm (Vietnam, Thailand, China, and India). Herein we report the first fossil record of Vietnamellidae based on a male and female imago from Mid-Cretaceous Burmese amber. We establish the new genus *Burmella* **gen. nov.** to accommodate these two new Mesozoic specimens. Their attribution to Vietnamellidae is supported by the rounded shape of the hind wings with arched outer margin, the course of thoracic sutures, and characteristics of venation, especially of MP and Cu of the forewings and associated intercalary veins of the cubital field. At the same time, *Burmella* **gen. nov.** clearly differs from *Vietnamella* by a diminished number of longitudinal and cross veins in the hind wings, and by the different shape of male genitalia. This first fossil record of Vietnamellidae supports an age of at least 100 Ma for this taxon.

## Keywords

*Burmella* gen. nov., Cretaceous, Ephemeroptera, fossil mayflies, new genus, new species, Myanmar, Pannota

## Introduction

The monogeneric family Vietnamellidae Allen, 1984 is generally regarded as monophyletic taxon within Pannota: Ephemerelloidea (Jacobus et al. 2005; Hu et al. 2017; Auychinda et al. 2020a). It was originally established by Tshernova (1972) with the type species *Vietnamella thani* Tshernova, 1972, based on larval specimens. The genus *Vietnamella* Tshernova, 1972 is endemic in the Oriental region with records from China, Thailand, India, and Vietnam (Tshernova 1972; Jacobus et al. 2005; Hu et al. 2017; Selvakumar et al. 2018; Auychinda et al. 2020a, b; Luo et al. 2020). So far there have been nine extant species formally described, which are *V. thani* Tshernova, 1972, *V. ornata* (Tshernova, 1972), *V. sinensis* (Hsu, 1936), *V. dabieshanensis* You & Su, 1987, *V. qingyuanensis* Zhou & Su, 1995, *V. guadunensis* Zhou & Su, 1995, *V. maculosa* Auychinda et al., 2020, *V. nanensis* Auychinda et al., 2020, and *V. chebalingensis* Tong, 2020.

*Vietnamella dabieshanensis* You & Su, 1987, *V. qingyuanensis* Zhou & Su, 1995, and *V. guadunensis* Zhou & Su, 1995 are regarded as synonyms of *V. sinensis* (see Hu et al. 2017), which leaves at present six valid described species within *Vietnamella*. Additional records have been reported from India and Thailand, but these have not been identified to species level (Selvakumar et al. 2018; Auychinda et al. 2020a, b), thus it is likely that there might be more extant species of *Vietnamella* discovered. However, so far there are no known fossil records of Vietnamellidae.

In this contribution, we present a fossil male and female adult mayfly specimen from Mesozoic Burmese Amber. These specimens are herein formally described as two new species in a new fossil genus *Burmella* gen. nov., which is placed within Vietnamellidae, thus constituting the first fossil record of this family.

## Materials and methods

The two specimens described in the present contribution are housed in the collection of the State Museum of Natural History Stuttgart (SMNS) under the inventory numbers BU-179 (holotype; male imago) and BU-321 (holotype; female imago). Both stones originate from the Hukawng Valley, Kachin State, Myanmar. The precise mine from which these stones originate is unknown. They were acquired from a local trader by Patrick Müller, Käßhofen, Germany, who generously donated the amber pieces to the SMNS.

Hukawng amber was assigned to the Early Cretaceous, Upper Albian, with a maximum age of  $98.79 \pm 0.62$  Ma, based on UePb zircon dating (see Shi et al. 2012), which is equivalent to the earliest Cenomanian (Gradstein et al. 2004). For more information on these amber deposits and their geological history see also Zherikhin and Ross (2000), Grimaldi et al. (2002), and Ross et al. (2010).

Drawings were made with a camera lucida on a Leica M205 C stereo microscope. Multiple photographs with different depth of field were taken through a Leica Z16

APO Macroscope equipped with a Leica DFC450 Digital Camera using Leica Application Suite v. 3.1.8. Photo stacks were processed with Helicon Focus Pro 6.4.1 to obtain combined photographs with extended depth of field, and subsequently enhanced with Adobe Photoshop CS3.

Anatomical terminology is based on Kluge (2004) and Bauernfeind and Sol-dán (2012).

## Systematic paleontology

**Subphylum Hexapoda Latreille, 1825**

**Class Insecta Linnaeus, 1758**

**Order Ephemeroptera Hyatt & Arms, 1890**

**Family Vietnamellidae Allen, 1984**

**Genus *Burmella* gen. nov.**

<http://zoobank.org/0A29850B-F977-47E1-948E-37B5C617BD95>

Figures 1–10, Table 1

**Type species.** *Burmella paucivenosa* sp. nov.

**Derivation of name.** The generic name of female gender is a composition of “*Burmar*” as an ancient term for Myanmar, combined with “*ella*”, a common ending of generic names in mayflies, and especially so within Ephemeroptera.

**Diagnosis.** Adults of *Burmella* gen. nov. differ from other mayfly genera by the following combination of features: *forewings* (a) with small number of cross veins; (b) pterostigma with simple veins, not anastomosed; (c) CuP smoothly curved towards wing base; (d) two secondary bifurcate veins in cubital field; (e) at least several free marginal intercalaries along ventral margin; *hind wings* (f) strongly rounded, small, as long as 0.08–0.14 of forewing length; (g) small number of cross veins; (h) triad RS present or absent; no MA and MP triads; (i) no secondary branches of cubital veins; (j) costal process developed, rounded apically, situated centrally; *abdomen* (k) with vestigial gill sockets recognizable at least on segments II–VI; *genitalia* (l) with large median projection of styliger plate, widely rounded apically; (m) three distal segments of forceps strongly elongated and slender; segment II longest, 5× as long as segment III; segments III and IV approximately of equal length; segment IV expanding apically; (n) penis lobes widely separated by V-shaped cleft; (o) no trace of paracercus. Additionally, *in female* (p) anterior part of eyes covered by anterolaterally expanded clypeal shield.

Subimago and larva unknown.

**Species composition.** *Burmella paucivenosa* sp. nov. (SMNS; BU-179); *Burmella clypeata* sp. nov. (SMNS; BU-321).

**Locality and horizon.** Hukawng Valley, Kachin State, Myanmar (Burma); Cenomanian, mid-Cretaceous.

**Table 1.** Measurements of fossil representatives of the genus *Burmella* gen. nov.

Adult characters	<i>Burmella paucivenosa</i> sp. nov. [SMNS, BU-179, male imago] (mm)	<i>Burmella clypeata</i> sp. nov. [SMNS, BU-321, female imago] (mm)
	Length of body	5.75
Length of right foreleg	2.51*	1.14*
Length of femur	0.83	0.42
Length of tibia	1.68	0.72*
Length of tarsus	–	–
Segment I	–	–
Segment II	–	–
Segment III	–	–
Segment IV	–	–
Segment V	–	–
Length of left foreleg	2.52*	1.64*
Length of femur	0.85	0.46
Length of tibia	1.67	1.18*
Length of tarsus	–	–
Segment I	–	–
Segment II	–	–
Segment III	–	–
Segment IV	–	–
Segment V	–	–
Length of right middle leg	2.78	–
Length of femur	1.45	–
Length of tibia	1.03	–
Length of tarsus	0.30	–
Segment I	0.08	–
Segment II	0.10	–
Segment III	0.10	–
Segment IV	0.11	–
Segment V	0.14	–
Length of left middle leg	2.70*	2.36
Length of femur	1.20	0.60
Length of tibia	1.02	1.34
Length of tarsus	0.48*	0.42
Segment I	–	0.08
Segment II	–	0.07
Segment III	–	0.07
Segment IV	–	0.08
Segment V	–	0.12
Length of right hind leg	2.47	1.71
Length of femur	1.02	0.71
Length of tibia	0.93	0.56
Length of tarsus	0.52	0.44
Segment I	0.07	0.09
Segment II	0.09	0.08
Segment III	0.10	0.07
Segment IV	0.12	0.08
Segment V	0.14	0.12
Length of left hind leg	2.07	2.60
Length of femur	1.00	0.98
Length of tibia	0.66	1.06
Length of tarsus	0.41	0.56
Segment I	0.05	0.11
Segment II	0.07	0.11
Segment III	0.07	0.10
Segment IV	0.10	0.10
Segment V	0.11	0.14
Length of right forewing	4.64	1.80
Length of left forewing	4.68	5.12
Length of right hind wing	0.66	0.45
Length of left hind wing	0.64	–
Hind/Fore wings length ratio	0.14	0.08
Length of cerci [right/left]	2.35*/1.24*	8.12/–

\* preserved part.

***Burmella paucivenosa* sp. nov.**

<http://zoobank.org/FEE2D9CE-A89A-4C7E-8619-2CC736309DBC>

Figures 1–6, Table 1

**Material examined.** *Holotype.* Male imago in Mid-Cretaceous Burmese amber, SMNS collection, inventory number BU-179. Well preserved specimen visible in lateral aspect. Due to fragility, the piece of amber is additionally embedded in translucent resin to seal the specimen from oxygen and prevent mechanical damage. Body and both pairs of wings completely preserved (Figs 1, 4–5); most part of right and left foretibiae and both foretarsi missing; most part of caudal filaments missing. For measurements see Table 1.

**Derivation of name.** The species epithet combines Latin “paucus”, few, and “venosus”, veined, referring to the reduced wing venation of the hind wing.

**Diagnosis.** *Male imago:* body length 5.75 mm; *forewings* with 3–4 marginal intercalaries connected with longitudinal veins, two free marginal intercalaries, no cross veins in anal field; *hind wings* strongly rounded, small, as long as 0.14× of forewing length, three cross veins between C–Sc, three cross veins between Sc–RA, one cross vein between RA–RSa, one cross vein between RA–RSp, RS not forked; *penis lobes* relatively simple, obliquely truncate apically, nearly tube-like; strong apical tooth on outer margin.

**Description.** Colouration relatively pale, yellowish-brown to dark brown; eyes and mesonotum darkest, dark brown to blackish; abdominal segments partly translucent; traces of dark brown maculation along of lateral margins of terga (Figs 1, 2, 4, 6).

**Head.** Compound eyes well-developed, large, widely rounded, medially contiguous; upper portion of compound eyes translucent and slightly yellowish apically, brownish-black basally; border between dorsal and ventral portions of compound eyes well distinguishable; lower portion of compound eyes brownish-black (Figs 1, 2A–C). Facets of compound eyes hexagonal. Ocelli poorly preserved, relatively small, without conspicuous colouration. Facial keel relatively small. Antennae slightly longer than head.

**Thorax.** General colouration yellowish-brown to brownish-black. Prothorax narrow, light brown. Mesonotal suture transverse, distinctly expressed; medioparapsidal suture relatively straight; lateroparapsidal suture distinctly curved laterally; scutellum not modified; no preserved natural colouration of pigmented area of mesonotum. Mesosternum with brownish basisternum and slightly paler furcasternum; basisternum elongated; furcasternal protuberances distinctly separated. Lateral sides of mesothorax light brown to brown, with blackish maculation. Metathorax brown to dark brown, blackish maculation dorsally (Fig. 2C, D).

**Wings.** *Forewings* hyaline, translucent, relatively narrow; venation well recognizable, light brown to dark brown; veins darker proximally and slightly paler distally; relatively small number of cross veins, especially in medial, cubital, and anal fields; no jagged edge along of ventral margin of forewings. Pterostigma with 3–4 simple veins. Vein sections between C and RA slightly frosted-brown distally; veins C and Sc brown to dark brown, visible all over their length; RS forked near base, after 0.14 of its length; iRS well-developed, connected with RSp by 5 cross veins, not approximated

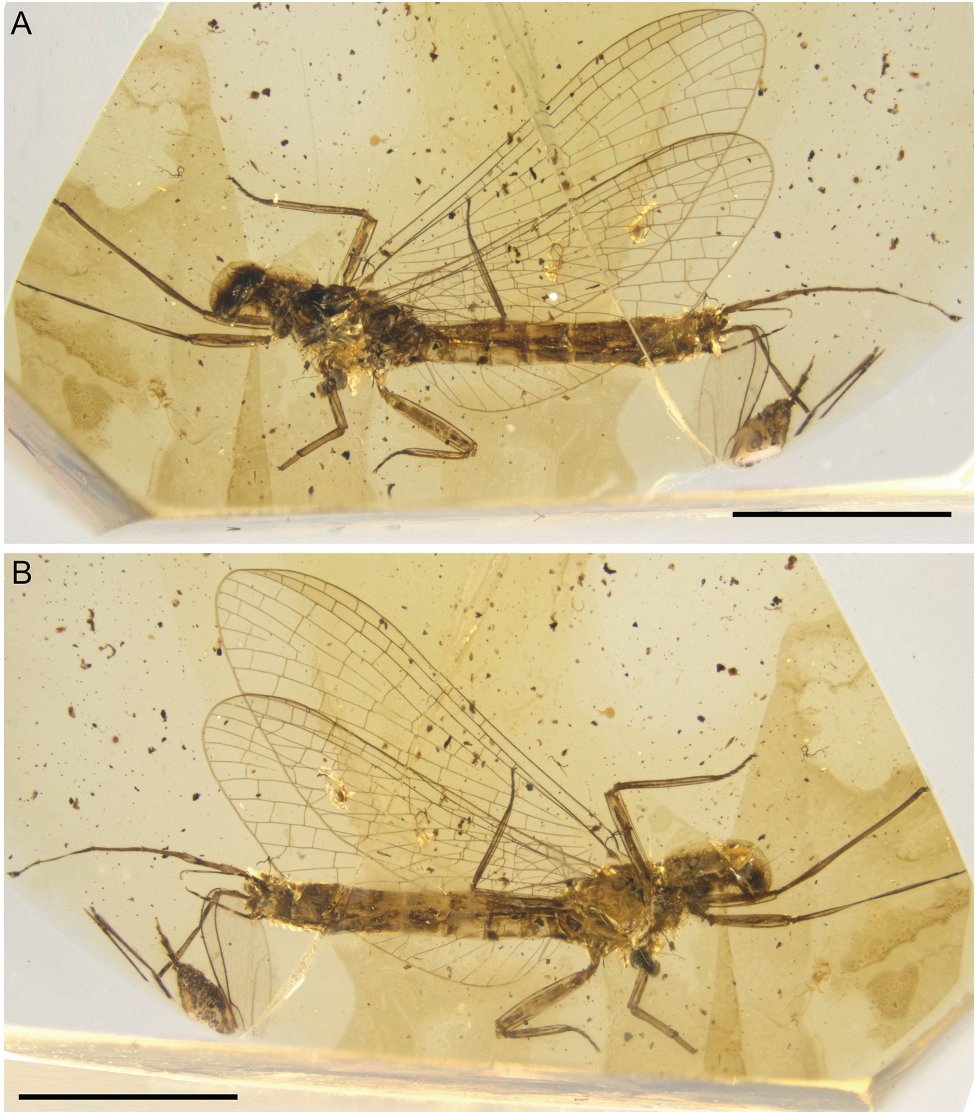


**Figure 1.** *Burmella paucivenosa* sp. nov., male imago, holotype, general lateral view **A** left side of body **B** right side of body. Scale bars: 2 mm.

to  $RSa_1$ ;  $MA$  fork slightly asymmetrical, forked after 0.60–0.62 of its length;  $MA_1$  and  $MA_2$  connected with  $iMA$  by 2–3 cross veins;  $MP$  asymmetrical, forked after 0.25 of its length,  $MP_1$  and  $MP_2$  basally connected by a single cross vein;  $iMP$  relatively short, connected with  $MP_1$  and  $MP_2$  by single cross veins from each side;  $CuP$  smoothly curved toward wing base, basally connected with  $CuA$  by cross vein  $cua-cup$ ,  $CuP$  connected with  $A_1$  by cross vein  $cup-a_1$ ,  $cua-cup$  located distally from  $cup-a_1$ ; in cubital field two secondary bifurcate veins  $iCu_{1+2}$  and  $iCu_{3+4}$  arising from  $CuA$  (i.e. four veins

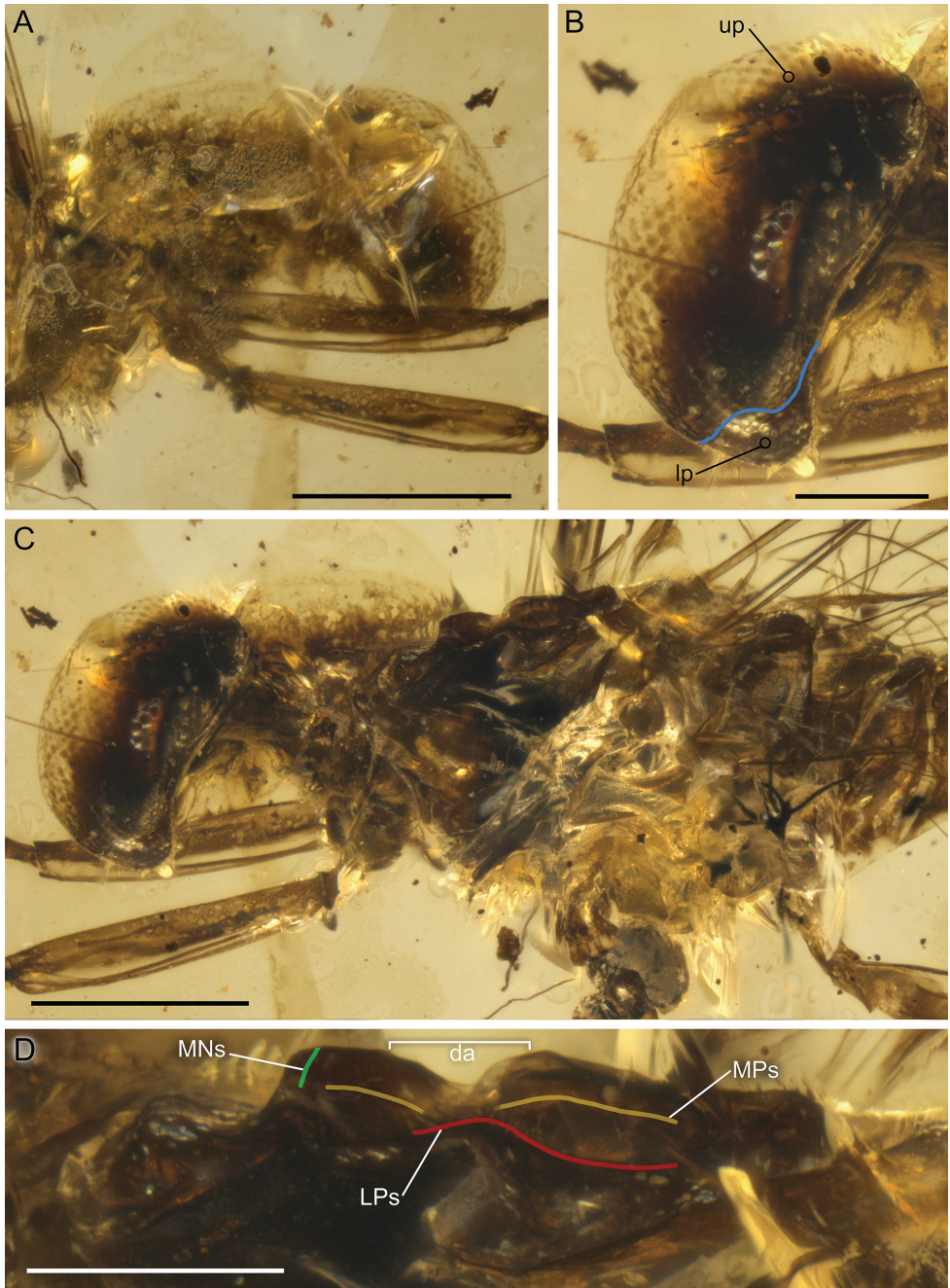


**Figure 2.** *Burmella paucivenosa* sp. nov., male imago, holotype **A** head, right lateral view **B** compound eye, left lateral view **C** head and thorax, left lateral view **D** mesothorax, left lateral view. Blue line – border between portions of compound eye, da – damaged area, lp – lower portion, LPs and red line – lateroparapsidal suture, MNs and green line – mesonotal suture, MPs and yellow line – medioparapsidal suture, up – upper portion. Scale bars: 0.5 mm (**A**, **C**); 0.2 mm (**B**, **D**).

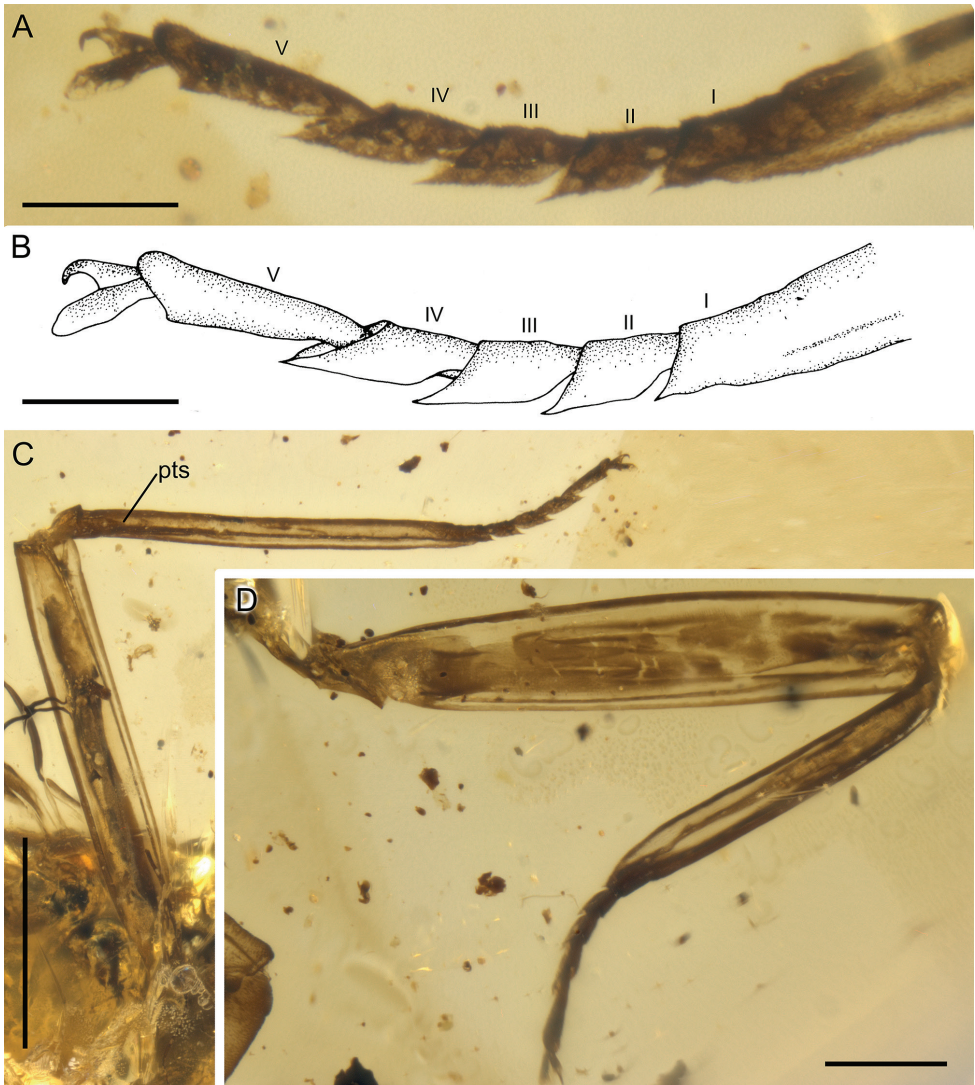


**Figure 3.** *Burmella paucivenosa* sp. nov., male imago, holotype **A, B** tarsus of right middle leg **C** right middle leg **D** left hind leg. I–V – tarsal segments, pts – patellotibial suture. Scale bars: 0.1 mm (**A, B**); 0.5 mm (**C**); 0.2 mm (**D**).

$iCu_1$ – $iCu_4$  each reaching basitornal margin of forewing); basal end of CuP closely approximated to CuA base;  $A_1$  closely approximated to  $A_2$ ; no cross veins in anal field. Several intercalaries ( $iRSa$ ,  $iRSa_2$ ,  $iMA$ ,  $iMP$ ) connected to longitudinal veins by cross-veins; two small, basally free marginal intercalaries in R and MP fields; no free intercalary veins in cubital and anal fields (Figs 1, 4).

**Hind wings** hyaline, translucent, strongly rounded, small, as long as 0.14 of forewing length; venation light brown to brown; venation significantly simplified, with

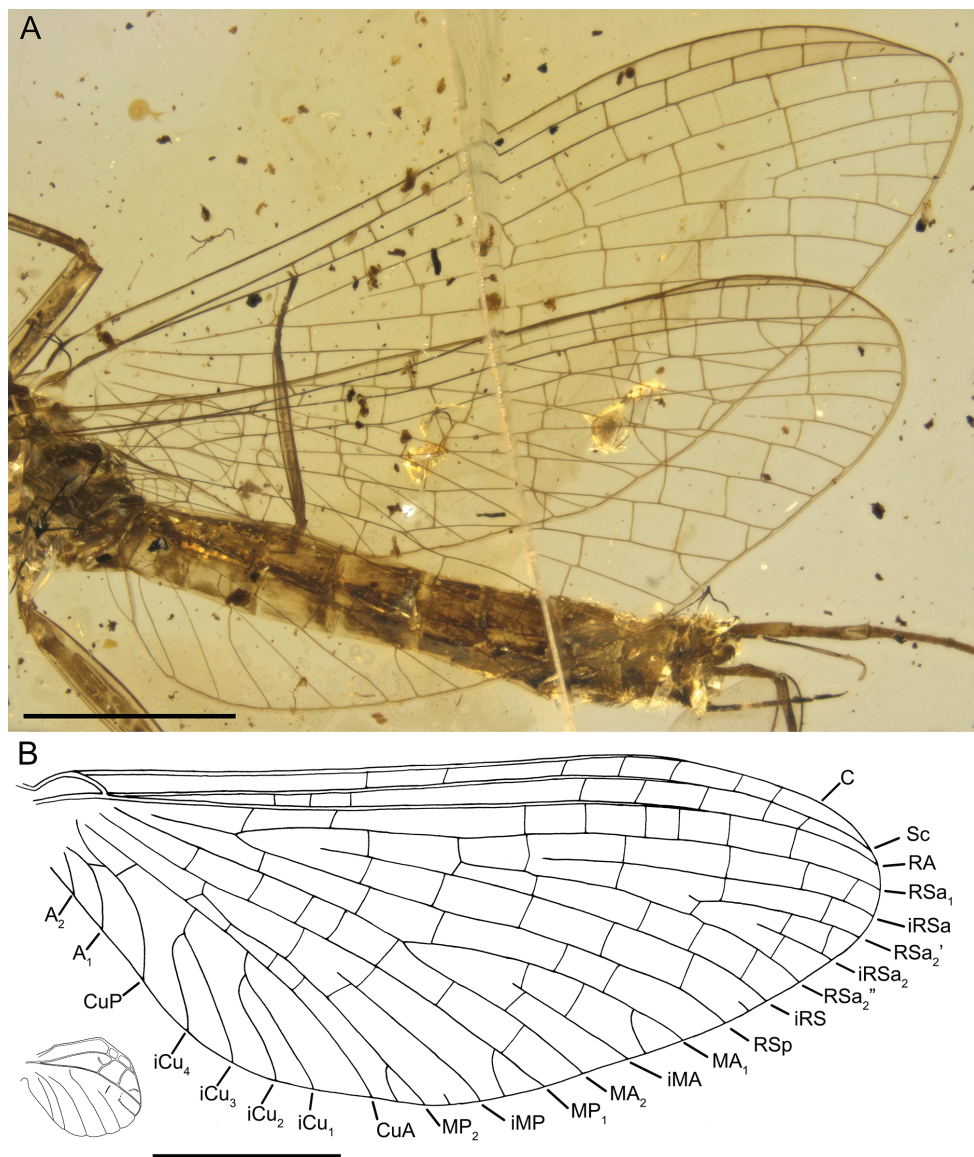


**Figure 4.** *Burmella paucivenosa* sp. nov., male imago, holotype **A** right and left wings position in amber **B** right forewing venation and size ratio of fore and hind wings. Scale bars: 1 mm.

strong reduction of number of longitudinal and cross veins; ventral margin of hind wings without jagged edge. Few cross veins between C–Sc (3 veins), Sc–RA (3 veins), RA–RSa (one vein), and RA–RSp (one vein); no triads of RS, MA and MP; MA connected with R; MP approaching CuA; no secondary branches of cubital veins; no free marginal intercalaries; costal process rounded apically, markedly protruding above anterior wing margin, situated at nearly middle of hind wing length (Fig. 5A, B).

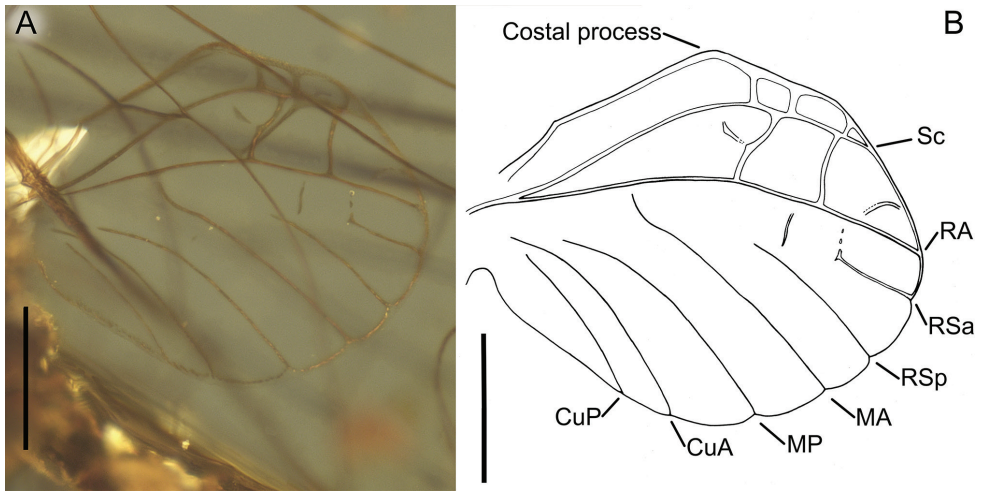


**Figure 5.** *Burmella paucivenosa* sp. nov., male imago, holotype **A** right hind wing in amber **B** right hind wing venation. Scale bars: 0.2 mm.

**Legs** well preserved, except of tarsi missing in both forelegs; margins of preserved leg segments without visible strong spines or setae. For measurements of leg segments see Table 1.

**Right foreleg:** length ratio of femur/tibia = 1/2.02; left foreleg: length ratio of femur/tibia = 1/1.96. Right middle leg completely preserved: length ratio of femur/tibia/tarsus = 1/0.71/0.21; length ratio of tarsomeres: 1/1.25/1.25/1.38/1.75 ( $5 > 4 > 3 = 2 > 1$ ). Left middle leg much shorter than right one, probably re-grown after previous injury, therefore with changed proportions of tarsomeres. Right and left hind legs completely preserved; right hind leg: length ratio of femur/tibia/tarsus = 1/0.91/0.51; length ratio of tarsomeres: 1/1.29/1.43/1.71/2.00 ( $5 > 4 > 3 > 2 > 1$ ). Left hind leg: length ratio of femur/tibia/tarsus = 1/0.66/0.41; length ratio of tarsomeres: 1/1.40/1.40/2.00/2.20 ( $5 > 4 > 3 = 2 > 1$ ). Patellotibial suture present on middle and hind legs, absent on forelegs. First tarsomere of middle and hind legs fused with tibia. Claws ephemeropteroid on preserved middle and hind legs, with outer claw hooked and inner claw blunt (Figs 1A, B, 3A–D).

**Abdominal segments** completely preserved, partly translucent, relatively pale, yellow to brown, with intensively brown maculation on terga laterally and sterna posteriorly. Vestigial gill sockets, not finger-like, recognizable on segments II–VI, poorly visible on segment VII due to influx of resin and cracks. Abdominal segments without large and prominent posterolateral projections; abdominal segments VIII–IX not elongated compared to previous segments. Abdominal sterna slightly paler than terga. Cerci brown, partly preserved; no trace of paracercus (Figs 1, 4, 6A, B).

**Genitalia** well preserved, light brown to brown, darker maculation on forceps. Styli ger plate angulate, mediocaudally deeply incised; median projection large, widely rounded apically, markedly protruding above anterior margin of styli ger. Basal segment

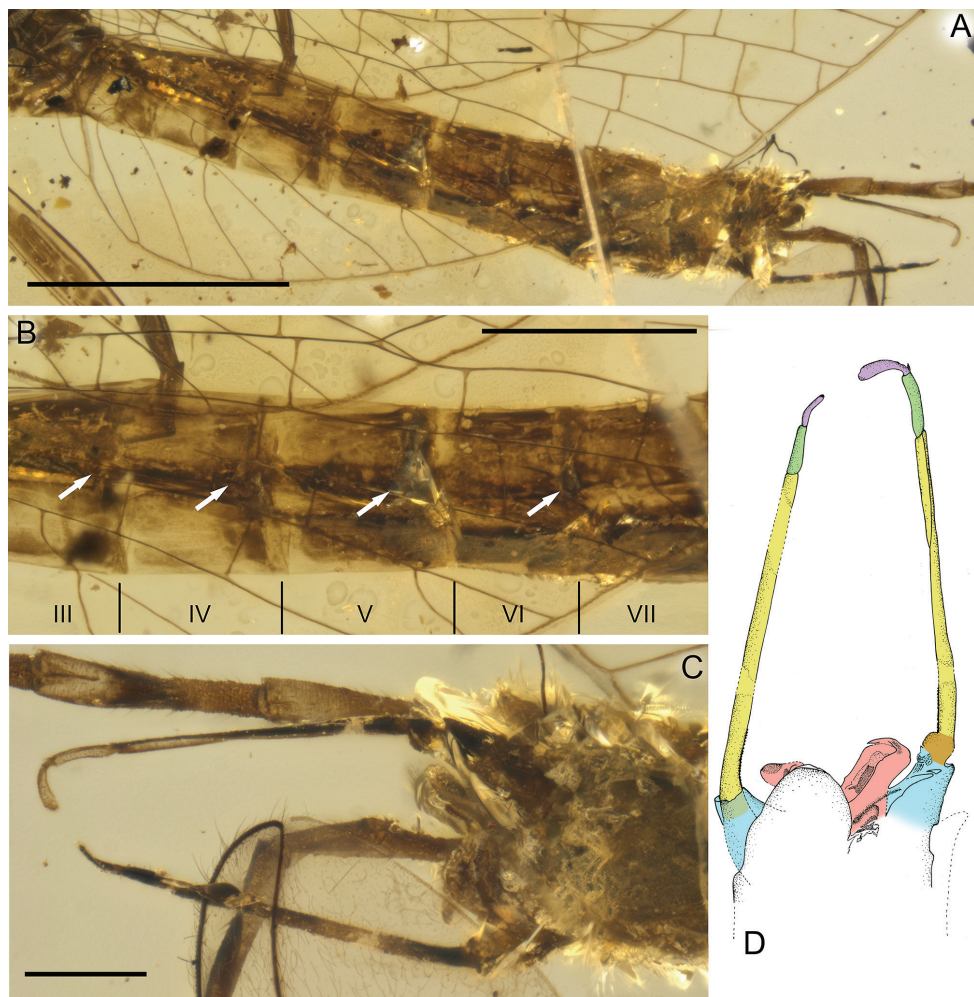


**Figure 6.** *Burmella paucivenosa* sp. nov., male imago, holotype **A** abdomen, left lateral view **B** abdominal segments III–VII, lateral view **C, D** genitalia, ventrolateral view. III–VII – numbers of segments, white arrows mark remnants of gill sockets, pink area – penis lobes, light blue area – gonobasis (styliker plate), brown area styliker segment I, yellow area –styliker segment II, light green area – styliker segment III, purple area – styliker segment IV. Scale bars: 1 mm (**A**); 0.5 mm (**B**); 0.2 mm (**C, D**).

I of forceps short, with rounded inner margin, slightly wider than long; segment II of forceps strongly elongated, slender distal segments III and IV much shorter, approximately of equal length; segment IV expanding apically; length ratio of forceps segments II–IV: 1.00/0.20/0.18 (Fig. 6C, D). Penis lobes widely separated by V-shaped cleft, relatively simple, obliquely truncate apically, nearly tube-like; structure of left penis lobe poorly visible; inner side of right penis lobe probably partly damaged or lost (i.e. looks semicircular from ventral side); strong apical tooth on outer margin; titillators not distinguishable (Fig. 6C, D).

**Affinities.** *Burmella paucivenosa* sp. nov. exhibits a combination of morphological characters allowing its attribution to Vietnamellidae, namely the presence of strongly rounded hind wings in combination with the presence of short intercalaries distally connected with longitudinal veins. Compared to other representatives of Vietnamellidae, *Burmella paucivenosa* sp. nov. is characterized by the presence of only two short free marginal intercalaries, while the number of these intercalary veins in all extant species and also in *Burmella clypeata* sp. nov. is significantly higher.

Within Vietnamellidae, *Burmella paucivenosa* sp. nov. can be attributed to the newly described genus *Burmella* gen. nov., as defined in Diagnosis (see above), mainly based on the following diagnostic characters: shape and structure of venation of hind wings, with reduced cross venation and distinct costal process situated centrally; lack of furcation of RS, MA, MP, CuA, and CuP in hind wings (Fig. 5); shape of male genitalia with deeply diverted penis lobes (Fig. 6C, D).

In the latter character, the male imago of *Burmella paucivenosa* sp. nov. differs from all other known male adults of Vietnamellidae. The genus *Vietnamella* is characterized by the presence of a club-shaped, elongated penis that is medially fused along its longitudinal axis, with only a small, V- or U-shaped incision apically (Tshernova 1972: 613, fig. 7; Hu et al. 2017: 385, figs 4C, 5C; Auychinda et al. 2020a: 8, fig. 4G; 2020b: 28, figs 7J, K, 8J, K). In contrast to *Vietnamella*, the tubular penis of *Burmella paucivenosa* sp. nov. is medially deeply split, with lobes strongly stretched laterally (Fig. 6C, D). Obvious differences are also visible in shape and proportions of forceps segments. In *Burmella paucivenosa* sp. nov. the 4-segmented forceps is strongly elongated and slender, with segment II being the longest, with the same width distally as segment III basally, while distal segment IV is markedly elongated and nearly subequal to segment III (Fig. 6C, D). On the contrary, in *Vietnamella* the forceps is only 3-segmented with segments significantly different in shape and proportions: Segment I is the longest one, while shortest segment III is small and rounded, which is typical for many species of Ephemeroidea (see Kluge 2004).

***Burmella clypeata* sp. nov.**

<http://zoobank.org/5F823D68-5C03-4138-8875-D80917D61452>

Figures 7–10, Table 1

**Material examined. Holotype.** Female imago in Mid-Cretaceous Burmese amber, SMNS collection, inventory number: BU-321. Well preserved specimen visible in dorsal/ventral aspect. Body and left forewings preserved except of lost distal part of C and Sc; left forewing twisted, covering dorsal side of abdomen; right forewings twisted, only partly preserved, distal part missing; foretibiae damaged; right antenna, foretarsi, right middle leg and left cercus missing (Figs 7, 8, 10). Left hind wing not visible. For measurements see Table 1.

**Derivation of name.** The species epithet refers to the laterally expanded clypeus that partly covers the eyes.

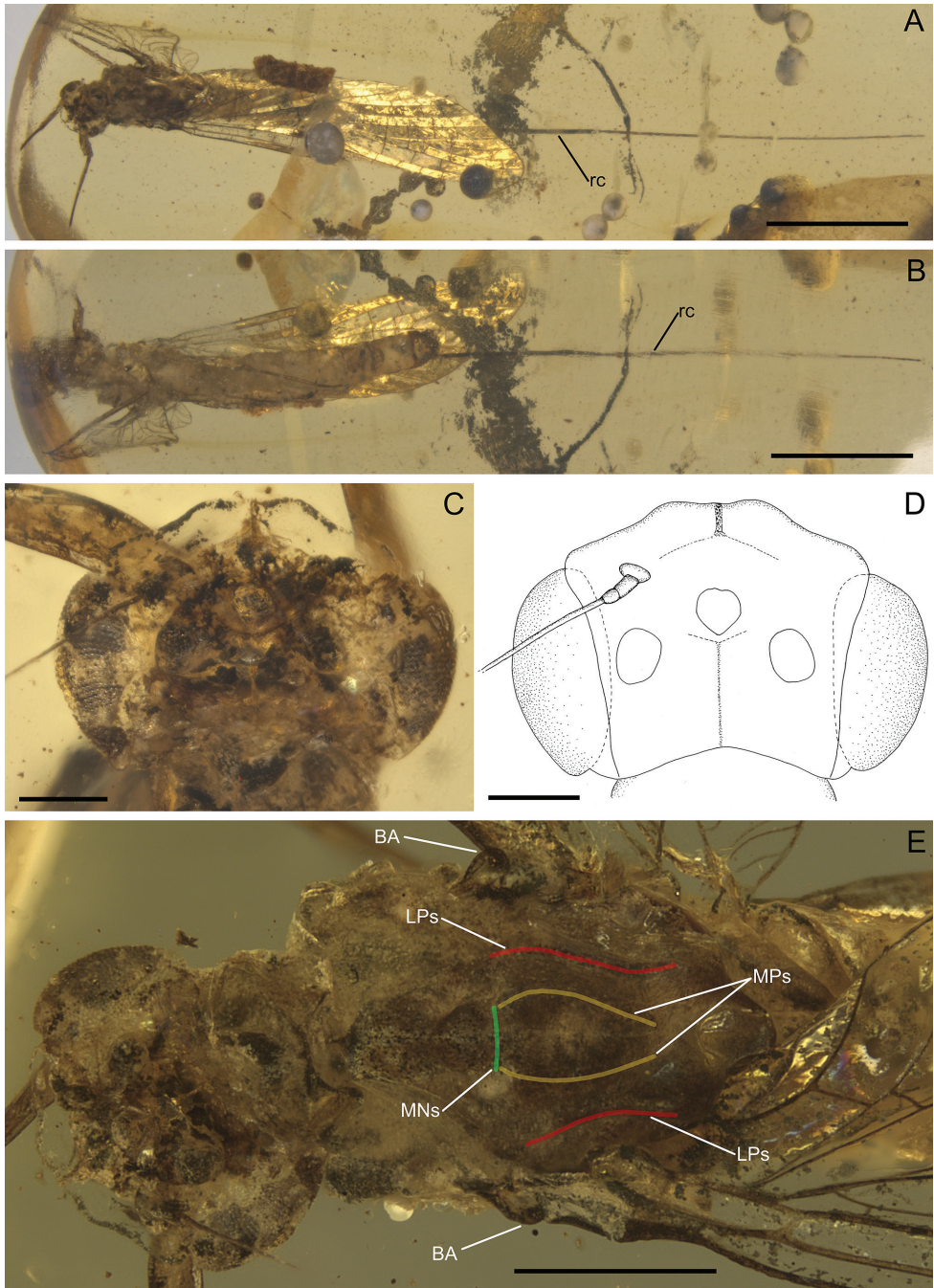


**Figure 7.** *Burmella clypeata* sp. nov., female imago, holotype **A** general dorsal view **B** general ventral view **C, D** head, dorsal view **E** head and thorax, dorsal view. BA – basal sclerite (basalare), LPs and red line – lateroparapsidal suture, MNs and green line – mesonotal suture, MPs and yellow line – medioparapsidal suture, rc – right cercus. Scale bars: 2 mm (**A, B**); 0.2 mm (**C, D**); 0.5 mm (**E**).

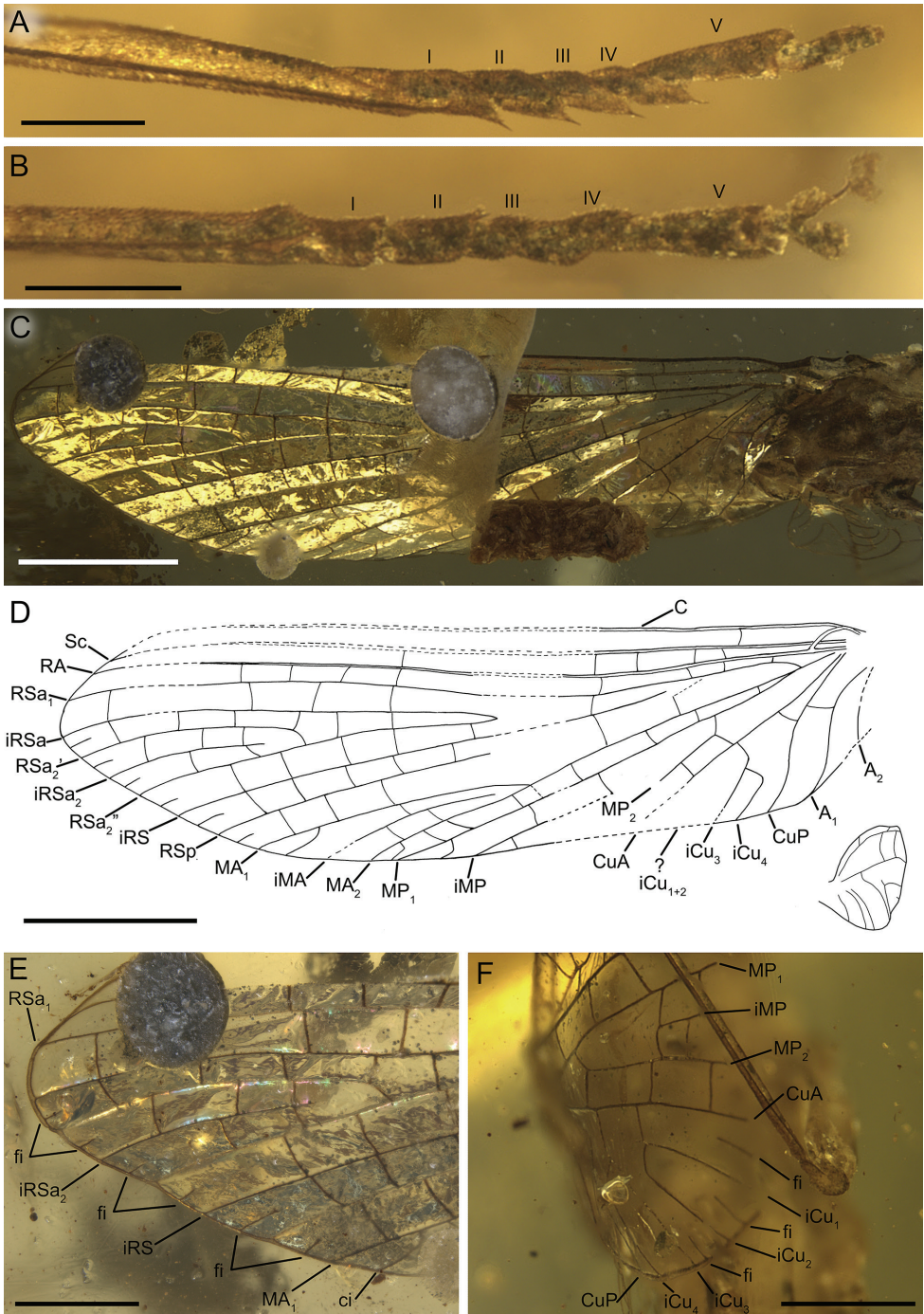


**Figure 8.** *Burmella clypeata* sp. nov., female imago, holotype **A** tarsus of left hind leg **B** tarsus of right hind leg **C** left forewing in amber **D** left forewing venation and size ratio of left fore- and right hind wings **E** distal part of left forewing **F** preserved basal part of right forewing. I–V – tarsal segments, ci – basally connected intercalary vein, fi – basally free intercalary vein. Scale bars: 0.1 mm (**A, B**); 1 mm (**C, D**); 0.5 mm (**E, F**).

**Diagnosis. Female imago:** body length 7.00 mm; *forewings* with at least four short marginal intercalaries in MA–MP field basally attached to longitudinal veins, six free marginal intercalaries in RS field; *hind wing* strongly rounded, small, as long as 0.08× of forewing length, two cross veins between C–Sc, two cross veins between Sc–RA; RS forked; *subgenital plate* more than 2.00× as wide as long, convex and widely rounded apically; *subanal plate* triangular, elongated, rounded apically without cleft.

**Description.** General colouration of body relatively pale, light brown to dark brown. Ventral side of body slightly darker than dorsal side. Body covered by blackish maculation (Figs 7A, B, 10).

**Head.** Clypeus expanded anterolaterally, partly covering anterior part of eyes. Eyes brown, elongated, relatively large, widely separated medially; facets of eyes hexagonal. Distance between eyes 0.73× of head width. Ocelli well preserved, large, without conspicuous colouration. Facial keel small. Antenna brown, approximately as long as head; segmentation hardly distinguishable, therefore not depicted (see Fig. 7C–D).

**Thorax.** General colouration brown to dark brown. Lateral aspect of thorax not visible. Prothorax narrow, brown. Mesonotal suture transverse, expressed; medioparapsidal suture poorly visible, straight; lateroparapsidal suture distinctly curved laterally; no preserved natural colouration of pigmented area of mesonotum. Ventral side of mesothorax poorly visible; basisternum relatively short and wide distally, furcasternal protuberances distinctly separated. Metathorax brown to dark brown, blackish maculation dorsally (Fig. 7E).

**Wings.** *Forewings* hyaline, translucent, relatively narrow; venation poorly recognizable due to wing deformation, pollution on surface and resin influxes [left wing], and damage of distal part [right wing]; venation well visible from dorsal, and partly from lateral side. Veins light brown to brown; relatively small number of cross veins; no jagged edge along of ventral margin (Fig. 8C–F).

General pattern of forewing venation similar to those of male imago of *Burmella paucivenosa* sp. nov., except for the following features: six free intercalary veins at least in RS field and CuA–CuP; at least four intercalaries in MA–MP field basally attached to longitudinal veins (Fig. 8C–F).

**Hind wings** hyaline, translucent, small, as long as 0.08 of forewing length; preserved wing is deformed due to embedding, but most probable was naturally strongly rounded, with shallow costal process; venation brown, significantly simplifies; strong reduction of number of longitudinal and cross veins; no jagged edge along of ventral margin. General structure and pattern of hind wing venation similar to those in male imago of *Burmella paucivenosa* sp. nov., except for the following features: a few cross veins between C–Sc (2 veins), and Sc–RA (2 veins); fork RS present, iRS short, no cross veins in RS field; costal process not prominent (Fig. 9A–C).

**Legs** well preserved, except for both forelegs with partly missing tibiae and tarsi; no visible strong spines or setae on margins of leg segments. Preserved part of forelegs darker than middle and hind legs, brown to intensively brown (Fig. 8A, B). For measurements of leg segments see Table 1.

Forelegs partly preserved [due to damage of foretibiae the ratio of femur/tibia is not calculated]. Left middle leg completely preserved: length ratio of femur/tibia/

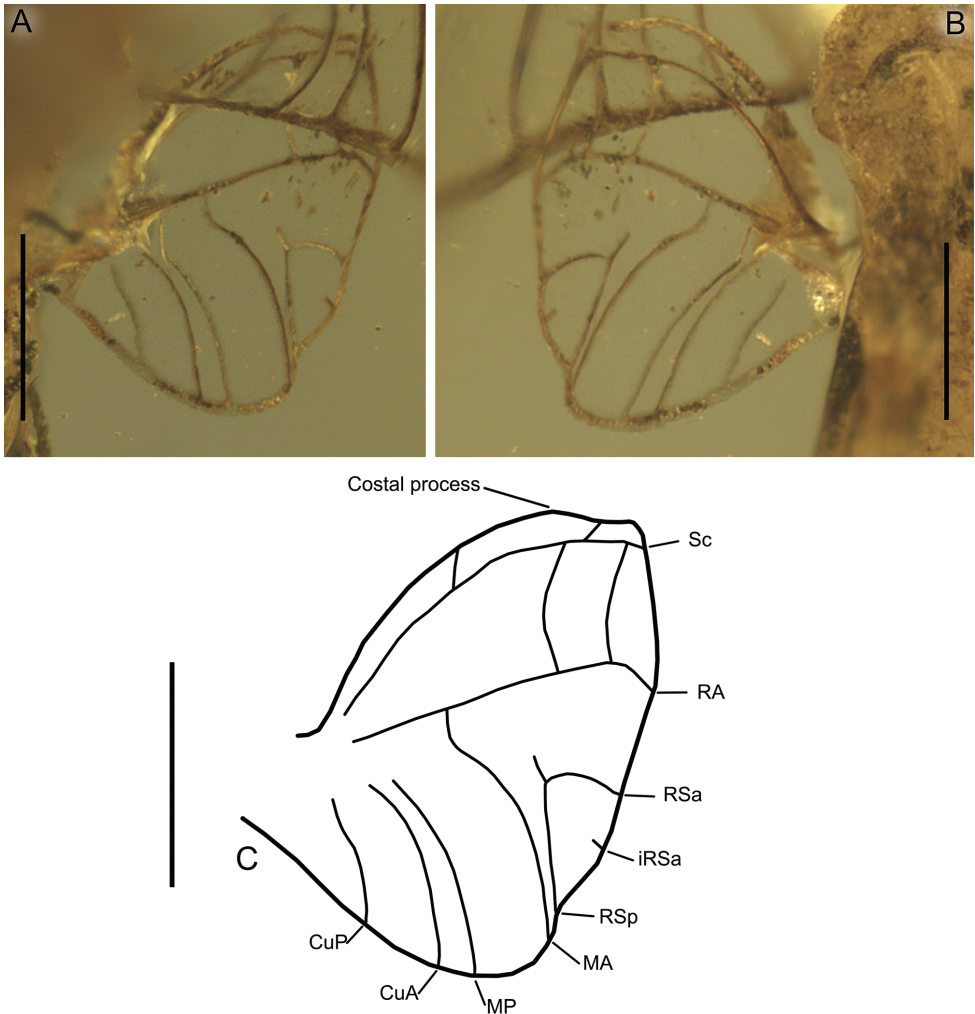


**Figure 9.** *Burmella clypeata* sp. nov., female imago, holotype **A** right hind wing, dorsal view **B** right hind wing, ventral view **C** right hind wing venation. Scale bars: 0.2 mm (**A, B**); 0.5 mm (**C**).

tarsus = 1/2.23/0.70; length ratio of tarsomeres: 1/0.88/0.88/1.00/1.50 ( $5 > 4 > 3 = 2 < 1$ ). Right hind leg much shorter than left one, probably re-grown after previous injury, therefore with changed proportions of tarsomeres: length ratio of femur/tibia/tarsus = 1/0.79/0.62; length ratio of tarsomeres: 1/0.89/0.78/0.89/1.33 ( $5 > 4 > 3 < 2 < 1$ ). Left hind leg: length ratio of femur/tibia/tarsus = 1/1.02/0.57; length ratio of tarsomeres: 1/1/0.91/0.91/1.27 ( $5 > 4 = 3 < 2 = 1$ ) (Figs 8A, B, 10A). Other leg characters similar to those in male imago of *Burmella paucivenosa* sp. nov.

**Abdominal segments** completely preserved, light brown to brown, with blackish maculation on terga and sterna; ventral side of abdomen paler than dorsal side. Vestigial gill sockets, not finger-like, well recognizable on segments II, V, and IV; on other segments

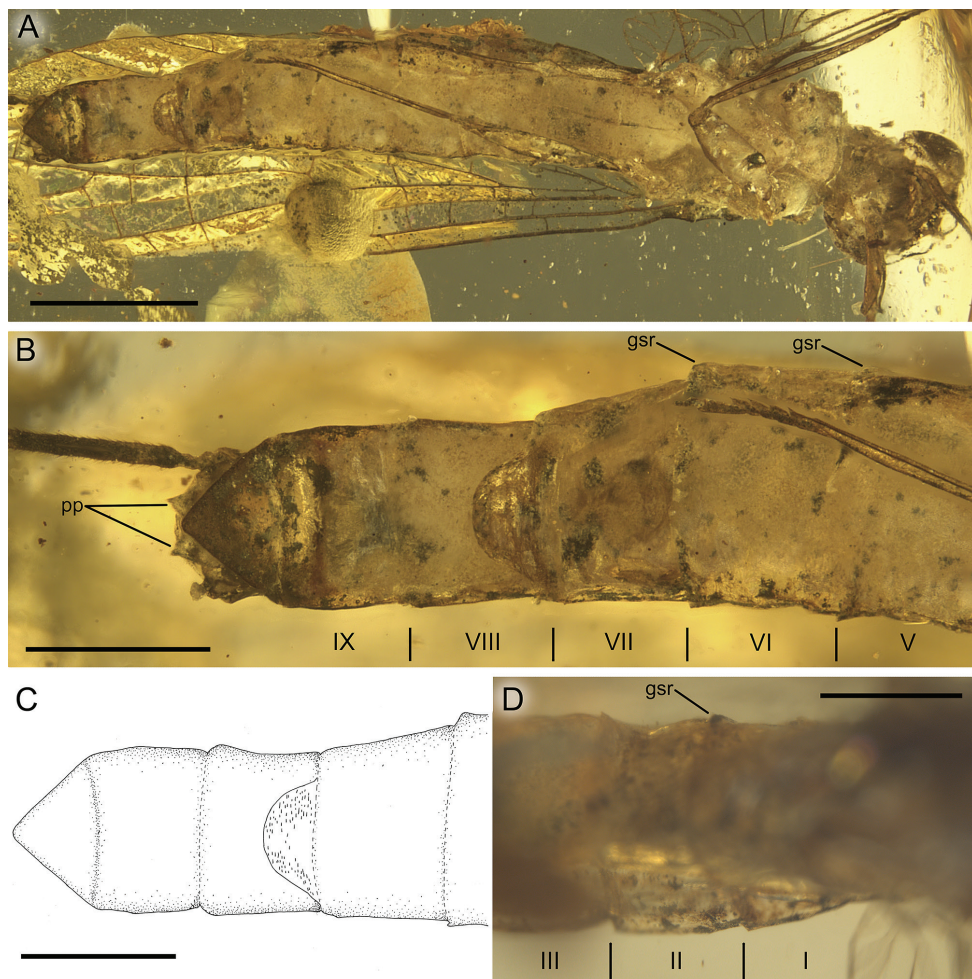


**Figure 10.** *Burmella clypeata* sp. nov., female imago, holotype **A** body, ventral view **B, C** apical part of abdomen, ventral view **D** basal segments of abdomen, dorsal view. I–III and V–IX – numbers of abdominal segments, gsr – remnant of gill socket, pp – paraproct plate. Scale bars: 1 mm (**A**); 0.5 mm (**B–D**).

gill sockets not distinguishable due to body position in amber. Abdominal segments without large and prominent posterolateral projections; no conspicuous elongation of distal segments compared to proximal ones. Subgenital plate relatively broad, more than 2.00× as wide as long, convex and widely rounded apically. Subanal plate triangular, elongated, moderately narrow and rounded apically without apical cleft. Right cercus completely preserved, brown, darker proximally, approximately as long as body (Fig. 10A–D).

**Affinities.** Attribution of *Burmella clypeata* sp. nov. to the newly described genus is confirmed based on the shape of hind wings, and specific venation.

On the other hand, some aspects of the venation of fore- and hind wings differ between *Burmella clypeata* sp. nov. and *Burmella paucivenosa* sp. nov. The forewings of

*Burmella clypeata* sp. nov. differ by the presence of numerous free marginal intercalaries between iRS and CuP, as well as the presence of at least one cross vein between  $A_1$  and  $A_2$ . In the hind wings differences between the extinct species described here refer to the number of cross veins between C–Sc and Sc–RA. The presence of RS furcation and blunt costal process in *Burmella clypeata* sp. nov. are also suitable for the separation of both species. In contrast to all other representatives of Vietnamellidae, the clypeus in the female of *Burmella clypeata* sp. nov. is anterolaterally expanded, as a result the anterior portion of eyes is partly covered by this clypeal shield (Fig. 7C–D; compare with e.g., Auychinda et al. 2020a: 9, figs A–E; 2020b: 30, fig. 9A).

We do however not per se exclude a possible conspecificity of both fossil specimens. This may be supported by a similar, small body size of both specimens, with similar proportions of male/female body length as in extant Vietnamellidae (for *Burmella* gen. nov. the ratio is 0.82; for *Vietnamella* between 0.92 and 0.96). Also, the anterolaterally expanded clypeus in *B. clypeata* may not exclude their conspecificity. Similar clypeal expansions present in one sex only have been reported in several extant and fossil species of Heptageniidae (e.g. in the subgenus *Ecdyonurus* (*Nestormeus*) Godunko, 2004), representing a morphological trait independently occurring in several unrelated taxa within the family (see Godunko 2007: 66, figs 1, 2; Hrivniak et al. 2018: 199, 204–205, figs 2–5). However, a clear difference in the venation of fore- and hind wings between *B. paucivenosa* sp. nov. and *B. clypeata* sp. nov. rather points to the presence of two different fossil species.

In any case, unless specimens of different sex are syninclusions and fossilized in mating position, we tend to describe males and females of the same genus as different species also to maintain nomenclatural stability (see e.g. Staniczek and Godunko 2016; Godunko et al. 2019).

### Remarks on the systematic position of *Burmella* gen. nov. as genus within Vietnamellidae (Ephemerelloidea)

Based on the available evidence, we propose the systematic position of *Burmella* gen. nov. as a distinct congener of the family Vietnamellidae, although its character distribution implies disturbing homoplasy of some characters within Ephemerelloidea (see also McCafferty and Wang 2000; Kluge 2004; Ogden et al. 2009).

However, *Burmella* gen. nov. shares most important apomorphic characters of Ephemerelloidea (compare also Kluge 2004):

(1) The basal connection of CuP with CuA and  $A_1$  by associated cross veins  $cua-cup$  and  $cup-a_1$ . As typical for most Ephemerelloidea,  $cua-cup$  in *Burmella* gen. nov. is located more distally than  $cup-a_1$ ;

(2) The specific arrangement of the cubital field with one or more bifurcated veins is another apomorphic feature of Ephemerelloidea, which is also present in *Burmella* gen. nov.;

(3) The apomorphic arrangement of thoracic sutures in Ephemerelloidea is also present in *Burmella* gen. nov., namely a transverse mesonotal suture and a lateroparap-

sidal suture with laterally curved posterior end, which is associated with specific lateral sclerotized area;

(4) The separated furcasternal protuberances count as yet another apomorphic character supporting this placement.

Within Ephemeroptera, *Burmella* gen. nov. shares the main wing apomorphy of Vietnamellidae, which is presence of strongly rounded hind wings with moderately arched foremargin. Except of Vietnamellidae, such a rounded shape of hind wings is only known in extant (*Baetisca* Walsh, 1863) and fossil (*Balticobaetisca* Staniczek & Bechly, 2002) genera of the family Baetiscidae Edmunds & Traver, 1954 (Staniczek and Bechly 2002: 8; Kluge 2004: 67, fig. 17C; Godunko and Krzemiński 2009: 127, fig. 1). However, the anteritornous forewing shape of *Burmella* gen. nov. as well as all the aforementioned apomorphic characters of Ephemeroptera precludes closer affinities with the posteritornous Baetiscidae. At the same time, the presence of marginal intercalaries attached to longitudinal veins, and the presence of free intercalary veins of forewings, also fits well with the character distribution in Ephemeroptera.

While the overall character distribution accounts for a placement of *Burmella* gen. nov. within Vietnamellidae, there are also considerable differences between the herein described species and the extant genus *Vietnamella* that justify its placement in a separate genus:

(1) A smaller number of cross veins in forewings, with only few, simple cross veins in pterostigma (in contrast to a well-developed cross venation, with simple and forked veins in the pterostigmatic area of *Vietnamella*) (Figs 1, 4, 8D–F; compare with Auychinda et al. 2020a: 28–30, figs 7H, 8H, 9H; 2020b: 9, fig. 5F);

(2) CuP of forewings smoothly curved toward the hind margin of wing and basally directed toward CuA (in contrast to CuP of *Vietnamella*, which is sharply curved at approximately 1/3 of its length) (Figs 4B, 8D; compare e.g. Kluge 2004: 318, fig. 95A);

(3) Distinctly diminished hind wings, as long as 0.08–0.14 of forewing length, with a few cross veins only (in contrast to *Vietnamella*, with well-developed cross venation and fore/hind length ratio at least 0.20) (Figs 5, 9; compare with Kluge 2004: 318, fig. 95B; Auychinda et al. 2020a: 28–30, figs 7I, 8I, 9I; 2020b: 9, fig. 5G);

(4) Cubital field of hind wings without secondary branches and cross venation, with simple CuA and CuP only (in contrast to well-developed branches of CuA and CuP in *Vietnamella*, connected by several cross veins) (Figs 5, 9);

(5) Rounded apically costal process of hind wings situated centrally (in *Vietnamella* costal process of hind wings is absent, with leading margin slightly concave centrally) (Figs 5, 9);

(6) Only a single longitudinal intercalary vein [iMP] between  $MP_1$  and  $MP_2$  of forewings (in contrast to *Vietnamella*, with iMP and 2–5 additional elongated intercalaries between  $MP_1$  and  $MP_2$ ) (Figs 1, 4, 8D; compare with Kluge 2004: 318, fig. 95A; Auychinda et al. 2020a: 28–30, figs 7H, 8H, 9H; 2020b: 9, fig. 5F);

(7) There are no traces of paracercus present (in *Vietnamella* a well-developed paracercus is present) (Figs 1, 4A, 6A, 6C, 10A, B; compare with Auychinda et al. 2020a: 31, fig. 10C Auychinda et al. 2020b, fig. 5N);

(8) Both fossil specimens are significantly smaller than known adults of *Vietnamella*. While the body size of male and female adults of *Vietnamella* varies within 12–17 mm, the adults of *Burmella* gen. nov. are approximately 2× smaller (5.75 mm the male, and 7.00 mm the female). The ratio of body length of fossil male and female is 0.82, which is a little less in compare to *Vietnamella* (the ratio is 0.92–0.96).

At the same time, *Burmella* gen. nov. shows significant differences in the structure and shape of male genitalia compared to both *Vietnamella* and other Ephemerelloidea. While the 3-segmented forceps of *Vietnamella* is relatively short, with enlarged segment I, a well recognizable border between segments I and II, and a nearly rounded, small, distal segment, the 4-segmented forceps of *Burmella* gen. nov. are even more elongated and slender, with two short segments distally. The longest segment II is distally as wide as the base of the segment III, and elongated segment IV is expanding apically. The penis lobes of *Burmella* gen. nov. are deeply separated by a V-shaped cleft and outstretched laterally. Overall, the genital morphology and arrangement of forceps segments appears to be a rather plesiomorphic condition resembling conditions like in Siphonuridae Ulmer, 1920 or Heptageniidae Needham, 1901.

This plesiomorphic condition of the genitalia however would imply a convergent, parallel development of both the 3-segmented forceps with elongated first segment and only one short segment distally, and a medially fused, stab-like penis in both *Vietnamella* and other Ephemerelloidea (Kluge 2004). However, all other synapomorphies *Burmella* gen. nov. shares with *Vietnamella* and other Ephemerelloidea in our opinion clearly outweigh the genital characters and justify its placement within Vietnamellidae. A more thorough phylogenetic discussion after a cladistic analysis will be conducted as soon as new Mesozoic material becomes available (Staniczek et al. in prep.)

The discovery of *Burmella* gen. nov. in about 100 Ma old Burmese amber however points to a surprisingly old age of Vietnamellidae, at the same time indicating that the major splits of Ephemerelloidea might have occurred earlier than previously assumed (Staniczek et al. 2018). Its discovery makes an Oriental origin of the group likely and supports the assumption of Vietnamellidae as endemic Oriental group within Ephemerelloidea.

## Acknowledgements

We are grateful to Patrick Müller, Kāshofen, Germany, for donating the specimens to SMNS. We would like to thank Kateřina Bláhová (IE BC CAS) for line drawings and Milan Pallmann (SMNS) for macro photographs. RJG acknowledges the financial support of the Grant Agency of the Czech Republic (No. 21-05216S) and institutional support RVO 60077344 (IE, BC CAS). The stay of RJG at SMNS was supported by a Georg Forster Research Fellowship for Experienced Researchers by the Alexander von Humboldt Foundation in 2019 and SYNTHESYS (<http://www.synthesys.info/>), which was financed by the European Community Research Infrastructure Action in 2020.

## References

- Auychinda Ch, Sartori M, Boonsoong B (2020a) Vietnamellidae (Insecta, Ephemeroptera) of Thailand. *ZooKeys* 902: 17–36. <https://doi.org/10.3897/zookeys.902.46844>
- Auychinda Ch, Jacobus LM, Sartori M, Boonsoong B (2020b) A new species of *Vietnamella* Tshernova 1972 (Ephemeroptera: Vietnamellidae) from Thailand. *Insects* 11(9): 1–18. <https://doi.org/10.3390/insects11090554>
- Bauernfeind E, Soldán T (2012) The Mayflies of Europe (Ephemeroptera). Apollo Books, Ollerup, 781 pp. <https://doi.org/10.1163/9789004260887>
- Godunko RJ (2007) Contribution to the knowledge of the fossil subgenus *Nestormeus* Godunko, 2004 (Ephemeroptera: Heptageniidae: *Ecdyonurus*) from the Baltic amber (Eocene). *Zootaxa* 1661: 63–68. <https://doi.org/10.5281/zenodo.179949>
- Godunko RJ, Krzemiński W (2009) New fossil findings of the mayfly genera *Balticobaetisca* Staniczek & Bechly, 2002 (Ephemeroptera: Baetiscidae) and *Borinquena* Traver, 1938 (Leptophlebiidae: Atalophlebiinae). In: International Perspectives in Mayfly and Stonefly Research. Proceedings of the 12<sup>th</sup> International Conference on Ephemeroptera and the 16<sup>th</sup> International Symposium on Plecoptera. *Aquatic Insects* 31(Suppl. 1): 125–136. <https://doi.org/10.1080/01650420802611187>
- Godunko RJ, Neumann Ch, Staniczek AH (2019) Revision of fossil Metretopodidae (Insecta, Ephemeroptera) in Baltic amber – Part 4: Description of two new species of *Siphloplecton* Clemens, 1915, with notes on the new *S. jaegeri* species group and with key to fossil male adults of *Siphloplecton*. *ZooKeys* 898: 1–26. <https://doi.org/10.3897/zookeys.898.47118>
- Gradstein FM, Ogg JG, Smith AG (2004) A Geologic Time Scale 2004. Cambridge University Press, Cambridge. <https://doi.org/10.1017/CBO9780511536045>
- Grimaldi DA, Engel MS, Nascimbene PC (2002) Fossiliferous Cretaceous amber from Myanmar (Burma): its rediscovery, biotic diversity, and paleontological significance. *American Museum Novitates* 3361: 1–71. [https://doi.org/10.1206/0003-0082\(2002\)361<0001:FC AFMB>2.0.CO;2](https://doi.org/10.1206/0003-0082(2002)361<0001:FC AFMB>2.0.CO;2)
- Hrivniak L, Sroka P, Godunko RJ, Palatov D, Poláček M, Manko P, Oboňa J (2018) Diversity of Armenian mayflies (Ephemeroptera) with the description of a new species of the genus *Ecdyonurus* (Heptageniidae). *Zootaxa* 4500(2): 195–221. <https://doi.org/10.11646/zootaxa.4500.2.3>
- Hu Z, Ma Zh-X, Luo J-Y, Zhou Ch-F (2017) Redescription and commentary on the Chinese mayfly *Vietnamella sinensis* (Ephemeroptera: Vietnamellidae). *Zootaxa* 4286(3): 381–390. <https://doi.org/10.11646/zootaxa.4286.3.5>
- Jacobus LM, McCafferty WP, Sites W (2005) Significant range extensions for *Kangella* and *Vietnamella* (Ephemeroptera: Ephemereillidae, Vietnamellidae). *Entomological News* 116: 268–270.
- Kluge NJ (2004) The Phylogenetic System of Ephemeroptera. Kluwer Academic Publishers, Dordrecht, 456 pp. <https://doi.org/10.1007/978-94-007-0872-3>
- Luo Y, Jiang J, Wang L, Shu Z, Tong X (2020) *Vietnamella chebalingensis*, a new species of the family Vietnamellidae (Ephemeroptera) from China based on morphological and molecular data. *Zootaxa* 4868(2): 208–220. <https://doi.org/10.11646/zootaxa.4868.2.2>

- McCafferty WP, Wang T-Q (2000) Phylogenetic systematics of the major lineages of pannotid mayflies (Ephemeroptera: Pannota). *Transactions of the American Entomological Society* 126(1): 9–101.
- Ogden TH, Gattolliat J-L, Sartori M, Staniczek AH, Soldan T, Whiting MF (2009) Towards a new paradigm in mayfly phylogeny (Ephemeroptera): combined analysis of morphological and molecular data. *Systematic Entomology* 34(4): 616–634. <https://doi.org/10.1111/j.1365-3113.2009.00488.x>
- Ross A, Mellish C, York P, Crighton B (2010) Burmese amber. In: Penney D (Ed.) *Biodiversity of Fossils in Amber from the Major World Deposits*. Rochdale: Siri Scientific Press.
- Selvakumar C, Sinda B, Vasanth M, Subramanian KA, Sivaramakrishnan KG (2018) A new record of monogeneric family Vietnamellidae (Insecta: Ephemeroptera) from India. *Journal of Asia-Pacific Entomology* 21: 994–998. <https://doi.org/10.1016/j.aspen.2018.07.015>
- Shi G, Grimaldi DA, Harlow GE, Wang J, Wang J, Yang M, Lei W, Li Q, Li X (2012) Age constraint on Burmese amber based on U-Pb dating of zircons. *Cretaceous Research* 37: 155–163. <https://doi.org/10.1016/j.cretres.2012.03.014>
- Staniczek AH, Bechly G (2002) First fossil record of the mayfly family Baetiscidae from Baltic amber (Insecta: Ephemeroptera). *Stuttgarter Beiträge zur Naturkunde (B)* 322: 1–11.
- Staniczek AH, Godunko RJ (2016) Revision of fossil Metretopodidae (Insecta: Ephemeroptera) in Baltic amber – Part 3: Description of two new species of *Siphloplecton* Clemens, 1915, with notes on the re-discovered lectotype of *Siphloplecton macrops* (Pictet-Baraban & Hagen, 1856). *Zootaxa* 4103(1): 1–24. <https://doi.org/10.11646/zootaxa.4103.1.1>
- Staniczek AH, Godunko RJ, Kluge NJ (2018) Fossil record of the mayfly family Ephemerellidae (Insecta: Ephemeroptera), with description of new species and first report of Ephemerellinae from Baltic amber. *Journal of Systematic Palaeontology* 16(15): 1319–1335. <https://doi.org/10.1080/14772019.2017.1388299>
- Tshernova OA (1972) Some new species of mayflies from Asia (Ephemeroptera, Heptageniidae, Ephemerellidae). *Entomologicheskoe Obozrenie* 51(3): 604–614.
- Zherikhin VV, Ross AJ (2000) A review of the history, geology and age of Burmese amber (Burmite). *Bulletin of the Natural History Museum, Geology* 56: 3–10.

# Species delimitation of *Margattea* cockroaches from China, with seven new species (Blattodea, Ectobiidae, Pseudophyllodromiinae)

Jia-Jun He<sup>1</sup>, Du-Ting Jin<sup>1</sup>, Yi-Shu Wang<sup>1</sup>, Yan-Li Che<sup>1</sup>, Zong-Qing Wang<sup>1</sup>

<sup>1</sup> College of Plant Protection, Southwest University, Beibei, Chongqing 400715, China

Corresponding author: Zong-Qing Wang ([zqwang2006@126.com](mailto:zqwang2006@126.com))

Academic editor: F. Legendre | Received 17 January 2021 | Accepted 1 April 2021 | Published 10 May 2021

<http://zoobank.org/E0949AC7-29FA-4691-ACD3-8C471C79D9AF>

**Citation:** He J-J, Jin D-T, Wang Y-S, Che Y-L, Wang Z-Q (2021) Species delimitation of *Margattea* cockroaches from China, with seven new species (Blattodea, Ectobiidae, Pseudophyllodromiinae). ZooKeys 1036: 121–151. <https://doi.org/10.3897/zookeys.1036.63232>

## Abstract

Nearly 450 *Margattea* specimens were collected from 27 locations in China and their morphology was examined. Then 68 *Margattea* COI sequences were obtained and used to carry out phylogenetic analyses as well as species delimitation analyses using General Mixed Yule Coalescent (GMYC), Automatic Barcode Gap Discovery (ABGD), and Poisson Tree Processes (bPTP). GMYC analysis resulted in 21 molecular operational taxonomic units (MOTUs) (confidence interval: 20–22), which was completely consistent with the result of the bPTP. There were 15 MOTUs using the ABGD method. The number of MOTUs was slightly different from the assigned morphospecies (16). As to the incongruence between molecular and morphological results, we checked the specimens again and made sure that most morphological differences were determined to be intraspecific differences (except the difference between *M. angusta* and *M. mckittrickae*), although a large genetic distance existed. Finally, 16 *Margattea* species from China were defined in this study, of which, seven new species are established, i.e. *Margattea deltodontia* J-J He & Z-Q Wang, **sp. nov.**, *Margattea cuspidata* J-J He & Z-Q Wang, **sp. nov.**, *Margattea caudata* J-J He & Z-Q Wang, **sp. nov.**, *Margattea paratraversa* J-J He & Z-Q Wang, **sp. nov.**, *Margattea disparilis* J-J He & Z-Q Wang, **sp. nov.**, *Margattea transversa* J-J He & Z-Q Wang, **sp. nov.**, and *Margattea bicruris* J-J He & Z-Q Wang, **sp. nov.**

## Keywords

ABGD, bPTP, cockroaches, COI, GMYC, intraspecific difference, morphology

## Introduction

Until now, 59 species have been included in the genus *Margattea* worldwide. Of these, 19 are from China (Wang et al. 2009; Liu et al. 2011; Beccaloni 2014). *Margattea* is known by the following characters: 1) eighth abdominal tergum unspecialized or specialized with a tuft; 2) median phallomere usually with accessory structure; 3) styli simple, cylindrical; and 4) symmetrical stripes and spots scattered on disc of pronotum, and in some species, the color of stripes and spots is similar to the body color (Roth 1989; Wang et al. 2009; Wang et al. 2014). As with other cockroach species, females of *Margattea* spp. are difficult to identify and match with males due to their strong resemblance in appearance and given that diagnostic characters are based on male genitalia (Wang et al. 2009, 2014).

DNA barcoding has proven to be a reliable and cost-effective method for identifying species in insect groups (Foster et al. 2004; Rach et al. 2008). General Mixed Yule-Coalescent (GMYC) (Pons et al. 2006), Automatic Barcode Gap Discovery (ABGD) (Puillandre et al. 2012), and Poisson-Tree-Processes (bPTP) (Zhang et al. 2013) have been used for species delimitation based on COI data (Che et al. 2017; Bai et al. 2018; Yang et al. 2019; Li et al. 2020).

In this study, we explore the diversity of *Margattea* species in China using both morphological features and GMYC, ABGD, and bPTP approaches to estimate the number of molecular operational taxonomic units (MOTUs), describe new species, and pair the female specimens with the males.

## Materials and methods

### Morphological study

Terminology mainly follows McKittrick (1964) (genitalia), Roth (2003), and Li et al. (2018) (venation). Venation abbreviations are as follows: cubitus anterior (CuA), cubitus posterior (CuP), media (M), radius (R), radius anterior (RA), radius posterior (RP), subcosta posterior (ScP), vannal (V), and postcubitus (Pcu).

Measurements are based on observed specimens. The genital segments of the studied specimens were dissected and immersed in 10% NaOH, heated to dissolve the fat, and rinsed with distilled water to make the segments and genitalia observable. They were then stored in glycerin. Genitalia were observed in glycerin using a MOTIC K400 stereomicroscope. All photos were made with a Leica DFC digital microscope camera attached to a Leica M205A stereomicroscope, and were modified with Adobe Photoshop CS6 (Adobe Systems, San Jose, CA, USA). Type materials are all deposited in the Institute of Entomology, Southwest University, Chongqing, China (SWU).

## DNA extraction, PCR and sequencing

DNA was extracted according to the Hipure Tissue DNA Mini Kit (Magen Biotech, Guangzhou). Fragments of COI were amplified using PCR. Primers used for the amplifications are LCO1490 (5'-GGTCAACAATCATAAGATATTGG-3') and HCO2198 (5'-TAAACTTCAGGGTGACCAAAAAATCA-3') (Folmer et al. 1994). Each PCR was performed in Analytik Jena Easy Cycler with 25 µl volumes using the aforementioned primers, followed by agarose gel electrophoresis. Amplification conditions were: initial denaturation at 98 °C for 2 min, followed by 35 cycles for 10 s at 98 °C, 10 s at 49 °C, and 1 min at 72 °C, with a final extension of 3 min at 72 °C.

## Sequence processing and phylogenetic analyses

A total of 81 COI sequences were used for analysis, of which 68 sequences are newly sequenced and nine sequences were downloaded from GenBank. Four sequences were selected as outgroups from species of four genera (*Allacta*, *Sorineuchora*, *Balta*, and *Shelfordina*) of the subfamily Pseudophyllodromiinae (Table 1). All sequences were aligned using MEGA 7 and adjusted visually after translation into amino acid sequences, whose lengths were 658 bp. The genetic divergence value was quantified by MEGA 7 based on Kimura 2-parameter (K2P) (Kumar et al. 2016). Maximum likelihood (ML) analysis was implemented in RAxML 7.3.0 (Stamatakis et al. 2008) using a GTR GAMMA model with 1000 bootstrap replicates.

We used three molecular species delimitation methods (GMYC, ABGD, bPTP) to delimit *Margattea* species based on COI sequences. For GMYC, time-resolved gene trees were estimated in BEAST 1.8.1 (Drummond and Rambaut 2007) with the parameters as follows: the uncorrelated lognormal (UCLN) relaxed clock model, the mean clock rate fixed to 1, the UPGMA starting tree and the tree prior as constant-size coalescent. The single-threshold GMYC method was then applied to generate the ultrametric gene tree using the SPLITS package (Ezard et al. 2009; Team 2013). Ultimately, we compared the groups delimited with the one-species null model using a likelihood ratio test. For ABGD, we used the Jukes-Cantor (JC69) model with a relative gap width  $X = 1.0$ , the rest of the parameters are set by default. For bPTP, we uploaded the converted file of the ML tree into the web site (<https://species.h-its.org>) with the default setting to obtain the results.

## Results

### Morphological delimitation of *Margattea*

Herein seven new species, *Margattea deltodonta* J-J He & Z-Q Wang, sp. nov., *Margattea cuspidata* J-J He & Z-Q Wang, sp. nov., *Margattea caudata* J-J He & Z-Q

**Table 1.** Samples used in this study. The location numbers correspond to Figure 11.

Species	Voucher ID	GenBank accession number	Collecting information	Location number
<b>ingroups</b>				
<i>M. speciosa</i>		KY349620		
	M14_5	MW970279	Jianfengling, Hainan, China; date and collector unknown	1
<i>M. angusta</i>	M28_6	MW970280	Putian, Fujian, China; 21 July 2013; Shun-Hua Gui, Yan Shi	5
		KY349624		
<i>M. mckittrickae</i>	M29_1	MW970281	Baoting, Hainan, China; 2 May 2013; Shun-Hua Gui, Yan Shi	2
	M29_2	MW970282		
<i>M. spinifera</i>	M28_2	MW970272	Putian, Fujian, China; 21 July 2013; Shun-Hua Gui, Yan Shi	5
	M28_3	MW970273		
	M28_7	MW970277	Guiping, Guangxi, China; 31 May–2 June 2014; Shun-Hua Gui, Xin-Ran, Jian-Yue Qiu	19
	M28_8	MW970278		
	M28_9	MW970274	Fuzhou, Fujian, China; 26 July 2013; Yan Shi	6
	M28_10	MW970275	Mt Wuyi, Fujian, China; 6–30 July 2013; Shun-Hua Gui, Yan Shi	8
	M28_11	MW970276	Mt Taimu, Ningde City, Fujian, China; 6–30 July 2013; Shun-Hua Gui, Yan Shi	7
		KY349644		
<i>M. spinosa</i>	M30_7	MW970299	Baoting, Hainan, China; 2 May 2013; Yan Shi	2
		KY349617		
<i>M. bisignata</i>	M19_1	MW970312	Nanling, Guangdong, China; 5–7 June 2010; Collector Unkown.	16
	M19_2	MW970313		
	M19_3	MW970314		
	M19_4	MW970317	Mt E'mei, Sichuan, China; 2 June 2011; Ke-Liang Wu	24
	M19_5	MW970318		
	M19_6, F	MW970307	Guiping, Guangxi, China; 31 May–2 June 2014; Shun-Hua Gui, Xin-Ran, Jian-Yue Qiu	19
	M19_7, F	MW970308	Jingxiu, Guangxi, China; 4–5 June 2014; Shun-Hua Gui, Xin-Ran Li	18
	M19_8	MW970316	Mt Dabie, Hubei, China; 2 July 2014; Xin-Ran Li	12
	M19_9	MW970315	Beibei, Chongqing, China; 23 May 2013; Jin-Jin Wang	23
	M19_10	MW970319	Mt E'mei, Sichuan, China; 2 July 2013; Jin-Jin Wang, Yang Li	24
	M_SY	MW970309	Nanchang, Jiangxi, China; 3 June 2017; Xin-Ran Li, Li-Li Wang; Meng Li	14
	SP6_SY	MW970311	Mt Lu, Jiangxi, China; date and collector unknown	13
	SP6_SY_2	MW970310		
		KY349607		
<i>M. multipunctata</i>	M42_1	MW970271	Xishuangbanna, Yunnan, China; 17 November 2009; Guo Tang, Zhi-Yuan Yao.	26
	M_DB	MW970270	Xishuangbanna, Yunnan, China; 27 May 2016; Zhi-Wei Qiu, Lu Qiu.	26
	DB	MW970269		
		KY349646		
<i>M. nimbata</i>	M13_1	MW970258	Beibei, Chongqing, China; 15–19 June 2016, Yang Li	23
	M13_2	MW970257		
	M13_3	MW970259		
	M_N	MW970260	Beibei, Chongqing, China; 9 June 2018; Collector Unkown.	
		KY349658		
	M13_4	MW970261	Mt Zijin, Jiangsu, China; 6–7 July 2014; Xin-Ran Li, Jian-yue Qiu, Yan Shi	11
<i>M. concava</i>	M27_1	MW970254	Mt Jianfengling, Hainan, China; 6 May 2013; Shun-Hua Gui, Yan Shi.	1
	M27_3	MW970255		
	M_AY	MW970256	Mt Jianfengling, Hainan, China; 24 April 2015; Lu Qiu, Qi-Kun Bai.	
	M27_4, F	MW970252	Mt Wuzhi, Hainan, China; 6 May 2013; Shun-Hua Gui, Yan Shi	2
	M27_5	MW970253	Mt Diaoluo, Hainan, China; 8 May 2013; Shun-Hua Gui, Yan Shi	4
		MF136391		
<i>M. cuspidata</i> sp. nov.	SP5	MW970300	Mt Daming, Guangxi, China; 2 July 2015; Lu Qiu, Qi-Kun Bai	20
	SP5_2	MW970301		
<i>M. caudata</i> sp. nov.	SP7	MW970283	Pu'er, Yunnan, China; 20 May 2016; Lu Qiu, Zhi-Wei Qiu	27
	SP7_2	MW970284		

Species	Voucher ID	GenBank accession number	Collecting information	Location number
<i>M. caudata</i>	SP7_3	MW970285		
sp. nov.	C3, F	MW970287		
	C4, F	MW970288		
	C5, F	MW970289		
	M901	MW970286		
<i>M. disparilis</i>	M_SC	MW970290	Xishuangbanna, Yunnan, China; 23 May 2016; Lu Qiu, Zhi-Wei Qiu	26
sp. nov.	SP9	MW970292		
	SP10	MW970291		
<i>M. deltodonta</i>	SP3_2	MW970294	Pingbian, Yunnan, China; 15 May 2016; Lu Qiu, Zhi-Wei Qiu	25
sp. nov.	SP3_3	MW970295		
	SP8_SP3	MW970298		
	CY03	MW970297		
	SP3	MW970293		
	SP3_2_2	MW970296		
<i>M. bicruris</i>	SP2_2	MW970303	Xishuangbanna, Yunnan, China; 23 May 2016; Lu Qiu, Zhi-Wei Qiu	26
sp. nov.	SP2_3	MW970304		
	SP2_4	MW970305		
	SP2_2_2	MW970302		
	M2	MW970306		
<i>M. transversa</i>	M9	MW970264	Pu'er, Yunnan, China; 20 May 2016; Lu Qiu, Zhi-Wei Qiu	27
sp. nov.	M903	MW970265		
	M904	MW970266		
	C2, F	MW970267		
	C7, F	MW970268		
		KY349661		
<i>M. paratransversa</i>	SP1	MW970262	Pu'er, Yunnan, China; 20 May 2016; Lu Qiu, Zhi-Wei Qiu	27
sp. nov.	SP1_2	MW970263		
<b>outgroups</b>				
<i>Allacta ornata</i>		KY349665		
<i>Sorineuchora nigra</i>		MF612149		
<i>Balta notulata</i>		KX051740		
<i>Shelfordina volubilis</i>		KY349562		

F: after voucher number means female sample.

Wang, sp. nov., *Margattea paratransversa* J-J He & Z-Q Wang, sp. nov., *Margattea disparilis* J-J He & Z-Q Wang, sp. nov., *Margattea transversa* J-J He & Z-Q Wang, sp. nov., and *Margattea bicruris* J-J He & Z-Q Wang, sp. nov. are established on the basis of morphological characters, including male genitalia, combined with molecular data. Species descriptions are provided below (Figs 4–10).

## Molecular analysis

All *Margattea* members were clustered together to form a monophyletic group in ML analysis (Fig. 1). Samples of *Margattea* species each formed monophyletic groups and most of branches with high support values, and females were recovered and grouped together with males (more details in Table 1). GMYC and bPTP analyses established 21 MOTUs as blue and purple bars indicate (Fig. 1); the ABGD analysis

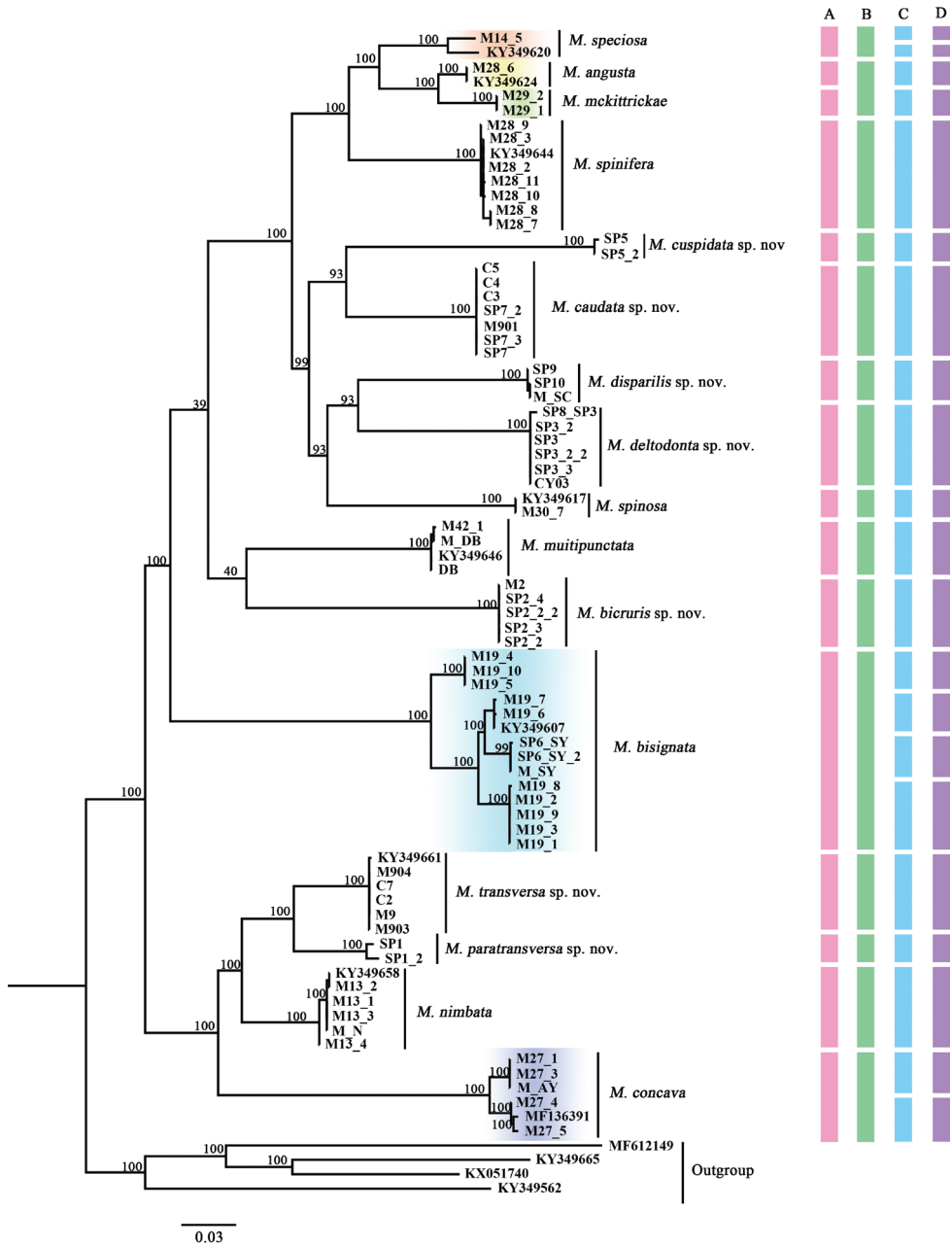


**Figure 1.** Maximum likelihood (ML) tree based on COI sequence. Branches labels is provided as bootstrap support values, some nodes without shown bootstrap value are given in Suppl. material 3: Fig. S1. Colored bars indicate different species delimitation by different methods **A** morphology (pink) **B** ABGD results (green) **C** GMYC results (blue) **D** bPTP results (purple). The colored clades on the tree (*M. speciosa*, *M. angusta*, *M. mckittrickae*, *M. bisignata*, and *M. concava*) correspond to clades with a disagreement between morphospecies and MOTUs.

established 15 MOTUs (green bars). Compared to the other two molecular divisions, ABGD results were mostly consistent with morphological results (revealed by pink bars) (Fig. 1).

#### Four methods to identify species

On the basis of morphological characters including male genitalia, we were able to identify 16 morphospecies of *Margattea*. ML analysis revealed each morphological species of the genus as a robust clade (Fig. 1). There were some similarities and differences in the results of these four methods. Both GMYC and bPTP divided all *Margattea* species into 21 MOTUs, while ABGD was different from the above two methods in that all species were divided into 15 MOTUs. And there were some disagreements between morphospecies and MOTUs, such as the colored clades on the ML tree. According to the GMYC and bPTP results, *M. speciosa* (with orange highlight) and *M. concava* (with lavender highlight) were grouped into two MOTUs. Moreover, *M. bisignata* (with light blue highlight) was divided into four MOTUs. And for ABGD, most species were consistent with morphospecies, except for *M. angusta* (with yellow highlight) and *M. mckittrickae* (with green highlight), which were considered to be one MOTU. As to the incongruence, we checked the specimens of *M. speciosa*, *M. concava*, and *M. bisignata* again and found there were no differences in male genitalia of their different samples (Figs 2, 3), so that the genetic variations among different samples of *M. speciosa*, *M. concava*, and *M. bisignata* were determined to be intraspecific differences despite a relatively large genetic distance existed (2.9% in *M. concava*, 3.1% in *M. speciosa*, and 5.9% in *M. bisignata*) (Suppl. material 1: Table S1). Also, upon examination of specimens of *M. angusta* and *M. mckittrickae*, we found some stable differences between the two species (in the former, the interstylar region barely protruding, right phallomere simple and hook-like, and in the latter, the interstylar region strongly produced, hook-like phallomere on the right side with a brush-shaped sclerite), although the genetic distance between them was only about 5%.

## Taxonomy

### Diagnosis of the genus *Margattea*

Third and fourth palpi both obviously longer than the fifth. Tegmina and wings usually fully developed, beyond end of abdomen, but slightly reduced in a few species, not reaching end of abdomen. Disc of pronotum usually with symmetrical maculae. ScP of tegmina simple, R multi-branched, M with 4–7 complete branches; hind wings of the ScP and RA expanded at base, CuA usually with 4–6 branches. Eighth abdominal tergum unspecialized or specialized with a tuft. Anteroventral margin of front femur type B<sub>2</sub>, or B<sub>3</sub>, rarely C<sub>2</sub>. Tarsal claws symmetrical and usually specialized, inner margin

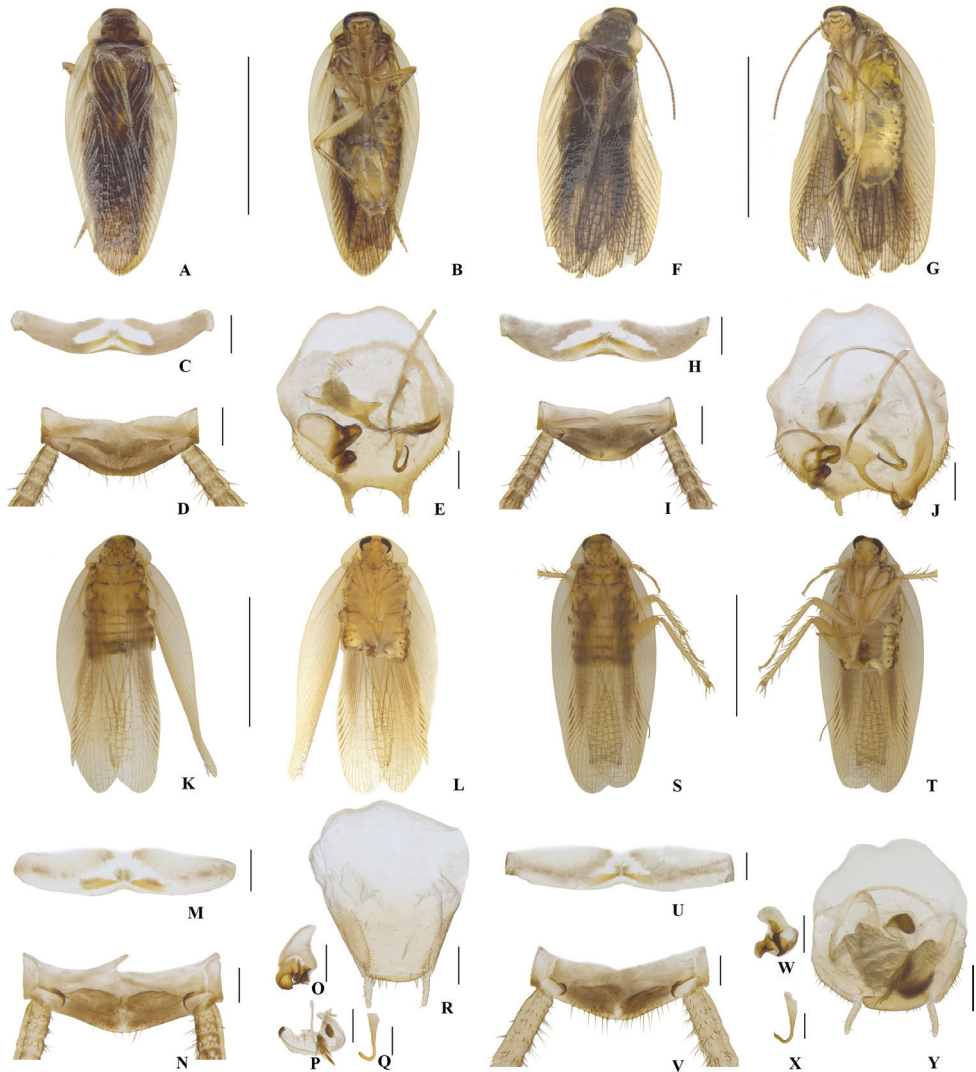


**Figure 2.** **A–J** *Margattea concava* **A–E** sample from Diaoluoshan, Hainan (voucher ID: M27\_5), male **F–J** sample from Jianfengling, Hainan (voucher ID: M\_AY), male **K–R** *Margattea mckittrickae*, sample from Baoting, Hainan (voucher ID: M29\_1), male **S–Y** *Margattea angusta*, male **A, F, K, S** dorsal view **B, G, L, T** ventral view **C, H, M, U** eighth abdominal terga, ventral view **D, I, N, V** supra-anal plate and paraprocts, ventral view **E, J, R, Y** subgenital plate and phallomeres, dorsal view **O, W** left phallomere, dorsal view **P** median phallomere, dorsal view **Q, X** hook-like phallomere, dorsal view. Scale bars: 5 mm (**A–B, F–G, K–L, S–T**), 0.5 mm (**C–E, H–J, M–R, V–Y**).

serrated. Styli simple, cylindrical. Hook phallomere on right. Median phallomere with accessory structure.

The genus *Margattea* Shelford, 1911 is closely related to *Balta* Tepper, 1893; however, they can be distinguished by the following characteristics: 1) In the former, the front femur is always of type  $B_2$ , or  $B_3$ , rarely  $C_2$ ; in the latter, the front femur always

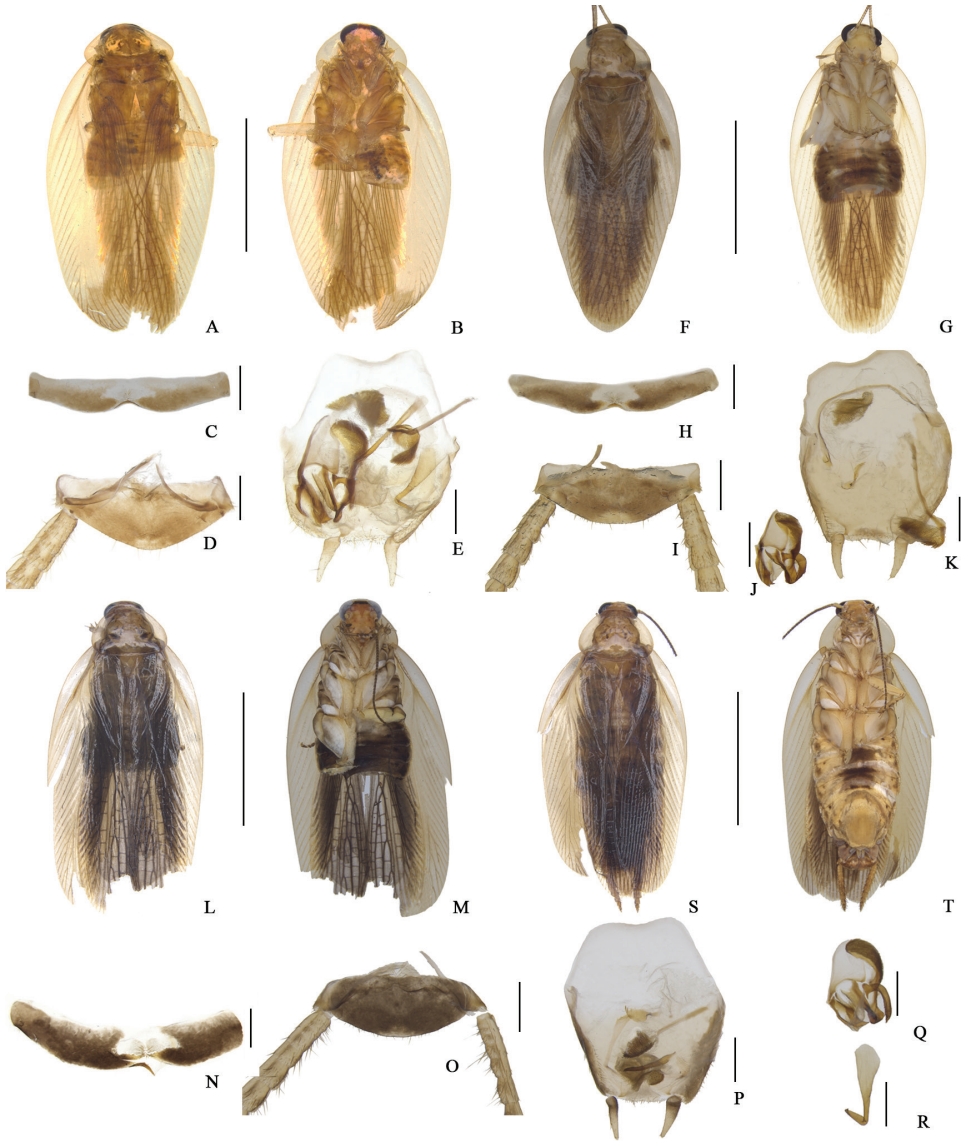


**Figure 3. A–R** *Margattea bisignata* **A–E** sample from E'meishan, Sichuan (voucher ID: M19\_4), male **F–K** sample from Dabieshan, Hubei (voucher ID: M19\_8), male **L–R** sample from Lushan, Jiangxi (voucher ID: SP6\_SY), male **S–T** sample from Guiping, Guangxi (voucher ID: M19\_6), female **A, F, L, S** dorsal view **B, G, M, T** ventral view **C, H, N** eighth abdominal terga, ventral view **D, I, O** supra-anal plate and paraprocts, ventral view **E, K, P** subgenital plate and phallomeres, dorsal view **J, Q** left phallomere, dorsal view **R** hook-like phallomere, dorsal view. Scale bars: 5 mm (**A–B, F–G, L–M, S–T**), 0.5 mm (**C–E, H–K, N–R**).

of type  $C_2$  or in a few, type  $B_3$ ; 2) in the former, the tarsal claws are symmetrical and specialized, but in the latter, the tarsal claws are asymmetrical and unspecialized; 3) in the former, the interstyler region is always convex or nearly straight, while in the latter, the interstyler region is always concave.

Key to species of *Margattea* from China

- 1 Tegmina basically reaching or extending beyond the end of abdomen.....2
- Tegmina barely reaching middle of abdomen ..*M. hemiptera* Bey-Bienko, 1958
- 2 The front femur Type B3.....3
- The front femur Type B2..... 11
- 3 Interstyler region have no produced or un conspicuous.....4
- Interstyler region strongly produced.....5
- 4 Pronotum pale yellow without dark maculae....*M. immaculata* Liu & Zhou, 2011
- Pronotum yellowish brown with maculae.....  
..... *M. mckittrickae* Wang, Che & Wang, 2009
- 5 Interstyler region produced nearly rectangle-shaped .....6
- Interstyler region produced not rectangle-shaped .....7
- 6 Posterior margin of interstyler region with a row of spines .....  
.....*M. perspicillaris* (Karny, 1915)
- Posterior margin of interstyler region without spines.....  
.....*Margattea angusta* Wang et al., 2014
- 7 Interstyler region produced nearly arc-shaped with a row of spines .....  
.....*M. spinifera* Bey-Bienko, 1958
- Interstyler region produced not arc-shaped ..... 8
- 8 Interstyler region extremely asymmetrical .....  
..... *M. disparilis* J-J He & Z-Q Wang, sp. nov.
- Interstyler region basically symmetrical .....9
- 9 The left and right edges of interstyler region curl inward..... 10
- The trailing edge of interstyler region curls upward .....  
.....*M. furcata* Liu & Zhou, 2011
- 10 The left end of the accessory structure of median phallomere with a slender bone.....*M. cuspidata* J-J He & Z-Q Wang, sp. nov.
- The accessory structure of median phallomere without bones.....  
..... *M. flexa* Wang et al., 2014
- 11 Male eighth tergum unspecialized .....12
- Male eighth tergum specialized ..... 14
- 12 Posterior margin of supra-anal plate with sharp protrusions .....  
..... *M. producta* Wang, Che & Wang, 2009
- Posterior margin of supra-anal plate not produced and nearly straight ..... 13
- 13 Ventral surface of body with brown spots.....  
.....*M. punctulata* (Brunner von Wattenwyl, 1893)
- Ventral surface of body without brown spots..... *M. limbata* Bey-Bienko, 1954
- 14 Styli dissimilar, the left bigger than the right....*M. pseudolimbata* Wang et al., 2014
- Styli similar ..... 15
- 15 Pronotal disc black brown with white maculae (specimens, the maculae of living body is fluorescent blue) ..... *M. multipunctata* Wang, Che & Wang, 2009
- Pronotal disc with scattered symmetrical maculae ..... 16

- 16 The accessory structure of left phallomere with brush-shaped sclerite ..... *M. bisignata* Bey-Bienko, 1970  
 – The accessory structure of left phallomere without brush-shaped sclerite..... 17
- 17 Median phallomere with spinelike sclerites..... 18  
 – Median phallomere without spinelike sclerites spinelike sclerites..... 21
- 18 Median phallomere with two or more spinelike sclerites ..... 19  
 – Median phallomere with only one spinelike sclerite ..... 20
- 19 Median phallomere with three spinelike sclerite .....  
 ..... *M. trispinosa* (Bey-Bienko, 1958)  
 – Median phallomere with two spinelike sclerite ..... *M. nimbata* (Shelford, 1907)
- 20 Interocular space without brown band .....  
 ..... *M. paratransversa* J-J He & Z-Q Wang, sp. nov.  
 – Interocular space with brown band ... *M. transversa* J-J He & Z-Q Wang, sp. nov.
- 21 Interstylar region strongly produced..... 22  
 – Interstylar region have no produced or un conspicuous..... 23
- 22 Interstylar region convex fishtail-shaped.....  
 ..... *M. caudata* J-J He & Z-Q Wang, sp. nov.  
 – Interstylar region convex triangular .....  
 ..... *M. deltodonta* J-J He & Z-Q Wang, sp. nov.
- 23 Interstylar region concave..... *M. concava* Wang, Che & Wang, 2009  
 – Interstylar region not concave ..... 24
- 24 Median phallomere with spines at apex..... *M. spinosa* Wang et al., 2014  
 – Median phallomere without spines at apex..... 25
- 25 Median phallomere forked at apex ..... *M. bicruris* J-J He & Z-Q Wang, sp. nov.  
 – Median phallomere unforked..... *M. speciosa* Liu & Zhou, 2011

***Margattea deltodonta* J-J He & Z-Q Wang, sp. nov.**

<http://zoobank.org/34AE83CF-363C-4738-B42D-20AE048DC6C0>

Figure 4A–N

**Type material.** *Holotype*: CHINA • ♂; Hongqi Reservoir, Mt Dawei, Pingbian County, Yunnan Province; 1550 m, 15-V-2016; Lu Qiu, Zhi-Wei Qiu leg; SWU-B-EC141501.

**Paratypes**: CHINA • 3♂♂; same data as holotype; SWU-B-EC141502-141504.

**Other material.** CHINA • 1♂; Hongqi Reservoir, Mt Dawei, Pingbian County, Yunnan Province; 1550 m; 17-V-2016; Lu Qiu, Zhi-Wei Qiu leg.

**Diagnosis.** This species is similar to *M. satsumana* (Asahina, 1979) in general appearance, but can be differentiated from the latter by the following characters: 1) median phallomere slender rod with base sharp, and apex expanded with three spines; while in the latter, base slightly expanded, and apex curved with some short spines; 2) subgenital plate not folded; while in the latter, folded inwards.

**Measurements (mm).** Male ( $n = 4$ ), pronotum: length  $\times$  width 1.6–2.1  $\times$  2.6–2.9, tergina length: 10.3–11.2, overall length: 12.5–13.1.

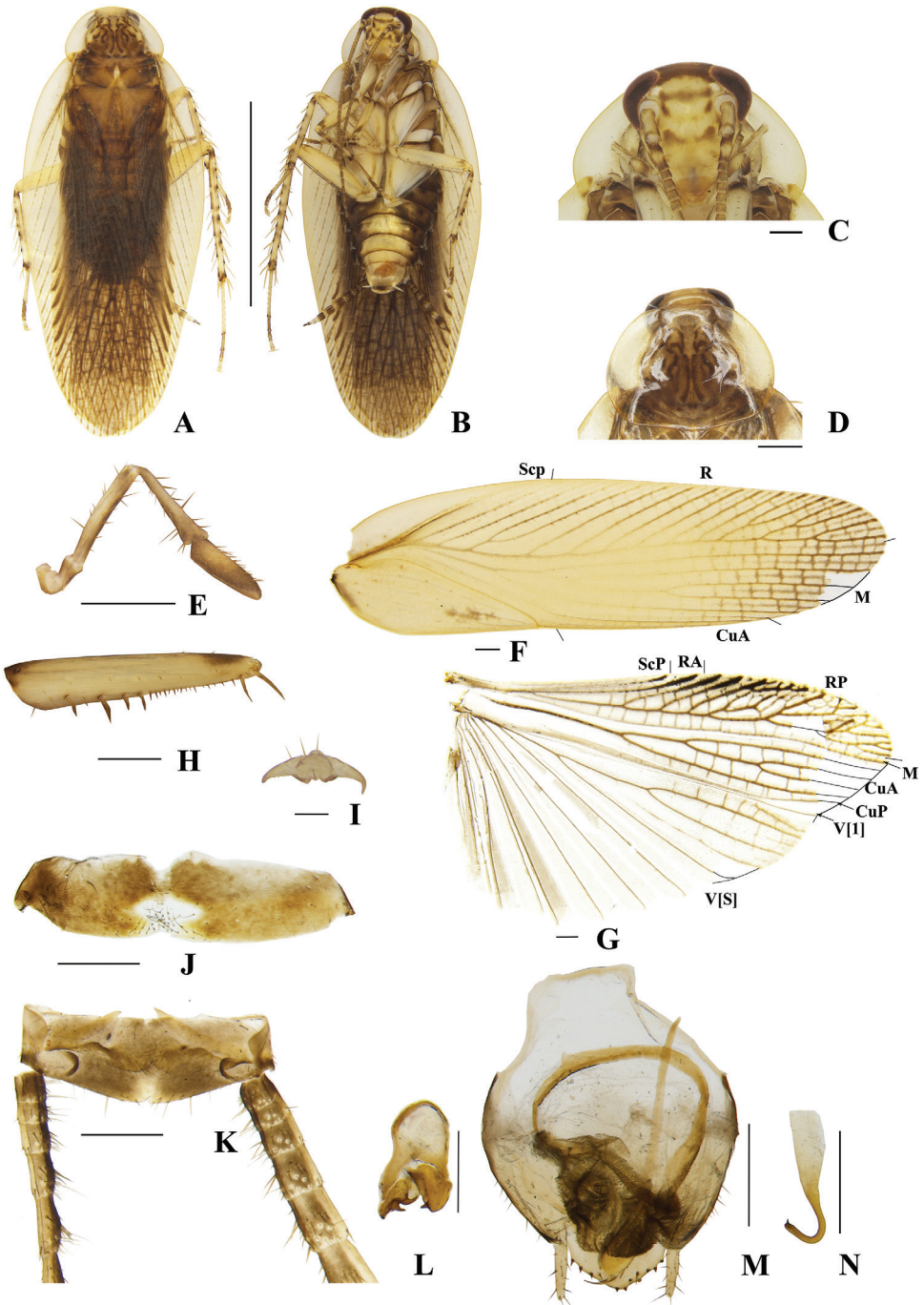


**Figure 4.** A–N *Margattea deltodonta* sp. nov., male **A** holotype, dorsal view **B** holotype, ventral view **C** head, ventral view **D** pronotum, dorsal view **E** maxillary palpi, ventral view **F** tegmen, dorsal view **G** hind wing, dorsal view **H** front femur, ventral view **I** tarsal claws **J** eighth abdominal terga **K** supra-anal plate and paraprocts, ventral view **L** left phallomere, dorsal view **M** subgenital plate and median phallomere, dorsal view **N** hook-like phallomere, dorsal view. Scale bars: 5 mm (**A**, **B**); 0.5 mm (**C**–**H**, **J**, **K**–**N**); 0.1 mm (**I**).

**Description. Male. Coloration:** body yellowish-brown (Fig. 4A, B). Face pale yellowish-brown. Interocular space with a dark brown band. Ocelli spots white, interocular space with a brown band. Antennae dark lined. Clypeus medium yellowish-brown (Fig. 4C). Maxillary palps dark yellowish-brown (Fig. 4E). Pronotal disc yellowish-brown with brown stripes and spots, and two lateral borders light brown (Fig. 4D). Tegmina medium brown, wings light lined (Fig. 4F, G). Abdomen yellowish-brown (Fig. 4B). Cerci dark yellowish-brown (Fig. 4K). Styli faint yellow (Fig. 4M). **Head:** vertex slightly exposed, interocular distance same length as antennal sockets space (Fig. 4C). Pronotum nearly trapezoidal, broader than long, the widest part after the midpoint, the front and posterior margins nearly straight, and the postero-lateral angle blunt and round; the disc with symmetrical irregular macules (Fig. 4D). The third and fourth palpi about same length, both obviously longer than the fifth, the fifth obviously expanded (Fig. 4E). **Tegmina and wings:** tegmina and wings fully developed, both extending beyond the end of abdomen (Fig. 4A, B). Tegmina with ScP simple, R multi-branched, M straight with five complete branches. Hind wings with ScP and RA expanded at apex; M straight and simple, without branches; CuA with four complete branches (Fig. 4F, G). **Legs:** anteroventral margin of front femur type  $B_2$  (Fig. 4H). Pulvilli present on four proximal tarsomeres. Tarsal claws symmetrical and specialized, inner margin serrated, arolia present (Fig. 4I). **Abdomen and genitalia:** eighth abdominal tergum specialized with a tuft (Fig. 4J). Supra-anal plate transverse, posterior margin convex, the middle slightly concave. Paraprocts simple, similar, splitting into two pieces, apex with tufts (Fig. 4K). Subgenital plate asymmetrical, both lateral margins slightly concave. Styli similar, slender with spines; interstyler region obviously convex with small spines (Fig. 4M). Left phallomere complex, irregular bone-shaped, with two short spines (Fig. 4L). Median phallomere slender rod-shaped with base sharp, and apex expanded with three long spines; the accessory structure arched, at rightmost end brush-shaped (Fig. 4M). Hook phallomere on the right side, apex curved inwards with a short spine (Fig. 4N).

**Female** unknown.

**Etymology.** The word “delt” and “odont” from Greek and means triangular, the species name “*deltodontus*” refers to the posterior margin of subgenital plate with small spines.

**Distribution.** China (Yunnan).

***Margattea cuspidata* J-J He & Z-Q Wang, sp. nov.**

<http://zoobank.org/7AD3ADF0-DA60-493B-A229-363CBC71F002>

Figure 5A–N

**Type material. Holotype:** CHINA • ♂; Mt Daming, Guangxi Province; 2-VII-2015; Lu Qiu, Qi-Kun Bai leg; SWU-B-EC141201. **Paratype:** CHINA • 1♂; same data as for holotype; SWU-B-EC141202.

**Diagnosis.** This species is similar to *M. flexa* Wang et al., 2014 in general appearance and male genitalia, but it can be differentiated from the latter by the following characters: 1) interstyler region obviously convex with both sides curved inwards, three

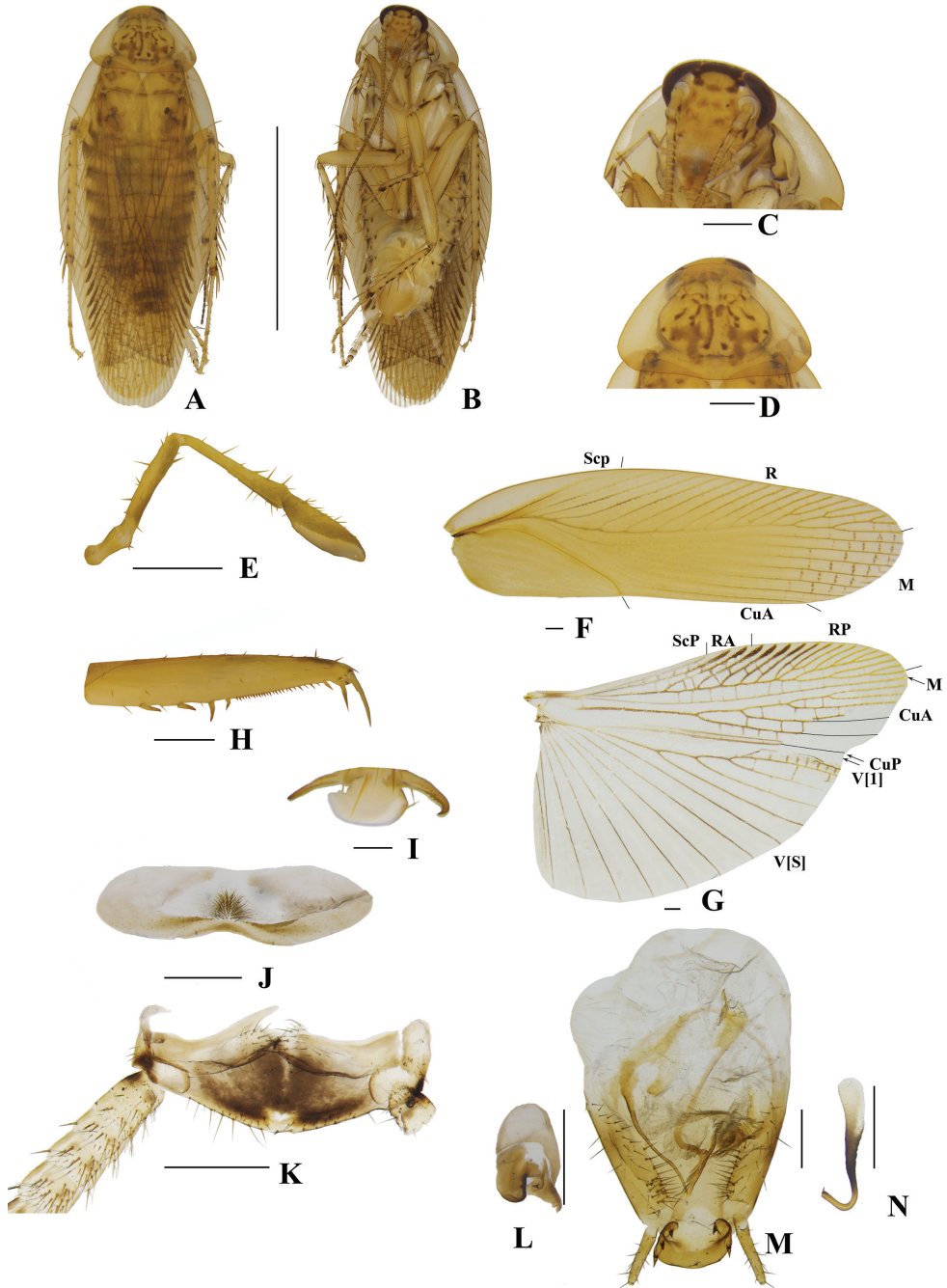


**Figure 5. A–N** *Margattea cuspidata* sp. nov., male **A** holotype, dorsal view **B** holotype, ventral view **C** head, ventral view **D** pronotum, dorsal view **E** maxillary palpi, ventral view **F** tegmen, dorsal view **G** hind wing, dorsal view **H** front femur, ventral view **I** tarsal claws **J** eighth abdominal terga **K** supra-anal plate and paraprocts, ventral view **L** left phallomere, dorsal view **M** subgenital plate and median phallomere, dorsal view **N** hook-like phallomere, dorsal view. Scale bars: 5 mm (**A, B**); 0.5 mm (**C–H, J, K–N**); 0.1 mm (**I**).

spines on each side, while in the latter, two sides curled up with 5–6 small thorns; 2) the left end of the accessory structure with a slender bone; the latter absent.

**Measurements (mm).** Male ( $n = 2$ ), pronotum: length  $\times$  width 1.6–2.1  $\times$  2.6–2.9, tegmina length: 10.3–11.2, overall length: 12.5–13.1.

**Description. Male. Coloration:** body yellowish-brown (Fig. 5A, B). Face yellowish-brown. Interocular space with a dark brown band. Ocelli spots white, interocelli space with a brown band. Antennae dark linen-colored. Clypeus dark yellowish-brown (Fig. 5C). Maxillary palps yellowish-brown (Fig. 5E). Pronotal disc yellowish-brown with dark brown stripes, and lateral borders light linen-colored (Fig. 5D). Tegmina pale yellow, wings medium brown (Fig. 5F, G). Abdomen pale yellowish-brown. Cerci pale yellowish-brown (Fig. 5K). Styli faint yellow (Fig. 5M). **Head:** vertex slightly exposed, distance between interocular same length as antennal sockets space (Fig. 5C). Pronotum nearly trapezoidal, broader than long, the widest part after the midpoint, the front and posterior margins nearly straight, and the postero-lateral angle blunt and round; the disc with symmetrical irregular macules (Fig. 5D). The third, fourth palpi of approximately same length, both obviously longer than the fifth, the fifth obviously expanded (Fig. 5E). **Tegmina and wings:** tegmina and wings fully developed, both extending beyond the end of abdomen (Fig. 5A, B). Tegmina with ScP simple, R multi-branched, M straight with six complete branches. Hind wings with ScP and RA expanded at apex; M straight and simple, without branches; CuA with five complete branches (Fig. 5F, G). **Legs:** anteroventral margin of front femur type B<sub>3</sub> (Fig. 5H). Pulvilli present on four proximal tarsomeres. Tarsal claws symmetrical and specialized, inner margin serrated, arolia present (Fig. 5I). **Abdomen and genitalia:** eighth abdominal tergum specialized with a tuft (Fig. 5J). Supra-anal plate transverse, posterior margin protruded. Paraprocts similar, splitting into two pieces, apex with tufts (Fig. 5K). Subgenital plate symmetrical, lateral borders flip inwards with spines and hairs. Styli similar, slender; interstyler region obviously convex, two sides convex and curved inwards, each side with three spines (Fig. 5M). Left phallomere complex, irregular bone-shaped, with a short spine (Fig. 5L). Median phallomere slender rod-shaped, obviously curved, apex with ordered long spines; the accessory structure arched, on at rightmost end with spines, left apex with a slender bone with apex sharp (Fig. 5M). Hook phallomere on the right side, apex curved inwards with a short spine (Fig. 5N).

**Female** unknown.

**Etymology.** The latin name “*cuspidatus*” refers to interstyler region obviously convex, two sides convex and curved inwards.

**Distribution.** China (Guangxi).

***Margattea caudata* J-J He & Z-Q Wang, sp. nov.**

<http://zoobank.org/D3FF2635-DB1C-42D1-B087-890314430081>

Figure 6A–N

**Type material. Holotype:** CHINA • ♂; Meizihu Reservoir, Pu'er City, Yunnan Province; 1400 m; 21-V-2016; Lu Qiu, Zhi-Wei Qiu leg; SWU-B-EC141301. **Paratypes:** CHINA • 6♂♂; 1 ♀, same data as holotype SWU-B-EC141302-141308.

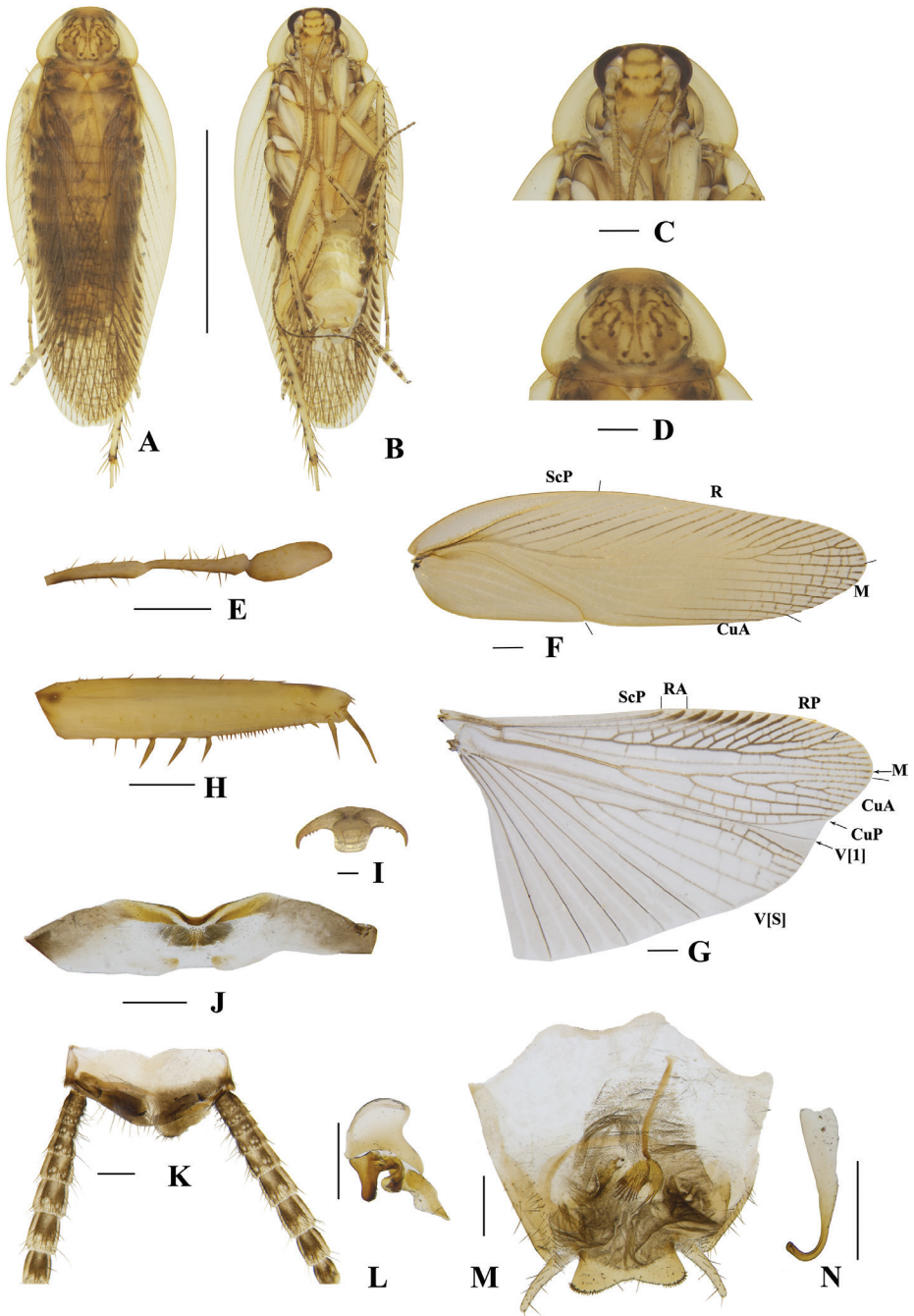


**Figure 6.** A–N *Margattea caudata* sp. nov., male **A** holotype, dorsal view **B** holotype, ventral view **C** head, dorsal view **D** pronotum, ventral view **E** maxillary palpi segments 3–5, ventral view **F** tegmen, dorsal view **G** hind wing, dorsal view **H** front femur, ventral view **I** tarsal claws **J** eighth abdominal terga **K** supra-anal plate and paraprocts, ventral view **L** left phallomere, dorsal view **M** subgenital plate and median phallomere, dorsal view **N** hook-like phallomere, dorsal view. Scale bars: 5 mm (**A**, **B**); 0.5 mm (**C**–**H**, **J**, **K**–**N**); 0.1 mm (**I**).

**Other materials.** CHINA • 2♀♀; Meizihu Reservoir, Pu'er City, Yunnan Province; 1400 m; 20-V-2016; Lu Qiu, Zhi-Wei Qiu leg.

**Diagnosis.** This species is similar to *M. mckittrickae* Wang, Che & Wang, 2009 in general appearance, but it can be differentiated from the latter by the following characters: 1) interstyler region obviously convex, fishtail-shaped, while the latter slightly convex; 2) left phallomere complex, irregular bone-shaped, while in the latter, two sides of left phallomere sheet-like; and 3) median phallomere with one accessory structure, while the latter with two accessory structures.

**Measurements (mm).** Male ( $n = 4$ ), pronotum: length  $\times$  width 2.7–2.8  $\times$  3.1–3.6, tegmina length: 10.4–12.6, overall length: 12.8–14.1. Female, pronotum: length  $\times$  width 2.5–3.0  $\times$  3.6–3.7, tegmina length: 9.0–9.1, overall length: 11.7–12.6.

**Description. Male. Coloration:** body pale brown with yellowish-brown (Fig. 6A, B). Face pale yellowish-brown. Interocular space with a brown band. Ocelli spots white, interocellar space with a brown band. Antennae light linen-colored. Clypeus medium yellowish-brown (Fig. 6C). Maxillary palps dark yellowish-brown (Fig. 6E). Pronotal disc pale yellowish-brown with brown stripes and two lateral borders light yellowish-brown (Fig. 6D). Tegmina yellowish-brown and wings medium brown (Fig. 6F, G). Abdomen pale yellowish-brown. Cerci yellowish-brown (Fig. 6K). Styli faint yellow (Fig. 6M). **Head:** vertex slightly exposed, interocular distance interocular same length as antennal socket space (Fig. 6C). Pronotum nearly trapezoidal, broader than long, the widest part after the midpoint, the front and posterior margins nearly straight, and postero-lateral angle blunt and round; disc with symmetrical irregular macules (Fig. 6D). Third and fourth palpi of approximately same length, both obviously longer than the fifth, fifth palp obviously expanded (Fig. 6E). **Tegmina and wings:** tegmina and wings fully developed, both extending beyond the end of abdomen (Fig. 6A, B). Tegmina with ScP simple, R multi-branched, M straight with five complete branches. Hind wings with ScP and RA expanded at apex; M straight and simple, without branches; CuA with 7 complete branches (Fig. 6F, G). **Legs:** anteroventral margin of front femur type B<sub>2</sub> (Fig. 6H). Pulvilli present on four proximal tarsomeres. Tarsal claws symmetrical and specialized, inner margin serrated, arolia present (Fig. 6I). **Abdomen and genitalia:** eighth abdominal tergum specialized with a tuft (Fig. 6J). Supra-anal plate transverse, posterior margin protruded. Paraprocts similar, splitting into two pieces, apex with tufts (Fig. 6K). Subgenital plate symmetrical, the middle of front margin slightly concave; the base of two lateral margins concave, apex flips inwards with tufts. Styli similar, slender, distinctly separated; interstyler region obviously convex, fishtail-shaped, middle space slightly concave, two lateral angles convex with short spines (Fig. 6M). Left phallomere complex, irregular bone-shaped, with short spine (Fig. 6L). Median phallomere slender rod-shaped, apex splitting into two parts, each with some long spines (Fig. 6M). Hook phallomere on the right side, apex curved inwards with a short spine (Fig. 6N).

**Female** with tegmina and wings slightly reduced.

**Etymology.** The latin name “*caudatus*” meaning “tail”, refers to the fishtail-shaped convexity on interstyler region.

**Distribution.** China (Yunnan).

***Margattea disparilis* J-J He & Z-Q Wang, sp. nov.**

<http://zoobank.org/484B73A3-9A9D-4922-81FB-CF7CE1E7C986>

Figure 7A–N

**Type material. Holotype:** CHINA • ♂; Wangtianshu Scenery Spot, Mengla County, Xishuangbanna Prefecture, Yunnan Province; 720 m; 23-V-2016; Lu Qiu, Zhi-Wei Qiu leg; SWU-B-EC141401. **Paratypes:** CHINA • ♂; Gougu Tropical Rainforest, Xishuangbanna Tropical Botanical Garden (CAS), Menglun Town, Jinghong City, Yunnan Province; 570 m; 26-V-2016; Lu Qiu, Zhi-Wei Qiu leg; SWU-B-EC141402.

**Other material.** CHINA • 1♂; Lvshilin (Green Stone Forest), Xishuangbanna Tropical Botanical Garden (CAS), Menglun Town, Jinghong City, Yunnan Province; 25-V-2016; Lu Qiu, Zhi-Wei Qiu leg.

**Diagnosis.** This species is similar to *M. flexa* Wang et al., 2014 in male genitalia, but it can be differentiated from the latter by the following characters: 1) interstyler region obviously irregularly convex, the left part obviously larger than the right, while in the latter, interstyler region obviously regularly convex; 2) the left part of the accessory structure of median phallomere with a brush, absent in the latter.

**Measurements (mm).** Male ( $n = 3$ ), pronotum: length  $\times$  width 2.4–2.6  $\times$  3.2–3.5, tegmina length: 9.3–9.9, overall length: 11.2–11.9.

**Description. Male. Coloration:** body yellowish-brown with pale brown (Fig. 7A, B). Face yellowish-brown. Interocular space with a dark brown band. Ocellar spots white and small, intercellular space with a brown band. Antennae light linen-colored. Clypeus medium yellowish-brown (Fig. 7C). Maxillary palps light yellowish-brown to yellowish-brown (Fig. 7E). Pronotal disc yellowish-brown with brown stripes and two lateral borders light yellow (Fig. 7D). Tegmina light fawn, wings and legs pale brown (Fig. 7F, G). Abdomen light linen with pale yellowish-brown. Cerci pale brown (Fig. 7K). Styli light yellowish-brown (Fig. 7M). **Head:** vertex slightly exposed, distance between interocular same length antennal sockets space (Fig. 7C). Pronotum nearly trapezoidal, broader than long, the widest part after the midpoint, the front and posterior margins nearly straight, and postero-lateral angle blunt and round; disc with symmetrical irregular macules (Fig. 7D). Third and fourth palpi of approximately the same length, both obviously longer than fifth, fifth palp obviously expanded (Fig. 7E). **Tegmina and wings:** tegmina and wings developed, both extending the end of abdomen (Fig. 7A–B). Tegmina with ScP simple, R multi-branched, M straight with seven complete branches. Hind wings with ScP and RA expanded at apex; M straight and simple, without branches; CuA with five complete branches (Fig. 7F, G). **Legs:** anteroventral margin of front femur type B<sub>3</sub> (Fig. 7H). Pulvilli present on four proximal tarsomeres. Tarsal claws symmetrical and specialized, inner margin serrated, arolia present (Fig. 7I). **Abdomen and genitalia:** eighth abdominal tergum specialized with a tuft (Fig. 7J). Supra-anal plate transverse, posterior margin convex. Paraprocts simple, similar, splitting into two pieces, base with tufts (Fig. 7K). Subgenital plate asymmetrical. Styli similar, slender, distinctly separated; interstyler region obviously irregularly convex, middle part concave, two lateral angles spherical with some short thorns, left angle obviously larger

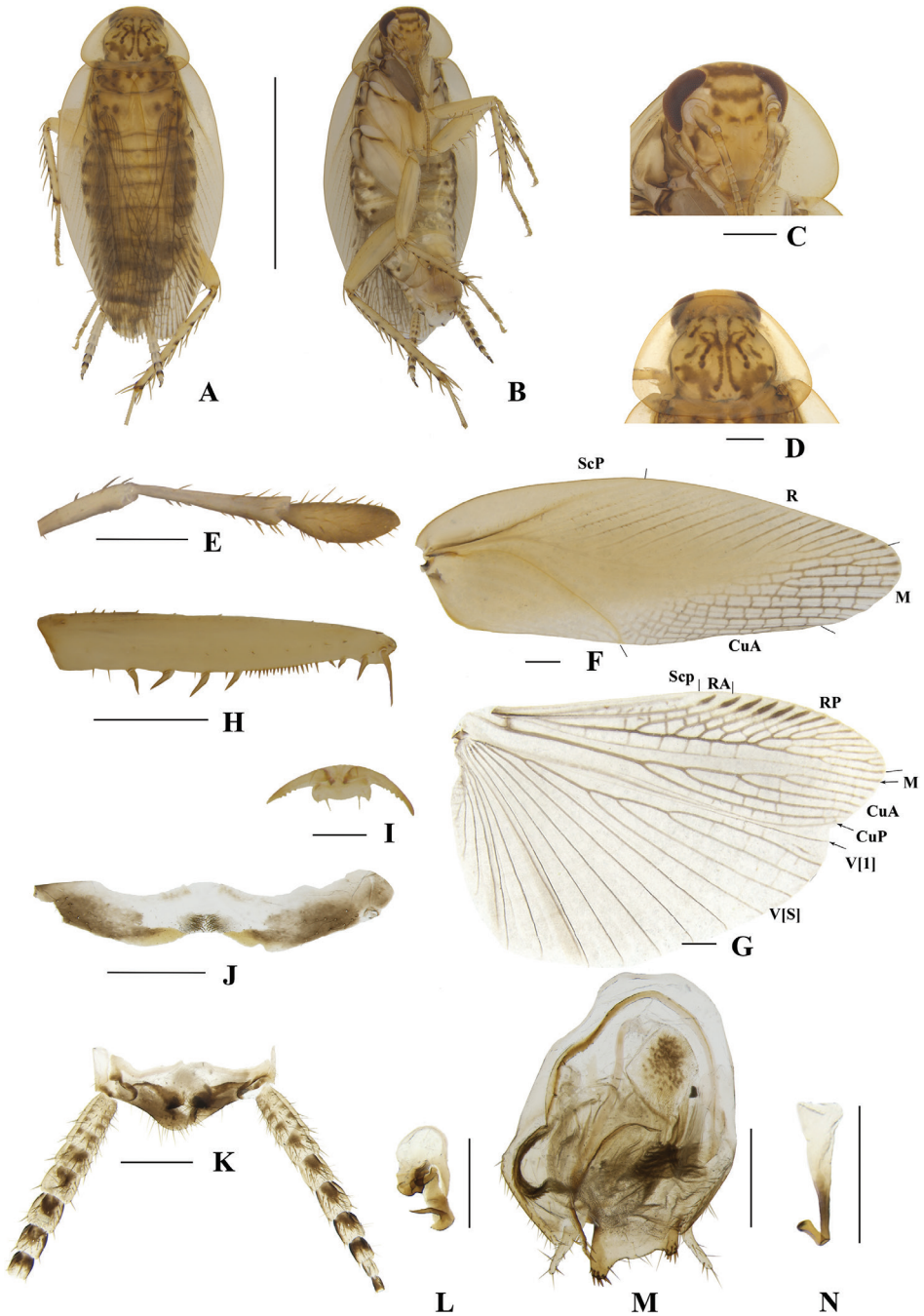


**Figure 7.** A–N *Margattea disparilis* sp. nov., male **A** holotype, dorsal view **B** holotype, ventral view **C** head, ventral view **D** pronotum, dorsal view **E** maxillary palpi segments 3–5, ventral view **F** tegmen, dorsal view **G** hind wing, dorsal view **H** front femur, ventral view **I** tarsal claws **J** eighth abdominal terga **K** supra-anal plate and paraprocts, ventral view **L** left phallomere, dorsal view **M** subgenital plate and median phallomere, dorsal view **N** hook-like phallomere, dorsal view. Scale bars: 5 mm (**A**, **B**); 0.5 mm (**C**–**H**, **J**, **K**–**N**); 0.1 mm (**I**).

than right (Fig. 7M). Left phallomere complex, irregular bone-shaped, with a long spine (Fig. 7L). Median phallomere slender rod-shaped, base splitting into some long spines; the accessory structure arched, at leftmost end with a brush (Fig. 7M). Hook phallomere on right side, base curved inwards with a short spine (Fig. 7N).

**Female** unknown.

**Etymology.** The latin name “*disparilis*” refers to the interstyler region obviously irregular convex.

**Distribution.** China (Yunnan).

***Margattea transversa* J-J He & Z-Q Wang, sp. nov.**

<http://zoobank.org/CA538705-BF0B-46C7-9708-29697F9F2ADD>

Figure 8A–N

**Type material. Holotype:** CHINA • ♂; Meizihu Reservoir, Pu'er City, Yunnan Province; 20-V-2016; Lu Qiu, Zhi-Wei Qiu leg; SWU-B-EC141801. **Paratypes:** CHINA • 2♂; same date as for holotype SWU-B-EC141802-141803.

**Other materials.** CHINA • 1♀; Meizihu Reservoir, Pu'er City, Yunnan Province; 20-V-2016; Lu Qiu, Zhi-Wei Qiu leg. • 1♀; Meizihu Reservoir, Pu'er City, Yunnan Province; 21-V-2016; Lu Qiu, Zhi-Wei Qiu leg.

**Diagnosis.** This species is similar to *M. nimbata* (Shelford, 1907) in male genitalia, but it can be differentiated from the latter by the following characters: 1) median phallomere base with a curved spine, while in the latter, with two curved spines; 2) a long piece of bone extends from the right side of the accessory structure, while absent in the latter; and 3) left phallomere with four long spines; the latter with two long spines.

**Measurements (mm).** Male ( $n = 3$ ), pronotum: length  $\times$  width 2.5–2.6  $\times$  3.2–3.9, tegmina length: 11.7–12.3, overall length: 14.0–14.1. Female, pronotum: length  $\times$  width 2.6–2.7  $\times$  3.2–3.4, tegmina length: 11.3–11.5, overall length: 13.4–13.6.

**Description. Male. Coloration:** body pale yellowish-brown with brown (Fig. 8A, B). Face yellowish-brown. Interocular space with a dark brown band. Ocelli spots white and big, interocelli space with a brown band. Antennae pale yellowish-brown. Clypeus medium yellowish-brown. Maxillary palps light yellowish-brown (Fig. 8E). Pronotal disc brownish-gray with brown stripes and two lateral borders light grey (Fig. 8D). Tegmina pale yellowish-brown, wings grey brown (Fig. 8F, G). Abdomen yellowish-brown. Cerci pale yellowish-brown to pale brown (Fig. 8K). Styli faint yellow (Fig. 8M). **Head:** vertex slightly exposed, interocular distance same length as antennal socket space (Fig. 8C). Pronotum nearly trapezoidal, broader than long, widest part after midpoint, front and posterior margins nearly straight, and postero-lateral angle blunt and round; disc with symmetrical irregular macules (Fig. 8D). Third and fourth palpi of approximately same length, both obviously longer than fifth palp, fifth palp obviously expanded (Fig. 8E). **Tegmina and wings:** tegmina and wings fully developed, both extending beyond the end of abdomen (Fig. 8A, B). Tegmina with ScP simple, R multi-branched, M straight with seven complete branches. Hind wings with ScP and RA expanded at base; M straight and simple, without branches; CuA with

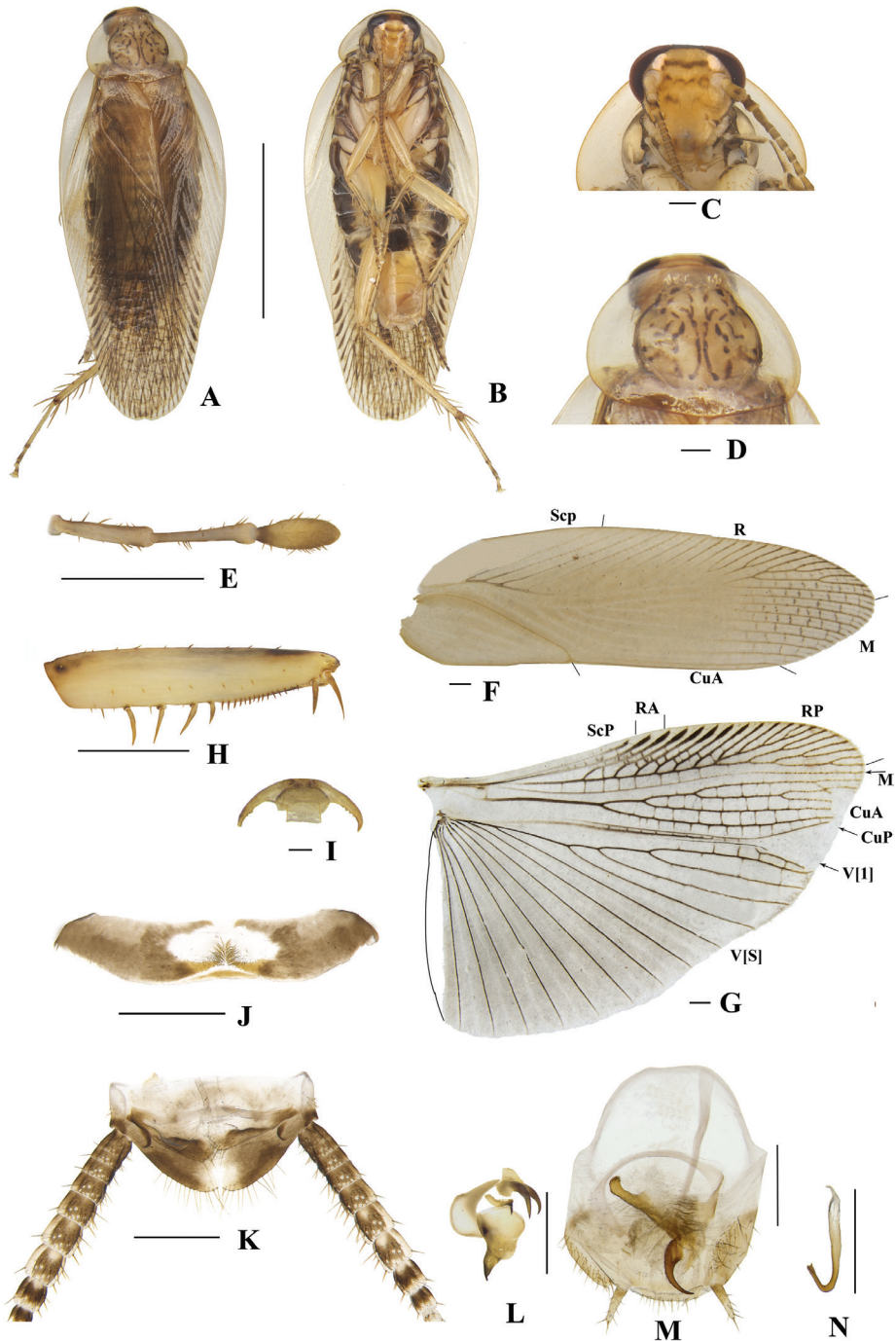


**Figure 8.** A–N *Margattea transversa* sp. nov., male **A** holotype, dorsal view **B** holotype, ventral view **C** head, ventral view **D** pronotum, dorsal view **E** maxillary palpi segments 3–5, ventral view **F** tegmen, dorsal view **G** hind wing, dorsal view **H** front femur, ventral view **I** tarsal claws **J** eighth abdominal terga **K** supra-anal plate and paraprocts, ventral view **L** left phallomere, dorsal view **M** subgenital plate and median phallomere, dorsal view **N** hook-like phallomere, dorsal view. Scale bars: 5 mm (**A**, **B**); 0.5 mm (**C**–**H**, **J**, **K**–**N**); 0.1 mm (**I**).

five complete branches (Fig. 8F, G). **Legs:** anteroventral margin of front femur type B<sub>2</sub> (Fig. 8H). Pulvilli present on four proximal tarsomeres. Tarsal claws symmetrical and specialized, inner margin serrated, arolia present (Fig. 8I). **Abdomen and genitalia:** eighth abdominal tergum specialized with a tuft (Fig. 8J). Supra-anal plate transverse, posterior margin convex. Paraprocts simple, similar, splitting into two pieces (Fig. 8K). Subgenital plate symmetrical. Styli similar, slender, distinctly separated (Fig. 8M). Left phallomere complex, irregular bone-shaped, with four spines (Fig. 8L). Median phallomere slender rod-shaped, apex with a curved spine; the accessory structure arched, at rightmost end blunt (Fig. 8M). Hook phallomere on the right side, base curved inwards with a short spine (Fig. 8N).

**Female** same as male.

**Etymology.** The latin name “*transversus*” refers to the interocular space having a dark brown transverse band.

**Distribution.** China (Yunnan).

***Margattea paratransversa* J-J He & Z-Q Wang, sp. nov.**

<http://zoobank.org/268B5D3F-BC3D-4A0B-93B7-6DC75B28FB60>

Figure 9A–N

**Type material. Holotype:** CHINA • ♂; Meizihu Reservoir, Pu'er City, Yunnan Province; 1400 m; 21-V-2016; Lu Qiu, Zhi-Wei Qiu leg; SWU-B-EC141701. **Paratype:** CHINA • 6♂♂; same data as holotype; SWU-B-EC141702-141707.

**Other material.** CHINA • 2♀; Meizihu Reservoir, Pu'er City, Yunnan Province; 1400 m; 20-V-2016; Lu Qiu, Zhi-Wei Qiu leg.

**Diagnosis.** This species closely resembles *Margattea transversa* sp. nov., but they can be distinguished by the following characteristics: 1) Left phallomere of the former with three long spines, while the latter with four long spines; 2) In the former, median phallomere apex with a slightly curved spine, while the median phallomere apex of latter with a distinct curved spine. In addition, this species is also similar to *M. nimbata* (Shelford, 1907) in general appearance, but it can be differentiated from the latter by the following characters: 1) median phallomere base with a curved spine, while in the latter, with two curved spines; 2) A long piece of bone extends from the right side of the accessory structure, while absent in the latter; and 3) left phallomere with three long spines; the latter with two long spines.

**Measurements (mm).** Male ( $n = 5$ ), pronotum: length  $\times$  width  $2.7\text{--}2.8 \times 3.1\text{--}3.6$ , tegmina length:  $10.4\text{--}12.6$ , overall length:  $12.8\text{--}14.1$ .

**Description. Male. Coloration:** body pale yellowish-brown with yellowish-brown (Fig. 9A, B). Face dark yellowish-brown. Interocular space with a brown band. Ocelli spots white. Antennae yellowish-brown. Clypeus pale brown (Fig. 9C). Maxillary palps light linen-colored (Fig. 9E). Pronotal disc light linen-colored with brown stripes and two lateral borders yellowish-white (Fig. 9D). Tegmina pale yellowish-brown, wings medium brown (Fig. 9F, G). Abdomen cream-colored to pale brown. Cerci yellowish brown (Fig. 9K). Styli faint yellow (Fig. 9M). **Head:** vertex slightly exposed, distance

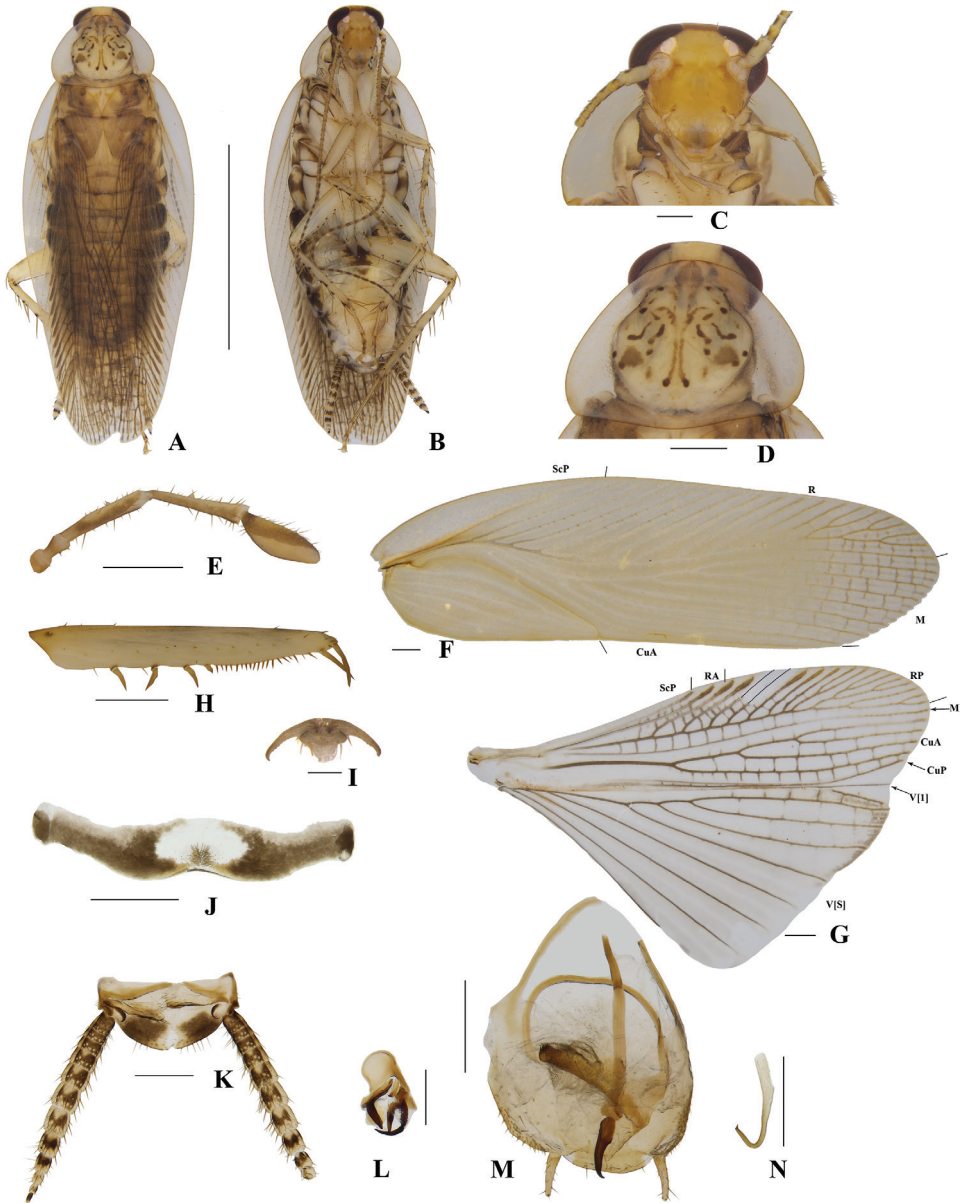


**Figure 9.** A–N *Margattea paratransversa* sp. nov., male **A** holotype, dorsal view **B** holotype, ventral view **C** head, ventral view **D** pronotum, dorsal view **E** maxillary palpi, ventral view **F** tegmen, dorsal view **G** hind wing, dorsal view **H** front femur, ventral view **I** tarsal claws **J** eighth abdominal terga **K** supra-anal plate and paraprocts, ventral view **L** left phallomere, dorsal view **M** subgenital plate and median phallomere, dorsal view **N** hook-like phallomere, dorsal view. Scale bars: 5 mm (**A**, **B**); 0.5 mm (**C**–**H**, **J**, **K**–**N**); 0.1 mm (**I**).

between interocular shorter than antennal socket space (Fig. 9C). Pronotum nearly trapezoidal, broader than long, the widest part after the midpoint, the front and posterior margins nearly straight, and the postero-lateral angle blunt and round; disc

with symmetrical irregular maculae (Fig. 9D). Third and fourth palpi of approximately same length, both obviously longer than fifth palp, fifth palp obviously expanded (Fig. 9E). **Tegmina and wings:** tegmina and wings fully developed, both extending beyond the end of abdomen (Fig. 9A, B). Tegmina with ScP simple, R multi-branched, M straight with seven complete branches. Hind wings with ScP and RA expanded at apex; M straight and simple without branches; CuA with five complete branches (Fig. 9F, G). **Legs:** anteroventral margin of front femur type B<sub>2</sub> (Fig. 9H). Pulvilli present on four proximal tarsomeres. Tarsal claws symmetrical and specialized, inner margin serrated, arolia present (Fig. 9I). **Abdomen and genitalia:** eighth abdominal tergum specialized with a tuft (Fig. 9J). Supra-anal plate transverse, posterior margin convex. Paraprocts simple, splitting into two pieces, apex with tufts (Fig. 9K). Subgenital plate symmetrical. Styli similar, slender, distinctly separated; interstyler region slightly convex (Fig. 9M). Left phallomere complex, irregular bone-shaped, with three long spines (Fig. 9L). Median phallomere slender rod-shaped, apex with a slightly curved spine; accessory structure arched, a long piece of bone extends from right side of accessory structure (Fig. 9M). Hook phallomere on right side, apex curved inwards with a short spine (Fig. 9N).

**Female** similar as male.

**Etyymology.** The species name “*paratransversa*” reflects its similarity to *M. transversa* sp. nov.

**Distribution.** China (Yunnan).

***Margattea bicruris* J-J He & Z-Q Wang, sp. nov.**

<http://zoobank.org/E491FDA2-CD3A-4B6F-B717-CB75FD06F8C4>

Figure 10A–L

**Type material. Holotype:** CHINA • ♂; Wangtianshu Scenery Spot, Mengla County, Xishuangbanna Prefecture, Yunnan Province; 23-V-2016; Lu Qiu, Zhi-Wei Qiu leg; SWU-B-EC141601. **Paratype:** CHINA • 2 ♂♂, same data as for holotype; SWU-B-EC141602-141603.

**Diagnosis.** This species is similar to *M. breviaalata* (Caudell, 1927) in male genitalia, but it can be differentiated from the latter by the following characters: 1) median phallomere slender rod, apex forked without spines; while in the latter, one side of splitting apex with 2 long spines; 2) left phallomere without a spine; the latter with a spine; and 3) supra-anal plate symmetrical, the front and the posterior margin straight; while in the latter, posterior margin convex, the middle part concave.

**Measurements (mm).** Male ( $n = 3$ ), pronotum: length  $\times$  width 2.1–2.2  $\times$  3.0–3.2, tegmina length: 9.9–10.9, overall length: 11.6–12.0.

**Description. Male. Coloration:** body pale yellow with yellowish-brown (Fig. 10A, B). Face pale yellowish-brown. Interocular space with a brown band. Ocelli spots white. Antennae pale yellowish-brown. Clypeus medium yellowish-brown (Fig. 10C). Maxillary palps light linen-colored (Fig. 10E). Pronotal disc pale yellowish-brown with

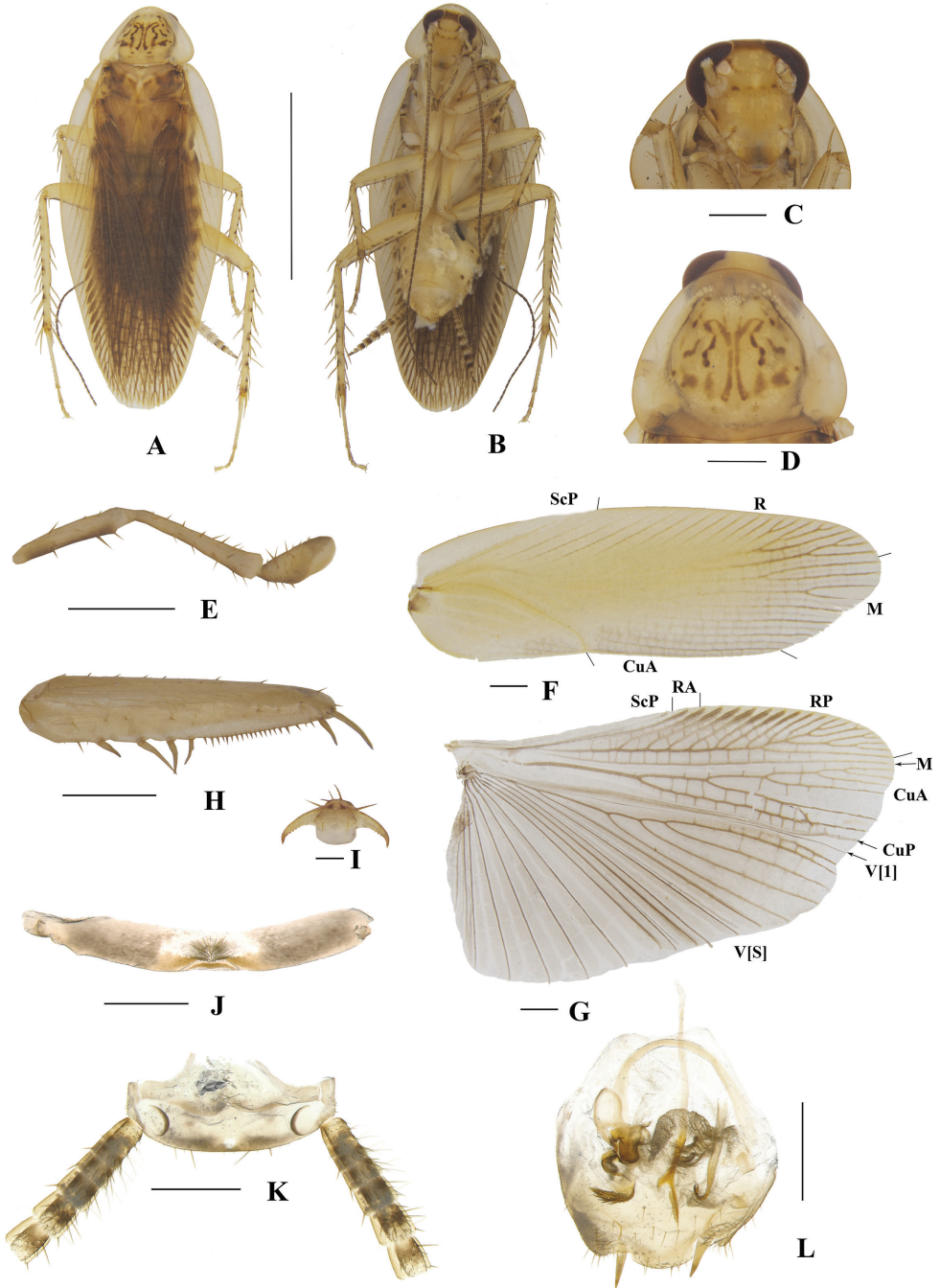


**Figure 10.** A–L *Margattea bicurvis* sp. nov., male **A** holotype, dorsal view **B** holotype, ventral view **C** head, ventral view **D** pronotum, dorsal view **E** maxillary palpi segments 3–5, ventral view **F** tegmen, dorsal view **G** hind wing, dorsal view **H** front femur, ventral view **I** tarsal claws **J** eighth abdominal terga **K** supra-anal plate and paraprocts, ventral view **L** subgenital plate and phallomeres, dorsal view. Scale bars: 5 mm (**A**, **B**); 0.5 mm (**C**–**H**, **J**, **K**–**L**); 0.1 mm (**I**).

yellowish-brown stripes, and two lateral light linen-colored borders (Fig. 10D). Tegmina light yellowish-brown, wings brownish grey (Fig. 10F, G). Abdomen cream-colored. Cerci yellowish-brown to pale brown (Fig. 10K). Styli faint yellow (Fig. 10L). **Head:** vertex slightly exposed, distance between interocular shorter than antennal sockets space (Fig. 10C). Pronotum nearly trapezoidal, broader than long, the widest part after midpoint, front and posterior margins nearly straight, and postero-lateral angle blunt and round; disc with symmetrical irregular stripes (Fig. 10D). Third and fourth palpi of approximately same length, both obviously longer than fifth palp, fifth palp obviously expanded (Fig. 10E). **Tegmina and wings:** tegmina and wings fully developed, both extending beyond the end of abdomen (Fig. 10A, B). Tegmina with ScP simple, R multi-branched, M straight with five complete branches. Hind wings with ScP and RA expanded at apex; M straight and simple, without branches; CuA with six complete branches (Fig. 10F, G). **Legs:** anteroventral margin of front femur type B<sub>2</sub> (Fig. 10H). Pulvilli present on four proximal tarsomeres. Tarsal claws symmetrical and specialized, inner margin serrated, arolia present (Fig. 10I). **Abdomen and genitalia:** eighth abdominal tergum specialized with a tuft (Fig. 10J). Supra-anal plate transverse. Paraprocts simple, similar, splitting into two pieces (Fig. 10K). Subgenital plate symmetrical. Styli similar, slender, distinctly separated. Left phallomere complex, irregular bone-shaped. Median phallomere slender rod-shaped with apex forked; the accessory structure arched, at leftmost end with a brush. Hook phallomere on right side, apex curved inwards with a short spine (Fig. 10L).

**Female** unknown.

**Etymology.** The Latin name “*bicruris*” refers to the median phallomere having the base forked.

**Distribution.** China (Yunnan).

## Discussion

The number of *Margattea* MOTUs (21) recovered from GMYC and bPTP analysis were greater than the number of species (16) determined by morphological characters. Of these, 13 MOTUs totally correspond to 13 species, while the remaining three species were overestimated as eight MOTUs. The ABGD method yielded 15 MOTUs because two morphospecies were considered as one MOTU. After re-examining the specimens, we still adhere to the morphological hypotheses, that is, 16 species. Our results therefore show that ABGD was, for *Margattea* with the parameters used, more in agreement with the morphological species hypotheses than the other methods tested. DNA-based identification methods were also proven to be useful in *Margattea* male and female matching. There is no denying that DNA-barcoding methods have performed well in the rapid identification and assessment of species diversity, in finding cryptic species, and in the matching of males and females (Yang et al. 2019; Li et al. 2020). However, when there is a divergence between the morphology and mo-



**Figure 11.** Twenty-seven collecting locations of *Margattea* species in China. The location corresponding to each number on the map was shown in Suppl. material 2: Table S2. The map originates from <https://www.simplemappr.net/>.

lecular results, we need to look for morphological evidence to show which approach is best supported.

For this group of cockroaches in our study, the intraspecific and interspecific K2P genetic distances (0.0–5.9% and 4.9–25.2%, respectively) were more or less similar to values found for other cockroach groups (*Cryptocercus*: 0.00–0.61% and 2.18–20.36% (Bai et al. 2018); Ectobiidae: 0.0–7.0% and 4.6–30.8% (Che et al. 2017)). There is an overlap, also known as no barcoding gap, between the intraspecific and interspecific distance according to our results; but this barcoding gap was treated as an artifact of insufficient sampling across lycaenid butterfly taxa by Wiemers et al. (2007). The maximum intraspecific genetic distance (5.9%) existed in *M. bisignata* samples. Four MOTUs were suggested within this species in the GMYC and bPTP analyses. No obvious variation could be discerned in these different geographical populations (Fig. 11) using morphological characters, including male genitalia, in spite of this larger genetic distance (Fig. 2). Therefore, we speculate that sufficient sampling of *M. bisignata* locations resulted in greater genetic distance. While the two morphospecies with an interspecific genetic distance of 5% were hypothesized as a single MOTU in ABGD, they did have obvious and stable morphological differentiation characters, which may be the result of insufficient sampling or rapid morphological differentiation.

## Acknowledgements

We are deeply grateful to Mr Zhi-wei Qiu (Chongqing) and Mr Lu Qiu (SWU) for collecting the specimens from Yunnan, China. We also thank Dr John Richard Schrock (Department of Biological Sciences, Emporia State University) for revising the English. This study is supported by the National Natural Sciences Foundation of China (no 31872271 and 31772506).

## References

- Bai QK, Wang LL, Wang ZQ, Lo N, Che YL (2018) Exploring the diversity of Asian *Cryptocercus* (Blattodea: Cryptocercidae): species delimitation based on chromosome numbers, morphology and molecular analysis. *Invertebrate Systematics* 32: 69–91. <https://doi.org/10.1071/IS17003>
- Beccaloni GW (2014) Cockroach Species File Online. Version 5.0/5.0. <http://Cockroach.SpeciesFile.org>
- Che YL, Gui SH, Lo N, Ritchie A, Wang ZQ (2017) Species delimitation and phylogenetic relationships in ectobiid cockroaches (Dictyoptera, Blattodea) from China. *PLoS ONE* 12: 1–25. <https://doi.org/10.1371/journal.pone.0169006>
- Drummond AJ, Rambaut A (2007) BEAST: Bayesian evolutionary analysis by sampling trees. *BMC Evolutionary Biology* 7: e214. <https://doi.org/10.1186/1471-2148-7-214>
- Ezard THG, Fujisawa T, Barraclough TG (2009) Splits: species limits by threshold statistics. <http://r-forge.r-project.org/projects/splits/> [accessed 5 July 2017]
- Folmer O, Black M, Hoeh W, Lutz R, Vrijenhoek R (1994) DNA primers for amplification of mitochondrial cytochrome c oxidase subunit I from diverse metazoan invertebrates. *Molecular Marine Biology and Biotechnology* 3: 294–299.
- Foster BT, Cognato AI, Gold RE (2004) DNA-based identification of the Eastern Subterranean Termite, *Reticulitermes flavipes* (Isoptera: Rhinotermitidae). *Journal of Economic Entomology* 97: 95–101. <https://doi.org/10.1093/jee/97.1.95>
- Kumar S, Stecher G, Tamura K (2016) MEGA7: Molecular Evolutionary Genetics Analysis version 7.0 for bigger datasets. *Molecular Biology and Evolution* 33: 1870–1874. <https://doi.org/10.1093/molbev/msw054>
- Li M, Che YL, Zheng YH, Wang ZQ (2017) The cockroach genus *Sorineuchora* Caudell, 1927 from China (Blattodea, Ectobiidae, Pseudophyllodromiinae). *ZooKeys* 697(1): 133–156. <https://doi.org/10.3897/zookeys.697.13617>
- Li M, Zhao QY, Chen R, He JJ, Peng T, Deng WB, Che YL, Wang ZQ (2020) Species diversity revealed in *Sigmella* Hebard, 1929 (Blattodea, Ectobiidae) based on morphology and four molecular species delimitation methods. *PLoS ONE* 15(6): e0232821. <https://doi.org/10.1371/journal.pone.0232821>
- Li XR, Zheng YH, Wang CC, Wang ZQ (2018) Old method not old-fashioned: parallelism between wing venation and wing-pad tracheation of cockroaches and a revision of terminology. *Zoomorphology* 137: 519–533. <https://doi.org/10.1007/s00435-018-0419-6>

- Liu XW, Zhou M (2011) Description of three new species of *Margattea* (Blattodea, Ectobiidae, Pseudophyllodromiinae) from China. *Acta Zootaxonomica Sinica* 36(4): 936–942.
- McKittrick FA (1964) *Evolutionary Studies of Cockroaches*. Cornell University Agricultural Experiment Station, Ithaca, New York, 197 pp.
- Pons J, Barraclough TG, Gomezzurita J, Cardoso A, Duran DP, Hazell S, Kamoun S, Sumlin WD, Vogler AP (2006) Sequence-based species delimitation for the DNA taxonomy of undescribed insects. *Systematic Biology* 55: 595–609. <https://doi.org/10.1080/10635150600852011>
- Puillandre N, Lambert A, Brouillet S, Achaz G (2012) ABGD, Automatic Barcode Gap Discovery for primary species delimitation. *Molecular Ecology* 21: 1864–1877. <https://doi.org/10.1111/j.1365-294X.2011.05239.x>
- Rach J, DeSalle R, Sarkar IN, Schierwater B, Hadrys H (2008) Character-based DNA barcoding allows discrimination of genera, species and populations in Odonata. *Proceedings of the Royal Society B – Biological Sciences* 275: 237–247. <https://doi.org/10.1098/rspb.2007.1290>
- Ramage T, Martins-simoes P, Mialdea G, Allemand R, Duploux A, Rousse P, Davies N, Roderick GK, Charlat S (2018) A DNA barcode-based survey of terrestrial arthropods in the Society Islands of French Polynesia: host diversity within the SymbioCode Project. *European Journal of Taxonomy* 272: 1–13. <https://doi.org/10.5852/ejt.2017.272>
- Roth LM (1989) The cockroach genus *Margattea* Shelford, with a new species from the Krakatau Islands, and re-descriptions of several species from the Indo-Pacific region (Dictyoptera: Blattaria: Blattellidae). *Proceedings of the Entomological Society of Washington* 91(2): 206–229.
- Roth LM (1991) New combinations, synonymies, redescrptions, and new species of cockroaches, mostly Indo-Australian Blattellidae. *Invertebrate Taxonomy* 5: 953–1021. <https://doi.org/10.1071/IT9910953>
- Roth LM (2003) Systematics and phylogeny of cockroaches (Dictyoptera: Blattaria). *Oriental Insects* 37: 1–186. <https://doi.org/10.1080/00305316.2003.10417344>
- Stamatakis A, Hoover P, Rougemont J (2008) A rapid bootstrap algorithm for the RAxML web servers. *Systematic Biology* 57: 758–771. <https://doi.org/10.1080/10635150802429642>
- Team RC (2013) R: A Language and Environment for Statistical Computing.
- Wang JJ, Li XR, Wang ZQ, Che YL (2014) Four new and three redescribed species of the cockroach genus *Margattea* Shelford, 1911 (Blattodea, Ectobiidae, Pseudophyllodromiinae) from China. *Zootaxa* 3827(1): 31–44. <https://doi.org/10.11646/zootaxa.3827.1.3>
- Wang ZQ, Che YL, Wang JJ (2009) Taxonomy of *Margattea* Shelford, 1911 from China (Dictyoptera: Blattaria: Blattellidae). *Zootaxa* 1974: 51–63. <https://doi.org/10.5281/zenodo.185116>
- Wiemers M, Fiedler K (2007) Does the DNA barcoding gap exist? – a case study in blue butterflies (Lepidoptera: Lycaenidae). *Frontiers in Zoology* 4(1): e8. <https://doi.org/10.1186/1742-9994-4-8>
- Yang R, Wang ZZ, Zhou YS, Wang ZQ, Che YL (2019) Establishment of six new *Rhabdoblatta* species (Blattodea, Blaberidae, Epilamprinae) from China. *ZooKeys* 851: 27–69. <https://doi.org/10.3897/zookeys.851.31403>
- Zhang J, Kapil P, Pavlidis P, Stamatakis AA (2013) General species delimitation method with applications to phylogenetic placements. *Bioinformatics* 29: 2869–2876. <https://doi.org/10.1093/bioinformatics/btt499>

## Supplementary material 1

### Table S1. Interspecific and intraspecific genetic distances

Authors: Jia-Jun He, Du-Ting Jin, Yi-Shu Wang, Yan-Li Che, Zong-Qing Wang

Data type: molecular data

Copyright notice: This dataset is made available under the Open Database License (<http://opendatacommons.org/licenses/odbl/1.0/>). The Open Database License (ODbL) is a license agreement intended to allow users to freely share, modify, and use this Dataset while maintaining this same freedom for others, provided that the original source and author(s) are credited.

Link: <https://doi.org/10.3897/zookeys.1036.63232.suppl1>

## Supplementary material 2

### Table S2. 27 collecting locations of *Margattea* species in China.

Authors: Jia-Jun He, Du-Ting Jin, Yi-Shu Wang, Yan-Li Che, Zong-Qing Wang

Data type: occurrence

Copyright notice: This dataset is made available under the Open Database License (<http://opendatacommons.org/licenses/odbl/1.0/>). The Open Database License (ODbL) is a license agreement intended to allow users to freely share, modify, and use this Dataset while maintaining this same freedom for others, provided that the original source and author(s) are credited.

Link: <https://doi.org/10.3897/zookeys.1036.63232.suppl2>

## Supplementary material 3

### Figure S1

Authors: Jia-Jun He, Du-Ting Jin, Yi-Shu Wang, Yan-Li Che, Zong-Qing Wang

Data type: image

Copyright notice: This dataset is made available under the Open Database License (<http://opendatacommons.org/licenses/odbl/1.0/>). The Open Database License (ODbL) is a license agreement intended to allow users to freely share, modify, and use this Dataset while maintaining this same freedom for others, provided that the original source and author(s) are credited.

Link: <https://doi.org/10.3897/zookeys.1036.63232.suppl3>

## Supplementary material 4

### Raw data

Authors: Jia-Jun He, Du-Ting Jin, Yi-Shu Wang, Yan-Li Che, Zong-Qing Wang

Data type: species data

Copyright notice: This dataset is made available under the Open Database License (<http://opendatacommons.org/licenses/odbl/1.0/>). The Open Database License (ODbL) is a license agreement intended to allow users to freely share, modify, and use this Dataset while maintaining this same freedom for others, provided that the original source and author(s) are credited.

Link: <https://doi.org/10.3897/zookeys.1036.63232.suppl4>



# First record of *Paegniodes* Eaton, 1881 (Ephemeroptera, Heptageniidae) from Thailand with description of a new species

Boonsatien Boonsoong<sup>1</sup>, Chonlakran Auychinda<sup>2</sup>,  
Michel Sartori<sup>3,4</sup>, Nuttakun Khanyom<sup>1</sup>

**1** Animal Systematics and Ecology Speciality Research Unit (ASESRU), Department of Zoology, Faculty of Science, Kasetsart University, Bangkok 10900, Thailand **2** Department of Biology and Health Science, Mahidol Wittayanusorn School, Salaya, Nakhon Pathom, Thailand **3** Museum of Zoology, Palais de Rumine, Place Riponne 6, CH-1005 Lausanne, Switzerland **4** University of Lausanne (UNIL), Department of Ecology and Evolution, CH-1015 Lausanne, Switzerland

Corresponding author: Boonsatien Boonsoong ([fscibtb@ku.ac.th](mailto:fscibtb@ku.ac.th))

---

Academic editor: L. Pereira-da-Conceicao | Received 23 February 2021 | Accepted 21 April 2021 | Published 10 May 2021

---

<http://zoobank.org/9A2C63EC-D583-418F-8277-3DAEC567EED6>

---

**Citation:** Boonsoong B, Auychinda C, Sartori M, Khanyom N (2021) First record of *Paegniodes* Eaton, 1881 (Ephemeroptera, Heptageniidae) from Thailand with description of a new species. ZooKeys 1036: 153–170. <https://doi.org/10.3897/zookeys.1036.64880>

---

## Abstract

A new species of Heptageniidae, *Paegniodes sapanensis* **sp. nov.**, is described based on larvae, subimagos, eggs, and COI data. The mayfly genus *Paegniodes* Eaton, 1881 is reported for the first time from Thailand. The larva of the new species can be distinguished from other known *Paegniodes* species by i) lamellae of gill I ca 1/4 of fibrilliform portion and ii) mandibles and basal segment of maxillary palp without dense setae on margin. The subimago characters useful to distinguish this new species from previously known species are i) the median stripes on abdominal terga and ii) shape of the female subgenital and subanal plates. The genetic distance between the new species and *P. cupulatus* (Eaton, 1871) was approximately 11%. The morphological characters of the new species are discussed and compared to other known species.

## Keywords

COI, diversity, mayfly, Southeast Asia

## Introduction

The poorly known mayfly genus *Paegniodes*, established by Eaton (1881), currently comprises two valid species: *P. cupulatus* (Eaton, 1871) from China (Ma et al. 2018; adults, larva, and egg) and *P. dao* Nguyen & Bae, 2004 from Vietnam (Nguyen and Bae 2004; larva only). Based on the unique characters of the imaginal and larval stages, Ma et al. (2018) clearly confirmed the generic status of *Paegniodes*, following Webb and McCafferty (2008). In addition, the complete mitochondrial genome of *P. cupulatus* was provided by Zhou et al. (2014).

In the past decade, knowledge about the diversity of the Heptageniidae in Thailand has continued to increase, and more species have been described and revised (Boonsoong and Braasch 2013; Boonsoong and Sartori 2015; Sutthacharoenthad et al. 2019). However, some genera of Thai heptageniid mayflies remain unclear and require taxonomic revision.

Here, we describe a new species of *Paegniodes* based on specimens from Nan province. In addition, the mitochondrial COI sequence data and a distribution map of the genus are provided.

## Materials and methods

*Paegniodes* larvae were collected by a hand-picking method from slow-flowing water in Nan Province in northern Thailand. The specimens were fixed and preserved in 95% ethanol for molecular and morphological studies. Mature larvae were reared using earthenware pots connected to an air supply until emergence of winged stages.

Measurements (given in mm) and photographs were taken using a NIKON SMZ800 stereoscopic microscope. For scanning electron microscopy (**SEM**), eggs were dried in a critical point drier (CPD7501) and coated with gold (Sputter Coater SC7620). The SEM photographs were obtained with a FEI Quanta 450 SEM. Final plates were prepared with Adobe Photoshop CC 2020.

The preserved specimens were dissected for DNA extraction. Total DNA was extracted using a genomic DNA purification kit (NucleoSpin, Macherey-Nagel, Germany), following the manufacturer's protocol. The COI amplification was performed using LCO1490 and HCO2198 (Folmer et al. 1994). The polymerase chain reaction (**PCR**) conditions and procedure were as described by Sutthacharoenthad et al. (2019). Purification and sequencing were conducted by Macrogen, Inc. (South Korea). The genetic distances between species were determined using Kimura-2-parameter distances (Kimura 1980), calculated with the MEGA X program (Kumar et al. 2018). Nucleotide sequences obtained in this study have been deposited in the GenBank database. Other *Paegniodes* sequences were also obtained from the Barcode of Life Data System (**BOLD**) and GenBank; details are presented in Table 1. The distribution map was generated with the SimpleMappr software (Shorthouse 2010).

**Table 1.** Sequenced specimens of the genus *Paegniodes* (new sequence indicated in bold).

Species	Locality	GenBank/BOLD Accession Number (GenSeq Nomenclature)
<i>P. sapanensis</i> sp. nov.	Nan, Thailand	MW633481 (genseq-2 COI)
<i>P. sapanensis</i> sp. nov.	Nan, Thailand	MW633482 (genseq-2 COI)
<i>P. dao</i> (BOLD identification)	Nan, Thailand	THMAY162
<i>P. cupulatus</i>	China	GBMH11533

The material is deposited in the collection of the Zoological Museum at Kasetsart University in Bangkok, Thailand (ZMKU) and at the Museum of Zoology in Lausanne, Switzerland (MZL).

## Taxonomy

### Order Ephemeroptera

### Family Heptageniidae

### Genus *Paegniodes* Eaton, 1881

#### *Paegniodes sapanensis* Boonsoong, Sartori & Auychinda, sp. nov.

<http://zoobank.org/1C749EC4-356B-4CCD-A22F-9C3AADD603AA>

Figures 1–10

**Materials examined. Holotype.** 1 female mature larva in alcohol, deposited in ZMKU, Thailand, Nan province, Bo Kluea district, Sapan waterfall, 19°11'25.8"N, 101°11'56.3"E, 800 m, 21.III.2020, B. Boonsoong leg.

**Paratypes.** 3 larvae in ethanol, deposited in ZMKU, same data as holotype; 2 larvae in ethanol, GBIFCH00834844, deposited in MZL same locality as holotype, 26.XI.2019, B. Boonsoong leg.; 1 male subimago (reared from larva), 2 female subimagos (reared from larvae), 2 larvae, all in ethanol, deposited in ZMKU, same locality as holotype, 29.XI.2020, B. Boonsoong leg.

**Description of larva.** Body length 16.2 mm (holotype) 10.0–13.5 mm (exuvia) 7.2–11.5 mm (immature), caudal filaments ca 1.5× of body length (immature).

General colouration dark brown with pale markings on tibiae and abdominal tergites.

**Colouration** (Figs 1, 10A–C). Head, thorax, legs, and abdomen dorsally dark brown. Head, thorax, legs, and abdomen ventrally whitish. Caudal filaments brown.

**Head. Head capsule.** Ovoid in shape and flattened, 1.8–2.5 mm in length, 2.5–4.1 mm in width, brown, without distinct markings (Fig. 2A); head capsule margins smooth. Compound eyes and base of ocelli black.

**Antenna** (Figs 2A, 10A). Antennae length slightly longer than head width, scape and pedicel dark brown, flagellum light brown.

**Labrum** (Fig. 2B). Triangular, width of labrum 1/3 of head capsule, with median notch on anterior margin, anterior margin with row of long, hair-like setae; dorsal surface with hair-like setae except at notch and nearby area.



**Figure 1.** *Paegniodes sapanensis* sp. nov., habitus of larva (Holotype).

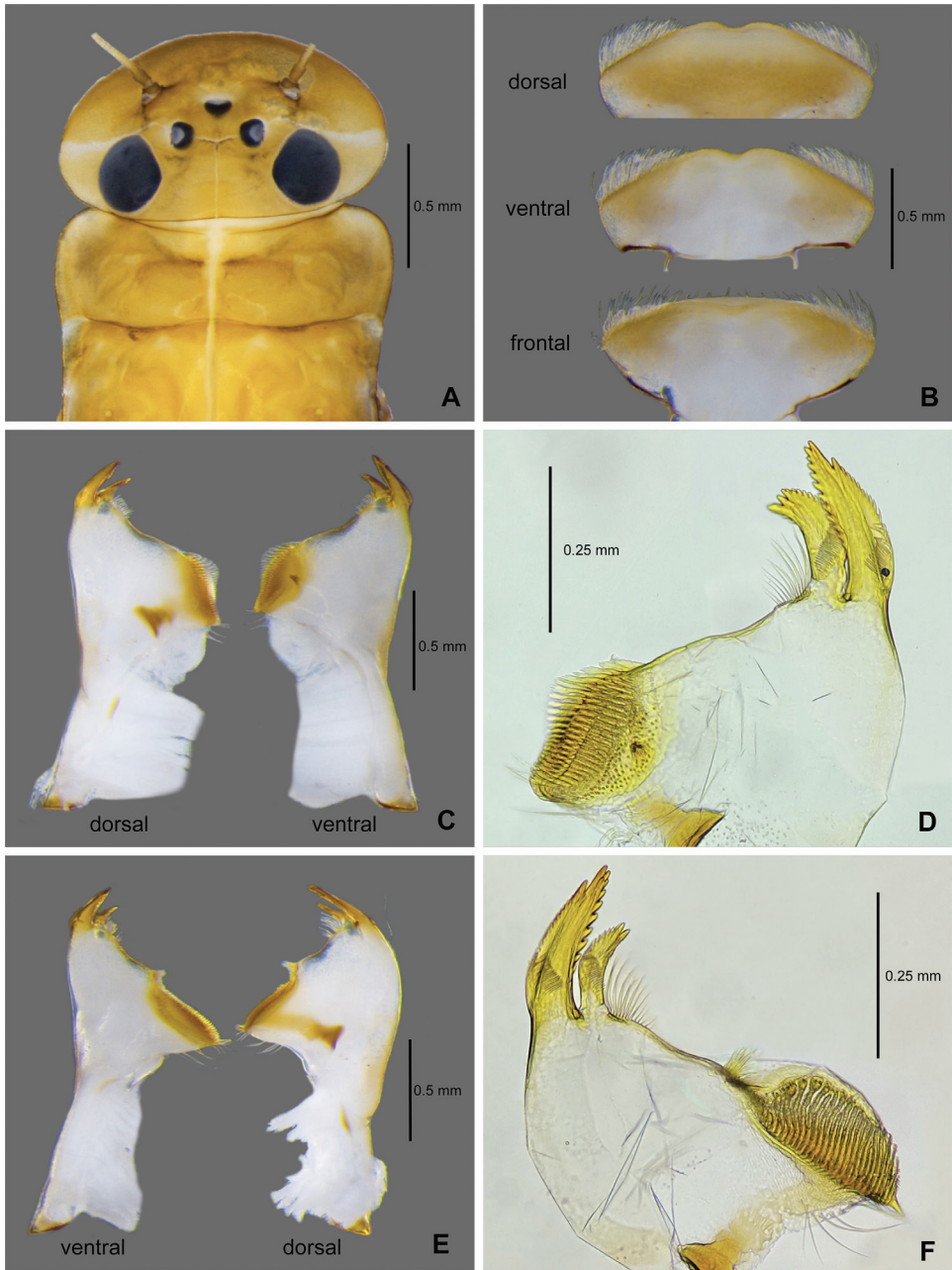


**Figure 2.** *Paegniodes sapanensis* sp. nov., larval morphology **A** head and pronotum **B** labrum **C** left mandible **D** enlargement of left mandible (ventral view) **E** right mandible **F** enlargement of right mandible (ventral view).

*Left mandible* (Fig. 2C). Outer and inner incisors acute with serrated margins, row of bristles located near inner incisor, row of fine serrated spines locate on base of outer and inner incisors, margin between inner incisor and mola slightly concave and

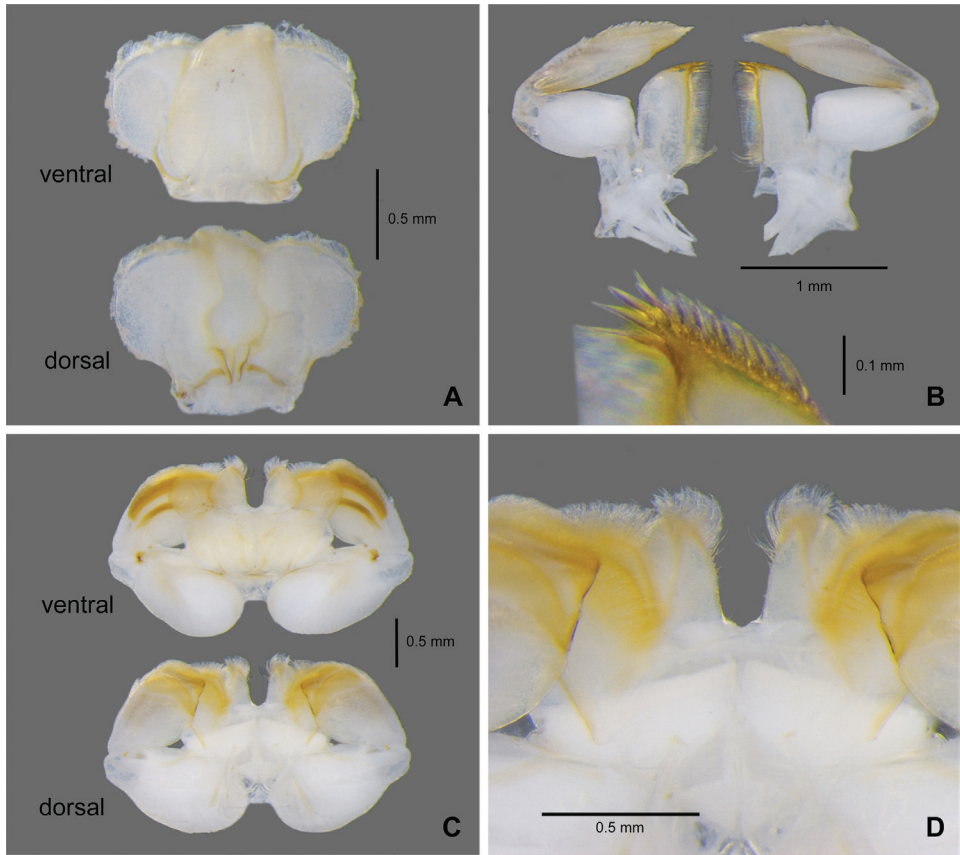


**Figure 3.** *Paegniodes sapanensis* sp. nov., larval morphology **A** hypopharynx **B** maxilla **C** labium (ventral view and dorsal view) **D** enlargement of labium (dorsal view).

smooth, one distinct denticle ventrally near mola area, setae present at apex of mola (Fig. 2D). Lateral margin without row of setae.

**Right mandible** (Fig. 2E). Outer and inner incisors acute with serrated margins, row of bristles located near inner incisor, row of fine serrated spines locate on base of outer and inner incisors, margin between inner incisor and mola slightly concave, tuft of setae locate on inner margin near mola, setae present at apex of mola (Fig. 2F). Lateral margin without row of setae.

**Hypopharynx** (Fig. 3A). Lingua subequal to superlingua, longer than broad, with medial tuft of long, stout setae. Superlingua distally almost straight, nearly square; each superlingua with notch on anterior margin, lateral margin rounded, with fine, long, simple setae along laterodistal margin.

**Maxilla** (Fig. 3B). Crown of galea-lacinia with a row of eight comb-shaped setae, apex of maxilla with three canines; two dentisetae, and one row of long setae on inner margin, with a row of submarginal setae on ventral surface; maxillary palpi two-segmented, apical one 1.6× length of basal segment; ventral surface of segment II with row of dense setae forming brush-like structure, apex of last segment apically lanceolate.

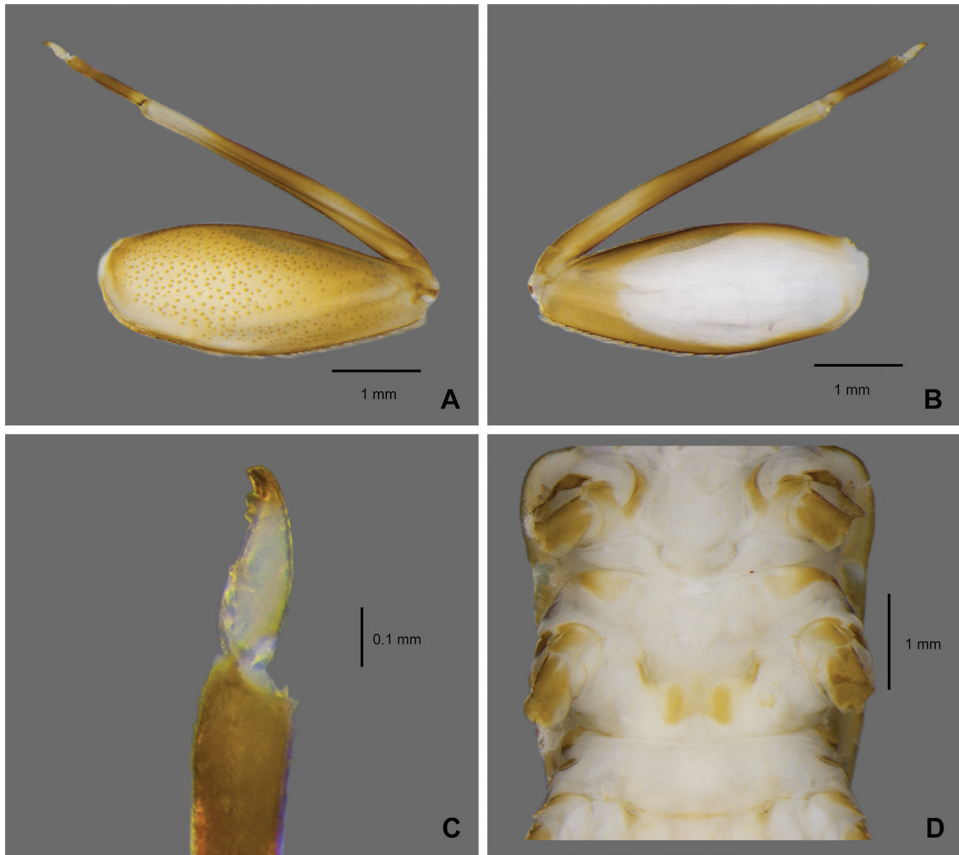


**Figure 4.** *Paegniodes sapanensis* sp. nov., larval morphology **A** foreleg (dorsal view) **B** foreleg (ventral view) **C** tarsal claw of foreleg **D** sternum.

**Labium** (Fig. 3C). Labium with U-shaped separation between glossae; shape of glossae conical, inner margin covered with dense setae, outer margin with row of setae; paraglossae moderately expanded laterally, with dense apical setae; basal segment of palp slightly longer than length of apical segment; apical segment slightly pentagonal, apex with broad projection (Fig. 3D); with dorsal transverse row of setae apically and setae brush ventrally.

**Thorax. Foreleg** (Fig. 4A) Coxa with well-developed, round dorsal plate; tibia subequal to femur in length, tarsus about  $\frac{1}{4}$  length of tibia; femur with regular row of bristles on outer margin and many scattered, mostly spatulate setae on dorsal surface, ventrally with whitish elongated oval area (Fig. 4B); tibia and apex of tarsus pigmented in light yellow; tarsus brown to dark; claw with a submedian denticle and three apical denticles (Fig. 4C). **Middle and hind legs** as foreleg but with patellar-tibial (fusion) sutures, apex of tibia with cluster of setae on inner surface, and claw with two or three apical denticles. Mesosternum with a distinct transverse yellow macula (Fig. 4D).

**Abdomen. Terga** (Fig. 6A). Terga pale brown, each tergum with two submedian pairs of pale dots; mature larva with distinct brown median stripes on terga II–VII,

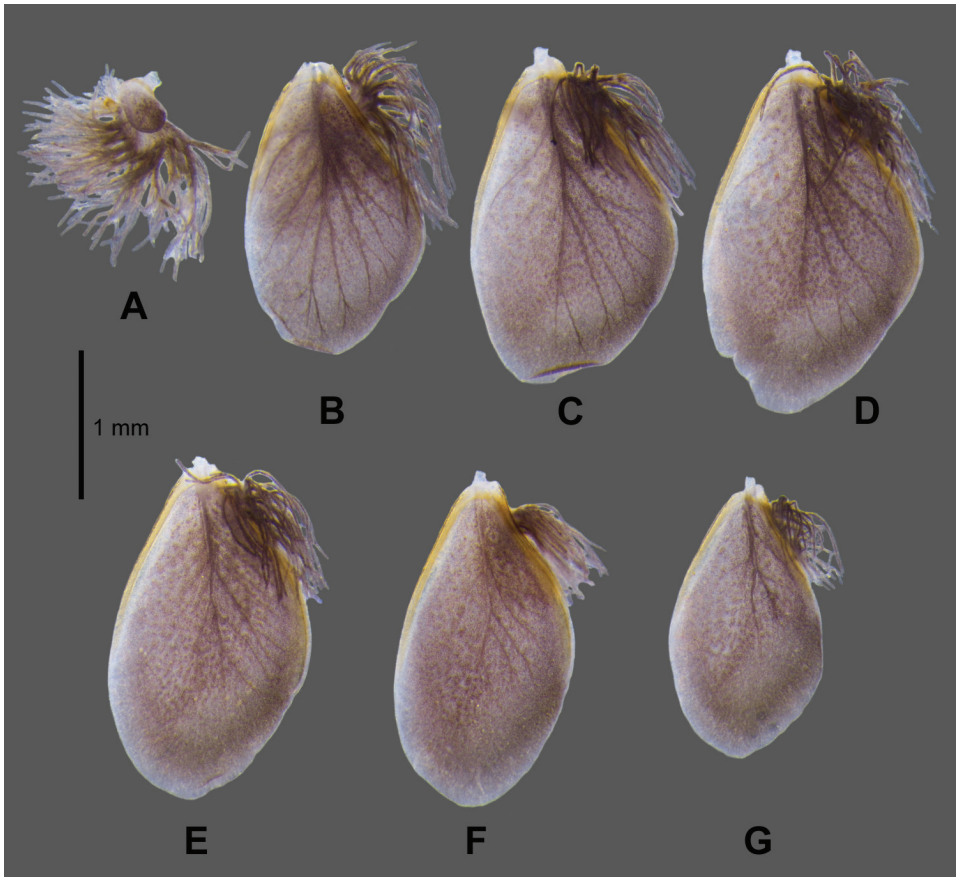


**Figure 5.** *Paegniodes sapanensis* sp. nov., larval morphology **A** gill I **B** gill II **C** gill III **D** gill IV **E** gill V **F** gill VI **G** gill VII.

with brown oblique stripes on lateral margin of terga III–VII, posterior margin of each tergum with row of strong and acute denticles, posterolateral projections extended into acute projections.

**Gills** (Fig. 5). Gills on abdominal segments I–VII; gill I (Fig. 5A) smaller than others, dorsal lamellae  $1/4$  in length of well-developed fibrilliform portion; gill II–VII similar in shape (Fig. 5B–G), lamellae much longer than fibrilliform portion, tracheation clearly visible, proximal half of lamellae margin thickened and sclerotised, gill IV (Fig. 5D) relatively larger than others.

**Caudal filaments** (Fig. 6B). Cerci subequal to paracercus in length, paracercus laterally with long setae on both margins of each segment, similar setae located on inner margins of cerci only.

**Diagnostic characters of larval stage.** The main diagnostic characters are: i) lamellae of gill I ca  $1/4$  of fibrilliform portion, ii) mandibles without dense hair-like setae on lateral margin, iii) basal segment of maxillary palp without hairlike setae on

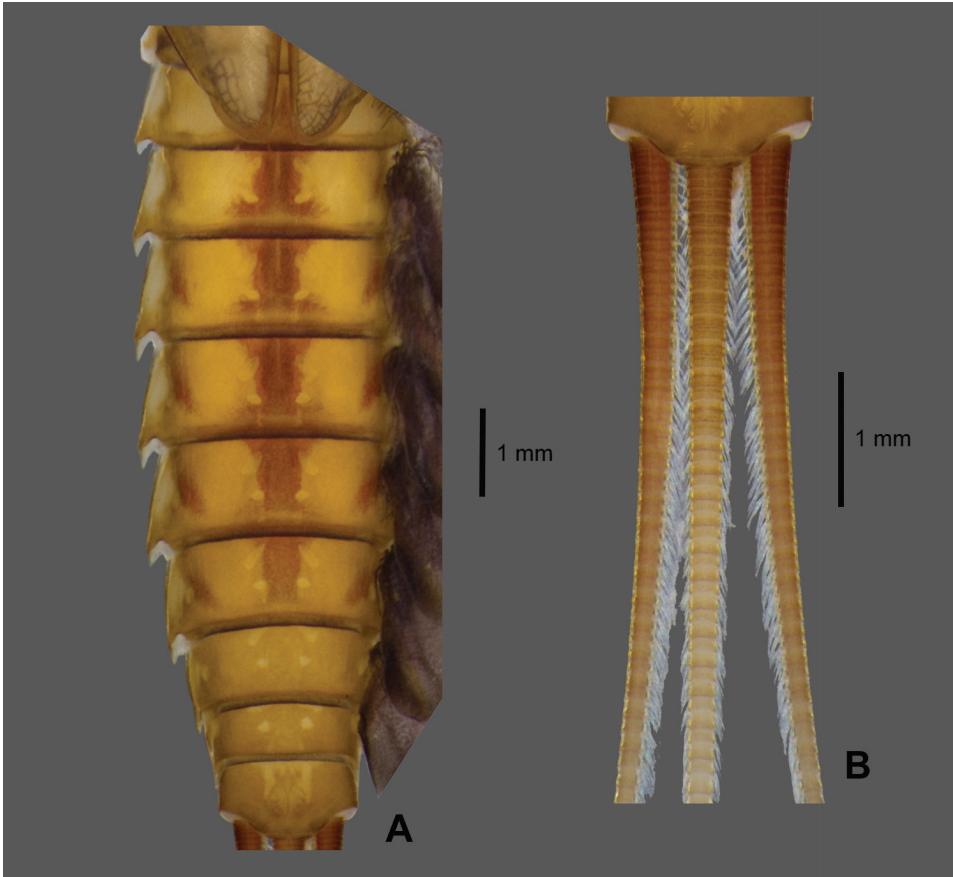


**Figure 6.** *Paegniodes sapanensis* sp. nov., larval morphology **A** terga II–X (dorsal view) **B** cerci and paracercus.

margins, and iv) apical segment of labial palp slightly pentagonal with broad projection at apex.

**Description of adult stages. Male subimago** (in ethanol Fig. 7, living Fig. 10E)

Body length 8.5 mm, cerci 17.5 mm, forewing 10.9 mm, hindwing 1.5 mm.

**Colouration** (Fig. 7). Head, thorax and abdomen dorsally yellowish brown. Head, thorax, and abdomen ventrally light yellow. Legs yellow. Caudal filaments brownish.

**Head** (Fig. 7A). Compound eyes separated by  $3.0\times$  width of median ocellus.

**Thorax** (Fig. 7A, D). Pronotum and mesonotum each with pair of dark dots; forewings semitransparent, veins yellowish to brown (Fig. 7B); hindwings 0.14 size of forewings (Fig. 7C). Legs yellowish to yellowish brown; femora brown with proximal and distal light maculae; tibiae uniformly brown; tibiae slightly shorter than femora. Forelegs (Fig. 7E): length of leg segments: femur 2.5 mm; tibia 2.3 mm; tarsus 2.0 mm (tarsal segments in order of decreasing length:  $2>3>4>1>5$ ). Midlegs: (Fig. 7F) length of leg segments: femur 2.4 mm; tibia 2.1 mm; tarsus 1.2 mm (tarsal segments in order of decreasing length  $2>1>5>3>4$ ). Hindlegs (Fig. 7G): length of leg segments: femur

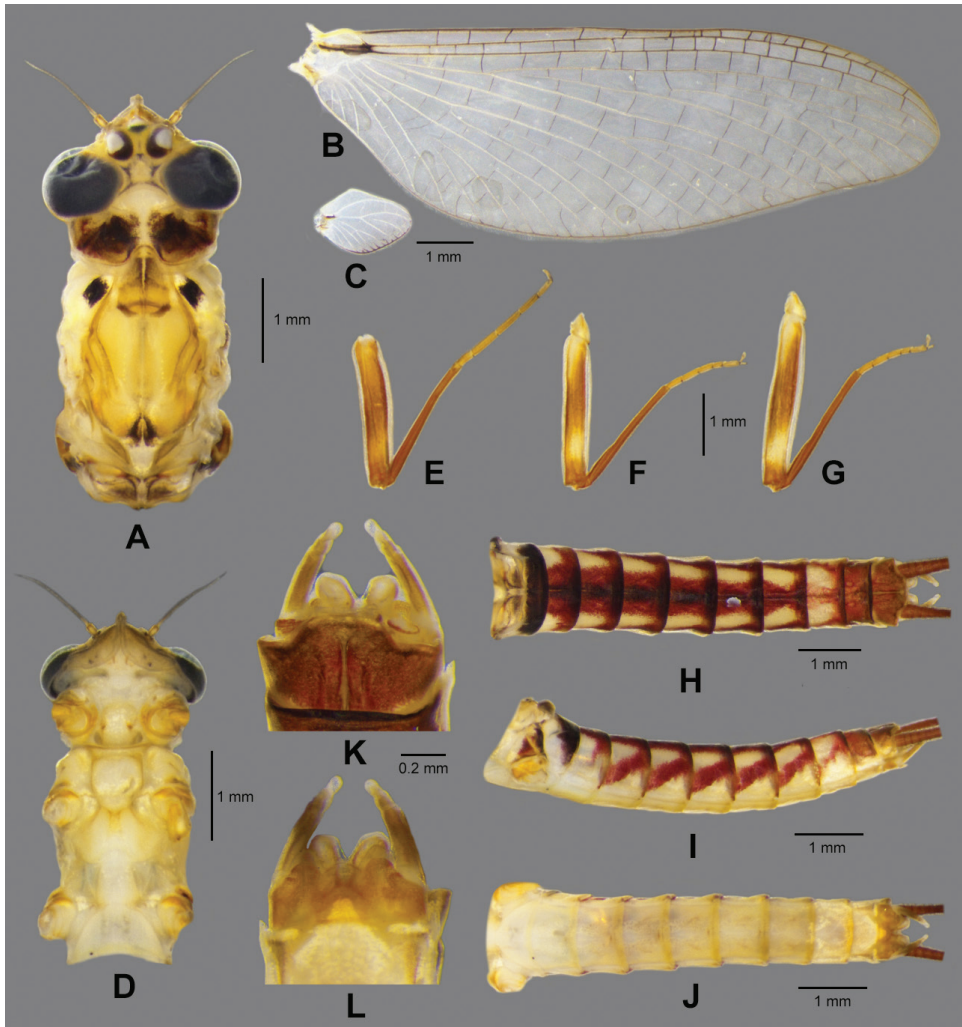


**Figure 7.** *Paegniodes sapanensis* sp. nov., male subimago **A** head and thorax (dorsal view) **B** forewing **C** hindwing **D** head and thorax (ventral view) **E** foreleg **F** middle leg **G** hind leg **H** abdomen (dorsal view) **I** abdomen (lateral view) **J** abdomen (ventral view) **K** genitalia (dorsal view) **L** genitalia (ventral view).

2.8 mm; tibia 2.2 mm; tarsus 1.2 mm (tarsal segments in order of decreasing length:  $1 \geq 5 > 2 \geq 3 > 4$ ). Each leg with two claws; one blunt, and one sharp and hooked.

**Abdomen.** Dorsally with ornamentation as in Fig. 7H, tergum I with transverse dark band, terga II–VII with distinct, reddish median band; laterally with pattern as in Fig. 7I, with clearly oblique stripes on terga III–VII but those on terga II and VIII less visible; all sterna predominantly light yellow (Fig. 7J). Combined length of two terminal segments of gonopods half the length of basal one (Fig. 7K, L). Penis lobes jointed at base, apices separated, each penis lobe apex slightly expanded laterally. Styliiger plate with concave posterior margin, but median part convex (Fig. 7L). Cerci reddish to brown.

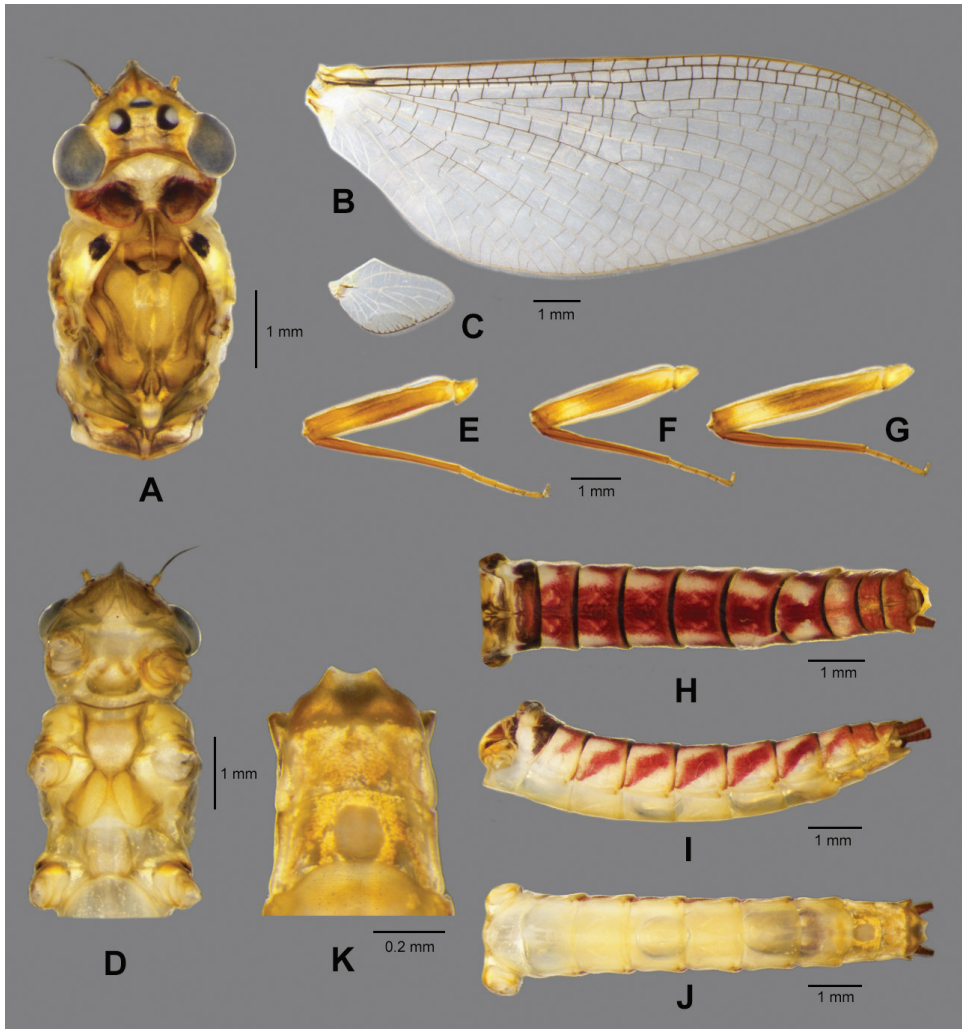


**Figure 8.** *Paegniodes sapanensis* sp. nov., female subimago **A** head and thorax (dorsal view) **B** forewing **C** hindwing **D** head and thorax (ventral view) **E** foreleg **F** middle leg **G** hind leg **H** abdomen (dorsal view) **I** abdomen (lateral view) **J** abdomen (ventral view) **K** genitalia (ventral view).

**Female subimago** (in ethanol Fig. 8, living Fig. 10D, F)

Body length 12.8 mm, cerci 20.0 mm, forewing 14.4 mm, hindwing 2.6 mm.

**Colouration** (Fig. 8). Head, thorax and abdomen dorsally brown. Head, thorax and abdomen ventrally light brown. Legs yellow. Caudal filaments brown.

**Head** (Fig. 8A). Compound eyes separated by 3.0× width of median ocellus.

**Thorax** (Fig. 8A, D). Pronotum and mesonotum each with pair of dark dots, sternum light brown; forewings semitransparent, veins yellowish to brown (Fig. 8B); hindwings 0.18 the size of the forewings (Fig. 8C). Legs yellowish to yellowish brown; femora brown with proximal and distal light maculae; tibiae uniformly brown; foreti-

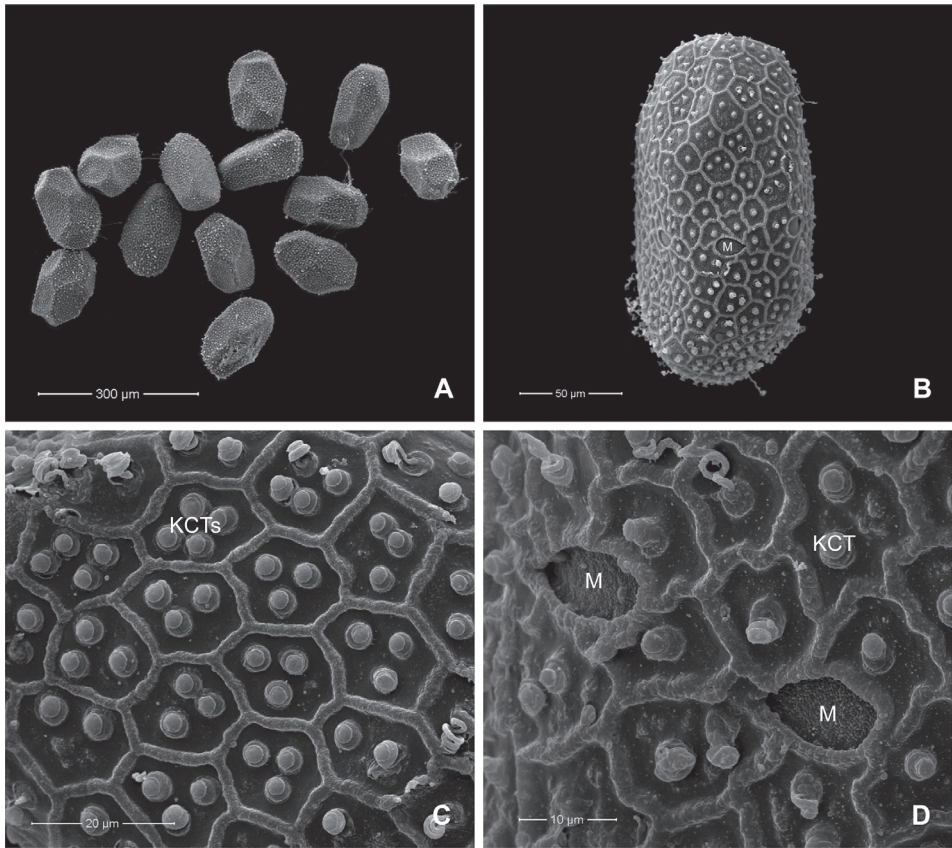


**Figure 9.** *Paegniodes sapanensis* sp. nov., scanning electron micrographs of egg (dissected from subimago) **A** eggs **B** general outline **C** chorionic surface **D** micropyle. M = micropyle, KCTs = knob-terminated coiled threads.

biae equal to femora; tibiae of midleg and hindleg slightly shorter than femora. Fore-legs (Fig. 8E): length of leg segments: femur 3.1 mm; tibia 3.1 mm; tarsus 1.7 mm (tarsal segments in order of decreasing length: 2>3>5>1>4). Midlegs (Fig. 8F): length of leg segments: femur 2.9 mm; tibia 2.7 mm; tarsus 1.4 mm (tarsal segments in order of decreasing length 2>1≥3≥5>4). Hind leg (Fig. 8G): length of leg segments: femur 3.5 mm; tibia 3.0 mm; tarsus 1.2 mm (tarsal segments in order of decreasing length: 5>1≥2>3>4). Each leg with two claws; one blunt, and one sharp and hooked.

**Abdomen.** Dorsally with ornamentation as in Fig. 8H, tergum I with dark band, with distinct reddish median band on terga II–VII; laterally with pattern as in Fig. 8I, with clearly oblique stripes on terga III–VII but those on terga II and VIII less visible; all sterna predominantly light yellow (Fig. 8J); subgenital plate (sternum VII) distally rounded and subanal plate (sternum IX) extended, with shallow median notch (Fig. 8K); cerci reddish brown, with tiny setae on surface.

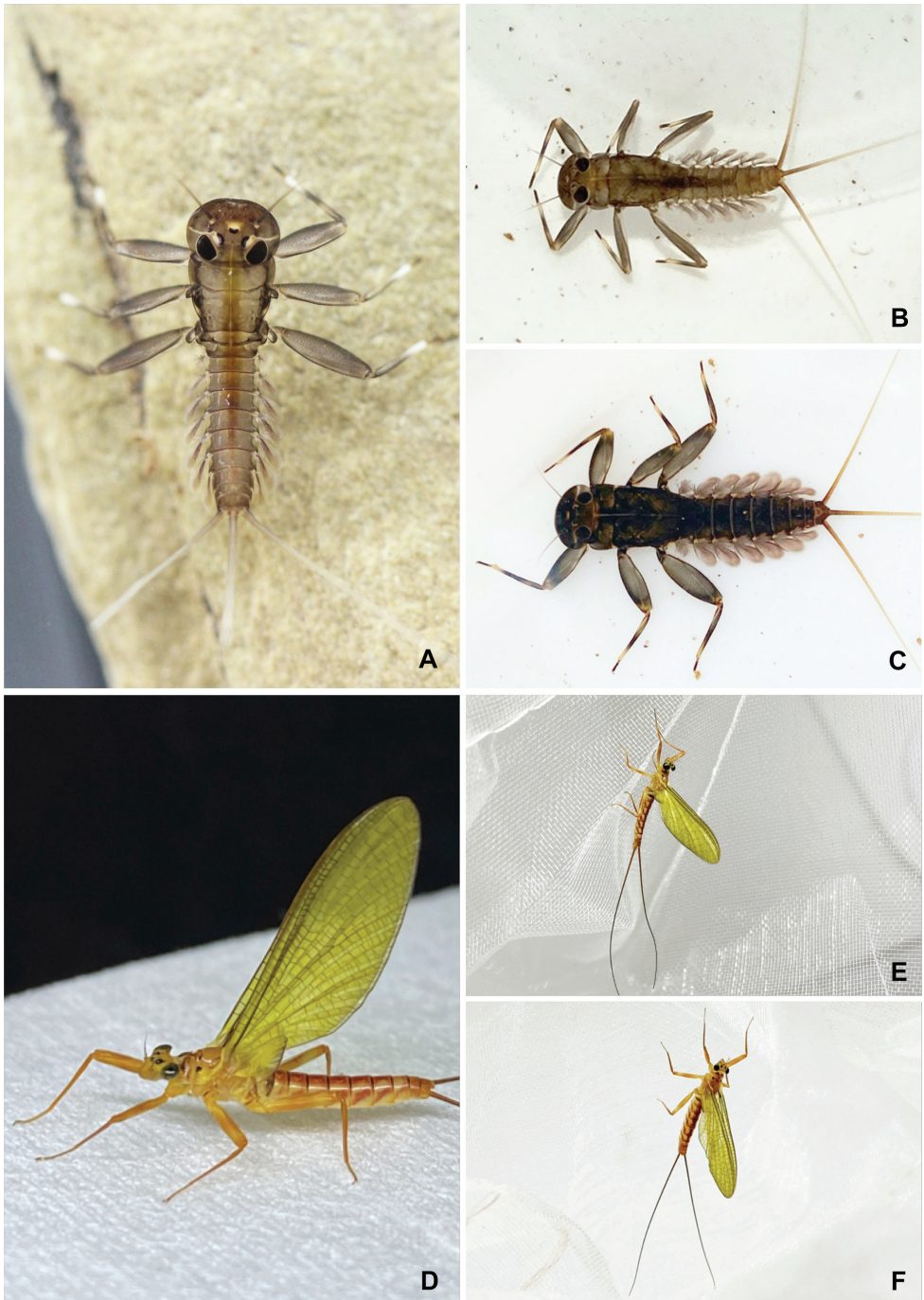


**Figure 10.** *Paegniodes sapanensis* sp. nov., habitus (live) **A** immature larva **B** male larva **C** female larva **D** closer view of female subimago **E** male subimago **F** female subimago.



**Figure 11.** Habitats of larvae of *Paegniodes sapanensis* sp. nov. **A** tributary of a Sapan stream **B** cobble substrate with bottom sand and gravel **C** stream bank with cobble.

**Description of egg.** (dissected from female subimago). Length ca 155–175  $\mu\text{m}$ , width ca 80–95  $\mu\text{m}$ ; elongate and oval in shape (Fig. 9A, B); chorionic surface covered with hexagonal and pentagonal mesh ridges, with 1–4 knob-terminated coiled threads

(KCTs) in between (Fig. 9C); tageniform micropyle in equatorial area (2 or 3 micropyles clearly visible on the same side) (Fig. 9D).

**Diagnostic characters of imaginal stage.** The diagnostic characters to distinguish our new species from *P. cupulatus* are: i) the median stripes on abdominal terga and ii) lateral margins of genital plates slightly concave near apex.

**Etymology.** The specific epithet is named for the Sapan waterfall (Bo Kluea district; tourist attraction of Nan province, Thailand), where the holotype is known.

**Distribution.** Nan province.

**Biological aspects.** The specimens were collected from tropical mountain streams (Fig. 11A) which are slightly disturbed by tourist activities. The larvae of the new species were found in flowing areas and the littoral zone of the streams, underneath a mostly cobble substrate (Fig. 11B, C).

**Molecular analysis.** Two COI sequences of *Paegniodes* were retrieved from BOLD system and GenBank (Table 1). One sequence from BOLD (THMAY162-12) was based on a specimen from the same locality (Namtok Sa Pan) as this study and this specimen was identified as *P. dao*. However, our Kimura 2-parameter (K2P) analysis revealed that intraspecific genetic divergence of the three sequences is very low (0.03%), and we considered all sequences as belonging to the same species. In addition, the interspecific distances (COI) between the new species and *Paegniodes cupulatus* ranged from 11.43–11.73%.

## Discussion

In this study, the morphology of the new species showed a close similarity to *P. cupulatus* (from China) in terms of mandibles, maxillary palp, gill I, and abdominal pattern (Table 2). Mandibles and basal segment of maxillary palp of *P. dao* (Nguyen and Bae 2004: fig. 1C, D) possess a dense, hair-like setal field on the lateral margin, which is not the case in *P. cupulatus* (Ma et al. 2018: fig. 4D, G) and *P. sapanensis* sp. nov. The dorsal lamellae of gill I of *P. cupulatus* and *P. sapanensis* sp. nov. represent at least 1/4 of

**Table 2.** Larval characters of *Paegniodes sapanensis* sp. nov. compared with known species (Nguyen and Bae 2004; Ma et al. 2018).

Species	<i>P. cupulatus</i>	<i>P. dao</i>	<i>P. sapanensis</i> sp. nov.
Distribution	China	Vietnam	Thailand
Mandibles	without dense hairlike setal field on lateral margin	with dense hairlike setal field on lateral margin	without dense hairlike setal field on lateral margin
Basal segment of maxillary palp	without dense hairlike setal fields on anterior and posterior margins	with dense hairlike setal fields on anterior and posterior margins	without dense hairlike setal fields on anterior and posterior margins
Number of comb-shape setae on the crown of the galea-lacinia	9	unknown	8
Shape of labial palp segment II	apex with broad projection	apically rounded	apex with broad projection
Number of apical denticles of tarsal claw	3	unknown	2–3
Lamellae of gill I	1/3	rudimentary	1/4

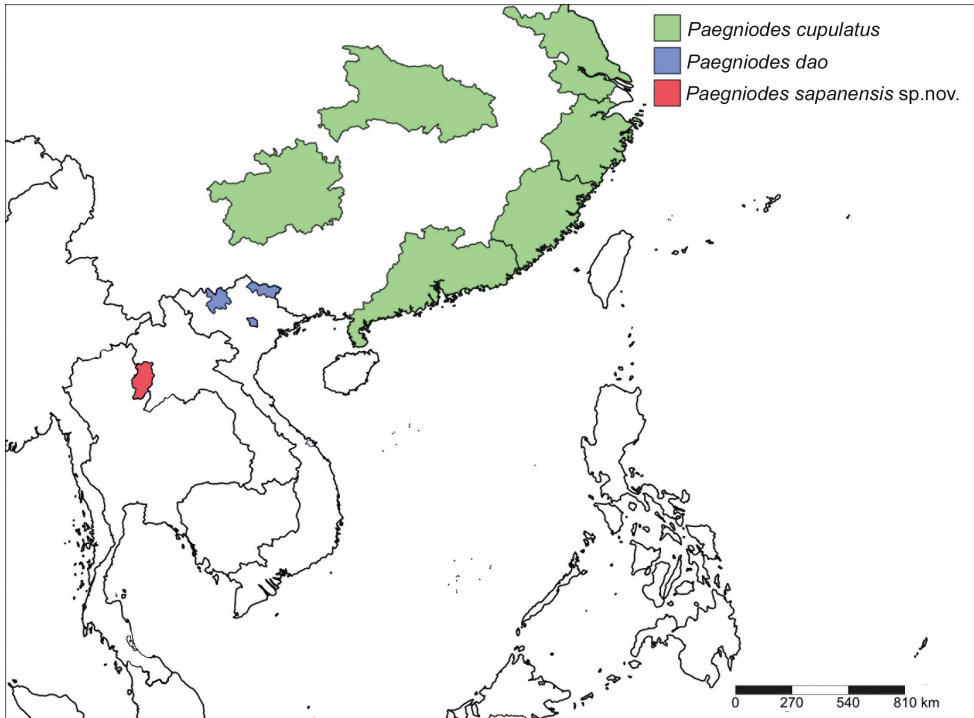


**Figure 12.** Distribution of the genus *Paegniodes* Eaton, 1881.

a fibrilliform portion, while this is barely visible in *P. dao* (Nguyen and Bae 2004: fig. 1G). In addition, the larvae of *P. cupulatus* and *P. sapanensis* sp. nov. possess the typical abdominal stripes, which are absent in *P. dao* (Nguyen and Bae 2004).

However, the new species can be separated from *Paegniodes cupulatus* by the colouration of mature nymphs of *P. sapanensis* sp. nov. which seem darker than that of *P. cupulatus*. On the abdominal terga of *P. cupulatus*, the pale dots are on both side of median stripe (Ma et al. 2018: fig. 1A), while pale dots of the new species are inside the median stripe (Fig. 6A). Size of lamellate in gill I of the new species is smaller than in *P. cupulatus* (Table 2). The imaginal stage of the new species also differs from *P. cupulatus* by the width of the median stripe on abdominal terga; in *P. cupulatus* this is narrower than in the new species. Lateral margins of subanal plate are slightly concave near apex in the new species but smooth in *P. cupulatus* (Ma et al. 2018: figs 6D, 8F).

The molecular analysis clearly supports *P. sapanensis* sp. nov. as a species separate from *P. cupulatus*, as the genetic distance between the two species is 11%, which is much higher than the value of 3.5% generally considered to represent the maximum intraspecific divergence (Hebert et al. 2003; Zhou et al. 2010). The intraspecific genetic distance of the new species was about 0.03%, which is not surprising, as all specimens were sampled in the same locality.

The combination characteristics of *Paegniodes* that distinguish it from all other genera in the subfamily Rhithrogeninae include: i) reduced lamellae on the gills I, ii) caudal filaments with interfacing setae, iii) short hindwings (usually less than 1/4 the length of the forewings), and iv) males having widely separated penes with strongly median titillators (Nguyen and Bae 2004; Webb and McCafferty 2008; Ma et al. 2018). The findings of this study revealed that the common characters in adults of *Paegniodes* were an abdomen with median and a pair of oblique stripes in both male and female subimagos, as also found in *P. cupulatus* and *P. dao* (Nguyen and Bae 2004; Ma et al. 2018). Additionally, the unique egg chorionic structure of *Paegniodes* includes hexagonal mesh ridges and 1–4 knobs between them (Ma et al. 2018). Unlike the relatively similar *Rhithrogeniella* (subfamily Ecdyonurinae), only one KCT is found between the ridges (Kang and Yang 1994; Sartori 2014).

The distribution of the genus *Paegniodes* is limited to Southeast Asia (Fig. 12). This is the first discovery of *Paegniodes* in Thailand after a decade of Ephemeroptera investigations. The genus *Paegniodes* is local and rare in Thailand, probably due to precise ecological requirements. In this study, we found the larvae in a unique microhabitat, located in slightly disturbed and mountain streams of Nan province.

Ma et al. (2018) expressed the view that the position of *Paegniodes* is apparently a plesiomorphic lineage of the subfamily Rhithrogeninae based on unique characteristics. The mouthparts and genitalia of the genus *Paegniodes* are closely related to *Rhithrogena*, but more plesiomorphic. However, the eggs of *Paegniodes*, unlike any genus in the subfamily Rhithrogeninae, are somewhat similar to the genus *Rhithrogeniella* (Ecdyonurinae). Our finding supports the taxonomic status of the genus *Paegniodes* suggested by Ma et al. (2018).

## Acknowledgements

This research has been supported by the Centre of Excellence on Biodiversity (BDC) Office of Higher Education Commission (BDC-PG2-161004). We are most grateful to our colleagues for assistance during field trips. We would like to thank the Department of Zoology and the Faculty of Science at Kasetsart University in Bangkok for their assistance and use of their facilities.

## References

- Boonsoong B, Braasch D (2013) Heptageniidae (Insecta, Ephemeroptera) of Thailand. *ZooKeys* 272: 61–93. <https://doi.org/10.3897/zookeys.272.3638>
- Boonsoong B, Sartori M (2015) A new species of *Compsoeuriella* Ulmer, 1939 (Ephemeroptera: Heptageniidae) from Thailand. *Zootaxa* 3936: 123–130. <https://doi.org/10.11646/zootaxa.3936.1.7>

- Eaton AE (1871) A Monograph on the Ephemeroidea. Transactions of the Entomological Society of London 1: 1–164.
- Eaton AE (1881) An announcement of new genera of the Ephemeroidea. Entomologist's Monthly Magazine 18: 21–27.
- Folmer O, Black M, Hoeh W, Lutz R, Vrijenhoek R (1994) DNA primers for amplification of mitochondrial cytochrome c oxidase subunit I from diverse metazoan invertebrates. Molecular Marine Biology and Biotechnology 3: 294–299.
- Hebert PDN, Cywinska A, Ball SL, DeWaard JR (2003) Biological identifications through DNA barcodes. Proceedings of the Royal Society B 270: 313–321. <https://doi.org/10.1098/rspb.2002.2218>
- Kang SC, Yang CT (1994) Heptageniidae of Taiwan (Ephemeroptera). Journal of Taiwan Museum 47: 5–36.
- Kimura M (1980) A simple method for estimating evolutionary rates of base substitutions through comparative studies of nucleotide sequences. Journal of Molecular Evolution 16: 111–120. <https://doi.org/10.1007/BF01731581>
- Kumar S, Stecher G, Li M, Knyaz C, Tamura K (2018) MEGA X: Molecular Evolutionary Genetics Analysis across computing platforms. Molecular Biology and Evolution 35: 1547–1549. <https://doi.org/10.1093/molbev/msy096>
- Ma ZX, Han N, Zhang W, Zhou CF (2018) Position and definition of the genus *Paegniodes* Eaton, 1881 based on redescription on the type species *Paegniodes cupulatus* (Eaton, 1871) (Ephemeroptera: Heptageniidae). Aquatic Insects 39(4): 362–374. <https://doi.org/10.1080/01650424.2018.1475675>
- Nguyen VV, Bae YJ (2004) A new species of poorly known mayfly genus *Paegniodes* Eaton (Ephemeroptera: Heptageniidae) from Vietnam. Entomological Research 34(4): 283–285. <https://doi.org/10.1111/j.1748-5967.2004.tb00124.x>
- Sartori M (2014) Status of the enigmatic Oriental genus *Rhithrogeniella* Ulmer, 1939 (Ephemeroptera, Heptageniidae). ZooKeys 429: 47–61. <https://doi.org/10.3897/zookeys.429.8116>
- Shorthouse DP (2010) SimpleMappR, an online tool to produce publication-quality point maps. <https://www.simplemappR.net> [accessed 11 Feb. 2021]
- Sutthacharoenthad W, Sartori M, Boonsoong B (2019) Integrative taxonomy of *Thalerosphyrus* Eaton, 1881 (Ephemeroptera, Heptageniidae) in Thailand. Journal of Natural History 53(23–24): 1491–1514. <https://doi.org/10.1080/00222933.2019.1657513>
- Webb JM, McCafferty WP (2008) Heptageniidae of the world. Part II: Key to the Genera. Canadian Journal of Arthropod Identification 7: 1–55. <https://doi.org/10.3752/cjai.2008.07>
- Zhou X, Jacobus LM, DeWalt RE, Adamowicz SJ, Hebert PDN (2010) Ephemeroptera, Plecoptera, and Trichoptera fauna of Churchill (Manitoba, Canada): insights into biodiversity patterns from DNA barcoding. Journal of the North American Benthological Society 29: 814–837. <https://doi.org/10.1899/09-121.1>
- Zhou D, Wang YY, Sun JZ, Han YK, Zhou CF (2016) The complete mitochondrial genome of *Paegniodes cupulatus* (Ephemeroptera: Heptageniidae). Mitochondrial DNA Part A 27(2): 925–926. <https://doi.org/10.3109/19401736.2014.926488>

# Corrigenda: A new species of *Chromis* damselfish from the tropical western Atlantic (Teleostei, Pomacentridae). ZooKeys 1008: 107–138. <https://doi.org/10.3897/zookeys.1008.58805>

Emily P. McFarland<sup>1,2</sup>, Carole C. Baldwin<sup>3</sup>, David Ross Robertson<sup>4</sup>,  
Luiz A. Rocha<sup>5</sup>, Luke Tornabene<sup>1,2</sup>

**1** School of Aquatic and Fishery Sciences, University of Washington, Seattle, WA 98195-5020, USA **2** Burke Museum of Natural History and Culture, Seattle, WA 98105, USA **3** Department of Vertebrate Zoology, National Museum of Natural History, Smithsonian Institution, Washington, DC, 20560, USA **4** Smithsonian Tropical Research Institute, Balboa, Republic of Panama **5** Department of Ichthyology, California Academy of Sciences, San Francisco, California 94118, USA

Corresponding author: Luke Tornabene ([ltorna1@uw.edu](mailto:ltorna1@uw.edu))

---

Academic editor: Kyle Piller | Received 11 March 2021 | Accepted 19 March 2021 | Published 10 May 2021

<http://zoobank.org/6336309E-41C5-459A-9F44-F20DDBCBE4C>

---

**Citation:** McFarland EP, Baldwin CC, Robertson DR, Rocha LA, Tornabene L (2021) Corrigenda: A new species of *Chromis* damselfish from the tropical western Atlantic (Teleostei, Pomacentridae). ZooKeys 1008: 171–172. <https://doi.org/10.3897/zookeys.1008.58805>. ZooKeys 1036: 171–172. <https://doi.org/10.3897/zookeys.1036.65739>

---

Following the publication of our paper (McFarland et al. 2020), it was brought to our attention by Andrew Bentley (University of Kansas) that Table 3 listed the holotype of the species *Chromis enchrysurus* Jordan & Gilbert, 1882 as KU 27029, and mislabeled the species as *Chromis enchrysurus*. We regret this mistake, as there are three syntypes of *C. enchrysurus*, none of which is the specimen listed. The corrected version of the table is provided here.

**Table 3.** Morphometrics and meristics of *Chromis vanbeberae* and *Chromis enchrysurus* specimens examined. Morphometric values are as percentage of SL.

	<i>Chromis vanbeberae</i>			<i>Chromis enchrysurus</i>	
	Holotype of <i>Chromis vanbeberae</i> USNM 446947	Average	Range	Average	Range
standard length	73.9	48.2	13.9–98.4	60.7	80.8–17.7
body depth	55.2	51.1	41.6–57.7	50.2	53.9–44.0
body width	19.4	19.1	16.5–21.6	17.5	19.2–13.8
head length	30.2	35.4	30.2–41.0	31.6	36.0–29.8
snout length	7.9	8.2	5.2–10.3	8.2	9.3–5.8
orbit diameter	11.8	14.6	11.5–17.4	11.7	14.7–10.0
interorbit width	10.7	10.6	8.6–12.1	10.6	14.0–9.2
caudal peduncle depth	16.1	15.1	13.3–16.4	14.0	15.6–9.8
upper jaw length	9.1	10.0	6.0–14.4	9.7	10.9–8.0
predorsal length	33.2	34.0	28.6–42.0	33.7	38.3–28.2
spinous dorsal base	48.6	44.1	35.5–50.2	46.7	50.8–36.6
soft dorsal base	18.9	16.5	13.4–18.9	14.6	18.0–10.4
1st dorsal spine	8.7	9.1	7.2–11.9	8.3	10.3–6.7
2nd dorsal spine	12.9	14.3	11.4–17.5	12.6	16.2–10.6
3rd dorsal spine	15.7	17.9	15.3–21.6	15.5	19.6–12.3
4th dorsal spine	19.4	20.2	16.6–24.5	17.4	22.4–13.5
5th dorsal spine	20.6	20.5	16.2–25.9	17.4	22.4–13.5
6th dorsal spine	19.8	18.6	15.5–23.7	17.0	21.6–13.3
last dorsal spine	16.4	13.8	10.3–17.4	12.3	16.1–9.3
longest dorsal ray	23.8	23.2	21.1–28.5	19.1	23.0–16.1
preanal length	64.1	67.0	63.2–69.7	66.5	69.9–63.1
1st anal spine	9.3	8.7	5.8–11.6	8.1	9.9–5.5
2nd anal spine	19.9	19.2	15.1–22.4	18.8	21.8–16.0
longest anal ray	23.4	24.1	18.9–28.0	19.9	26.3–16.3
caudal length	41.0	36.8	29.7–44.9	31.4	35.8–27.3
longest pectoral ray	34.2	33.8	31.1–38.1	31.2	33.7–28.6
prepelvic length	35.2	38.4	35.2–43.6	37.3	41.7–33.8
pelvic spine length	22.2	20.3	18.7–22.4	20.0	31.2–17.2
1st pelvic soft ray	40.9	35.4	28.8–43.2	23.4	36.8–30.8
dorsal rays	12	12.7	12–13	12.2	11–15
anal rays	12	12.6	12–13	12.1	11–13
pored lateral line scales	17	16.5	15–17	17.2	16–18
upper gill rakers	7	7.3	7–8	7.5	7–8
lower gill rakers	17	16.9	16–18	16.8	16–18

## Reference

McFarland EP, Baldwin CC, Robertson DR, Rocha LA, Tornabene L (2020) A new species of *Chromis* damselfish from the tropical western Atlantic (Teleostei, Pomacentridae). ZooKeys 1008: 107–138. <https://doi.org/10.3897/zookeys.1008.58805>

# Corrigendum: Chinese species of *Carinostigmus* Tsuneki (Hymenoptera, Crabronidae), including three new species and a new record to China. ZooKeys 987: 115–134. <https://doi.org/10.3897/zookeys.987.55317>

Nawaz Haider Bashir<sup>1</sup>, Li Ma<sup>1</sup>, Qiang Li<sup>1</sup>

<sup>1</sup> Department of Entomology, College of Plant Protection, Yunnan Agricultural University, Kunming, Yunnan, 650201, China

Corresponding author: Li Ma ([maliwasps@aliyun.com](mailto:maliwasps@aliyun.com)); Qiang Li ([liqiangkm@126.com](mailto:liqiangkm@126.com))

---

Academic editor: T. Dörfel | Received 21 April 2021 | Accepted 22 April 2021 | Published 10 May 2021

---

<http://zoobank.org/C90EBAA3-2E67-4CE4-B843-ADA84F12678F>

---

**Citation:** Bashir NH, Ma L, Li Q (2021) Corrigendum: Chinese species of *Carinostigmus* Tsuneki (Hymenoptera, Crabronidae), including three new species and a new record to China. ZooKeys 987: 115–134. <https://doi.org/10.3897/zookeys.987.55317>. ZooKeys 1036: 173–174. <https://doi.org/10.3897/zookeys.1036.67684>

---

It has come to our attention that in the work referenced above, Figure 1 has a location error. The correct version of Figure 1 is reproduced here. The major changes are as follows: *C. iwatai* was collected from Yunnan: Baoshan, instead of Yunnan: Menglian Dai; *C. kaibuanus* was collected from Yunnan: Jinghong, instead of Yunnan: Guangnan county; and *C. filippovi* was collected from Sichuan: Mount Emei, instead of Sichuan: Emeishan city.

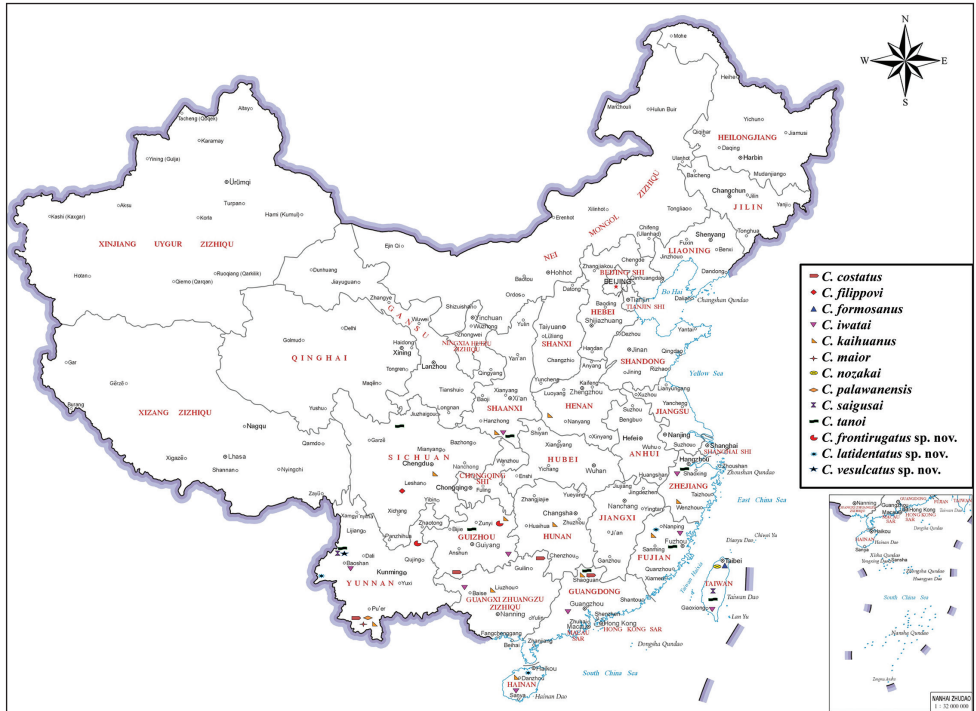


**Figure 1.** Distribution of *Carinostigmus* from China.

**References**

Bashir NH, Ma L, Li Q (2020) Chinese species of *Carinostigmus* Tsuneki (Hymenoptera, Crambionidae), including three new species and a new record to China. *ZooKeys* 987: 115–134. <https://doi.org/10.3897/zookeys.987.55317>